

Exploration of Host- Pathogen Interactions in the Australian Skink *Tiliqua rugosa*

By

Robert Liam O'Reilly
BSc (Honours)

Thesis
Submitted to Flinders University
for the degree of

Doctor of Philosophy

College of Science and Engineering
31st January 2023



Table of Contents

Thesis Abstract	iv
Declaration	vii
List of Contributors	viii
Co-Author Contributions	ix
List of Conference Presentations	x
General Acknowledgements	xi
Thesis General Introduction	1
Chapter 1: Foreword	21
Chapter 1: Fine scale population structure coincides with a parapatric tick boundary and MHC genotypes in a long-lived monogamous lizard.....	22
Abstract	23
Introduction.....	24
Methods.....	28
Study area and tissue collection	28
Group delineation for MHC I allele frequency and SNP analysis.....	28
MHCI Amplification and Sequencing	29
Sequencing and Genotyping.....	31
Statistical Analysis.....	32
Results.....	34
Sample sizes and groupings	34
MHC	34
DArTSeq	35
Discussion	36
Figures	39
Tables.....	42
References	45
Chapter 1: Supplementary Material.....	52
Chapter 2: Foreword	58
Chapter 2: Viral abundance and sub-population variation in <i>Tiliqua rugosa</i> over an ecological gradient using flow cytometry	59
Abstract	60
Introduction.....	61



Methods.....	64
Sample collection.....	64
Sample preparation	64
Flow Cytometry Analysis.....	65
Spatial and Statistical Analysis	65
Results.....	67
Discussion	67
Figures	Error! Bookmark not defined.
Tables.....	76
References	77
Chapter 2: Supplementary Material.....	81
Chapter 3: Foreword	84
CHAPTER 3: Spatial distribution of the shingleback nidovirus between Western Australia and South Australia using RT-qPCR	85
Abstract	86
Introduction.....	87
Methods.....	88
Sampling.....	89
RT-qPCR.....	90
Results.....	91
Sampling.....	91
RT-PCR.....	91
Discussion	93
Interpretation of results	93
Conclusion.....	95
Figures	96
Tables.....	101
References	102
Chapter 3: Supplementary Material.....	107
Chapter 4: Foreword	119
CHAPTER 4: Differential gene expression analysis of a non-model organism (<i>Tiliqua rugosa</i>) suggests upregulation of adaptive immune genes with the bobtail flu.....	120
Abstract	121
Introduction.....	122



Methods.....	124
Tissue collection.....	124
Iso-Seq to generate a pseudo-reference genome.....	124
Isoseq3.....	125
Cogent.....	126
ANGEL: Robust Open Reading Frame Prediction.....	127
BLASTX and BLAST2GO.....	127
NovaSeq.....	127
Differential expression analysis in R.....	128
Results.....	129
IsoSeq.....	129
Isoseq3.....	130
Cogent.....	130
ANGEL: Robust Open Reading Frame Prediction.....	130
CD-HIT.....	130
Blastx and Blast2GO.....	131
NovaSeq.....	131
Differential expression analysis.....	131
Discussion.....	133
Interpretation of results.....	133
Conclusion.....	136
Figures.....	137
Tables.....	140
References.....	151
Chapter 4: Supplementary Material.....	156
Thesis Discussion.....	180
Summary and Discussion.....	180
References.....	185



Thesis Abstract

Newly emerging pathogens and disease outbreaks in areas previously undetected are an increasing concern as climate change causes host and vector distributions to shift.

Fluctuating conditions require hosts to be able to tolerate changing pathogen diversity and abundance to survive. Understanding host-pathogen interactions in a common wild species may provide insight in how other species could respond to disease outbreaks. This thesis explores the host-pathogen interactions in an iconic Australian skink, *Tiliqua rugosa* that is widely distributed across the southern half of Australia and has close interactions with humans.

First, I explore immune genes of a *T. rugosa* population in Mount Mary, South Australia, across an ecological gradient. Using genome wide SNPs, I also investigated the *T. rugosa*'s population structure driven by two parasitic tick species over an ecological gradient. I found an association with certain Major Histocompatibility Complex class I (MHC I) alleles and tick infestation type — these alleles were also under selection. SNP data showed that the genetic differentiation shown by the MHC data was not simply reflective of a population differentiation that occurs across the whole genome. In the future, by understanding this differentiation in this system, and the association with tick vectors, studies may find evidence of the beginnings of a species divergent event without geographic barriers restricting gene flow.

Since MHC I is an antigen recognition molecule, the positive selection found could also be explained by varying viral abundances across the ecological gradient, and not necessarily via tick vectors. There are currently only two known viruses in *T. rugosa* (*Shingleback nidovirus 1* and Adenovirus), both of which are respiratory viruses. Therefore, I investigated the viral communities in the oral cavity of *T. rugosa* using flow cytometry and compared viral abundances across the ecological gradient of arid to humid environmental conditions. This presents a novel application of flow cytometry in a reptile system. I found two viral sub-populations, that are yet to be characterised, in greater than 95% of sampled lizards, and significant abundance variations across the gradient. These results support the positive



selection found, as could be explained by pathogen mediated selection, and shows how changing environmental conditions influence viral abundances.

At the start of this PhD, there was one known virus in *T. rugosa* —the *Shingleback nidovirus 1* — that had been associated with the bobtail flu. The bobtail flu was detected in the surrounding Perth Hills, Western Australia, and had a severe impact on the *T. rugosa*'s local wildlife population. However, there were also anecdotal reports of *T. rugosa* with bobtail flu symptoms in other states, including at Mount Mary, South Australia. I therefore aimed to determine whether the bobtail flu had come across from Perth and was in the Mount Mary study site. I sampled *T. rugosa* between Perth-Adelaide using reverse transcription real-time PCR (RT-qPCR) to screen for the *Shingleback nidovirus 1*' presence or absence in an individual. I found one positive sample (out of 91 samples) in a wild *T. rugosa* individual east of the Perth Hills. I did not find any positive samples in South Australia, or at the Mount Mary study site. This is the first attempt at identifying the *Shingleback nidovirus 1*'s distribution between Perth and Adelaide. My results also show that the viruses found using flow cytometry were not the *Shingleback nidovirus 1*, which then suggests there is at least one new virus for this species.

Finally, I explored how the bobtail flu effects *T. rugosa* by conducting a differential gene expression analysis using transcriptomics, between those diagnosed with the bobtail flu and those suffering from major trauma. Because *T. rugosa* does not currently have a reference genome, both long read (Iso-Seq) and short read (NovaSeq) sequencing technologies were used for the analysis. I found evidence that suggests the bobtail flu seems to suppress the host's innate immune system, although further investigation is required. The suppression of the host's immune system is particularly important should the bobtail flu be confirmed in South Australia in the future, as a closely related endangered species (*Tiliqua adelaidensis*) distributions overlaps with *Tiliqua rugosa* and could potentially be at risk.



This thesis uses novel and innovative techniques to understand how pathogens, parasites, and disease effect a common reptile species. As a non-model organism there is limited viral and genetic research on *T. rugosa* in response to pathogens, parasites, and disease. This thesis creates a framework for future research in this species to expand on while providing some insights into parasites and pathogens potentially affecting a species population structure; viruses shifting in abundance with changing environmental conditions on a fine scale; shows monitoring viruses and their distributions being accessible to non-model organisms; and how a respiratory disease effects a lizards immune system using transcriptomics.



Declaration

I certify that this thesis does not incorporate without acknowledgment any material previously submitted for a degree or diploma in any university; and that to the best of my knowledge and belief it does not contain any material previously published or written by another person except where due reference is made in the text.

Robert Liam O'Reilly



List of Contributors

Recipient of the Australian Government Research Training Program (AGRTP) support and stipend

Research and conference grants awarded:

- Holsworth Wildlife Research Endowment 2018- 2021
- European Society for Clinical Virology travel grant, Nov 2019
- Research funding Grant, Royal Society of South Australia, 2018



Co-Author Contributions

Supervisor Michael G. Gardner
College of Science and
Engineering
Flinders University, Australia

Associated Supervisor Michael P. Schwarz
College of Science and
Engineering
Flinders University, Australia

List of Co-Authors

Robert L. O'Reilly (RLO), Michael G. Gardner (MGG), Tessa Bradford (TB), Mike P Schwarz (MPS), Stephanie S. Godfrey (SSG), Steven J. Coopers (SJC), Terry Bertozzi (TB), James Paterson (JP), Jim Mitchell (JM), Carmel Maher (CM), Dale Burzacott (DB)

Chapter	Concept & design	Planning & implementation	Data collection	Analysis & interpretation	Writing & formatting
1	RLO, MGG, MPS	RLO, MGG	RLO, DB	RLO	RLO, TB, SSG, TB, SJC, MPS, MGG
2	RLO, JP, MGG	RLO, JP	RLO,	RLO, JP	RLO, JP, MGG, JM
3	RLO, MGG	RLO,	RLO	RLO	RLO, MGG
4	RLO, MGG	RLO,	RLO	RLO, CM, MGG	RLO, MGG



List of Conference Presentations

- O'Reilly, R., Gardner, M.G. The bobtail flu, is it as severe as the man flu? Conference talk, Australian Society of Herpetology Conference, Brisbane, 10-13th December, 2018.
- O'Reilly, R., Schwarz, M., Gardner, M.G. Exploration of the Shingleback nidovirus in an Australian skink, Poster presented at World Congress of Herpetology in Dunedin, New Zealand, 5-10th of January, 2020.
- O'Reilly, R., Schwarz, M., Gardner, M.G. Exploration of the Shingleback nidovirus in an Australian skink, Conference talk, European Society of Clinical Virology workshop in Vienna, Austria, 23-24th of January, 2020
- O'Reilly, R., Paterson, J., Mitchell, J., Gardner, M.G. Viral abundance and sub-population variation in *Tiliqua rugosa* over an ecological gradient using flow cytometry, Conference Talk, Ecological Society of Australia, (Online), 22-26th of November, 2021



General Acknowledgements

I would like to thank everyone who has helped me in some way with this PhD project over the past four years. Whether with motivational support; someone to bounce ideas off; or assisting in the project itself. It is very, very much appreciated. I'd like to give a special mention and thanks to certain people and groups that without them the project wouldn't have been possible:

Firstly, Wattle Grove Veterinary Hospital and Kanyana Wildlife Rehabilitation Centre, in Perth, Western Australia, who assisted this project by collecting samples from sick lizards during intake in their facilities and sending them to me in Adelaide.

Dr Mark O'Dea who invited me to the Antimicrobial Resistance and Infectious Diseases (AMRID) laboratory at Murdoch University, in Perth, for two weeks and showed me the ropes.

Alf Rebola who was nice enough to offer his car for me to use while in Perth for those two weeks.

Far West Coast Aboriginal Corporation and Nullarbor Parks Board, as well as the Aboriginal elders who gave permission to do research on their land in the Nullarbor.

Michelle Clanahan, my fellow lizard hunter, who came on the remote three-week field trip across the Nullarbor. She was an amazing volunteer who went well above and beyond.

Paula and Ken Everet, Michelle's cousins, who welcomed us into their homes in Perth to stay for the weekend midway through the Nullarbor field trip while we dropped off samples and regrouped for the last leg of the trip. You are the nicest of people, I can't thank you enough.

I'd like to thank my partner, Dr Olivia Miller, who has been there whenever I needed her. Making life easier and always understanding the stresses and commitments a PhD demands.

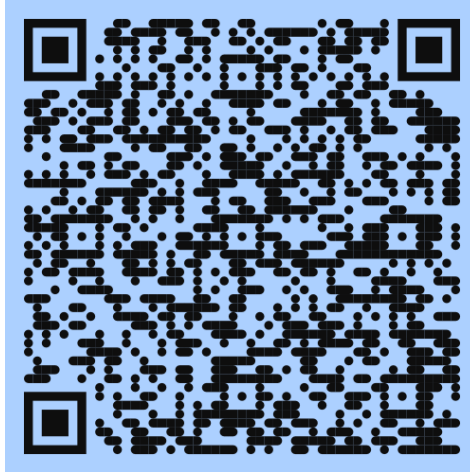
Obee, my dog, who forces me to leave the house for walks while trying to write up. If it wasn't for him I probably wouldn't have left the house at all.

My supervisors Mike Schwarz and Mike Gardner for giving me the opportunity, and the time they dedicated to this project.



Lastly, lab mates past and present. It is difficult to find a work-life balance during PhD.

Having a group of good people in the lab to socialise with, hiking, partying, even just coffee dates, it made my time during PhD more enjoyable — see below.



Here is a flash back.



Thesis General Introduction

Introduction

Many different organisms suffer from disease. However, what is disease? The medical definition is that disease is a condition that negatively affects the normal biological functioning of an individual (Sartorius *et al.*, 2006). Disease can be triggered by a pathogen causing abnormalities within an individual and resulting in acute or chronic sickness or death (Berg 2000; Grove and Joshi 2014; Perez-Molina and Molina 2018). There are many types of pathogens that can cause disease, for example - fungi, viruses, bacteria, and protozoans (Nami *et al.*, 2019; Oliver *et al.*, 2018; Bossart *et al.*, 2019; Kirk *et al.*, 2015). The impacts of disease can be devastating and there are numerous documented occurrences where pathogens have rapidly reduced the overall abundance of wild animal populations. For example, in 2015, approximately 200,000 Saiga antelope died within a three-week period in a mass mortality event caused by the bacterium *Pasteurella multocida* (Kock *et al.*, 2018). This extreme example shows how quickly pathogens can decimate populations and species, particularly when environmental factors such as temperature and humidity create perfect conditions to spread.

Disease can not only decimate populations but can even cause extinction of species. In 2007, there was great concern for amphibians, as the globally spread, highly virulent, fungus *Batrachochytrium dendrobatidis* caused chytridiomycosis disease in amphibians, resulting in the extinction, or decline, of up to 200 different frog species (Skerratt *et al.*, 2007). This disease continues to impact amphibian populations globally (Cádiz *et al.*, 2019; Miller *et al.*, 2018), with concerns about the limited recovery (12%) of the declined species (Scheele *et al.*, 2019). However, studies have suggested the impacts of this disease are not restricted to amphibians but a cascading effect on ecosystems that has severely reduced biodiversity (Scheele *et al.*, 2019; Zipkin and DiRenzo 2022). Studies such as these highlight the importance of ongoing monitoring of known infectious pathogens in order to prevent such catastrophic events (Durmus and Ülgen 2017).

Some pathogens, however, have the ability to spread not only within species and populations, but can be transferred across phyla (Brito *et al.*, 2017; Ramos *et al.*, 2019). One mechanism for this spread is that of vectors with multiple hosts. Vectors are classified as any



agent (organism or inanimate object) that transmits a pathogen to another organism (Last 2001). The two most notorious pathogen vectors are mosquitos and ticks. Ticks are not only vectors of pathogens, in that they transmit infectious agents horizontally (different life stages, multiple hosts), but also reservoirs for pathogens which can be stored in the ovaries and passed on vertically (mother to offspring) (Anderson 1989; Szabo *et al.*, 2013; Ajith Kumar *et al.*, 2013). Another example of a reservoir host are the rodents that carried the black plague in the classic outbreak of 1346-1352 (Ligon 2006). Rodents are the reservoir host of the bacterium (*Yersinia pestis*), and fleas are the vectors that transmitted the pathogen to humans. This disease resulted in the death of one third of the world population at the time (Ligon 2006).

Although less prominent in disease literature, reptiles can also act as potential reservoirs for zoonotic pathogens (Ramos *et al.*, 2019). For example, antibodies for *Flaviviridae* viruses such as the Japanese Encephalitis Virus (JEV) and St Louis encephalitis, that can infect humans, have been serologically detected in turtles and snakes — indicating previous infection (Whitney *et al.*, 1968; Lee 1968; Shortridge *et al.*, 1975; Ariel 2011).. A study by Klenk *et al.*, (2004) found that juvenile alligators (*Alligator mississippiensis*) are a competent host for West Nile Virus (a zoonosis) and had a longer amplification cycle (greater than two weeks) than birds (maximum seven days) which were previously thought to be the only reservoir host. The transmission cycle of West Nile Virus is not exclusive to the larger reptiles either, experimental transmission studies have detected WNV viremia titers in lizards (Green Iguanas (*Iguana iguana*), Western Fence-Lizards (*Sceloporus occidentalis*), and Red-Ear Sliders (*Trachemys scripta elegans*) (Klenk and Komar 2003; Steinman *et al.*, 2006; Reisen *et al.*, 2007; Marschang 2011; Machain-Williams *et al.*, 2013; Dahlin *et al.*, 2016). Future research may discover other reptiles are component reservoirs for WNV which could help explain where the virus overwinters when the vectors (mosquitos and ticks) are not active West Nile virus and Japanese Encephalitis virus are just two examples of diseases with severe consequences when they infect humans, but where a reptile could act as reservoirs for the disease. Diseases of this nature have driven the increase in studies of viruses in reptiles and the reptile immune system (Ariel 2011; Marschang *et al.*, 2021). Additionally, the complex eco-epidemiology of WNV in the wild, with its ability to infect multiple taxa, is



the perfect example of why host-pathogen interactions should be investigated when new viruses emerge. However, spillover events are not the only concern. Cross-species infection from a widely distributed common species, to an endangered species are also a conservation concern.

Recently, a novel nidovirus has been discovered in a lizard. Globally, this is the first ever case of a nidovirus reported in lizards. The virus has been associated with a severe upper respiratory infection in its host, the sleepy lizard (*Tiliqua rugosa*) (O’Dea *et al.*, 2016).

Mortality rates in wild populations are unconfirmed but are anecdotally reported as high. As this is a relatively newly discovered virus, there are many unknowns that need to be addressed. Systematic virology, the study of the host and its response to infection, provides an excellent framework for investigating these unknowns. This review provides the groundwork for developing such a study, commencing the discussion with the broad concepts related to disease and immunity, before exploring a specific system.

This review first introduces disease immunity at a cellular level before exploring the two types of immune systems, innate and adaptive, at both a cellular and genetic level. The review then focuses on the reptile immune system, highlighting key areas that need to be understood when researching virology in this system, and what these mean in relation to reptile defence against disease. Finally, I focus on the novel nidovirus and the associated disease, where I identify unknowns and the future research needed to address these.

Main Body

Disease Immunity

The immune systems are a defence mechanism that has evolved in all multicellular organisms to combat pathogens or material that could harm an individual (Boehm 2012; Bailey 2013). Immunity to disease is important for the survival of an individual, population, or species. There are two broad, but interconnected, types of immune system—innate and adaptive (Medzhitov and Janeway 1998; Delves and Roitt 2000; Medzhitov and Janway 2000; Boehm 2012; Riera Roma *et al.*, 2016). The innate immune system is non-specific and attacks anything deemed foreign, from pathogens to particulates (Medzhitov and Janway 2000; Kasuga *et al.*, 2021). The adaptive is more specific and responds more quickly than the innate in cases of reinfection (Viver *et al.*, 2011). The adaptive generates a specific antibody



for a specific pathogen. The retention of these antibodies effectively serves as “memory”, enabling the rapid identification and response to specific pathogens when reinfected (Vivier *et al.*, 2011; Engels and Wienands 2018). This rapid response can reduce the severity of infection, or even eliminate it altogether.. Invertebrates have only innate immune systems, while vertebrates, including reptiles, have both innate and adaptive immune systems (Bailey 2013; Zimmerman 2010a; Zimmerman 2016).

Understanding the immune system at both a genetic and mechanistic cellular level can increase the efficacy of medical treatments (Shanley *et al.*, 2021), and lead to new diagnostic methods (Abraham *et al.*, 2021; Mustafa and Makhawi, 2021) even when the responsible agent has yet to be identified. For example, if a serological assay indicates higher than normal levels of antibodies it can be inferred that a pathogen is influencing its host despite the cause of this immune response being unknown (Crowther 2002). Further, by comparing healthy and sick individuals’ immune genes, we can understand the host’s genetic adaptations to disease (Patterson and Germolec 2006; Osterlund *et al.*, 2012).

Innate and Adaptive Immune Response

The innate immune system is the host’s first line of defence against pathogens (Romo *et al.*, 2016). The first component in defence is physical barriers to prevent pathogens from entering the host’s skin such as mucous membranes, and even the stomach. The innate system also has cells called leukocytes, to combat pathogens that pass through these physical barriers. There are multiple types of leukocytes including, but not limited to, macrophages and dendritic cells—each playing a specific role in overcoming infection. Dendritic cells are the stimulators of the adaptive response, whereas the macrophages are the heavy lifters, controlling inflammatory responses, increasing the number of other leukocytes at the infection site, phagocytosing antigens, and then downregulating the response afterwards to prevent tissue damage (Banchereau and Steinman 1998; Arango Duque and Descoteaux 2014).

Another type of innate defence are protein molecules on the surfaces of cells called Pattern Recognition Receptors (PRRs). These detect unique structures on pathogens called pathogen associated molecular patterns (PAMPs) (Kumar 2011; Kawai and Akira 2011). There are four types of pattern recognition receptors, Toll-like receptors (TLR), C-type lectin receptors



(CLR), RIG-like receptor (RLR), and Nod-like receptors (NLR), each recognising different types of PAMPs. Toll-like receptors detect viral nucleic acids and bacterial lipoproteins (Xia *et al.*, 2021). C-type lectin receptors recognise carbohydrates of fungi and viruses and are expressed on monocytes and macrophages and dendritic cells, neutrophils, B and T-cells (Kumar 2011; Iwasaki and Medzhitov 2010). Retinoic acid-inducible gene-I-like receptors are also sensors of viral infections that reside in the cytosol of cells. NOD-cytosolic receptors are also in the cytosol, however, they detect bacterial infection.

Previously, it was thought that the innate system was separate from the adaptive, however, we now know that they work in conjunction (Medzhitov 2000). The adaptive immune system is triggered after an innate response is initiated. While the innate system is non-specific, the adaptive system responds to specific antigens once the innate macrophages and dendritic cells have broken down the pathogen and presented it to the adaptive response (Delves and Roitt 2000). The adaptive system has two types of responses, cell mediated and humeral. Cell mediated is detection and response within the cell, and the humeral response protects the extracellular spaces. The key components involved in the adaptive system are two types of lymphocytes (subset of leucocytes), B-cells and T-cells, with T-cells comprising of cytotoxic T-cells (TC) and helper T-cells (TH) (Delves and Roitt 2000). Cytotoxic T-cells have one job, to target virally infected cells (or tumours) and kill them (Akdis 2011; Arango Duque and Descoteaux 2014). Helper T-cells boost the response of the immune systems, and B-cells produce specific antibodies. In addition to the T- and B-cells, PRR's are a crucial part of the adaptive system (Takeuchi and Akira 2010). These are molecules located on the surface of all cells that identify antigens, binding to them before signalling the T-cells for cell destruction (Bailey *et al.*, 2013; Rierra Romo *et al.*, 2016).

The Major Histocompatibility Complex (MHC) is one such PRR. It is a protein molecule on the surface of every nucleic cell (Knapp 2005; Sommer 2005). The genes of MHC are one of the most polymorphic regions known and it plays a key role in the adaptive immune system in all jawed vertebrates. Major Histocompatibility Complex class I is intracellular and identifies viruses, tumours, and sometimes self-peptides (autoimmune disease) (Bonneaud 2005; Beouwer 2010). MHC class II is extracellular and involves identification of bacteria. There are a number of studies on the MHC of most taxa, which discuss the role of MHC, from kinship



avoidance to pathogen recognition, as well as the mechanisms involved with recognising continuously evolving pathogens (Lewis 1998; Zelano, *et al.*, 2002; Bernatchez *et al.*, 2003; Spurgin and Richardson 2010; Ujvari and Belov 2011; Jones *et al.*, 2015).

The process, wherein the innate and adaptive systems work conjointly to fight infection, can be broadly described as follows. The innate system detects a foreign pathogen that macrophages and neutrophils/dendritic respond to, causing local inflammation. The leucocytes firstly 'stick' to the pathogen preventing cell penetration and secondly, to engulf the pathogen before breaking it down (Delves and Roitt 2000). In dendritic cells, a peptide of the pathogen is then taken up and presented on the surface of the cells by the protein molecule MHC class I. This in turn triggers a cytotoxic T-cell to destroy the infected cell. It is important to note, that both B and T cells need to be activated by antigen presenting cells before they become specific to a particular antigen. Before this, they are 'naïve' cells that are not specific. That is why there is some time delay in the adaptive response to an unknown pathogen, whereas reinfection has a much faster adaptive response, as specific T and B-cells have already been activated for that particular pathogen (Riera Romo *et al.*, 2016).

Non-avian Reptile Immune System

The reptile immune system is functionally the same as mammals in that they have both innate and adaptive immune systems (Zimmerman *et al.*, 2010b; Zimmerman 2016). The reptile innate immune system contains non-specific leukocytes, lysozymes, and antimicrobial peptides. Identified leukocytes in reptiles are similar to mammals with monocytes, heterophiles, basophils and eosinophils. The function of these cells is the same in both non-avian reptiles and mammals (Montali 1988; Zimmerman 2010a; Zimmerman 2016; Ghorai *et al.*, 2018). The innate immunity of reptiles is strong and broad (Zimmerman 2010a). However, the reptile adaptive immune system is slow in comparison to the mammals. In fact, it takes six – eight weeks for antibody levels to peak after primary response (Zimmerman 2016). Antibodies from the primary response have also been detected up to 34 weeks (Origgi *et al.*, 2001) — whereas mammals peak antibody levels are reached around one week from infection (Zimmerman 2010a). There are two major differences that non-



avian reptiles have compared with mammals that could explain such a comparatively slow response. These differences are in the lymph and the thermoregulatory systems.

First, reptiles do not have lymph nodes to transport the immune response around the organism. However, they do have lymphoid tissue – spleen, thymus, and bone marrow – where T-cell maturation takes place for the adaptive immune system (Zimmerman 2010; Rios and Zimmerman 2015). Hussein *et al.*, (1978) showed the importance of these organs when the removal of partial or total organs resulted in a lower humeral response.

The second major difference when considering reptile immunology, is thermoregulation. Mammals innately thermoregulate their bodies, and in response to pathogens raise the temperature (fever), whereas reptiles cannot (Zimmerman 2016). Instead, non-avian reptiles behaviourally raise their body temperatures by moving into the sun and basking for longer periods of time (Rakus *et al.*, 2017). The importance of this becomes apparent when you consider the biological processes of ectotherms slows right down when cold, and this includes the immune response (Brames 2007). This reduction in response could result in higher susceptibility to infection and disease. In fact, one hypothesis suggests the evolution of the energetically costly strategy of thermoregulation in endotherms is in response to pathogens (Logan 2019).

This temperature dependent immune response also makes diagnostic tools for screening complicated. Diagnostic tools such as immunological assays, use different types of antibodies and titre levels – depending on the assay – to indicate current infection or previous infection (Crowther 2002; Jacobson and Origgi 2002; Wang *et al.*, 2018). However, it becomes troublesome to determine infection in an understudied and wild species when not only the levels of specific antibodies are temperature dependent, but the types of antibodies might be different as well. Mammals have five different immunoglobulin isotypes, IgG, IgA, IgD, IgE, and IgM, each with their own shape and purpose. For example, IgM eliminates pathogens in the early stages of the humeral response before IgG levels reach peak levels, while IgG plays a key role that provides the majority of antibody defence against pathogens (Abadi and Pirofski 1998). However, most reptiles have only three types of immunoglobulins, IgM, IgD, and IgY (Zimmerman *et al.*, 2010a; Pettinello and Dooley 2014). While IgM and IgD are functionally the same as their mammalian counterparts, the



reptilian IgY has been proposed to be the precursor to the mammalian IgG and IgE (Ghorai-Pruiam 2018). There have been some studies that have found some of the other types of immunoglobulins (IgA, and IgE) in certain types of squamates and it appears to be species dependent (Wei *et al.*, 2009; Deza and Espinel 2008; Zimmerman 2016).

The study of non-avian reptiles has largely been neglected in comparison to that of other more economically valuable species. Of the four reptilian classes, Crocodylia, Sphenodontia, Squamata, and Testudines, the few studies that look at reptile immune systems are largely limited to Crocodylia and Testudines. A review by Zimmerman (2010a), found that only 20 percent of the literature on reptile immune systems were of Squamata. Considering Squamata is the largest order of reptiles, there are still a lot of unknowns with regards to immune defence against pathogens which should be addressed, as Squamates play an important role in ecosystems as both prey and predator species.

Species of focus – *Tiliqua rugosa*

Life History

Tiliqua rugosa are a common long-lived skink, with records of lizards older than 40 years in the wild. They are a relatively large, slow-moving reptile, with the average Snout-to-Vent Length (SVL) for an adult greater than 30cm (Bull 1987). *Tiliqua rugosa* have a relatively wide home range of 400m and exhibit complex sociality, monogamy, often returning to the same mate every year (Bull and Freake 1999; Bull 2000). *Tiliqua rugosa* spend only six to eight weeks in mating pairs during springtime and spend the rest of the year alone (Bull 2000).

Complex sociality has been shown to have multiple benefits for populations, such as predator defence and shared parental care (Krause and Ruxton 2002). However, this level of sociality also comes at a cost. There is increased risk of infection from disease and parasite transmission (May & Anderson 1987; Read & Keeling 2003; Hughes *et al.*, 2002). During times of social interaction, such as mating season, paired *T. rugosa* share refuges under Mallee scrub and blue bush, where they pass on parasites and pathogens (Bull *et al.*, 2012).



Parasites, Pathogens, and Disease of Tiliqua rugosa

Tiliqua rugosa are commonly infested with both ectoparasites (ticks), and endoparasites (nematodes, helminths, and blood parasites)(Norval *et al.*, 2019). These parasites can spread pathogens that cause disease (Norval *et al.*, 2019; Staines *et al.*, 2020). Ticks are an ectoparasite with a four-stage life cycle – egg, larvae, nymph, and adult. Each stage they attach to a new lizard, this means one tick will come into contact with three lizards by the time it is an adult. Pathogens therefore have the potential to spread widely. Interestingly, ticks also have the ability to transmit pathogens and blood parasites not just horizontally but also vertically, mother to offspring, by storing pathogens in ovaries and passing on to the next clutch (Brossard and Wikel 2005; Kwan *et al.*, 2017).

Generally, these parasites do not affect the overall health of the *T. rugosa* (Norval *et al.*, 2019). However, over infestation can start to take a toll, resulting in reduced movement capabilities, reduced mating fitness, and anaemia (Smallridge and Bull 1999; Smallridge and Bull 2000; Bouma *et al.*, 2007). To date, however, there is only one major disease recorded that severely affects this species, and that is the bobtail flu. There is a detailed review by Norval *et al.*, (2019), of parasites that infect *T. rugosa*. I, therefore, briefly discuss common parasites that infest *T. rugosa*, and their overall impact on this host.

The most heavily researched parasites of *T. Rugosa* are ticks; *Amblyomma limbatum* and *Bothriocroton hydrosauri* (Bull *et al.*, 1981; Godfrey and Gardner 2017). Previous research has examined aspects of the effects of two species of ticks on the *T. rugosa* host, at a study site near Mount Mary, SA (- 33.886041, 139.354746) over the last 40 years (Godfrey and Gardner 2017). Their distributions abut and form a parapatric boundary that is concordant with an ecological gradient (Bull *et al.*, 1989; Bull and Possingham 1995).

Tiliqua rugosa also acts as an intermediate host for a micro parasite, *Hemolivia mariae*. *Hemolivia mariae* is a blood parasite that commonly infects these two tick species as definitive invertebrate hosts, while having the ability to then infect *T. rugosa* as an intermediate vertebrate host (Smallridge and Bull 1999). A study by Smallridge and Bull (2000) showed *H. mariae* transmitted from infected tick to lizards, with a prevalence of 11.5%. Body condition loss was significantly correlated with infected males, while infected



females had no significant correlation. This reduced body condition and consequently, reduced mate fitness. Recently, it was found that an intracellular bacterial parasite known as *Rickettsia* spp., of the spotted fever group strain, were found in 83% of *B. hydrosauri* whereas no *A. limbatum* were infected (Staines *et al.*, 2020). It is yet unknown how these susceptibility differences across the ecological gradient influence *T. rugosa*.

The major disease *T. rugosa* has been reported to suffer from, the 'Bobtail flu', has been observed since the early 1990's. There is limited peer reviewed literature on the Bobtail flu, only veterinary reports as early as 1990, and predominantly from Kanyana Wildlife Rehabilitation Centre in Perth. In 2004 Kanyana were awarded a 64-thousand-dollar grant to set up a facility specifically for the sick *T. rugosa*, as the intake numbers were around 200 a year (Kanyana Annual Report 2014-15). Mortality rates of untreated *T. rugosa*, in the wild, are unknown but are suspected to be high. This disease is an Upper Respiratory Tract Infection (URTI), inhibiting normal respiratory function. Symptoms present as sneezing; wheezing; lethargy; serous to mucopurulent discharge from eyes and nose, resulting in vision impairment; loss of appetite; and loss of body condition (O'Dea *et al.*, 2016). Death can occur as a result of suffocation, where the glottis is blocked by mucus. Treatment involves using both a broad-spectrum antibiotic (Enrofloxacin) and antiprotozoal (Metronidazole), in conjunction with oral rehydration, resulting in an 84% survival rate (O'Dea *et al.*, 2016). Treatment for six weeks is recommended, or re-infection is suggested to be likely. This coincides with what is known of reptile's slow immune response, where antibodies reach peak levels around 6-8 weeks (Wetherall and Turner, 1972; Zimmerman *et al.*, 2010a). It is interesting that a combination of antibiotics and antiprotozoal medication are used to treat a respiratory infection associated with a virus. It is likely used as a preventative of potential secondary infections—along with regular rehydration—until the respiratory disease had been overcome by the slow reptile immune system.

In 2011, research was conducted using PCR to determine potentially infectious agents as the cause of this URTI. Doctors Mark Bennett, Tim Hyndman, and student Brett de Poister associated with Murdoch University, specifically looked at herpesviruses and adenoviruses, possibly because they are common viruses in other reptiles. However, they met with little success (Moller, 2014). It was not until 2016, with the help of next generation sequencing



technologies that the shingleback nidovirus was identified – and associated with the disease (O’Dea *et al.*, 2016).

Shingleback nidovirus 1

The *Shingleback nidovirus 1* (ShNV) was the first virus known to affect *T. rugosa* and also the first nidovirus ever discovered in a lizard. It was initially characterised in the *Coronaviridae* family – the same family as the Severe Acute Respiratory Syndrome (SARS) – although, in the subfamily *Torovirinae*. The *Shingleback nidovirus 1* was placed within a relatively new genus (at the time) coined *Barnivirus* (Figure 1) (O’Dea *et al.*, 2016; Zhang *et al.*, 2018). The genus was first proposed by Stenglein *et al.*, (2014) after the discovery of the Ball Python Nidovirus (BPNV) and was distinct from the genus *Torovirus* and *Bafinivirus* (Figure 1). The genus then expanded to include six distinct viruses; *Ball python nidovirus*; *Ball python nidovirus 1*; *Morelia viridis nidovirus*; *Python nidovirus*; *Bellinger river virus*; and the *Shingleback nidovirus 1* (Figure 1) (Stenglein *et al.*, 2014; Bodewes *et al.*, 2014; Uccellini *et al.*, 2014; O’Dea *et al.*, 2016; Dervas *et al.*, 2017; Zhang *et al.*, 2018). However, these reptile nidoviruses were later reclassified into the family *Tobaniviridae*, subfamily *Serpentovirinae* by the International Committee on Taxonomy of Viruses (Dervas *et al.*, 2020, Parrish *et al.*, 2021, Walker *et al.*, 2019).

Virus isolation of the *Shingleback nidovirus 1* has so far been unsuccessful. However, because of the molecular phylogenetics we can interpret the shape and structure of this virus (O’Dea *et al.*, 2016). The partially characterised viral contig is 23,832 nt in length, which is just short of the characteristic length of its subfamily (26-32kb) (Gorbalenya *et al.*, 2006; King *et al.*, 2012). The virus is a (+) single strand RNA, in a capsid envelope with spiked epitopes, a standard form of viruses from the *Nidovirales* order (Gorbalenya *et al.*, 2006; King *et al.*, 2012). It is these spiked epitopes that mediate virus attachment to the host cell-surface receptors, and which host antibodies bind to before triggering further immune responses. It is not yet known the extent that the *Shingleback nidovirus 1* contributes to the bobtail flu as 12 % of infected individuals were asymptomatic, and not all lizards displaying clinical symptoms were positive for the virus (O’Dea *et al.*, 2016). It has also been suggested that an Adenovirus co-contributes to the disease (Hyndman and Shilton 2018). It is likely that



therefore multiple hosts are plausible (Ahlquist *et al.*, 2003; Woolhouse and Gowtage-Sequeria 2005; Elena *et al.*, 2009). This is concerning as the *T. rugosa* distribution in South Australia, overlaps with the closely related and endangered *Tiliqua adelaidensis* (Pygmy bluetongue) (Cogger 2014, Smith *et al.*, 2009). We do not know if there are other viruses that commonly infect this species, although it is very likely there are. We do not know the pathogenesis of this virus — only assumptions based on closely related viruses and observations in veterinary clinics (Stenglein *et al.*, 2014; Zhang *et al.*, 2018). We do not know how the virus affects the host genetically. Immune response genes like MHC class I, and Interferon type I, are known to evolve over time to detect viruses, while viruses evolve to become undetectable (Acevedo-Whitehouse & Cunningham 2006; Spurgin and Richardson 2010). Therefore, selective viral pressures could impact population structure of the host. The aim of this PhD is to address some of these unknowns.



References

- Abadi J., Pirofski L. (1998). Isotype. In: Delves PJ, editor. *Encyclopedia of Immunology* (Second Edition). Oxford: Elsevier. P. 1514-1516.
- Abraham R.S. and Butte, M.J. (2021). The new “wholly trinity” in the diagnosis and management of inborn errors of immunity. *The Journal of Allergy and Clinical Immunology: In Practice*. **9(2)**: 613-625
- Acevedo-Whitehouse K., Cunningham A.A. (2006). Is MHC enough for understanding wildlife immunogenetics? *Trends in Ecology and Evolution*. **21**:433-438.
- Ahlquist P., Noueiry A.O., Lee W-M., Kushner D.B., Dye B.T. (2003). Host factors in positive-strand RNA virus genome replication. *Journal of Virology* **77**:8181-8186.
- Ajith Kumar K.G., Ravindran R., Johns J., Chandy G., Rajagopal K., Chandrasekhar L., George A.J., Ghosh S. (2018). Ixodid Tick Vectors of Wild Mammals and Reptiles of Southern India. *Journal of arthropod-borne diseases* **12**:276-285.
- Akdis M., Burgler S., Cramer R., Eiwegger T., Fujita H., Gomez E., Klunker S., Meyer N., O’Mahony L., Palomares O. (2011). Interleukins, from 1 to 37, and interferon- γ : Receptors, functions, and roles in diseases. *Journal of Allergy and Clinical Immunology* **127**:701-721.
- Anderson J.F. (1989). Epizootiology of Borrelia in Ixodes Tick Vectors and Reservoir Hosts. *Clinical infectious diseases* **11**: S1451-S1459.
- Arango Duque G., Descoteaux A. (2014). Macrophage cytokines: involvement in immunity and infectious diseases. *Frontiers in Immunology* **5**:491-491.
- Ariel E. (2011). Viruses in reptiles. *Veterinary Research* **42**:100.
- Bailey M, Christoforidou Z, Lewis M. 2013. Evolution of immune systems: Specificity and autoreactivity. *Autoimmunity Reviews* **12**:643-647.
- Banchereau J., Steinman R.M. (1998). Dendritic cells and the control of immunity. *Nature* **392**:245-252.
- Beiki H., Liu H., Huang J., Manchanda N., Nonneman D., Smith T.P.L., Reecy J.M., Tuggle C.K. (2019). Improved annotation of the domestic pig genome through integration of Iso-Seq and RNA-seq data. *BMC genomics* **20**:344.
- Berg T.P.V.D. (2000). Acute infectious bursal disease in poultry: A review. *Avian Pathology* **29**:175-194.
- Bernatchez L., Landry C. (2003). MHC studies in nonmodel vertebrates: what have we learned about natural selection in 15 years? *Journal of evolutionary biology* **16**:363-377.
- Bodewes R., Lempp C., Schürch A.C., Habierski A., Hahn K., Lamers M., von Dörnberg K., Wohlsein P., Drexler J.F., Haagmans B.L. (2014). Novel divergent nidovirus in a python with pneumonia. *Journal of General Virology* **95**:2480-2485.
- Boehm T. (2012). Evolution of Vertebrate Immunity. *Current Biology* **22**: R722-R732.
- Bonneaud C., Richard M., Faivre B., Westerdahl H., Sorci G. (2005). An MHC class I allele associated to the expression of T-dependent immune response in the house sparrow. *Immunogenetics* **57**:782-789.
- Bossart G.D., Romano T.A., Peden-Adams M.M., Schaefer A.M., Rice C.D., Fair P.A., Reif J.S. (2019). Comparative Innate and Adaptive Immune Responses in Atlantic Bottlenose Dolphins (*Tursiops truncatus*) With Viral, Bacterial, and Fungal Infections. *Frontiers in Immunology* **10**.



- Bouma M.J., Smallridge C.J., Bull C.M., Komdeur J. (2007). Susceptibility to infection by a haemogregarine parasite and the impact of infection in the Australian sleepy lizard *Tiliqua rugosa*. *Parasitology research* **100**:949-954.
- Brames H. (2007). Aspects of Light and Reptilian Immunity. *Iguana* **14**:1
- Brito B.P., Rodriguez L.L., Hammond J.M., Pinto J., Perez A.M. (2017). Review of the Global Distribution of Foot-and-Mouth Disease Virus from 2007 to 2014. *Transboundary and Emerging Diseases* **64**:316-332.
- Brooker M. (2016). Bobtail skink (*Tiliqua rugosa*) observations on the Darling Scarp, Perth, Western Australia, 1985-2015. **30**:131-147.
- Brouwer L., Barr I., Van De POL M., Burke T., Komdeur J., Richardson D.S. (2010). MHC-dependent survival in a wild population: evidence for hidden genetic benefits gained through extra-pair fertilizations. *Molecular Ecology* **19**:3444-3455.
- Bull C., Burzacott D., Sharrad R. (1989). No competition for resources between two tick species at their parapatric boundary. *Oecologia* **79**:558-562.
- Bull C., Sharrad R., Petney T. (1981). Parapatric boundaries between Australian reptile ticks. *The Proceedings of the Ecological Society of Australia* **11**:95-107.
- Bull C.M. (2000). Monogamy in lizards. *Behavioural Processes* **51**:7-20.
- Bull C.M. (1987). A population study of the viviparous Australian lizard *Trachydosaurus rugosa* (Scincidae). *Copeia* **3**: 749-757.
- Bull C.M., Burzacott D. (2001). Temporal and spatial dynamics of a parapatric boundary between two Australian reptile ticks. *Molecular Ecology* **10**:639-648.
- Bull C.M., Godfrey S.S., Gordon D.M. (2012). Social networks and the spread of *Salmonella* in a sleepy lizard population. *Molecular Ecology* **21**:4386-4392.
- Bull C.M., Possingham H. (1995). A model to explain ecological parapatry. *The American Naturalist* **145**:935-947.
- Cádiz A., Reytor M.L., Díaz L.M., Chestnut T., Burns J.A., Amato G. (2019). The Chytrid Fungus, *Batrachochytrium dendrobatidis*, is Widespread Among Cuban Amphibians. *EcoHealth* **16**:128-140.
- Crowther J.R. (2002). In The ELISA guidebook: Validation of Diagnostic Tests for Infectious Diseases, Chapter 8. Humana Press, Totowa, New Jersey, **42**: 301-347.
- Dahlin C.R., Hughes D.F., Meshaka W.E., Coleman C., Henning J.D. (2016). Wild snakes harbor West Nile virus. *One Health* **2**:136-138.
- Delves P.J., Roitt I.M. (2000). The Immune System. *New England Journal of Medicine* **343**:37-49.
- Dervas E., Hepojoki J., Laimbacher A., Romero-Palomo F., Jelinek C., Keller S., Smura T., Hepojoki S., Kipar A., Hetzel U. (2017). Nidovirus-Associated Proliferative Pneumonia in the Green Tree Python (*Morelia viridis*). *Journal of Virology* **91**.
- Deza F.G., Espinel C.S., Beneitez J.V. (2007). A novel IgA-like immunoglobulin in the reptile *Eublepharis macularius*. *Development and Comparative Immunology*. **31**: 596–605.
- Durmuş S., Ülgen K.Ö. (2017). Comparative interactomics for virus-human protein-protein interactions: DNA viruses versus RNA viruses. *FEBS open bio* **7**:96-107.
- Elena S.F., Agudelo-Romero P., Lalić J. (2009). The evolution of viruses in multi-host fitness landscapes. *The open virology journal* **3**:1-6.
- ESRI (2011). ArcGIS Desktop: Release 10. Redlands, CA: Environmental Systems Research Institute.



- Engels N., Wienands J. (2018). Memory control by the B cell antigen receptor. *Immunological Reviews* **283**:150-160.
- Ghorai S.M., Priyam M. (2018). Reptilia: Cellular Immunity in Reptiles: Perspective on Elements of Evolution. In: Cooper EL, editor. *Advances in Comparative Immunology*. Cham: *Springer International Publishing*. P. 773-791.
- Godfrey S.S., Ansari T.H., Gardner M.G., Farine D.R., Bull C.M. (2014). A contact-based social network of lizards is defined by low genetic relatedness among strongly connected individuals. *Animal Behaviour* **97**:35-43.
- Godfrey S. S. and Gardner M.G. (2017). Lizards, ticks and contributions to Australian parasitology: C. Michael Bull (1947–2016). *International Journal for Parasitology: Parasites and Wildlife* **6**:295-298.
- Gorbalenya A.E., Enjuanes L., Ziebuhr J., Snijder E.J. (2006). Nidovirales: Evolving the largest RNA virus genome. *Virus Research* **117**:17-37.
- Grover A., Joshi A. (2014). An overview of chronic disease models: a systematic literature review. *Global journal of health science* **7**:210-227.
- Hughes W.O., Eilenberg J., Boomsma J.J. (2002). Trade-offs in group living: transmission and disease resistance in leaf-cutting ants. *Proceedings of the Royal Society of London B: Biological Sciences* **269**:1811-1819.
- Hussein M.F., Badir N., El Ridi R. Akef, M. (1978). Effect of seasonal variation on lymphoid tissues of the lizards, *Mabuya Quinquetaeniata* licht and *Uromastix aegyptia* forsk. *Development and Comparative Immunology*. **2**: 469-478.
- IBM Corp. Released (2017). IBM SPSS Statistics for Windows, Version 25.0. Armonk, NY: IBM Corp.
- Jacobson E.R., Origgi F. (2002). Use of serology in reptile medicine. *Seminars in Avian and Exotic Pet Medicine* **11**:33-45.
- Jones M.R., Cheviron Z.A., Carling M.D. (2015). Spatially variable coevolution between a haemosporidian parasite and the MHC of a widely distributed passerine. *Ecology and Evolution* **5**:1045-1060.
- Kanyana Wildlife Centre. 2014–2015 Annual Report. Perth, WA: Kanyana Wildlife Centre; 2015.
- Kaplan A.J., Stacy N.I., Jacobson E., Le-Bert C.R., Nollens H.H., Origgi F.C., Green L.G., Booterabi S., Bolten A., Hernandez J.A. (2015). Development and validation of a competitive enzyme-linked immunosorbent assay for the measurement of total plasma immunoglobulins in healthy loggerhead sea (*Caretta caretta*) and green turtles (*Chelonia mydas*). *Journal of Veterinary Diagnostic Investigation* **28**:5-11.
- Kasuga Y., Zhu B., Jang K.J., Yoo J.S. (2021). Innate immune sensing of coronavirus and viral evasion strategies. *Experimental & molecular medicine*. **53(5)**: 723-736
- Kawai T., Akira S. (2011). Toll-like Receptors and Their Crosstalk with Other Innate Receptors in Infection and Immunity. *Immunity* **34**:637-650.
- King A.M.Q., Adams M.J., Carstens E.B., Lefkowitz E.J., editors (2012). Order – Nidovirales. Virus Taxonomy. *Elsevier*. P. 784-794.
- Kirk M.D., Pires S.M., Black R.E., Caipo M., Crump J.A., Devleeschauwer B., Döpfer D., Fazil A., Fischer-Walker C.L., Hald T. (2015). World Health Organization Estimates of the Global and Regional Disease Burden of 22 Foodborne Bacterial, Protozoal, and Viral Diseases, 2010: A Data Synthesis. *PLOS Medicine* **12**: e1001921.



- Klenk K., Snow J., Morgan K., Bowen R., Stephens M., Foster F., Gordy P., Beckett S., Komar N., Gubler D. (2004). Alligators as West Nile virus amplifiers. *Emerging infectious diseases* **10**:2150-2155.
- Klenk K., Komar N. (2003). Poor replication of West Nile virus (New York 1999 strain) in three reptilian and one amphibian species, *American Journal of Tropical Medicine*. **69**:260–262
- Knapp L.A. (2005). The ABCs of MHC. *Evolutionary Anthropology: Issues, News, and Reviews* **14**:28-37.
- Kock R.A., Orynbayev M., Robinson S., Zuther S., Singh N.J., Beauvais W., Morgan E.R., Kerimbayev A., Khomenko S., Martineau H.M. (2018). Saigas on the brink: Multidisciplinary analysis of the factors influencing mass mortality events. *Science Advances* **4**:eaao2314.
- Krause J., and Ruxton G.D. (2002). Living in groups. Oxford: Oxford University Press
- Kumar H., Kawai T., Akira S. (2011). Pathogen Recognition by the Innate Immune System. *International Reviews of Immunology* **30**:16-34.
- Kwan J.Y., Griggs R., Chicana B., Miller C., Swei A. (2017). Vertical vs. horizontal transmission of the microbiome in a key disease vector, *Ixodes pacificus*. *Molecular Ecology* **26**:6578-6589.
- Last J.M. (2001). A dictionary of epidemiology. 4th ed. New York: Oxford University Press,
- Lee H.W. (1968). Multiplication and antibody formation of Japanese encephalitis virus in snakes: proliferation of the virus. *Seoul Journal of Medicine*. **9**:157-161.
- Lewis K. (1998). Pathogen Resistance as the Origin of Kin Altruism. *Journal of Theoretical Biology*. **193**:359-363.
- Ligon B.L. (2006). Plague: A Review of its History and Potential as a Biological Weapon. *Seminars in Pediatric Infectious Diseases* **17**:161-170.
- Michael Logan (2019). Did pathogens facilitate the rise of endothermy? *Ideas in Ecology and Evolution*. **12**:1
- Machain-Williams C., Padilla-Paz M., Weber S.E., Cetino-Trejo R., Juarez-Ordaz J., Lorono-Pino M. (2013). Antibodies to West Nile virus in wild and farmed crocodiles in southeastern Mexico, *Journal of Wildlife Diseases*. **49**
- Marschang R.E. (2011). Viruses infecting reptiles. *Viruses*. **3**:2087–2126.
- Marschang R.E., Meddings J.I., Ariel E. (2021). Viruses of Reptiles. In *Studies in Viral Ecology*, C.J. Hurst (Ed.). <https://doi.org/10.1002/9781119608370.ch13>
- Medzhitov R., Janeway C. (2000). Innate Immunity. *New England Journal of Medicine* **343**:338-344.
- Medzhitov R., Janeway Jr C.A. (1998). Innate immune recognition and control of adaptive immune responses. *Seminars in Immunology* **10**:351-353.
- May R.M., Anderson R.M. (1987). Transmission dynamics of HIV infection. *Nature*. **326**: 137–142.
- Merchant M.E., Pallansch M., Paulman R.L., Wells J.B., Nalca A., Ptak R. (2005). Antiviral activity of serum from the American alligator (*Alligator mississippiensis*). *Antiviral Research* **66**:35-38.
- Miller C.A., Tasse Taboue G.C., Ekane M.M.P., Robak M., Sesink Clee P.R., Richards-Zawacki C., Fokam E.B., Fuashi N.A., Anthony N.M. (2018). Distribution modeling and lineage



- diversity of the chytrid fungus *Batrachochytrium dendrobatidis* (Bd) in a central African amphibian hotspot. *PLoS One* 13:e0199288.
- Moller C.A. (2014). The haematology of bobtail lizards (*Tiliqua rugosa*) in Western Australia: reference intervals, blood cell morphology, cytochemistry and ultrastructure. Master's thesis, Murdoch University, Perth.
- Montali R.J. (1988). Comparative pathology of inflammation in the higher vertebrates (reptiles, birds and mammals). *Journal of Comparative Pathology* 99:1-26.
- Mustafa M.I. and Makhawi A.M. (2021). SHERLOCK and DETECTR: CRISPR-Cas systems as potential rapid diagnostic tools for emerging infectious diseases. *Journal of Clinical Microbiology* 59(3):e00745-20
- Nami S., Aghebati-Maleki A., Morovati H., Aghebati-Maleki L. (2019). Current antifungal drugs and immunotherapeutic approaches as promising strategies to treatment of fungal diseases. *Biomedicine & Pharmacotherapy* 110:857-868.
- Nash D., Mostashari F., Fine A., Miller J., O'Leary D., Murray K., Huang A., Rosenberg A., Greenberg A., Sherman M. (2001). The Outbreak of West Nile Virus Infection in the New York City Area in 1999. *New England Journal of Medicine* 344:1807-1814.
- Norval G., Ross K.E., Sharrad R.D., Gardner M.G. (2019). Taking stock: a review of the known parasites of the sleepy lizard, *Tiliqua rugosa* (Gray, 1825), a common lizard endemic to Australia. *Transactions of the Royal Society of South Australia*. 143:2, 216-234.
- O'Dea M.A., Jackson B., Jackson C., Xavier P., Warren K. (2016). Discovery and Partial Genomic Characterisation of a Novel Nidovirus Associated with Respiratory Disease in Wild Shingleback Lizards (*Tiliqua rugosa*). *PLoS One* 11: e0165209.
- Oliver G.F., Carr J.M., Smith J.R. (2019). Emerging infectious uveitis: Chikungunya, dengue, Zika and Ebola: A review. *Clinical & Experimental Ophthalmology* 47:372-380.
- Österlund P., Strengell M., Sarin L.P., Poranen M.M., Fagerlund R., Melén K., Julkunen I. (2012). Incoming Influenza A Virus Evades Early Host Recognition, while Influenza B Virus Induces Interferon Expression Directly upon Entry. *Journal of Virology* 86:11183-11193.
- Patterson R.M., Germolec D.R. (2006). Gene Expression Alterations in Immune System Pathways following Exposure to Immunosuppressive Chemicals. *Annals of the New York Academy of Sciences* 1076:718-727.
- Pérez-Molina J.A., Molina I. (2018). Chagas disease. *The Lancet* 391:82-94.
- Pettinello R D.H. (2014). The Immunoglobulins of Cold-Blooded Vertebrates. *Biomolecules* 4:1045-1069.
- R Core Team. (2013). R: a language and environment for statistical computing. Vienna, Austria: R Foundation for Statistical Computing.
- Rakus K., Ronsmans M., Vanderplasschen A. (2017). Behavioural fever in ectothermic vertebrates. *Developmental & Comparative Immunology* 66:84-91.
- Ramos C.P., Santana J.A., Morcatti Coura F., Xavier R.G.C., Leal C.A.G., Oliveira Junior C.A., Heinemann M.B., Lage A.P., Lobato F.C.F., Silva R.O. (2019). Identification and Characterization of *Escherichia coli*, *Salmonella* Spp., *Clostridium perfringens*, and *C. difficile* Isolates from Reptiles in Brazil. *BioMed Research International* 2019: 9530732.
- Read J.M., Keeling M.J. (2003). Disease evolution on networks: the role of contact structure. *Proceedings of the Royal Society London. Series B Biological Sciences*. 270: 699–708



- Reisen, W.K. Brault A.C., Martinez V.M, Fang Y., Simmons K., Garcia S. (2007). Ability of transtadially infected *Ixodes pacificus* (Acari: Ixodidae) to transmit West Nile virus to song sparrow or western fence lizards, *Journal Medical Entomology*. **44**:320–327.
- Riera Romo M., Pérez-Martínez D., Castillo Ferrer C. (2016). Innate immunity in vertebrates: an overview. *Immunology* **148**:125-139.
- Sartorius N. (2006). The three aspects of malady. *Croatian medical journal* **47**:350-351.
- Scheele B.C., Pasmans F., Skerratt L.F., Berger L., Martel A.N., Beukema W., Acevedo A.A., Burrowes P.A., Carvalho T., Catenazzi A., De la Riva I. (2019). Amphibian fungal panzootic causes catastrophic and ongoing loss of biodiversity. *Science* **363(6434)**: 1459-1463
- Skerratt L.F., Berger L., Speare R., Cashins S., McDonald K.R., Phillott A.D., Hines H.B., Kenyon N. (2007). Spread of chytridiomycosis has caused the rapid global decline and extinction of frogs. *EcoHealth* **4**:125-134.
- Shanley L.C., Mahon O.R., Kelly D.J., Dunne, A. (2021). Harnessing the innate and adaptive immune system for tissue repair and regeneration: Considering more than macrophages. *Acta Biomaterialia*. **133**: 208-221
- Shortridge K.F., Oya A., Konayashi M., Yip D.Y. (1975). Arbovirus infections in reptiles: Studies on the presence of Japanese encephalitis virus antibody in plasma of the turtle. *Southeast Asian Journal of Tropical Medicine and Public Health* **6**:161-169.
- Smallridge C.J., Bull C.M. (2000). Prevalence and intensity of the blood parasite *Hemolivia mariae* in a field population of the skink *Tiliqua rugosa*. *Parasitology Resources* **86**:655-660.
- Smallridge C.J., Bull C.M. (1999). Transmission of the blood parasite *Hemolivia mariae* between its lizard and tick hosts. *Parasitology research* **85**:858-863.
- Sommer S. (2005). The importance of immune gene variability (MHC) in evolutionary ecology and conservation. *Frontiers in zoology* **2**:16-33.
- Spurgin L.G., Richardson D.S. (2010). How pathogens drive genetic diversity: MHC, mechanisms and misunderstandings. *Proceedings of the Royal Society of London. Series B, Biological Sciences* **277**:979-988.
- Steinman A., Banet-Noach C., Grinfeld L., Grinfeld L., Aizenberg Z., Lahav D (2006). Experimental infection of common garter snakes (*Thamnophis sirtalis*) with West Nile virus, *Vector Borne Zoonotic Diseases*. **6**:361–368.
- Stenglein M.D., Jacobson E.R., Wozniak E.J., Wellehan J.F.X., Kincaid A., Gordon M., Porter B.F., Baumgartner W., Stahl S., Kelley K. (2014). Ball Python Nidovirus: a Candidate Etiologic Agent for Severe Respiratory Disease in *Python regius*. *mBio* **5(5)**: e01484-14.
- Szabó M., Pinter A., Labruna M. (2013). Ecology, biology and distribution of spotted-fever tick vectors in Brazil. *Frontiers in Cellular and Infection Microbiology* **3**.
- Takeuchi O., Akira S. (2010). Pattern Recognition Receptors and Inflammation. *Cell* **140**:805-820.
- Uccellini L., Ossiboff R.J., de Matos R.E., Morrissey J.K., Petrosov A., Navarrete-Macias I., Jain K., Hicks A.L., Buckles E.L., Tokarz R. (2014). Identification of a novel nidovirus in an outbreak of fatal respiratory disease in ball pythons (*Python regius*). *Virology Journal* **11**:144.



- Ujvari B., Belov K. (2011). Major histocompatibility complex (MHC) markers in conservation biology. *International Journal of Molecular Sciences* **12**:5168-5186.
- Vivier E., Raulet D.H., Moretta A., Caligiuri M.A., Zitvogel L., Lanier L.L., Yokoyama W.M., Ugolini S. (2011). Innate or Adaptive Immunity? The Example of Natural Killer Cells. *Science* **331**:44.
- Wang J., Peng T., Zhang X., Yao K., Ke Y., Shao B., Wang Z., Shen J., Jiang H. (2018). A novel hapten and monoclonal antibody-based indirect competitive ELISA for simultaneous analysis of alternariol and alternariol monomethyl ether in wheat. *Food Control* **94**:65-70.
- Wei Z., Wu Z., Ren L. (2009). Expression of IgM, IgD, and IgY in a reptile, *Anolis carolinensis*. *Journal of Immunology*. **183**: 3858–3864
- Wetherall J., Turner K. (1972). Immune response of the lizard, *Tiliqua rugosa*. *Australian Journal of Experimental Biology and Medical Science* **50**:79-95.
- Whitney E., Jamnback H., Means R., Watthews T.H. (1968) Arthropod-borne virus survey in St. Lawrence County, New York. Arbovirus reactivity in serum from amphibians, reptiles, birds and mammals. *American Journal of Tropical Medicine and Hygiene* **17**:645-650
- Woolhouse M.E.J., Gowtage-Sequeria S. (2005). Host range and emerging and reemerging pathogens. *Emerging infectious diseases* **11**:1842-1847.
- Xia P., Wu Y., Lian S., Yan L., Meng X., Duan Q., Zhu, G. (2021). Research progress on Toll-like receptor signal transduction and its roles in antimicrobial immune responses. *Applied Microbiology and Biotechnology*. **105(13)**: 5341-5355
- Zelano B., Edwards S., xa V. (2002). An Mhc Component to Kin Recognition and Mate Choice in Birds: Predictions, Progress, and Prospects. *The American Naturalist* **160**:S225-S237.
- Zhang H., Jiang J., Wang Z., Chang X., Liu X., Wang S., Zhao K., Chen J. (2011). Development of an indirect competitive ELISA for simultaneous detection of enrofloxacin and ciprofloxacin. *Journal of Zhejiang University. Science. B.* **12**:884-891.
- Zhang J., Finlaison D.S., Frost M.J., Gestier S., Gu X., Hall J., Jenkins C., Parrish K., Read A.J., Srivastava M. (2018). Identification of a novel nidovirus as a potential cause of large scale mortalities in the endangered Bellinger River snapping turtle (*Myuchelys georgesii*). *PLoS One* **13**: e0205209.
- Zimmerman L. (2016). The Immune System in Reptiles. *Encyclopedia of Immunobiology*. In eLS, John Wiley & Sons, Ltd (Ed.)
- Zimmerman L.M., Vogel L.A., Bowden R.M. (2010a). Understanding the vertebrate immune system: insights from the reptilian perspective. *The Journal of Experimental Biology* **213**:661.
- Zimmerman L.M. Paitz R.T., Vogel L.A., Bowden R.M. (2010b). Variation in the seasonal patterns of innate and adaptive immunity in the red-eared slider (*Trachemys scripta*). *The Journal of Experimental Biology* **213**:1477.
- Zipkin E.F., DiRenzo G.V. (2022). Biodiversity is decimated by the cascading effects of the amphibian-killing chytrid fungus. *PLoS Pathog* **18(7)**: e1010624.



Chapter 1: Foreword

Each chapter of this PhD thesis is written as a publishable manuscript as they will be submitted to journals after thesis submission. Chapter 1 outlines how pathogens and parasites influence the host genetics both on a specific gene region, as well as on a genome-wide scale to determine whether selection on a small functional region could possibly affect population structure, and what this could mean for the species in the future. This chapter is in preparation to be submitted to Molecular Ecology.



Chapter 1: Fine scale population structure coincides with a parapatric tick boundary and MHC genotypes in a long-lived monogamous lizard

Robert L. O'Reilly¹, Tessa M. Bradford², Michael P. Schwarz¹, Stephanie S. Godfrey³,
Steven J. B. Cooper⁴, Terry Bertozzi² and Michael G. Gardner¹

¹ Flinders University, SA, Australia

² South Australian Museum, SA 5000, Australia.

³ Department of Zoology, University of Otago, Dunedin, New Zealand

⁴ Australian Centre for Evolutionary Biology and Biodiversity, School of Biological Science,
The University of Adelaide, Adelaide, SA 5005, Australia

Corresponding author: robert.liam.oreilly@gmail.com

Keywords: MHC, Magic genes, DArTSeq, Adaptive divergence, Parasite mediated selection,
Egerniinae



Abstract

Understanding the processes leading to speciation has been a long-standing question in biology. Historically it has been accepted that restriction to gene flow by large geographic barriers is a key contributor to species divergence. However, selective forces such as assortative mating or pathogen mediated selection could overcome gene flow without a geographic barrier, if strong enough. We aimed to assess whether there were selective pressures being applied to the lizard species *Tiliqua rugosa* at a fine scale across a tick parapatric boundary in Mount Mary, South Australia. Group delineations were based on tick species attached to *T. rugosa* at the time of sampling (defined as *Amblyomma limbatum* only present, *Bothriocroton hydrosauri* only present, both tick species present, and no ticks present). We analysed the allele frequencies of the Major Histocompatibility Complex (MHC) class I peptide binding region of *T. rugosa* ($n = 165$) sampled across the site, also testing for selection and deviations from Hardy-Weinberg equilibrium. We also attempted to observe whether these selective forces could be observed on the *T. rugosa*'s ($n = 173$) population structure using genome wide SNPs (DArTseq). We found significant ($p = 0.028$) MHC class I allele frequency variations between those with *B. hydrosauri* and those with both tick species attached to the lizards at the time of sampling. We also found deviations from Hardy-Weinberg equilibrium ($p = 0.038$), and heterozygosity deficiency in the *B. hydrosauri* group. A PCoA analysis on the SNP data found clear separation, although low explained variation, between *T. rugosa* grouped by *A. limbatum* and *B. hydrosauri*. Structure analysis did not show distinct separation in the *T. rugosa*. Future research will combine historical recapture data (~40 years) on *T. rugosa* across the site, to ensure only one tick species has been observed on a lizard when recaptured to give better support to group delineation. These added data combined with deeper sequencing of those lizards may provide better insight into the *T. rugosa*'s population structure and the role of pathogen mediated genetic divergence.



Introduction

Understanding what mechanisms drive species diversification has been a fundamental question in evolutionary biology. Hard geographical barriers (e.g. mountains, rivers) can restrict gene flow, leading to allopatric divergence (Butlin *et al.*, 2008). Reproductive isolation and divergence can also occur without hard geographical barriers (e.g. mountains) leading to sympatric or parapatric speciation (Blanckaert *et al.*, 2020; Grant and Grant 2002; Kautt *et al.*, 2016; Michalak *et al.*, 2001). Parapatric speciation is when subpopulations develop reproductive isolation with some, but not complete, restriction to gene flow (Gavrilets *et al.*, 2000), whereas sympatry occurs when subpopulations diverge with no restriction to gene flow (Dieckmann and Doebeli 1999; Fitzpatrick *et al.*, 2008). Sympatric speciation continues to remain controversial, constantly being debated and redefined (Fitzpatrick *et al.*, 2008; Hollander *et al.*, 2013; Mallet *et al.*, 2009; Michalak *et al.*, 2001; Smadja and Butlin 2011). The debate seems to stem from what is a clear definition of sympatric speciation, what are the important processes influencing the event, and how frequently does it occur? There is a good review by Fitzpatrick *et al.*, (2008). Fitzpatrick *et al.*, (2008) also suggest splitting hairs on what is sympatric or allopatric speciation is less important than evaluating the processes that cause divergence with modelling, assessment of gene flow, and testing for selection, as this will give a better understanding on speciation. In order to diversify when sub-populations are connected via gene flow, genes affecting multiple traits are needed to strengthen barrier effects to achieve reproductive isolation, or a trait needs to be under divergent selection that is also associated with assortative mating (Perini *et al.*, 2020; Smadja and Butlin 2011). For example, a locally adaptive trait, i.e. resistance to a certain pathogen, that varies in strength within a population could generate this barrier to gene flow (Sakamoto and Innan 2020), particularly if the resistance trait is selected for in mate choice. These genes have been referred to as ‘multiple effect traits’(Perini *et al.*, 2020), or ‘magic traits’ (Gavrilets 2004; Servedio *et al.*, 2011). To be classed as a ‘magic traits’ gene, it must satisfy three criteria: i) the trait must be subjected to divergent selection; ii) the trait must support non-random mating; and iii) the trait must be of a magnitude that is ecologically relevant (Garduno-Paz *et al.*, 2020; Maan and Seehausen 2011; Servedio *et al.*, 2011).



A region of genes that has the potential to be classed as magic trait genes and influences diversification and speciation with gene flow is the Major Histocompatibility Complex (MHC) (Andreou *et al.*, 2017; Meléndez-Rosa *et al.*, 2020). These molecules allow the detection of pathogens, by distinguishing self-peptides from non-self-peptides, then binding and presenting pathogens to T-cells. There are two main classes of MHC, class I which defends against intracellular pathogens such as viruses, and class II that defends against extracellular pathogens like bacteria (Knapp 2005). The self and non-self-distinguishing ability (of both classes) is enabled by the highly diverse peptide-binding region (PBR), with higher genetic diversity incurring resistance to a greater number of pathogen types (Rudensky *et al.*, 1991; Aeschlimann *et al.*, 2003; Chaplin 2010; Spurgin & Richardson 2010).

This high diversity of the MHC, has been shown to influence mate choice in multiple taxa *Gasterosteus aculeatus* (Andreou *et al.*, 2017; Eizaguirre *et al.*, 2009b; Eizaguirre *et al.*, 2012); *Ctenophorus decresii* (Hacking *et al.*, 2018); *Cheirogaleus medius* (Schwensow *et al.*, 2008) — with clear impacts of MHC-based mate choice on offspring survival (Agbali *et al.*, 2010; Brouwer *et al.*, 2010). Given that MHC is involved in the adaptation of hosts to pathogens and parasites (Biedrzycka *et al.*, 2018; Fraser and Neff 2010; Froeschke and Sommer 2012; Hacking *et al.*, 2018; Jones *et al.*, 2015; Kloch *et al.*, 2010; Loiseau *et al.*, 2011; Savage and Zamudio 2016; Schad *et al.*, 2012; Schwensow *et al.*, 2010; Schwensow *et al.*, 2017; Sepil *et al.*, 2013; Srithayakumar *et al.*, 2011; Zhang *et al.*, 2015; Zhang and He 2013) and can influence mate choice (Agbali *et al.*, 2010; Andreou *et al.*, 2017; Dearborn *et al.*, 2015; Pearson *et al.*, 2017; Sakamoto and Innan 2020; Zelano *et al.*, 2002), these genes could potentially be classed as a magic trait gene (Kamiya *et al.*, 2014; Garduno-Paz *et al.*, 2020). However, little is known about the involvement of MHC genes at the early stages of speciation.

Here, we asked whether there were allele frequency variations on MHC class I in a population of an Australian skink *Tiliqua rugosa* (Gray, 1825), over an ecological gradient near Mount Mary in South Australia. *Tiliqua rugosa* are long lived (40+ years), monogamous lizards (Bull 2000). The population has been extensively studied over the past 39 years (Bull *et al.*, 1981; Bull *et al.*, 1989; Chilton & Bull 1993; Bull & Burzacott 2001; Chilton *et al.*, 2009; Bull *et al.*, 2012; Godfrey and Gardner 2017). The study population — part of a wider and



continuous population — of *T. rugosa* at Mount Mary is within a 30 km by 30 km area distributed across an ecological gradient (Bull & Burzacott 2001) with no physical barriers preventing interbreeding. The arid northern area of the site is dominated by the chenopod bluebush (*Maireana sedifolia*), while the southern area has higher rainfall and is primarily mallee scrub (*Eucalyptus socialis*) (Bull & Burzacott 2001; Kerr *et al.*, 2003).

Roughly coincident with this ecotone is the distribution of two reptile tick species, *Amblyomma limbatum* in the north-east and *Bothriocroton hydrosauri* in the south-west (Smyth 1973; Bull & Burzacott 2001). These two tick species use *T. rugosa* as the primary host, forming a parapatric boundary where the ecotone changes (Bull & Burzacott 2001). This parapatric boundary was first mapped in the area in 1968 and has been shown to be relatively stable with minor shifts of 1–2 km over a 17-year period (Smyth 1973; Bull *et al.*, 1989; Bull & Burzacott 2001). The ranges of the tick species abut, with ~1km overlap, and there is no hybridization between them (Bull *et al.*, 1989). *Bothriocroton hydrosauri*'s distribution is known to be restricted to the southern area of the site where conditions are more humid (Bull and Possingham 1995, Bull and Burzacott 2001). Experimental studies have shown *B. hydrosauri* desiccate in the conditions similar to the northern region of the site (Bull and Smyth 1973). By contrast, *A. limbatum* do not occur in the southern region of the site where conditions are more humid, even though experiments show they are able to survive in such environments (Godfrey and Gardner 2017). It is currently unknown what inhibits *A. limbatum* from moving south. However, it is unlikely a result of any interaction between the host and parasite as *T. rugosa* are passive carriers of both species of ticks and can move freely across the ecological gradient. Therefore, they do not inhibit *A. limbatum*'s dispersal into the south-west region.

Both *A. limbatum* and *B. hydrosauri* are known to vector at least two parasites; *Hemolivia mariae* (Smallridge and Bull 1999) and *Rickettsia* spp. (Staines *et al.*, 2020). Differences in the prevalence, susceptibility, and transmission of *Rickettsia* via the ticks is currently being explored, although it has been documented for *Hemolivia mariae* (Bouma *et al.*, 2007; Smallridge and Bull 1999; Smallridge and Bull 2000). Studies show that *B. hydrosauri* were more susceptible to infection from *H. mariae* than *A. limbatum*, and transmission from the ticks to *T. rugosa* can occur (Smallridge and Bull 1999; Smallridge and Bull 2000). It was also



found that *H. mariae* infection in *T. rugosa* does reduce the lizard's home ranges however, individuals with greater home ranges were more at risk of infection (Bouma *et al.*, 2007). Other cellular pathogen communities associated with lizards either side of the tick boundary have not been fully examined (Norval *et al.*, 2019; Smallridge and Bull 1999; Smallridge and Bull 2000; Staines *et al.*, 2020). Given that there are distribution limitations for these two tick species (Petney and Bull 1984), it is likely that intracellular pathogen differences occur between the tick species.

Considering the varying transmission of parasites from these ticks to the lizards and the ecological gradient, it is reasonable to suggest there would be varying selective pressures on the lizard's immune genes (such as MHC), that over time could alter the MHC peptide binding region's diversity between the two sides of the boundary. We firstly aimed to examine the MHC class I allele frequency variation in *T. rugosa* across the parapatric boundary. We predicted there would be differences correlated with tick species infesting the lizard due to the varying susceptibility of pathogens between tick species, resulting in transmission differences in the lizards. Our second aim was to use genome-wide single nucleotides polymorphisms (SNPs) to determine if there is population differentiation across large or small areas of the genome. We hypothesised that any differentiation might be confined to small regions of the genome that could support MHC under selection.



Methods

Study area and tissue collection

The site (30 km by 30 km) has an extensive 40-year continuous history of research on the *T. rugosa* population and the parapatric boundary of the ticks (Bull *et al.*, 1981; Bull *et al.*, 1989; Bull and Burzacott 2001; Bull *et al.*, 2017; Godfrey and Gardner 2017). Tissue samples (toe clips) from *T. rugosa* (n = 173) were obtained near Mount Mary in South Australia (- 33.922222°, 139.284167°) (Figure 1), and stored in ethanol. Tissue collection was conducted between September-December (in 2015 & 2016), when *T. rugosa* are most active (Bull and Burzacott 2001). Individuals were selected by random encounter along pre-existing road transects and hand captured as per Bull and Burzacott (2001) and GPS recorded. This method does not require baiting or trapping (Bull 1995; Bull and Burzacott 2001). Sampled lizards were identified with unique toe clip number or given a new toe clip number if new. Lizards were checked for ticks and the tick species was recorded. Sampling followed animal ethics approval E424/17.

Group delineation for MHC I allele frequency and SNP analysis

For both the MHC and SNP analyses, we assigned individual lizards into groups determined by which species of tick had been attached to them when captured. The groupings were 'A. *limbatum* only present' = 1; 'B. *hydrosauri* only present' = 2; 'Both tick species present' = 3, and 'No ticks present' = 4. The reason was to determine if a particular tick had any association to allele frequency variation at MHC class I loci and genome wide SNP loci, which could indicate parasite or pathogen driven selection. These lizards do not have any family associations so familial relationships are unlikely to have been overrepresented in the sampling (Godfrey *et al.*, 2014).

As the two tick species are limited in their distribution across the site, we generated an estimate of the current position of the parapatric boundary, between the two tick species, at the time of sampling. We did this by using the GPS coordinates of *T. rugosa* individuals which had both tick species attached at the time of sampling (2016). By using only those individuals and creating a polynomial line of best fit equation (order of 6) to represent the boundary, we can determine a *T. rugosa* individual's position to the boundary and explore how variation in



the principal coordinates analysis (PCoA) is explained spatially across the study site. The boundary line had randomised coordinates along the line equation, generated in Excel (version 2102), and the line points converted from points to line in ArcGIS (ESRI, 2011).

MHCI Amplification and Sequencing

DNA was extracted from tissue samples of 165 individuals using DNeasy Blood and Tissue kits (Qiagen, Valencia, CA) following the manufacturer's protocols and quantified using a Qubit and 1.5% agarose gel electrophoresis. DNA from 23 individuals were split into two samples as technical replicates (total n = 188, including replicates).

We targeted a 242 bp fragment of exon2, of the α -1 domain of MHC class I, using primers previously developed for *T. rugosa* (Ansari *et al.*, 2015). The α -1 and α -2 domains of the MHC molecule make up the hypervariable peptide binding region that recognises antigens. The polymerase chain reaction (PCR) was set up as a two-step process. The first PCR amplified the target DNA, while the second PCR attached unique indexes and sequencing adapters to each amplicon (See [MHC I indexes](#))(Pearson *et al.*, 2016a). These unique indexes were 8 bp in length (forwards and reverse) which allow for sample identification after sequencing (Pearson *et al.*, 2016a) and were previously used successfully in another study (Hacking *et al.*, 2017). The forward locus specific primer was α 1 F2_tagF 5' *ACGACGTTGTAAAAACGGCGGTGTCKGAGCCYRGCCAG*-3', that includes an attached 15 bp sequence adapter (in italics) used to add Illumina sequencing adapters and indexes via complementary sequence in a second PCR. The reverse locus specific primer was α -1 R1_tagR 5' *CATTAAGTTCCCATTATGKCHDRTCCAGWRMTGRGGGT*-3' that also includes an attached 16bp sequence adapter (in italics). Four blank samples (negative controls) were also included to give a total of 192 samples These blank samples continued through the sequencing pipeline, as negative controls, for the purpose of quality control. For the first PCR, each reaction composed of 25 μ l, containing: 1 x MRT buffer (Hayden *et al.*, 2008), 0.4 μ M of each primer (forward and reverse), 1 unit of Immolase (5 U/ μ l) and 2.6 – 59 ng/ μ l of DNA. The PCR cycle consisted of 95°C for 10 minutes; 35 cycles of 94°C for 45 seconds, 58°C for 45 seconds and 72°C for 60 seconds; 72°C for 6 minutes; 25°C for 2 minutes (Pearson *et al.*, 2015). Successful amplification of MHC I loci was determined by the presence of a band (between 200 – 300bp) on 1.5 % agarose gel under a UV imager (Bio-Rad Laboratories,



California, USA). The first stage PCR products were cleaned using an epMotion 5075 pipetting robot and a 384-well filter plate (Millipore, USA) on a Merck Millipore vacuum manifold (Merck KGaA, Germany), following the manufacturer's protocols. The cleaned PCR product was re-suspended in 20 μ l of 10 mM TRIS pH 8.0.

The second PCR incorporated 1 x MRT buffer, 0.5 U of Immolase (5 U/ μ l), in a total volume of 8 μ l. Then 2 μ l of each unique index combination were added to each well (0.4 μ M each index; forward and reverse), followed by 2 μ l of PCR1 product (DNA template) to give a total volume of 12 μ l per PCR. Cycling conditions were 95°C for 10 minutes; 8 cycles of 92°C for 15 seconds, 54°C for 60 seconds and 72°C for 1 min 30 seconds; 72°C for 6 minutes; 25°C for 2 minutes (Hacking *et al.*, 2017). Successful attachment of indexes to amplicons was determined by comparative band shifts (38–40 bp) between PCR1 and PCR2 on electrophoresis gels (1.5% agarose). The amplicons from PCR2 were pooled together and then purified using AMPure magnetic beads (1:1 ratio) following manufacturer's protocols (Agencourt Bioscience Corporation, Massachusetts). The magnetic beads bind to the DNA fragments leaving smaller fragments (less 100 bp) behind i.e. adapter dimers. The cleaned products were checked on an Agilent 2200 tape station to confirm removal of any adapter dimers or any other contamination. Samples were then sent to Australian Genome Research Facility (AGRF) (Adelaide) for sequencing on an Illumina MiSeq with 300 bp paired-end reads (forward (R1) and reverse (R2)), that allowed for the full sequencing of products due to a 50 bp overlap.

DARTSeq assays

We used the same individuals as in the MHC Class I analysis ($n = 165$), with nine added individuals that were collected later in 2016 after the MHC analysis (total $n = 174$). The extracted DNA was then sent to Diversity Arrays Technology (Canberra, Australia) for reduced representation genome sequencing using the DARTseq platform. Diversity Arrays Technology uses hybridised solid-state technology on an open platform, to assay the presence or absence of specific DNA fragments from relatively small amounts of genomic DNA (Hassani *et al.*, 2020; Jaccoud *et al.*, 2001; Wenzl *et al.*, 2004), by using a combination of restriction enzyme digestion and adapter ligation before amplification (Wenzl *et al.*, 2004). DART then use proprietary methods post sequencing for quality control including a blast



alignment to confirm success. The genome reference that DArT used for our study was 'AnoleLizard_v2' (*Anolis carolinensis*), as this is currently the closest genome reference to *T. rugosa* at the time of processing, with a minimum 70% identity match.

Sequencing and Genotyping

MHC

The forward and reverse reads were paired in PEAR (version 0.9.8) (Zhang *et al.*, 2014) and clustered to their corresponding sample, in individual files. The quality and length distribution of the reads were then analysed using FastQC (version 0.11.9) before genotyping (Andrews 2010). Negative controls (n = 4) were then removed from the pipeline (filtered n = 188), after confirming negative controls produced no reads, and technical replicates had similar number to their repeated sample.

To remove errors resulting from the any amplification of adapter dimers, insertion/deletion sequencing errors, and pseudo variants we used Genome Analysis Toolkit (GATk) version 3.6 (Li and Durbin 2009), to map the paired-end reads to two previously published loci (Tiru-UA*03 and Tiru-UA*04) characterised from the transcriptome of *T. rugosa* by Ansari *et al.*, (2015). GATk uses Burrows Wheeler Alignment (BWA-MEM) algorithm that aligns based on predicted likelihood from the given read data (Li 2013). We considered reads that did not align to the characterised loci as sequencing errors and they were removed from further analyses (You *et al.*, 2012).

After eliminating sequencing errors, single-nucleotide polymorphisms (SNPs) were called using GATk's haplotype caller on individual files and then concatenated and genotyped using GATk's genotype caller (Li *et al.*, 2009). The aligned reads (BAM files) were compared to the predicted likelihood genotypes (VCF files) in Integrative Genomics Viewer (IGV) (Version 2.3) (Thorvaldsdóttir *et al.*, 2013). We visually checked heterozygous SNPs using IGV, for approximately equal proportion of reads for each allele to identify and remove any erroneous reads, as using Haplotype caller's hard filtering parameters did not remove them all (You *et al.*, 2012). The SNPs identified by GATk, or allele variants, were assigned arbitrary numbers in Excel.



DArTseq

Data received from DArTseq was analysed using the DartR package in RStudio, R version 3.6.0. (R Core Team 2018). Other metrics were attached to the genlight file including defined groups for each sample i.e., 'A. limbatum only present', 'B. hydrosauri only present', 'Both tick species present', 'No ticks present', and the GPS coordinates of each sample. Raw data were filtered using high thresholds. call rate threshold of 1, removing all missing data; the reproducibility threshold was set at 1 for 100% reproducibility, all monomorphic loci were removed, secondaries — repeated fragments for a particular locus — were also automatically removed as this can double the signal. In order to remove linked loci a $R^2 = 0.7$ threshold was set as these individuals are not assumed to be highly related and therefore a lower threshold is suitable (Godfrey *et al.*, 2014, Piza-Roca *et al.*, 2019). In the DartR package, the R^2 threshold is less conservative the closer to 1, inverse to the biological R^2 value indicating relatedness where high R^2 value indicates high relatedness. Linked loci were removed using a loop that assessed the number of connections a linked locus had (most to least), then the locus with the highest connections was removed — before looping again ([Script 1](#)) (Dorey *et al.*, 2021). This conservative method enables the retention of some loci that would be removed with hard filtering (Dorey *et al.*, 2021).

Statistical Analysis

MHC

To test for MHC allelic variation between groups, pairwise F-statistics (F_{ST}) were calculated for each locus using GenAlex (version 6.503), to determine if there was significant genetic variability between lizards groups (ticks attached) (Peakall and Smouse 2012). Fisher's Exact tests were performed on the numbers of each allele between groups, to determine if there were any significant allele frequency differences between groups in RxC contingency tables in Windows' command line (Zaykin *et al.*, 2008). Tests were carried out on each locus with 10,000 randomised permutations to generate P values, to account for unequal group sizes (Zaykin *et al.*, 2008).

We implemented χ^2 tests using GenAlex 6.503 to determine if any of the groups deviated from Hardy-Weinberg equilibrium (HWE) (Peakall and Smouse 2012, Reece *et al.*, 2011,



Zaykin *et al.*, 2008). Expected versus observed genotype frequencies were graphed for each group and locus, to determine if there was a deficiency of heterozygosity in any of the groups. Observed heterozygosities of each group were examined using RxC to test if there were any significant differences between groups (Zaykin *et al.*, 2008). Allele frequencies and pie charts were calculated and plotted in Excel 2013 for each group and each locus to detect any patterns. To determine whether allele frequency variations were associated with ticks attached we performed a Principal Component Analysis (PCA), on the allele sequences for both MHC class I loci.

We tested the ratio of non-synonymous to synonymous nucleotide substitutions (dN/dS) to determine whether selection was occurring at sites by using PAML codeml (Pearson *et al.*, 2016b; Xu and Yang 2013). We tested three different selection scenarios: Neutral (M0), slightly selective (M7), and positively selective (M8). Akaike Information Criterion (AIC), was used to determine model of best fit i.e. M0, M7 or M8. However, since our sample size was small and uneven (Yang *et al.*, 2005), we also used a bias-adjustment (AICc). The difference between each model's AICc was calculated (Δi), and the model with the lowest $\Delta AICc$ score was considered the model of best fit (Yang and Nielsen 2002; Yang *et al.*, 2005).

DArTSeq

A Principle Coordinates Analysis (PCoA) was performed on the SNP data, in DartR (version 1.8.3) to determine SNP variation among the delineated groups (Gruber *et al.*, 2018; R Core Team 2018). Principle coordinates analysis was determined preferred for these analyses, rather than PCA, to determine similarities or dissimilarities that explain variation between samples and groups (Mohammadi and Prasanna 2003). The PCoA scores of explained variation for each sample were then extracted and used for a discriminant analysis in SPSS (IBM Corp 2017) and spatial mapping in ArcGIS (ESRI 2011).

The PCoA scores of all groups were extracted and using SPSS (version 25) we performed a non-parametric pairwise Mann-Whitney U test on the lizards with *A. limbatum* only, and *B. hydrosauri* only for PCo1 – PCo5. The extracted PCoA scores were input into ArcGIS and each PCo axis was tested against the GPS coordinates of individuals using a coloured scaled range. This was to observe any patterns in relation to the parapatric boundary. The SNP data were tested for deviations from HWE after removing linked loci from within each group,



using DartR package (version 1.8.3) in RStudio (version 4.0.3) (Gruber *et al.*, 2018; R Core Team 2018). In order to analyse the population's genetic structure the SNP data was exported from DartR to be run on Flinders University's HPC 'DeepThought' using STRUCTURE (version 2.3.4) (Flinders 2021, Pritchard *et al.*, 2000). The structure output was then input into CLUMPAK's [online server](#) for visualisation of the population structure (Kopelman *et al.*, 2015).

Results

Sample sizes and groupings

In total 173 *T. rugosa* individuals (165 for MHC; a further eight for DArTseq) were sampled (See, [MHC and DArTseq samples](#)). Group delineation for the MHC analysis consisted of: *A. limbatum* = 38; *B. hydrosauri* = 67; both tick species present = 20; and no ticks attached = 40. Group delineation for the DArTSeq analysis consisted of: *A. limbatum* = 40; *B. hydrosauri* = 67; both tick species = 25; no ticks attached = 41.

MHC

Samples were successfully amplified and sequenced (total n = 188, 165 samples, another 23 technical replicates) while the four negative controls did not return reads. The four negative controls had minimal reads (58 – 138 reads). Read coverage per individual ranged from 16,000 to 69,000 reads. FastQC quality analysis on R1 and R2 reads showed 7,978,126 reads each ([MHC Reads file](#)). GATK mapped the sequences back to two MHC loci previously identified in *T. rugosa* (Ansari *et al.*, 2015): Tiru-UA*03 and Tiru-UA*04. Four SNPs were called by GATK's haplotype caller for Tiru-UA*04, and six for Tiru-UA*03. IGV showed all heterozygous SNPs called had relatively equal proportions of reads for each allele. The technical replicates (n = 23) had the exact same MHC nucleotide sequences as their corresponding samples and were therefore removed from the statistical analysis (n = 165). Analysis of the allelic variation revealed four different amino acid allele sequences at Tiru-UA*04 (Figure 2; Figure S4).

There was minimal differentiation in MHC allele frequencies overall between the delineated groups for both loci (Tiru-UA*03, P = 0.317; Tiru-UA*04, P = 0.110) (Table 1). However, there was a significant difference of MHC allele frequencies between the delineated '*B. hydrosauri*



only' group and 'both ticks present' group for locus Tiru-UA*04, Fisher's exact $P = 0.028$ (Table 1). F_{st} values for locus Tiru-UA*04 in lizards from the '*B. hydrosauri*' group were $p = 0.246$, while 'both ticks present' lizards were $p = 0.024$ (Table S1). Tiru-UA*03 had low – negative values within all groups (Table S1).

Pairwise contingency tables (Fisher's exact) (P values) for heterozygosity and homozygosity between groups, for each loci, did not show any significant differences (Fisher's exact) between groups at either locus (Tiru-UA*03, $P = 0.730$; Tiru-UA*04, $P = 0.694$) (Table S2). There was a significant deviation from Hardy-Weinberg equilibrium of locus Tiru UA*04 for lizards infested only with *B. hydrosauri* ($P = 0.038$, Table 2), and were found with fewer observed heterozygotes than expected for each genotype (Figure 3).

Multi-variate Principal Component Analysis (PCA) of all groups using both loci, indicated minimal variation between groups. There were similar results when only comparing *A. limbatum* only group and *B. hydrosauri* only group (See supplementary material). The results of Paml codeml indicated no selection at Tiru-UA*03 as the model of best fitness was M0 (neutral) (Table 3). However, for Tiru-UA*04 the model of best fit was M8 (Table 3) for sites 22 and 30 are under positive selection (Table 4). Site 22 of Tiru-UA*04 had a posterior probability of 0.987 for being positively selected, whereas site 30 was just below the $P > 95\%$ significance threshold with 0.943 (Table 4).

DARTSeq

The raw data consisted of 61,774 SNPs for 173 individuals grouped in four groupings. There was 11.9% missing data reported within the file. For the call rate, 61% of the data had less than 5% missing data, which was then filtered for 0% missing data ($n = 173$; SNPs = 20,356). Analyses of reproducibility indicated 45% of the data had 100% reproducibility ($n = 173$; SNPs = 9,234). Thirty-six monomorphic loci were reported and then removed from the data. Linked loci were removed from within each group using $R^2 = 0.7$ threshold ($n = 173$; SNPs = 3,271). Thirty-two loci across all groups significantly deviated ($p < 0.05$) from Hardy Weinberg Equilibrium (Figure S4). Two loci (29090556-37-G/A and 29130860-6-T/A), deviated from HWE in each group, except for 'both ticks present' where neither loci were found.



The PCoA of all groups showed PCo1 and PCo2 explained 2.2% of the total variation (Figure 4). Visually, there appears to be minor separation between *A. limbatum* only and *B. hydrosauri* groups between PCo 1 and PCo2 axis, while lizards with both ticks clustered with *A. limbatum* only lizards (Figure 4). In contrast, the group that had no ticks attached, are spread horizontally along the x axis. The pairwise non-parametric Mann-Whitney U test showed significant differences between *A. limbatum* only and *B. hydrosauri* groups for PCo1 ($p = 0.027$) and PCo4 ($p = 0.000$) while PCo2 was just outside of significance ($p = 0.058$) (Table 5). The PCo1 scores for all lizards were spatially visualised using a colour gradient showing negative ranged scores (in green, -5.397 to -2.158) associated with the lizard samples predominantly with *A. limbatum* attached in the north-east of the site, while the positive PCo1 scores (in red, 0.874 to 6.519) are associated with the *T. rugosa* samples with *B. hydrosauri* attached in the south-west (Figure 5). Structure analysis showed no population structure (See supplementary material)

Discussion

Our study has several important findings. Firstly, MHC variation at a single locus was suggestive with host's tick type attached, with significant differences between lizards with *B. hydrosauri* only and those with both tick species attached. Secondly, lizards with only *B. hydrosauri* attached showed heterozygosity deficiency and positive selection on codon sites of differentiated alleles. Thirdly, analysis of genome wide markers indicates that only a small proportion of the genome was contributing to differentiation. Finally, the distribution of genetic variation at both MHC was surprisingly fine-scale (km's) given the wide distribution of the species across temperate and semi-arid Australia.

We found significant allele frequency differences at one MHC I locus (Tiru-UA*04) between lizards with *B. hydrosauri* only present, and those with both ticks present (Table 1, Figure 2), where as locus Tiru-UA*03 were synonymous. Exploring further, we then found significant heterozygote deficiency in *T. rugosa* with *B. hydrosauri* only present (Table 2; and Figure 3). tested for selection (negative, neutral, positive) on the allele variants from *T. rugosa* with *B. hydrosauri* only (Table 3) and confirmed there was positive selection at site 22 of locus Tiru-UA*04 (Table 4). These suggest that selective pressures are influencing a portion of the lizard population at the study site and may be accompanied by assortative mating which



requires further exploration. We cannot determine the cause of the selection pressures at this stage, assortative mating is one possible explanation. Demographic distance could be another (Otto *et al.*, 2008). The distance across the study site may reduce the potential interactions of lizards on one side of the boundary compared to the other (e.g. Lizards in the north-east of the study rarely or never have contact with those in the south-west, even though there are no physical barriers)(Figure 1).However, as pathogen mediated selection has been associated with MHC (Carrington *et al.*, 1999; Savage and Zamudio 2016; Schwensow *et al.*, 2017; Zhang and He 2013), and MHC class I recognises viruses, our results likely indicate the potential presence of viruses in the system—predominantly in the more humid south-west side of the study site and less prevalent in the arid north-east. The selective pressure that seems to be on *T. rugosa* in the south-west of the study site could be explained by transmission differences, via the different ticks species, to the lizards (Smallridge and Bull 1999; Smallridge and Bull 2000); or external environment variations influencing the microorganism community.

The MHC results also give further evidence for pathogen-mediated selection (PMS). Pathogen-mediated selection is the theory that pathogens are a driving force for the MHC diversity observed in vertebrates (Spurgin and Richardson 2010). While the mechanisms of PMS — heterozygote advantage, rare-allele advantage, and fluctuating selection — are still under debate (Spurgin and Richardson 2010), there is evidence that pathogens drive MHC diversity (Biedrzycka *et al.*, 2018; Fraser and Neff 2010; Savage and Zamudio 2016; Schad *et al.*, 2012; Schwensow *et al.*, 2017; Westerdahl *et al.*, 2005; Zhang and He 2013). Our results give support to pathogens as driving differentiation of populations and call for further work to explore these potential drivers.

Genome wide SNPs (generated using DArTSeq) were used to determine whether these selection pressures might be influencing a small region of the genome. Principal Coordinate Analysis (PCoA) of all *T. rugosa* samples grouped by tick species attached, showed low level variation (2.2%) between those with *B. hydrosauri* only present and attached and *A. limbatum* only present (Figure 4). The Mann-Whitney U showed significant differences for PCo1 and PCo4 between those lizards grouped as *A. limbatum* only present and '*B. hydrosauri* only present' (Table 5). While the variation in the PCoA of all groups is only



minor (2.2%), this could suggest a small region of the genome under selection — likely a functional region. The MHC genes are a functional region of the genome that we have shown to be under selection in our study site. While we cannot determine if the minor variation is caused by pressures on the MHC genes in this species, it could explain the observed pattern. These results provide further evidence for why MHC could be referred to as a ‘magic trait’ gene (Andreou *et al.*, 2017; Meléndez-Rosa *et al.*, 2020). These results meet the three criteria needed to be a magic trait gene; i) we showed that the one locus of MHC class I in one population of *T. rugosa* has significantly different allele frequency variations within the population; ii) we showed heterozygosity deficiency in the lizards of one area of the site compared to the rest of the site, that could suggest assortative mating (Eizaguirre *et al.*, 2009b, Schad *et al.*, 2005) ; and iii) as MHC diversity is key for pathogen recognition and defence, it affects survival fitness of vertebrates making it ‘of a magnitude ecologically relevant’ (Eizaguirre *et al.*, 2009a, Piertney and Oliver 2006). That there is some pattern at the genome level indicates that the pressures in this system are working on the functional regions of their genome, can be detected at the genomic level, and could be the beginnings of divergence in this species. We cannot make such a conclusion from this study, as structure analysis shows one population, but further research will investigate this hypothesis more deeply as a genome for this particular species becomes available soon. Research will also determine the role parasites may play in driving diversification during the early stages of host differentiation in this system.



Figures

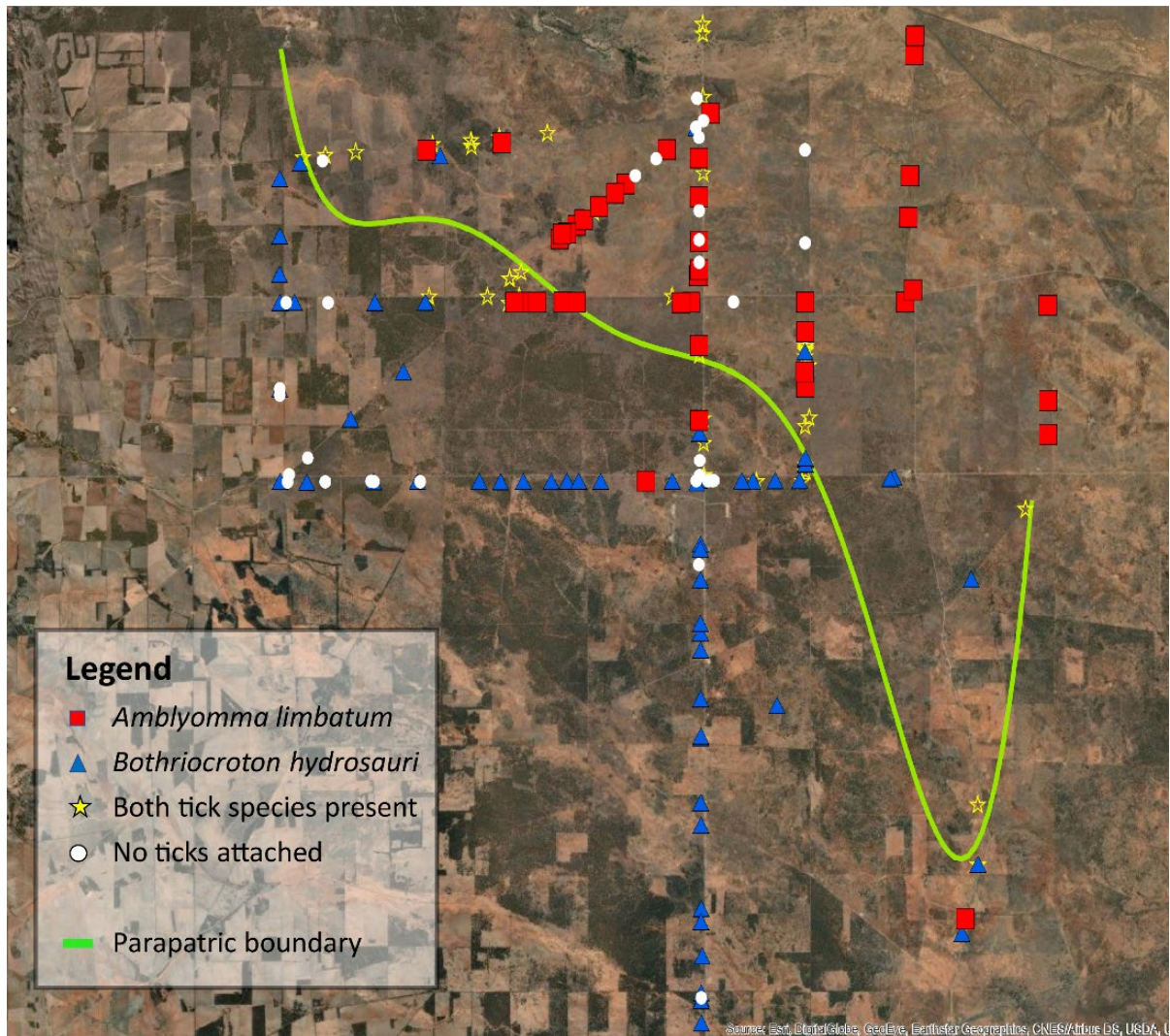


Figure 1 Sample distribution of *Tiliqua rugosa* individuals (n = 178) captured at the study site near Mount Mary, South Australia (-33.922222°, 139.284167°) for MiSeq sequencing of MHC loci and DArTSeq sequencing. Legend indicates which tick species were attached to the *Tiliqua rugosa* at the time of sampling. Parapatric boundary indicates an estimate based on samples collected in 2016 that had both tick species attached.

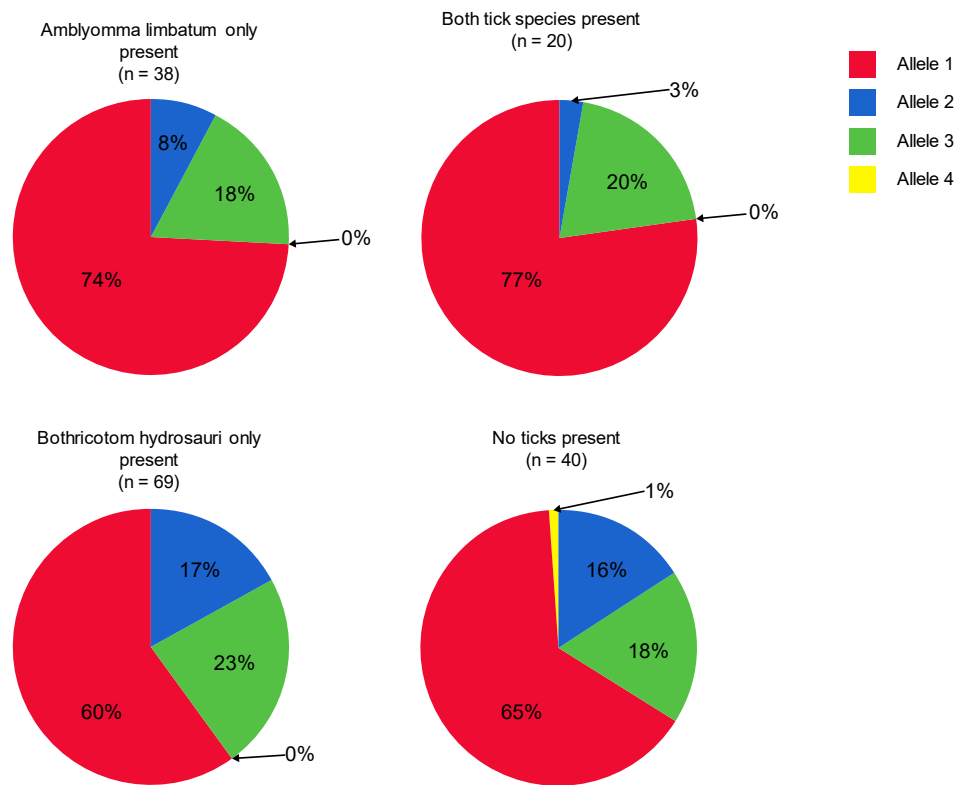


Figure 2 Allele frequencies for MHC class I locus **Tiru-UA*04** within *Tiliqua rugosa* defined by their tick status. Alleles 1 = red, Allele 2 = Blue, Allele 3 = green, and Allele 4 = Yellow

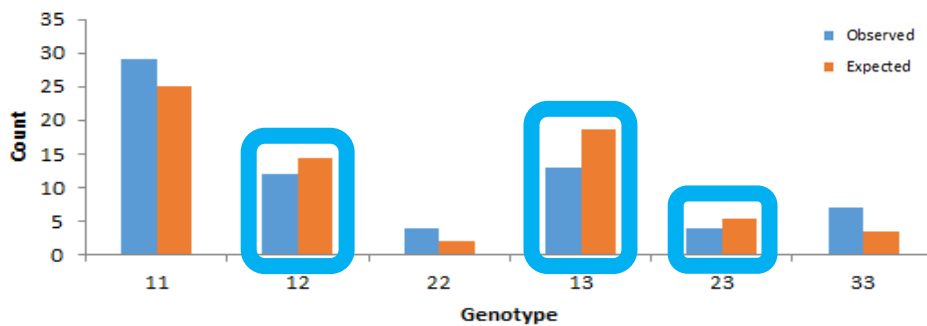


Figure 3 A significant deficiency of observed heterozygosity for MHC class I locus **Tiru-UA*04** in *Tiliqua rugosa* lizards with *Bothriocroton hydrosauri* only attached ($P = 0.038$).



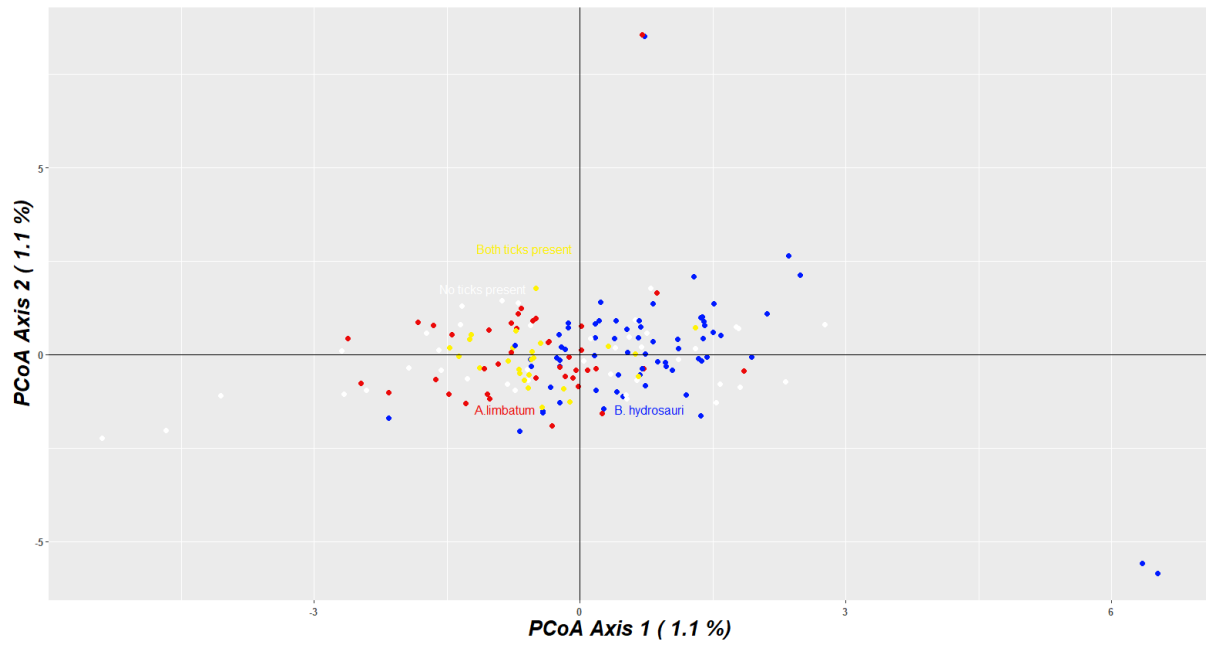


Figure 4 Principal Coordinate Analysis (PCoA) using SNP data of *Tiliqua rugosa* individuals group based on tick species attached. *Amblyomma limbatum* = Red; *Bothriocroton hydrosauri* = Blue; Both ticks present = Yellow; No ticks present = White.



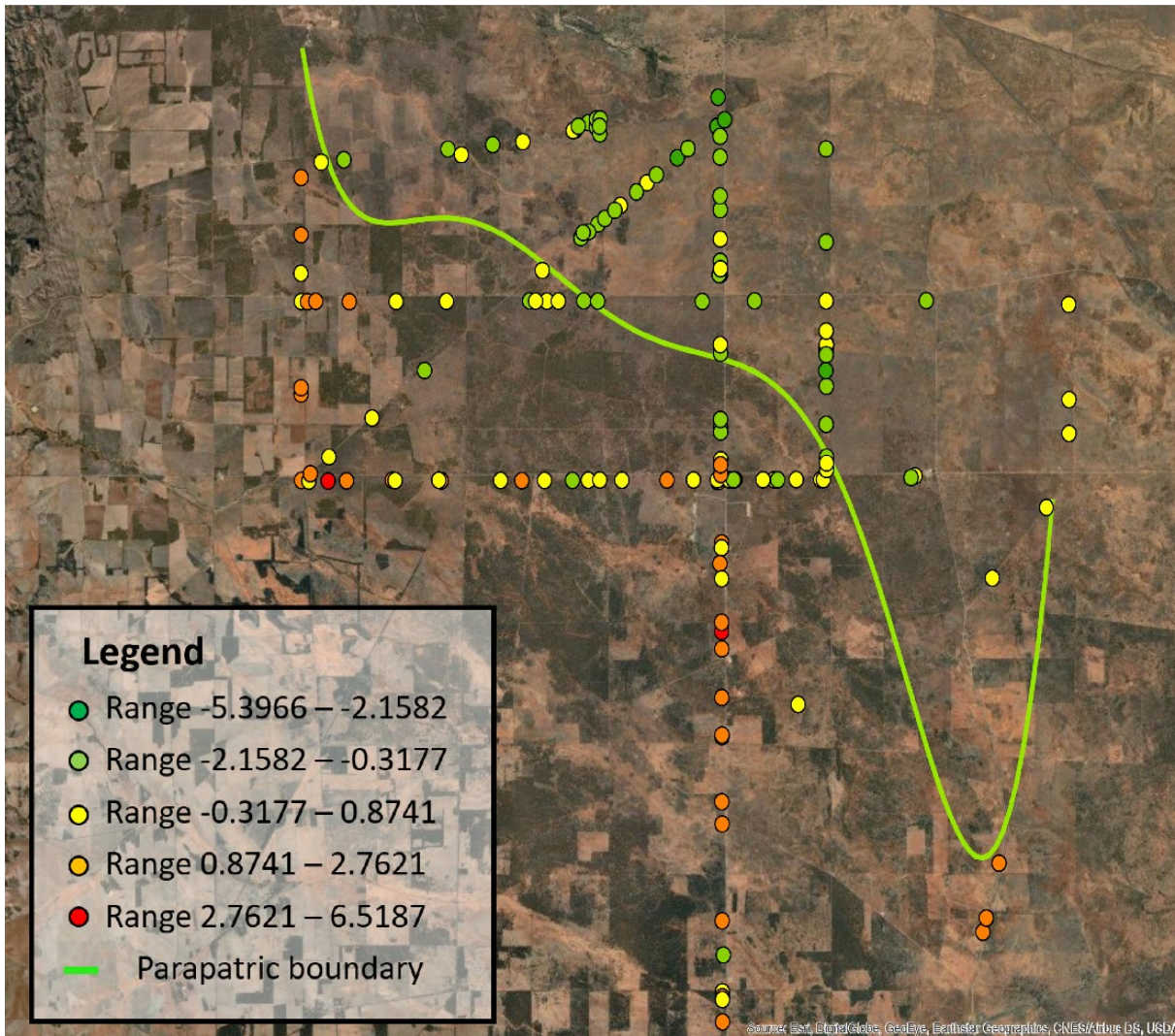


Figure 5 PCo1 scores for individuals of *Tiliqua rugosa* of SNP data ranked using a gradient scale over the parapatric boundary. Range indicates correlation to PCo1's Principal Coordinate Analysis. Negative scores were in green (-5.397 to -2.158) ranging to positive in red (0.874 to 6.519).



Tables

Table 1 Tests of between groups allele frequencies via Fisher's exact test (P values) on contingency tables for each of the two MHC class I loci genotyped. Bold P values are significant at the 0.05 level.

Pairwise Contingency tables	Tiru-UA*03	Tiru-UA*04
<i>A. limbatum</i> vs No ticks present	1.000	0.328
<i>A. limbatum</i> vs <i>B. hydrosauri</i>	0.546	0.115
<i>A. limbatum</i> vs Both tick species present	0.340	0.889
<i>B. hydrosauri</i> vs Both tick species present	1.000	0.028*
<i>B. hydrosauri</i> vs No ticks present	0.235	0.503
Both tick species present vs No ticks present	0.545	0.122
Between all groups	0.317	0.110

Table 2 Tests of conformance to Hardy-Weinberg equilibrium for the two MHC class I loci genotyped in this study. Bold P values are significant at the 0.05 level.

Group	Locus	DF	ChiSq	P Value
<i>A. limbatum</i>	Tiru-UA*03	3	0.117	0.990
	Tiru-UA*04	3	0.452	0.929
<i>B. hydrosauri</i>	Tiru-UA*03	10	0.626	1.000
	Tiru-UA*04	3	8.441	0.038*
Both tick sp.	Tiru-UA*03	3	0.247	0.970
	Tiru-UA*04	3	0.334	0.953
None	Tiru-UA*03	3	0.263	0.967
	Tiru-UA*04	6	5.973	0.426

Key: ns=not significant, * P<0.05, ** P<0.01, *** P<0.001

Table 3 M0 (one ω ratio), M7 (nearly neutral with beta), M8 (positive selection with beta ($\omega_0 \leq 1$, $\omega_1 > 1$)) AICc (AIC with bias adjustment for small sample sizes) Δ AICc Difference between the value of the AICc of a model and the best model $\omega_1 = dN/dS$ ω_2 = Estimated ω for sites under positive selection p_0 = Proportion of sites with $\omega \leq 1$ p_1 = Proportion of positively selected sites ($\omega > 1$)

MHC I	ln L	AIC	AIC _c	Δ AIC _c	Parameters
Tiru-UA*03					
M0	-191.995875	385.99175	386.99175	0-Best model	$\omega_1 = 0.66424$
M7	-191.325668	386.651336	398.651336	11.659586	
M8	-190.287038	388.574076	428.574076	41.582326	$p_0 = 0.910$, $p_1 = 0.090$, $\omega_2 = 7.592$
Tiru-UA*04					
M8	-182.429397	372.858794	332.858794	0-Best model	$p_0 = 0.970$, $p_1 = 0.030$, $\omega_2 = 137.702$
M0	-185.928707	373.857414	375.857414	42.99862	$\omega_1 = 0.94452$
M7	-185.348976	374.697952	386.697952	53.839158	



Table 4 Bayes Empirical Bayes (BEB) analysis of selection on the two MHC class I loci genotyped in this study.

Tiru-UA03 (Pr(w>1) post mean +- SE for w)			Tiru-UA04 (Pr(w>1) post mean +- SE for w)		
30 V	0.861	7.318 +- 4.001	22 A	0.987*	2.058 +- 1.016
			30 G	0.943	2.047 +- 1.004

Positively selected sites (*: P>95%; **: P>99%)

Table 5 Non-parametric Mann-Whitney U pairwise analysis comparing PC scores from SNP data between *Tiliqua rugosa* lizards with *Amblyomma limbatum* attached and those infested with *Bothriocroton hydrosauri*. Significant values with less than 0.05 in bold.

	PC1	PC2	PC3	PC4	PC5
Chi-Square	4.899	3.591	1.914	27.052	0.028
df	1	1	1	1	1
Asymp. Sig.	0.027	0.058	0.167	0.000	0.868



Data Availability

Data and scripts are stored on a GitHub repository and will be publicly available once published.



References

- Agbali M, Reichard M, Bryjová A, Bryja J, Smith C (2010). Mate choice for nonadditive genetic benefits correlate with MHC dissimilarity in the rose bitterling (*Rhodeus ocellatus*). *Evolution* **64**: 1683-1696.
- Andreou D, Eizaguirre C, Boehm T, Milinski M (2017). Mate choice in sticklebacks reveals that immunogenes can drive ecological speciation. *Behavioural Ecology* **28**: 953-961.
- Andrews S (2010). FastQC: A Quality Control Tool for High Throughput Sequence Data.
- Ansari TH, Bertozzi T, Miller RD, Gardner MG (2015). MHC in a monogamous lizard—Characterization of class I MHC genes in the Australian skink *Tiliqua rugosa*. *Developmental and Comparative Immunology* **53**: 320-327.
- Biedrzycka A, Bielański W, Ćmiel A, Solarz W, Zając T, Migalska M *et al.*, (2018). Blood parasites shape extreme MHC diversity in a migratory passerine. *Molecular Ecology*.
- Blanckaert A, Bank C, Hermisson J (2020). The limits to parapatric speciation 3: evolution of strong reproductive isolation in presence of gene flow despite limited ecological differentiation. *Philosophical Transactions of the Royal Society B: Biological Sciences* **375**: 20190532.
- Bouma MJ, Smallridge CJ, Bull CM, Komdeur J (2007). Susceptibility to infection by a haemogregarine parasite and the impact of infection in the Australian sleepy lizard *Tiliqua rugosa*. *Parasitology Research* **100**: 949-954.
- Brouwer L, Barr I, Van De POL M, Burke T, Komdeur J, Richardson DS (2010). MHC-dependent survival in a wild population: evidence for hidden genetic benefits gained through extra-pair fertilizations. *Molecular Ecology* **19**: 3444-3455.
- Bull C, Sharrad R, Petney T (1981). Parapatric boundaries between Australian reptile ticks. *The Proceedings of the Ecological Society of Australia* **11**: 95-107.
- Bull C, Burzacott D, Sharrad R (1989). No competition for resources between two tick species at their parapatric boundary. *Oecologia* **79**: 558-562.
- Bull CM (1995). Population ecology of the sleepy lizard, *Tiliqua rugosa*, at Mt Mary, South Australia. *Australian Journal of Ecology* **20**: 393-402.
- Bull CM, Possingham H (1995). A model to explain ecological parapatry. *The American Naturalist* **145**: 935-947.
- Bull CM (2000). Monogamy in lizards. *Behavioural Processes* **51**: 7-20.
- Bull CM, Burzacott D (2001). Temporal and spatial dynamics of a parapatric boundary between two Australian reptile ticks. *Molecular Ecology* **10**: 639-648.
- Bull CM, Gardner MG, Sih A, Spiegel O, Godfrey SS, Leu ST (2017). Why is social behavior rare in reptiles? Lessons from sleepy lizards. *Advances in the Study of Behavior* **49**: 1-26.
- Bull M, Smyth M (1973). The distribution of three species of reptile ticks, *Aponomma hydrosauri*, *Amblyomma albolimbatum*, and *Amblyomma limbatum*, water balance of nymphs and adults in relation to distribution. *Australian Journal of Zoology* **21**: 103-110.
- Butlin RK, Galindo J, Grahame JW (2008). Sympatric, parapatric or allopatric: the most important way to classify speciation? *Philosophical Transactions of the Royal Society B: Biological Sciences* **363**: 2997-3007.
- Carrington M, Nelson GW, Martin MP, Kissner T, Vlahov D, Goedert JJ *et al.*, (1999). HLA and HIV-1: Heterozygote Advantage and B*35-Cw*04 Disadvantage. *Science* **283**: 1748.



- Dearborn DC, Gager AB, Gilmour ME, McArthur AG, Hinerfeld DA, Mauck RA (2015). Non-neutral evolution and reciprocal monophyly of two expressed Mhc class II B genes in Leach's storm-petrel. *Immunogenetics* **67**: 111-123.
- Dieckmann U, Doebeli M (1999). On the origin of species by sympatric speciation. *Nature* **400**: 354-357.
- Dorey JB, Groom SVC, Velasco-Castrillón A, Stevens MI, Lee MSY, Schwarz MP (2021). Holocene population expansion of a tropical bee coincides with early human colonisation of Fiji rather than climate change. *Molecular Ecology* **30**: 4005–4022.
- Eizaguirre C, Lenz TL, Traulsen A, Milinski M (2009a). Speciation accelerated and stabilized by pleiotropic major histocompatibility complex immunogenes. *Ecology Letters* **12**: 5-12.
- Eizaguirre C, Yeates SE, Lenz TL, Kalbe M, Milinski M (2009b). MHC-based mate choice combines good genes and maintenance of MHC polymorphism. *Molecular Ecology* **18**: 3316-3329.
- Eizaguirre C, Lenz TL, Kalbe M, Milinski M (2012). Divergent selection on locally adapted major histocompatibility complex immune genes experimentally proven in the field. *Ecology Letters* **15**: 723-731.
- ESRI. 2011 ArcGIS desktop: release 10. Redlands, CA: Environmental Systems Research Institute
- Fitzpatrick BM, Fordyce JA, Gavrillets S (2008). What, if anything, is sympatric speciation? *Journal of Evolutionary Biology* **21**: 1452-1459.
- Flinders U (2021). Deep Thought (HPC). Flinders University.
- Fraser BA, Neff BD (2010). Parasite mediated homogenizing selection at the MHC in guppies. *Genetica* **138**: 273.
- Froeschke G, Sommer S (2012). Insights into the complex associations between MHC class II DRB polymorphism and multiple gastrointestinal parasite infestations in the striped mouse. *PLoS One* **7**: e31820.
- Garduno-Paz MV, Huntingford FA, Garrett S, Adams CE (2020). A phenotypically plastic magic trait promoting reproductive isolation in sticklebacks? *Evolutionary Ecology* **34**: 123-131.
- Gavrillets S, Li H, Vose MD (2000). Patterns of Parapatric Speciation. *Evolution* **54**: 1126-1134.
- Gavrillets S (2004). *Fitness landscapes and the origin of species*. Princeton University Press: Princeton.
- Godfrey SS, Ansari TH, Gardner MG, Farine DR, Bull CM (2014). A contact-based social network of lizards is defined by low genetic relatedness among strongly connected individuals. *Animal Behaviour* **97**: 35-43.
- Godfrey SS, Gardner MG (2017). Lizards, ticks and contributions to Australian parasitology: C. Michael Bull (1947–2016). *International Journal for Parasitology: Parasites and Wildlife* **6**: 295-298.
- Grant BR, Grant PR (2002). Simulating secondary contact in allopatric speciation: an empirical test of premating isolation. *Biological Journal of the Linnean Society* **76**: 545-556.
- Gruber B, Unmack PJ, Berry OF, Georges A (2018). dartr: An r package to facilitate analysis of SNP data generated from reduced representation genome sequencing. *Molecular Ecology Resources* **18**: 691-699.



- Hacking J, Bradford T, Pierce K, Gardner M (2017). *De novo genotyping and segregation analysis reveals high diversity and evidence for copy number variation at the MHC in an Australian dragon lizard*: Unpublished manuscript.
- Hacking J, Stuart-Fox D, Godfrey S, Gardner M (2018). Specific MHC class I supertype associated with parasite infection and colour morph in a wild lizard population. *Molecular Ecology*.
- Hassani SMR, Talebi R, Pourdad SS, Naji AM, Fayaz F (2020). In-depth genome diversity, population structure and linkage disequilibrium analysis of worldwide diverse safflower (*Carthamus tinctorius* L.) accessions using NGS data generated by DArTseq technology. *Molecular Biology Reports* **47**: 2123-2135.
- Hayden MJ, Nguyen TM, Waterman A, Chalmers KJ (2008). Multiplex-Ready PCR: A new method for multiplexed SSR and SNP genotyping. *BMC Genomics* **9**: 80-80.
- Hollander J, Smadja CM, Butlin RK, Reid DG (2013). Genital divergence in sympatric sister snails. *Journal of Evolutionary Biology* **26**: 210-215.
- Jaccoud D, Peng K, Feinstein D, Kilian A (2001). Diversity Arrays: a solid state technology for sequence information independent genotyping. *Nucleic Acids Research* **29**: 25-25.
- Jones MR, Cheviron ZA, Carling MD (2015). Spatially variable coevolution between a haemosporidian parasite and the MHC of a widely distributed passerine. *Ecology and Evolution* **5**: 1045-1060.
- Kautt AF, Machado-Schiaffino G, Meyer A (2016). Multispecies Outcomes of Sympatric Speciation after Admixture with the Source Population in Two Radiations of Nicaraguan Crater Lake Cichlids. *PLOS Genetics* **12**: e1006157.
- Kloch A, Babik W, Bajer A, Siński E, Radwan J (2010). Effects of an MHC-DRB genotype and allele number on the load of gut parasites in the bank vole *Myodes glareolus*. *Molecular Ecology* **19**: 255-265.
- Knapp LA (2005). The ABCs of MHC. *Evolutionary Anthropology: Issues, News, and Reviews* **14**: 28-37.
- Kopelman NM, Mayzel J, Jakobsson M, Rosenberg NA, Mayrose I (2015). Clumpak: a program for identifying clustering modes and packaging population structure inferences across K. *Molecular Ecology Resources* **15**: 1179-1191.
- Li H, Durbin R (2009). Fast and accurate short read alignment with Burrows-Wheeler transform. *Bioinformatics* **25**: 1754-1760.
- Li H, Handsaker B, Wysoker A, Fennell T, Ruan J, Homer N, Gabor M, Abecasis G, Durbin R (2009). The sequence alignment/map format and SAMtools. *Bioinformatics* **25**: 2078-2079.
- Li H (2013). Aligning sequence reads, clone sequences and assembly contigs with BWA-MEM. *Preprint at arXiv:13033997v2*.
- Loiseau C, Zoorob R, Robert A, Chastel O, Julliard R, Sorci G (2011). *Plasmodium relictum* infection and MHC diversity in the house sparrow (*Passer domesticus*). *Proceedings of the Royal Society of London Series B, Biological Sciences* **278**: 1264-1272.
- Maan ME, Seehausen O (2011). Ecology, sexual selection and speciation. *Ecology Letters* **14**: 591-602.
- Mallet J, Meyer A, Nosil P, Feder JL (2009). Space, sympatry and speciation. *Journal of Evolutionary Biology* **22**: 2332-2341.



- Meléndez-Rosa J, Bi K, Lacey EA (2020). Mating system is correlated with immunogenetic diversity in sympatric species of Peromyscine mice. *PLOS ONE* **15**: e0236084.
- Michalak P, Minkov I, Helin A, Lerman DN, Bettencourt BR, Feder ME, Korol, A.B., Nevo, E. (2001). Genetic evidence for adaptation-driven incipient speciation of *Drosophila melanogaster* along a microclimatic contrast in “Evolution Canyon,” Israel. *Proceedings of the National Academy of Sciences* **98**: 13195.
- Mohammadi SA, Prasanna BM (2003). Analysis of Genetic Diversity in Crop Plants—Salient Statistical Tools and Considerations. *Crop Science* **43**: 1235-1248.
- Norval G, Ross KE, Sharrad RD, Gardner MG (2019). Taking stock: a review of the known parasites of the sleepy lizard, *Tiliqua rugosa* (Gray, 1825), a common lizard endemic to Australia. *Transactions of the Royal Society of South Australia*: 1-19.
- Otto SP, Servedio MR, Nuismer SL (2008). Frequency-dependent selection and the evolution of assortative mating. *Genetics* **179**(4):2091-112
- Peakall P, Smouse R (2012). GenAEx 6.5: genetic analysis in Excel. Population genetic software for teaching and research—an update. *Bioinformatics* **28**: 2537-2539.
- Pearson S, Tobe S, Fusco D, Bull C, Gardner M (2015). Piles of scats for piles of DNA: deriving DNA of lizards from their faeces. *Australian Journal of Zoology* **62**: 507-514.
- Pearson S, Bradford T, Ansari T, Bull C, Gardner M (2016a). MHC genotyping from next-generation sequencing: detailed methodology for the gidgee skink, *Egernia stokesii*. *Transactions of the Royal Society of South Australia* **140**: 244-262.
- Pearson SK, Bull CM, Gardner MG (2016b). *Egernia stokesii* (gidgee skink) MHC I positively selected sites lack concordance with HLA peptide binding regions. *Immunogenetics*: 1-13.
- Pearson SK, Godfrey SS, Schwensow N, Bull CM, Gardner MG (2017). Genes and Group Membership Predict Gidgee Skink (*Egernia stokesii*) Reproductive Pairs. *Journal of Heredity* **108**: 369-378.
- Perini S, Rafajlović M, Westram AM, Johannesson K, Butlin RK (2020). Assortative mating, sexual selection, and their consequences for gene flow in *Littorina*. *Evolution* **74**: 1482-1497.
- Petney T, Bull C (1984). Microhabitat selection by two reptile ticks at their parapatric boundary. *Australian Ecology* **9**: 233-239.
- Piertney S, Oliver M (2006). The evolutionary ecology of the major histocompatibility complex. *Heredity* **96**: 7-21.
- Piza-Roca C, Strickland K, Kent N, Frere CH (2019). Presence of kin-biased social associations in a lizard with no parental care: the eastern water dragon (*Intellagama lesueurii*). *Behavioral Ecology* **30**: 1406-1415.
- Pritchard JK, Stephens M, Donnelly P (2000). Inference of Population Structure Using Multilocus Genotype Data. *Genetics* **155**: 945-959.
- R Core Team (2018). R: a language and environment for statistical computing. R Foundation for Statistical Computing: Vienna, Austria.
- Reece JB, Meyers N, Urry LA, Cain ML, Wasserman SA, Minorsky PV *et al.*, (2011). *Campbell Biology: Australian Version* 9th edn. Person Education Australia.
- Sakamoto T, Innan H (2020). Establishment process of a magic trait allele subject to both divergent selection and assortative mating. *Theoretical Population Biology* **135**: 9-18.
- Savage AE, Zamudio KR (2016). Adaptive tolerance to a pathogenic fungus drives major histocompatibility complex evolution in natural amphibian populations. *Proceedings of*



the Royal Society of London Series B, Biological Sciences **283**:
doi:10.1098/rspb.2015.3115.

- Schad J, Ganzhorn JU, Sommer S, Yoder A (2005). Parasite burden and constitution of Major Histocompatibility Complex in the Malagasy mouse lemur *Microcebus murinus*. *Evolution* **59**: 439-450.
- Schad J, Dechmann DKN, Voigt CC, Sommer S (2012). Evidence for the 'Good Genes' Model: Association of MHC Class II DRB Alleles with Ectoparasitism and Reproductive State in the Neotropical Lesser Bulldog Bat, *Noctilio albiventris*. *PLOS ONE* **7**: e37101.
- Schwensow N, Fietz J, Dausmann K, Sommer S (2008). MHC-associated mating strategies and the importance of overall genetic diversity in an obligate pair-living primate. *Evolutionary Ecology* **22**: 617-636.
- Schwensow N, Dausmann K, Eberle M, Fietz J, Sommer S (2010). Functional associations of similar MHC alleles and shared parasite species in two sympatric lemurs. *Infection, Genetics and Evolution* **10**: 662-668.
- Schwensow N., Mazzone C.J., Marmesat E., Fickel J., Peacock D., Kovaliski J., Sinclair, R., Cassey, P., Cooke, B., Sommer, S. (2017). High adaptive variability and virus-driven selection on major histocompatibility complex (MHC) genes in invasive wild rabbits in Australia. *Biological Invasions* **19**: 1255-1271.
- Sepil I, Lachish S, Hinks AE, Sheldon BC (2013). MHC supertypes confer both qualitative and quantitative resistance to avian malaria infections in a wild bird population. *Proceedings of the Royal Society B: Biological Sciences* **280**: 20130134.
- Servedio MR, Doorn GSV, Kopp M, Frame AM, Nosil P (2011). Magic traits in speciation: 'magic' but not rare? *Trends in Ecology & Evolution* **26**: 389-397.
- Smadja CM, Butlin RK (2011). A framework for comparing processes of speciation in the presence of gene flow. *Molecular Ecology* **20**: 5123-5140.
- Smallridge CJ, Bull CM (1999). Transmission of the blood parasite *Hemolivia mariae* between its lizard and tick hosts. *Parasitology Research* **85**: 858-863.
- Smallridge CJ, Bull CM (2000). Prevalence and intensity of the blood parasite *Hemolivia mariae* in a field population of the skink *Tiliqua rugosa*. *Parasitology Research* **86**: 655-660.
- Spurgin LG, Richardson DS (2010). How pathogens drive genetic diversity: MHC, mechanisms and misunderstandings. *Proceedings of the Royal Society of London Series B, Biological Sciences* **277**: 979-988.
- Srithayakumar V, Castillo S, Rosatte RC, Kyle CJ (2011). MHC class II DRB diversity in raccoons (*Procyon lotor*) reveals associations with raccoon rabies virus (*Lyssavirus*). *Immunogenetics* **63**: 103-113.
- Staines M, Bradford T, Graves SR, Bull S, Gardner MG (2020). Proposing a new hypothesis: *Rickettsia* spp. as a mechanism maintaining parapatry between two Australian reptile tick species. *Austral Ecology* **45**: 488-492.
- Thorvaldsdóttir H, Robinson JT, Mesirov JP (2013). Integrative Genomics Viewer (IGV): high-performance genomics data visualization and exploration. *Briefings in Bioinformatics* **14**: 178-192.
- Wenzl P, Carling J, Kudrna D, Jaccoud D, Huttner E, Kleinhofs A *et al.*, (2004). Diversity Arrays Technology (DArT) for whole-genome profiling of barley. *Proceedings of the National Academy of Sciences of the United States of America* **101**: 9915.



- Westerdahl H, Waldenström J, Hansson B, Hasselquist D, von Schantz T, Bensch S (2005). Associations between malaria and MHC genes in a migratory songbird. *Proceedings of the Royal Society B: Biological Sciences* **272**: 1511.
- Xu B, Yang Z (2013). PAMLX: a graphical user interface for PAML. *Molecular Biology and Evolution* **30**: 2723-2724.
- Yang Z, Nielsen R (2002). Codon-substitution models for detecting molecular adaptation at individual sites along specific lineages. *Molecular Biology and Evolution* **19**: 908-917.
- Yang Z, Wong WS, Nielsen R (2005). Bayes empirical Bayes inference of amino acid sites under positive selection. *Molecular Biology and Evolution* **22**: 1107-1118.
- You N, Murillo G, Su X, Zeng X, Xu J, Ning K *et al.*, (2012). SNP calling using genotype model selection on high-throughput sequencing data. *Bioinformatics* **28**: 643-650.
- Zaykin DV, Pudovkin A, Weir BS (2008). Correlation-based inference for linkage disequilibrium with multiple alleles. *Genetics* **180**: 533-545.
- Zelano B, Edwards S, xa, V (2002). An MHC Component to Kin Recognition and Mate Choice in Birds: Predictions, Progress, and Prospects. *The American Naturalist* **160**: S225-S237.
- Zhang J, Kobert K, Flouri T, Stamatakis A (2014). PEAR: a fast and accurate Illumina Paired-End reAd mergeR. *Bioinformatics* **30**: 614-620.
- Zhang L, Wu Q, Hu Y, Wu H, Wei F (2015). Major histocompatibility complex alleles associated with parasite susceptibility in wild giant pandas. *Heredity* **114**: 85-93.
- Zhang M, He H (2013). Parasite-mediated selection of major histocompatibility complex variability in wild Brandt's voles (*Lasiopodomys brandtii*) from Inner Mongolia, China. *BMC Evolutionary Biology* **13**: 149-163.



Chapter 1: Supplementary Material

Below are some analyses that were performed when exploring the MHC and SNP data but are not the focus of the manuscript.

MHC

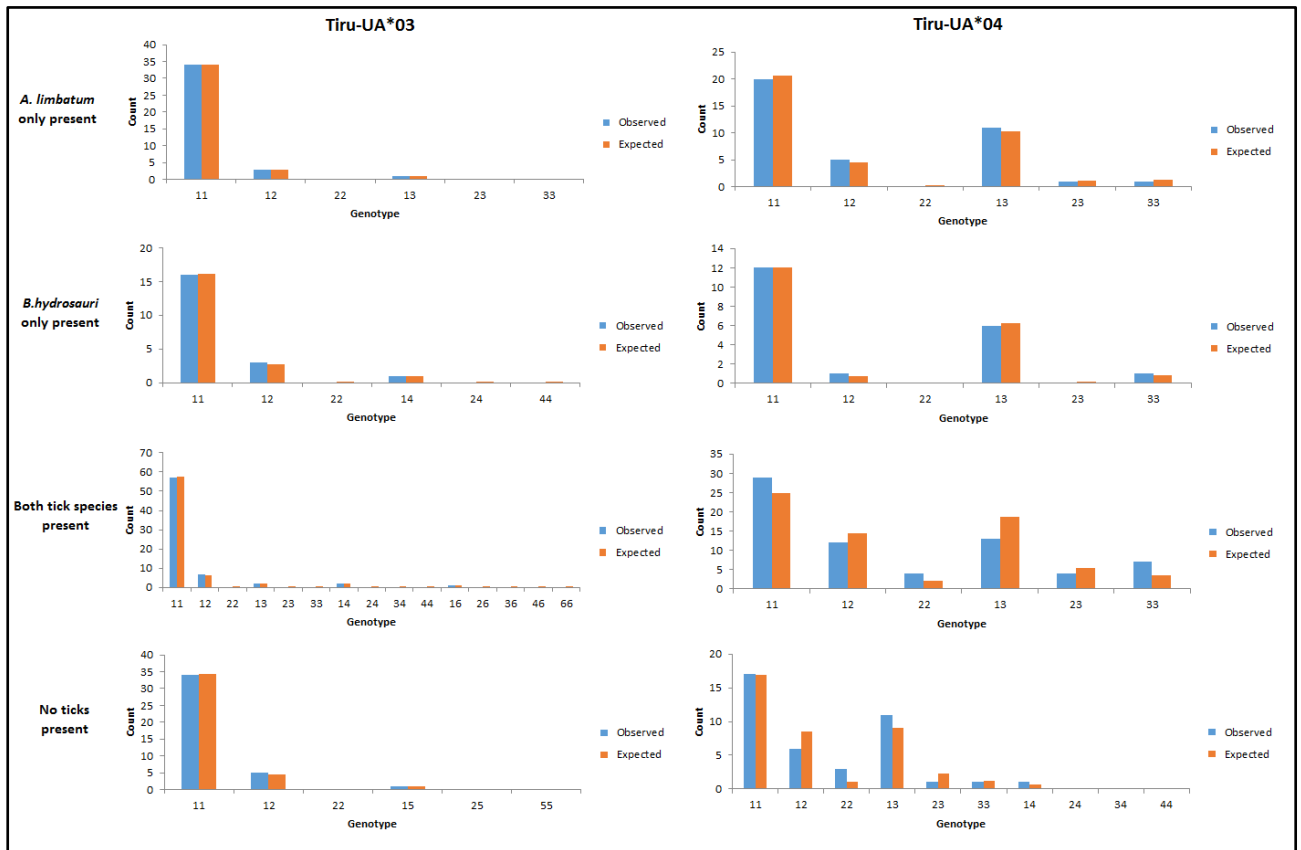


Figure S1: Expected heterozygosity and observed generated in GenAlex on loci **Tiru-UA*03** and **Tiru-UA*04** MHC class I data, for each group (*Amblyomma limbatum* only present, *Bothriocroton hydrosauri* only present, Both tick species present, and no ticks present).



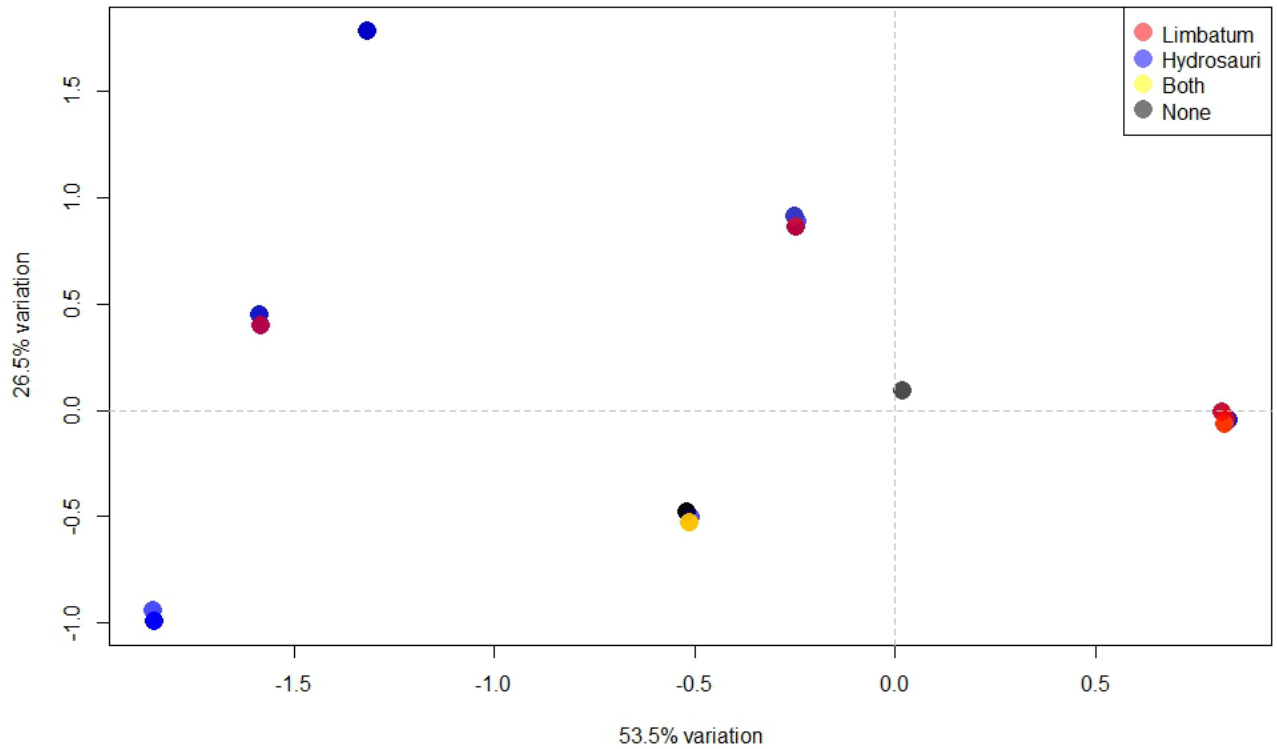


Figure S2: Principal component analysis (PCA) using MHC data of two loci (Tiru-UA*03; Tiru-UA*04) and 165 individual *Tiliqua rugosa* grouped by tick species attached when captured. Red = *Amblyomma limbatum*; Blue = *Bothriocroton hydrosauri*; Yellow = Both ticks present; Grey = No ticks present.



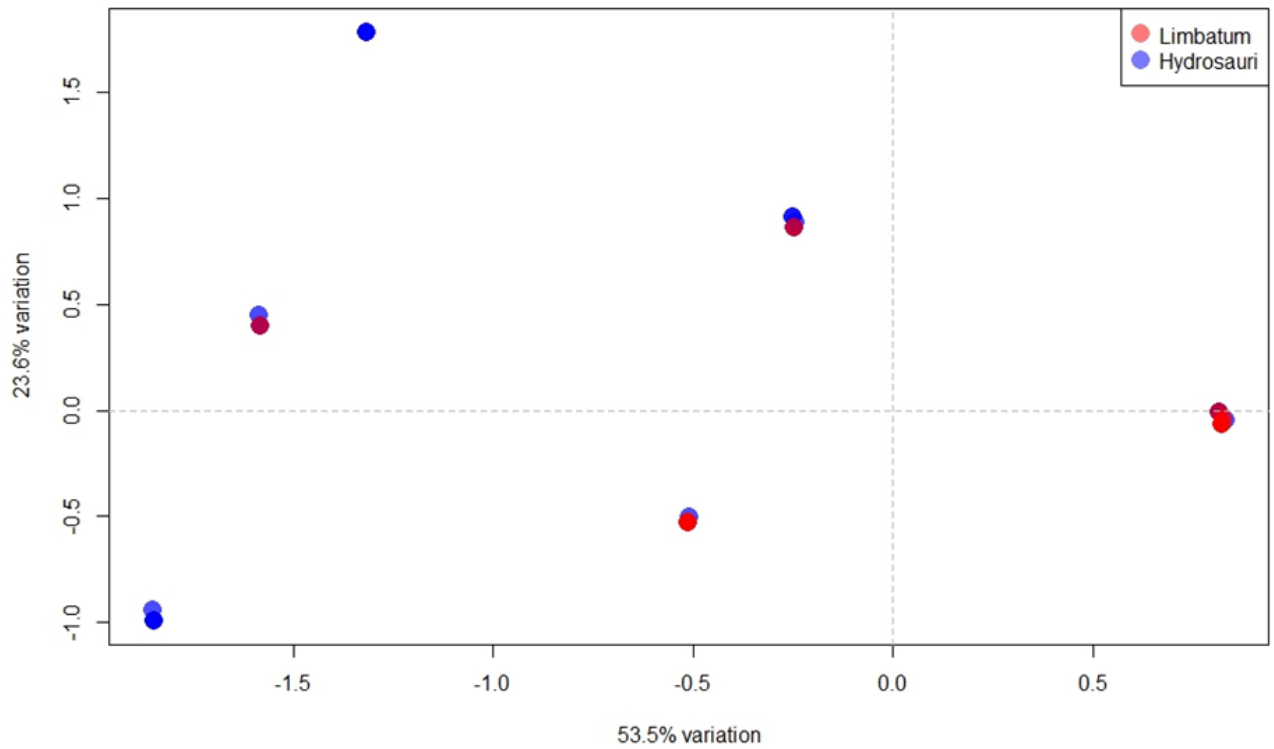


Figure S3: Principal component analysis (PCA) using MHC data of two loci (Tiru-UA*03; Tiru-UA*04) and two groups at either side of the parapatric boundary. Red = *Amblyomma limbatum*; Blue = *Bothriocroton hydrosauri*



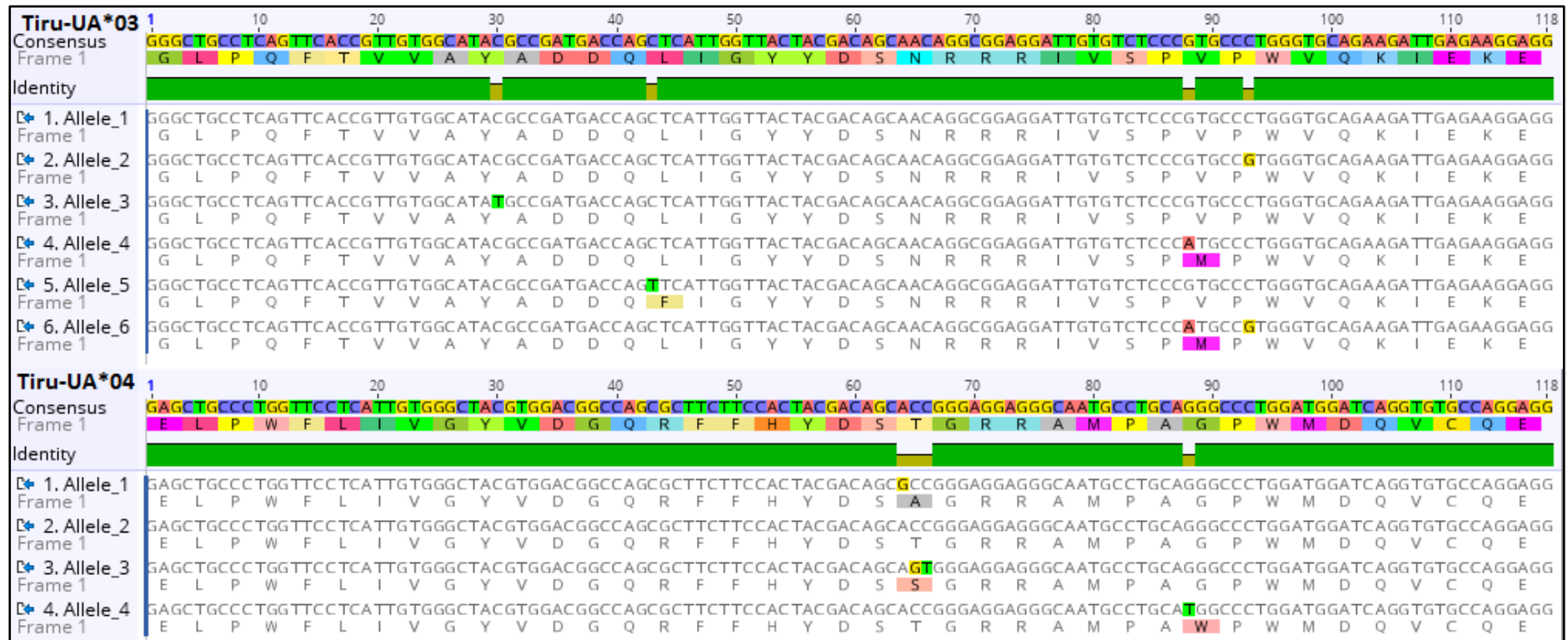


Figure S4: Alignment of the two MHC class I loci genotyped, Tiru-UA*03 and Tiru-UA*04, showing Synonymous and non-synonymous substitutions. The small, highlighted letters indicate a nucleotide substitution. The large, highlighted letter blocks indicate where a nucleotide substitution resulted in a change in an amino acid.



Table S1: F-statistics of each group for both MHC class I loci (Tiru-UA*03; Tiru-UA*04) genotyped in this study on *Tiliqua rugosa*

Group	Locus	F _{ST}
<i>A. limbatum</i> only present	Tiru-UA*03	-0.045
	Tiru-UA*04	-0.073
<i>B. hydrosauri</i> only present	Tiru-UA*03	-0.065
	Tiru-UA*04	0.246
Both tick species present	Tiru-UA*03	-0.088
	Tiru-UA*04	0.024
No tick present	Tiru-UA*03	-0.069
	Tiru-UA*04	0.087
Overall	Tiru-UA*03	0.005
	Tiru-UA*04	0.019

Table S2: F-statistics (F_{ST}) of *Tiliqua rugosa* MHC class I loci grouped by tick species attached at the time of sampling.

Group	Group	Fst
<i>A. limbatum</i>	<i>B. hydrosauri</i>	0.012
<i>A. limbatum</i>	Both tick species present	-0.010
<i>B. hydrosauri</i>	Both tick species present	0.000
<i>A. limbatum</i>	No tick present	0.020
<i>B. hydrosauri</i>	No tick present	-0.007
Both tick species present	No tick present	0.009

Table S3: Heterozygosity vs Homozygosity contingency tables Fisher's Exact (P values) for each loci between groups

Pairwise Contingency tables	Tiru-UA*03	Tiru-UA*04
<i>A. limbatum</i> vs No ticks present	0.735	1.000
<i>A. limbatum</i> vs <i>B. hydrosauri</i>	0.417	0.838
<i>A. limbatum</i> vs Both tick species present	0.417	0.393
<i>B. hydrosauri</i> vs Both tick species present	0.744	0.442
<i>B. hydrosauri</i> vs No ticks present	0.795	0.686
Both tick species present vs No ticks present	0.714	0.280
Between all groups	0.730	0.694

DARTSeq



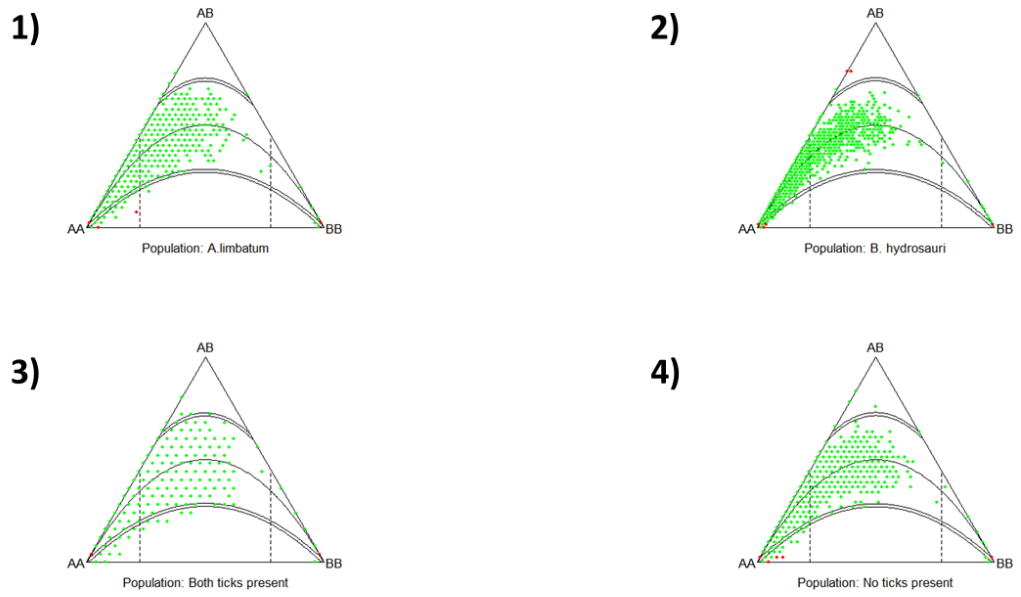


Figure S4: Figure represents Hardy-Weinberg Equilibrium analysis of SNP data for all *Tiliqua rugosa* groups (1 = *Amblyomma limbatum* group; 2 = *Bothriocroton hydrosauri* group; 3 = Both ticks present; 4 = No ticks present). Red dots indicate loci that deviate from Hardy-Weinberg Equilibrium



Chapter 2: Foreword

Chapter 2 uses a novel technique to observe viral abundance variations in a reptile, across an ecological gradient at the study site in Mount Mary, South Australia. The chapter aims to determine whether the selective pressures observed in Chapter 1 could be the result of viruses in the system that are not associated with the two tick species in the study site. As the only known viruses in this species currently are respiratory viruses, samples were taken as if screening for those viruses.



Chapter 2: Viral abundance and sub-population variation in *Tiliqua rugosa* over an ecological gradient using flow cytometry

Robert L. O'Reilly¹, James S. Paterson¹, Jim G. Mitchell¹ and Michael G. Gardner¹

¹Flinders University, Bedford Park, Adelaide, SA, Australia

Corresponding author: robert.liam.oreilly@gmail.com

Keywords: Reptile virology, Viruses, Lizard, Flow cytometry, Ecological variation



Abstract

Environmental conditions influence viral and bacterial communities in the environment and host. Fluctuating conditions require hosts to be able to tolerate changing pathogen diversity and abundance to survive. We examined the viral communities in the oral cavity of an iconic Australian reptile, the sleepy lizard (*Tiliqua rugosa*), over an ecological gradient of arid to humid environmental conditions with the use of flow cytometry. We found two viral, a bacterial and an unknown sub-population. One viral sub-population was found in 97% of lizards, with high abundance in 52% of those lizards. The second viral sub-population was found in all individuals, but only in high abundance in 21% of lizards. There were significant differences in Virus 1 abundances between the arid north-east of the site and the middle of the site — concordant with a tick parapatric boundary ($p = 0.003$). As there are currently only a serpentinovirus and adenovirus known to infect this species, yet to be confirmed in South Australia, and since two sub-populations were discovered in our system, we propose it could represent these two viruses infecting this host. This study presents a novel approach in determining viral communal abundances in relation to varying ecological environments in an Australian reptile. These data further add to the understanding of reptile virology and the relationship pathogens have with their host's external environment.



Introduction

Disease ecology is increasingly viewed as critical research in understanding and identifying emerging and re-emerging pathogens. The field has diversified over the years to include parasitology, virology, epidemiology, immunology, even sociology and spatial behaviour (Albery *et al.*, 2021; Brandell *et al.*, 2020; Garchitorena *et al.*, 2017; Wilcox and Gubler 2005). One study by Giles *et al.*, (2018) highlights the importance of monitoring spatial behaviour and climate fluctuations in a host with known pathogens. Giles *et al.*, (2018) associated a change in migration of the grey-headed flying fox (*Pteropus poliocephalus*) in search of flowering Eucalypt trees, during an El Niño event, to unprecedented clusters of spillover events of the Hendra virus (*Hendra henipavirus*) in NSW and QLD. Grey-headed foxes are a reservoir for this zoonotic virus, and while the virus cannot be transmitted to humans from bats, as it needs horses as an amplifier, these shifting migration patterns in response to climate change are a concern for those in the equine industry. This extreme example shows the importance of monitoring animal movement in relation to climate shift. This is particularly important in ectotherms which rely on external environmental conditions for biological and immunological function (Zimmerman 2016).

Reptiles have been known to change their behaviour by basking for longer in order to increase their body temperature when infected with a disease, in an attempt to increase their core temperatures allowing greater immune response (Rakus *et al.*, 2017; Vaughn *et al.*, 1974). One study by Longo and Zamudio (2017) has shown temperature fluctuations in the common Coquí (*Eleutherodactylus coqui*) gives a survival advantage to host in warm-wet season, and disadvantage or increased susceptibility to the fungal pathogen *Batrachochytrium dendrobatidis* (Bd) during cool-dry conditions. Environmental conditions also influence viral and bacterial communities in both the external environment as well as internal. The influence could be either direct (where the virus cannot survive outside of the host in certain conditions, i.e. dry, humid, cool) or indirect (where the environment affects the transmission vectors, e.g. ticks and mosquitos) or hosts. Mosquitos, for example, are well known vectors for a multitude of viruses, and their distribution touches every continent around the world except Antarctica. As global temperature increases, there is concern that mosquito distributions will shift bringing disease to previously uninfected areas (Reinhold *et al.*, 2018).



As the COVID-19 pandemic has highlighted, viruses can move fast and evolve rapidly given the right circumstances. Being able to determine viral ‘hot spots’ or abundances is an important and crucial part of viral ecology. Traditionally this has been done with virus isolation cultures and counts however, this is time consuming and can be difficult on newly emerged viruses without much information — particularly in reptiles where reptilian cell lines need to be sourced (Ariel 2011; Brussaard 2004). Another method which can give highly precise counts of virus particles, while having the flexibility of specificity or non-specific targeting is flow cytometry. Flow cytometry uses the forward and side scatter of wavelengths to distinguish both horizontal and vertical measurements of particles (Adan *et al.*, 2017). By measuring the number of particles within known volumes over a defined amount of time, flow cytometry has many uses. This technique has been adapted for characterising immunological cells in reptiles (de Carvalho *et al.*, 2017; Zimmerman Laura *et al.*, 2010); determining lymphoma cells in canines (Comazzi and Riondato 2021; Riondato and Comazzi 2021); and even viral and bacterial communities abundances in the mouths of children (Carlson-Jones *et al.*, 2020). The use of flow cytometry for viral abundance is a novel and efficient way to assess viral abundances in different environments.

Here, we examined the viral abundance and sub-population structure of a *Tiliqua rugosa* population in the mid north region of South Australia using a novel flow cytometry technique. This site has been thoroughly researched since 1981 (Bull *et al.*, 1981; Godfrey and Gardner 2017). The study site, 12km by 12km, has an ecological gradient ranging from arid in the north-east to more humid with more leaf litter (largely from *Eucalyptus*) in the southwest (Petney and Bull 1984), and is concordant with a tick parapatric boundary (Bull *et al.*, 1981). A parapatric boundary is defined as an area where two species’ ranges abut and the species do not hybridise (Bull and Possingham 1995). The tick species in the southwest region, *Bothriocroton hydrosauri*, is prone to desiccation in dry conditions and therefore limited in moving north-west. This north-west arid region is inhabited by another tick species, *Amblyomma limbatum* (Petney and Bull 1984). It is still not yet known what inhibits *A. limbatum* from moving further south.

The ecological variation across the site would enable varying pathogen pressures on their hosts, particularly at the vector stage of transmission (such as ticks) — which is influenced heavily by environmental conditions (Harvell *et al.*, 2002; Rohr and Cohen 2020). Previous



studies found variation in transmission and susceptibility of pathogens and parasites across the parapatric boundary at the site. Studies which include the transmission of *Salmonella enterica* over *T. rugosa*'s social networks (Bull *et al.*, 2012); susceptibility differences of a blood parasite (*Hemolivia mariae*) (Smallridge and Bull 1999) and the zoonotic bacteria *Rickettsia* spp. (Staines *et al.*, 2020) in these two reptile ticks; to the prevalence of the blood parasite in *T. rugosa* transmitted via the ectoparasites (Smallridge and Bull 2000). Genetic research of *T. rugosa* have found allele frequency variations and positive selection occurring on the Major Histocompatibility Complex (MHC) class I immune genes, in the south-west region of the site, where *B. hydrosauri* inhabit (Chapter 1).

The MHC class I is an antigen recognition molecule in all vertebrates that identifies viruses and triggers an immune response (Knapp 2005; Wieczorek *et al.*, 2017). Currently, there are only two known viruses that infect this genus, a serpentovirus (*Shingleback nidovirus 1*), that was previously classified as a coronavirus and has been associated with an upper respiratory tract disease labelled the "bobtail flu" (O'Dea *et al.*, 2016). The second virus is an adenovirus, that is also believed to be contributing to the disease (Hyndman and Shilton 2018). The transmission variations observed, along with the selection pressure differences of immune genes associated with viral recognition across the ecological gradient, could indicate there are differences in viral abundance at the site applying varying selection pressures on these lizards. Therefore, we aim to determine if there was any viral abundance and sub-population variation in relation to the ecological gradient or associated with the parapatric boundary in these lizards.



Methods

Sample collection

Samples were obtained by driving along predetermined transects (Bull *et al.*, 1981) at a study site near Mount Mary, South Australia (-33.922222°, 139.284167°) (Figure 1). Individual lizards were captured along these transects by using the random encounter method where any seen while driving the transects are captured. The random encounter method reduces selection bias and does not require trapping or baiting (Bull and Burzacott 2001). Captured lizards had GPS location taken before an oral swab of the glottis (Figure 2). The 80 mm flocked swabs were rotated 360° on the glottis, twice for all swabs, before being placed in 1.5 mL cryovials (O’Dea *et al.*, 2016). The cryovials contained 1 mL of sterile phosphate buffered saline (PBS) and samples were snap-frozen in liquid nitrogen on location, then stored at -80°C on return to the laboratory (Carlson-Jones *et al.*, 2020). No animals sampled in this chapter showed any clinical symptoms of illness. Samples obtained in this chapter are new, they do not correspond to samples in chapter 1.

Sample preparation

Frozen samples were thawed in ice to prevent particle damage, and then vortexed for 2 minutes to elute all particles into solution. The 1 mL solution was then transferred to a new vial and glutaraldehyde was added (0.5% final concentration) before the sample was kept in the dark for 15 minutes. Glutaraldehyde is used as a fixative, which has been shown to successfully inactivate various infectious agents, such as bacteria and viruses, while maintaining particle structure (Brussaard 2004; Graham and Jaeger 1968; Rittenbury and Hench 1965). Samples were diluted in TE buffer (10 mM Tris, 1mM EDTA) at 1:10 however, fourteen samples required further dilution (1:100) based on their preliminary flow cytometry data ([Abundance summary](#)). The samples were then stained using SYBR Green I (1:20,000 dilution, Molecular Probes, USA) and incubated for 10 minutes at 80°C, as previously optimised for visualisation in (Brussaard 2004; Carlson-Jones *et al.*, 2016; Paterson *et al.*, 2012). Control samples were sterile swabs prepared consistently to lizard swab samples. All samples, including controls, were analysed in triplicate (Carlson-Jones *et al.*, 2020).



Flow Cytometry Analysis

Samples were analysed on a CytoFLEX S (Beckman Coulter) using a violet laser (405 nm wavelength) to measure the light scatter (SSC and FSC), while green fluorescence was measured using the blue laser (488 nm wavelength). Viral and bacterial sub-populations were differentiated based on their differences in side-scatter, a proxy of size, and SYBR Green fluorescence, a proxy for the amount of nucleic acid present in each cell or particle (Brussaard 2004). The parameters were set to run at 10 $\mu\text{L}/\text{min}$ for two minutes (Carlson-Jones *et al.*, 2016). Regions were identified from clustering of particles cytograms in the software program FlowJo™ version 10 (Becton 2021) using ‘gates’ and applied across all samples (including controls) and all sessions before calculating abundances. Abundances were calculated in Excel (version 2205) where analysis consisted of first determining the background noise averages for each region. These noise values were then subtracted from the sample before scaling up from 20 μL , to amount per tube (1 mL), and then to environment (tube \times dilution). The regions were averaged using each sample triplicate. Ordinal variables for prevalence analysis were defined using the top third of the abundance counts as ‘High’ (High = $>3.72 \times 10^6$ particles per mL). The bottom third of abundance counts as ‘Low’ (Low = $<3.11 \times 10^6$ particles per mL), while the ‘Medium’ was in between (Medium = $3.11 \times 10^6 - 3.72 \times 10^6$ particles per mL).

Spatial and Statistical Analysis

Abundance data and GPS coordinates for each individual lizard was imported into QGIS version 3.3 (QGIS Development Team 2022) to visually observe regional abundances spatially across the study site to determine if ecological variation influenced viral communities — i.e. identify if there were “hot spots”. Abundance data for each region, for each lizard sample, were converted to raster data before performing an Inverse Weighted Distance (IWD) interpolation (weighting power = 2.000). This analysis infers abundances of missing data across the study site, by giving more weight to points with data while giving less weight the further from a data point. The assumption with inverse weighted interpolation is that conditions change the more distance from the data point’s local conditions (Shepard 1968). Interpolation analysis have previously been used for epidemiology in human studies, as a way to account for irregularly spaced data points to provide continuous patterns (Blanco *et al.*, 2017; Hoek *et al.*, 2001; Messina *et al.*, 2011).



Due to the sample distribution with a large area of missing data points in the north-west area of the map, a buffer layer was created for each data point with a 3 km radius. The IWD layer was then clipped to the buffer layer to reduce assumptions made with missing data over the large area. Statistical analyses were conducted in SPSS (version 25) to determine if there were significant differences between geographic location and viral abundance. A Kruskal-Wallis test was performed using the Monte Carlo correction, on the entire abundance data for each group against each microbiological population. The Kruskal-Wallis test is a non-parametric comparison of variable means that is able to test more than two variables, however it does not tell the direction of significance. A Mann-Whitney U test was then used independently as a post hoc test to corroborate the Kruskal-Wallis, by comparing all combinations of groups and subpopulation regions.

To estimate where the parapatric boundary line lies between sides for grouping, a polynomial line of best fit (order of 6) was used on lizard samples obtained in Chapter 1, that had both ticks attached to a lizard. Having both ticks attached indicates the current parapatric boundary line at the time of sampling — due to the limitation of *B. hydrosauri*'s movement north-east into arid conditions. This estimate, along with using satellite data to assess the vegetation surrounding the sample, determined which group the sample belonged to. Mallee scrub indicates higher rain fall or proximity to a water source (e.g. dam) which could affect viral abundances in that area. Samples north-east of the boundary line were grouped as '*A. limbatum* side', while samples south-west of the boundary line were grouped '*B. hydrosauri*', and those within 1 km either side were grouped as 'near boundary'. This was because the boundary has been known to shift ~1 km depending on yearly rainfall (Bull and Burzacott 2001).



Results

Forty-two lizards had an oral swab of the glottis (Figure 2), taken across the study site (Figure 1) during September – November 2019. Of those 42 lizards, fourteen had duplicate swabs collected for comparison. Sample sizes per group consisted of northern side with *A. limbatum* n = 12, southern side with *B. hydrosauri* n = 12, and those ‘near the boundary’ n = 18. No lizards were found while sampling in the north-west of the study site (Figure 1), although they are known to be in the area.

Using flow cytometry, four distinct sub-populations were identified and labelled as: Virus 1, Virus 2, Bacteria, and Unknown — based on particle size and clustering (Figure 3). Virus 1 (V1) was found in 95.24% of lizards at the time of sampling with 52.38% in high abundance (Table S1). Virus 2 (V2) was detected in all lizards (100%), however only 21.43% were in high abundance (Table S1). Bacteria were found in 92% of individuals, and in the low abundance range (Low = $<3.11 \times 10^6$ cells per mL) (Table S1). The unidentified (unknown) region showed clear population clustering (Figure 3) and was found in 97.62% of lizard samples, of which 33.33% had high abundance (High = $>3.72 \times 10^6$ particles per mL (Figure 5; Table S1).

When grouped by location, ‘near boundary’ had individuals with high abundance of Unknown (16.67%), Virus 1 (72.22%), and Virus 2 (11.11%) (Figure 5; Table S1). Individuals on the arid, *Amblyomma limbatum* side of the boundary, had high abundance of Unknown (41.67%) and Virus 1 (16.67%). There were no individuals that had a high abundance of Virus 2 however, 81.67% had a low level, with 8.33% of medium abundance (Medium = 3.11×10^6 – 3.72×10^6 particles per mL). The *B. hydrosauri* side, had a high abundance of Unknown (50%), Virus1 (58.33%), and Virus 2 (58.33%) (Figure 5; Table S1). All individuals in each group had low abundance of bacteria (Low = $<3.11 \times 10^6$ cells per mL). A Kruskal-Wallis test, with a Monte Carlo correction returned a significant result (H = 8.23, df = 2, p = 0.014) (Table 1) between ‘near boundary’ group and ‘*A. limbatum* side’. The post hoc Mann-Whitney U test showed significance (U = 41.000, p = 0.015) between those collected on the ‘*A. limbatum* side’ and ‘Near boundary’ for Virus 1 (Table 2).

Discussion

These results support the prediction that there are viruses in this system with varying abundances, potentially influencing MHC immune gene diversity disproportionately across



the study site (Chapter 1). We found two distinct viral sub-populations in this system, as well as bacteria, and unidentified (unknown) region. Both of the viral sub-populations were in more than 95% of individuals across the site. Virus 1 was found to be in higher abundance within individuals (52.38%) compared to Virus 2 (21.43%). Although Virus 2 was in higher prevalence (100%) than Virus 1 (95.24%). When comparing viral abundance levels within grouped lizards, the higher abundance level observed was predominantly found on the humid southern side — where *B. hydrosauri* occurs (Figure 5). The higher viral abundance in the southwest of the site coincides with the selective pressures on MHC class I genes found in Chapter 1. It is well known that pathogen richness and diversity has previously been linked to MHC's high polymorphism and influence the selective processes that maintain it (Prugnolle *et al.*, 2005, Spurgin and Richardson 2010). A study by Wang *et al.*, (2017) was able to show a direct link to the abundance levels of two specific amphibian viruses (*Frog virus 3* and *Ambystoma tigrinum virus*) and observed positive selection on the MHC class I in the black-spotted pond frog (*Pelophylax nigromaculatus*). Therefore, it is logical that the disproportionate viral abundances seen in our study could also be influencing the host's genetics in this study system.

Although analyses between the northeast and southwest of the site, 'A. limbatum side' and 'B. hydrosauri side' respectively, showed non-significance with Virus 1 ($p = 0.076$) and Virus 2 ($p = 0.068$) (Table S4), it is still suggestive of a difference between the sides of the study site. Particularly when considering comparative analyses of 'Near Boundary' and 'B. hydrosauri side' revealed Virus 1 ($p = 0.369$) and Virus 2 ($p = 0.196$) to be highly non-significant. It is likely that 'Near Boundary' and 'B. hydrosauri side' are similar in climate conditions as *B. hydrosauri* ticks desiccate in the arid environment. The significant ($p = 0.003$) difference between 'Near Boundary' and 'A. limbatum side' (Table S3) is explained as a result of the change from humid region into the arid conditions of the northeast that coincides with the parapatric boundary (Bull and Burzacott 2001). Ambient humidity and temperature do influence virus viability, particularly respiratory viruses (Pica and Bouvier 2012). However, there are inconsistencies in the literature on specifics (Pica and Bouvier 2012, Yang and Marr 2012). General consensus seems to be that enveloped viruses survive better than nonenveloped when in aerosol form (Yang and Marr 2012). As the swabs in our study were of the glottis, a part of the upper respiratory system, it is likely that Viruses 1



and 2 are respiratory viruses (Parrish *et al.*, 2021; Schumacher 2011). Currently, there are only two known viruses identified in *T. rugosa*, the *Shingleback nidovirus 1* (ShNV1) (O’Dea *et al.*, 2016), and an adenovirus (Hyndman and Shilton 2018) — both of which are respiratory viruses. The *Shingleback nidovirus 1* has been associated with an upper respiratory tract infection in these lizards, termed “the bobtail flu”. It is a single strand positive RNA virus with an enveloped capsid and is highly transmissible between individuals (O’Dea *et al.*, 2016). The adenovirus is a non-enveloped double strand DNA virus also thought to be contributing to the bobtail flu (Hyndman and Shilton 2018). If the viral sub-populations found in this study are identified in the future with metagenomics as these two viruses, perhaps the structural differences (and therefore viability differences) between these viruses, such as enveloped vs non-enveloped, could explain the patterns observed here (Figure 4; Figure 5). Future research will screen samples for these viruses.

If these viruses are identified as the known serpentovirus and adenovirus, this study would then provide epidemiological information on how these viruses’ abundances are influenced in the rural Australian Outback. Currently there is no published information on the ShNV or the adenovirus in the wild such as distribution, abundances, or viability. However, the lizards swabbed in this study showed none of the clinical signs of being infected by a respiratory virus (O’Dea *et al.*, 2016; Schumacher 2011). Research at this Mt Mary study site has been continuously conducted on *T. rugosa* over the past 40 years as part of a long-term study system (Bull *et al.*, 1981; Godfrey and Gardner 2017). There have been very few observations of any lizards showing clinical symptoms of the bobtail flu (Smyth *et al.*, 2014). Although, the ShNV has been found to be asymptomatic in 12% of individuals (O’Dea *et al.*, 2016), it is more likely given the >95% infection of both viruses found in our study while displaying no symptoms, that these are newly discovered viruses in this species. In which case, our study would provide the first record of these novel viruses in *T. rugosa*.

One caveat with this study’s method is the inability to give species level identification of the viruses and identify the unknown sub-population (Figure 3). Unfortunately, without the identification of these viruses there are too many unknowns to postulate with any support. Future research must first identify the viruses. Using currently available primers and probes, samples could be screened for the ShNV and Adenovirus using reverse transcription real-time PCR (RT-qPCR) (O’Dea *et al.*, 2016) or by adapting a recently developed and highly



sensitive flow cytometry method (Paterson *et al.*, 2022). However, as these viruses are likely novel, a common method to identify new viruses is using metagenomics (Houldcroft *et al.*, 2017, Thomson *et al.*, 2016). Once the viruses are identified, research could explore how the transmission of the viruses occurs, such as examining whether the viruses modes of transmission are of one four common modes of respiratory viruses: contact, fomite, droplets, or aerosols (Leung 2021). Transmission could occur in this species from refuge sharing (Kerr *et al.*, 2003); or via social networks that has previously been shown to spread pathogens (Bull *et al.*, 2012); tick vectors (Bouma *et al.*, 2007); or even their food source (these lizards are opportunistic omnivores). Future research could also include consistent sampling throughout the season to determine the viral seasonality in response to shifts in humidity and temperature (Fisman 2012, Price *et al.*, 2019). Identifying viral seasonality could also provide insight on whether the infection is chronic or transmitted throughout the season.

Our study highlights how flow cytometry is a robust and cost-effective method to identify microbial abundances in areas that may have varying climates. This study also suggests that using flow cytometry to determine viral abundance and sub-population structure in oral cavity of lizards can be conducted and should be used in conjunction with sequencing technologies. To our knowledge, the use of flow cytometry to determine viral abundance variations over an ecological gradient has never been achieved in reptiles making the use of this method novel. Although the flow cytometry method has been used in humans and human wastewater to calculate viral and bacterial abundances (Carlson-jones *et al.*, 2016, Carlson-jones *et al.*, 2020, Hisee *et al.*, 2020). Our study has potentially discovered two viral sub-populations in this species that may be contributing to the genetic selective pressures seen in these lizards in Chapter 1. Future research will delve into identifying these viruses, identifying the transmission vectors, and exploring whether there are temporal or seasonal fluctuations.



Figures

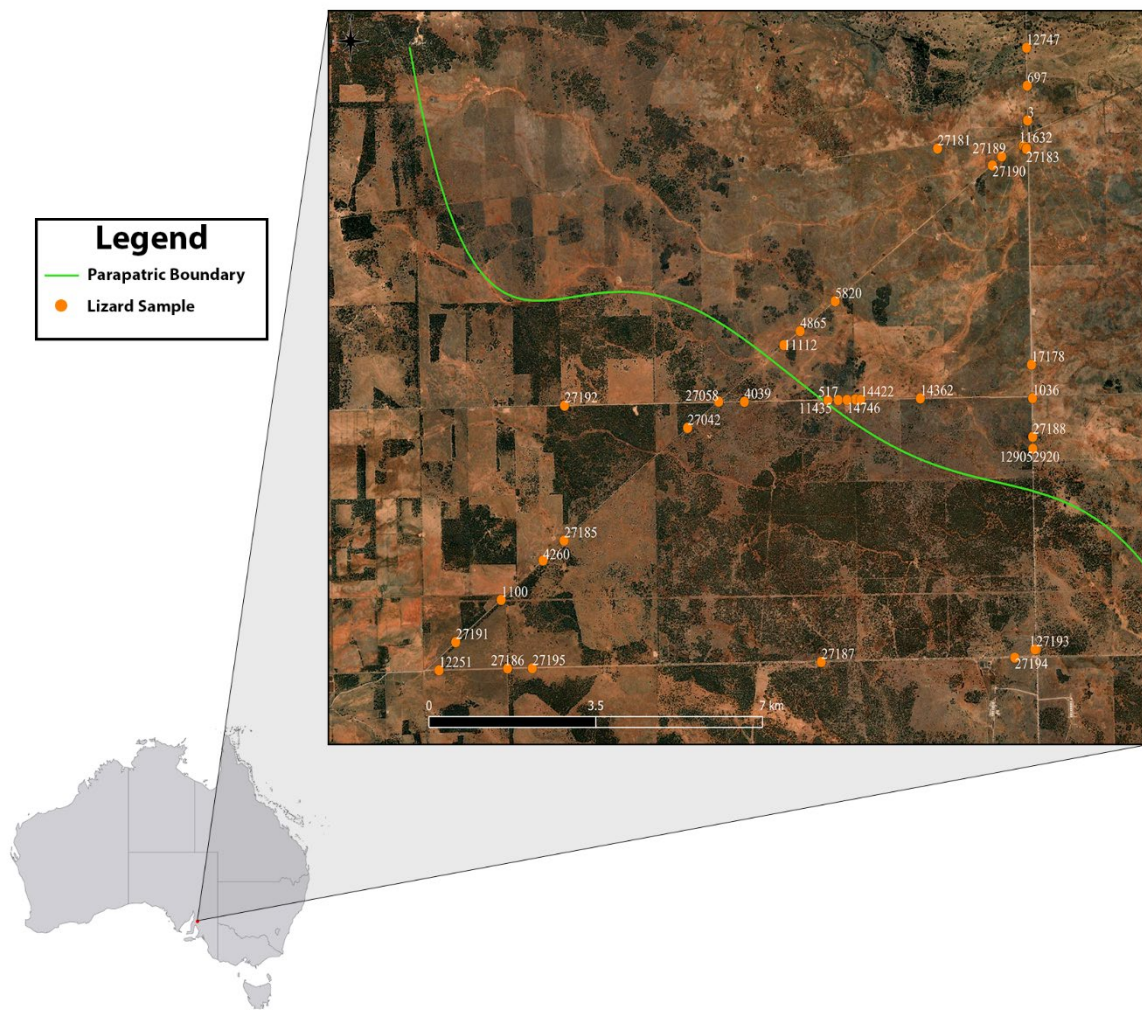


Figure 1: Study site near Mount Mary, South Australia ($-33.928306, 139.291000$) showing oral swab samples collected from *Tiliqua rugosa* (orange). Numbers associated with the orange dots are lizard identification numbers. The parapatric boundary, where tick species *Amblyomma limbatum* and *Bothriocroton hydrosauri* abut, is represented as a green line. The boundary was estimated from previous lizard samples where both tick species were attached to the lizard then using a polynomial line of best fit (order of 6).



Figure 2: Swab sample was in the oral cavity, on the glottis located directly behind the tongue (green arrow). Each swab was rotated 360° on the glottis twice before being stored in 1 mL of Phosphate-buffered saline and snap frozen at -80°C.

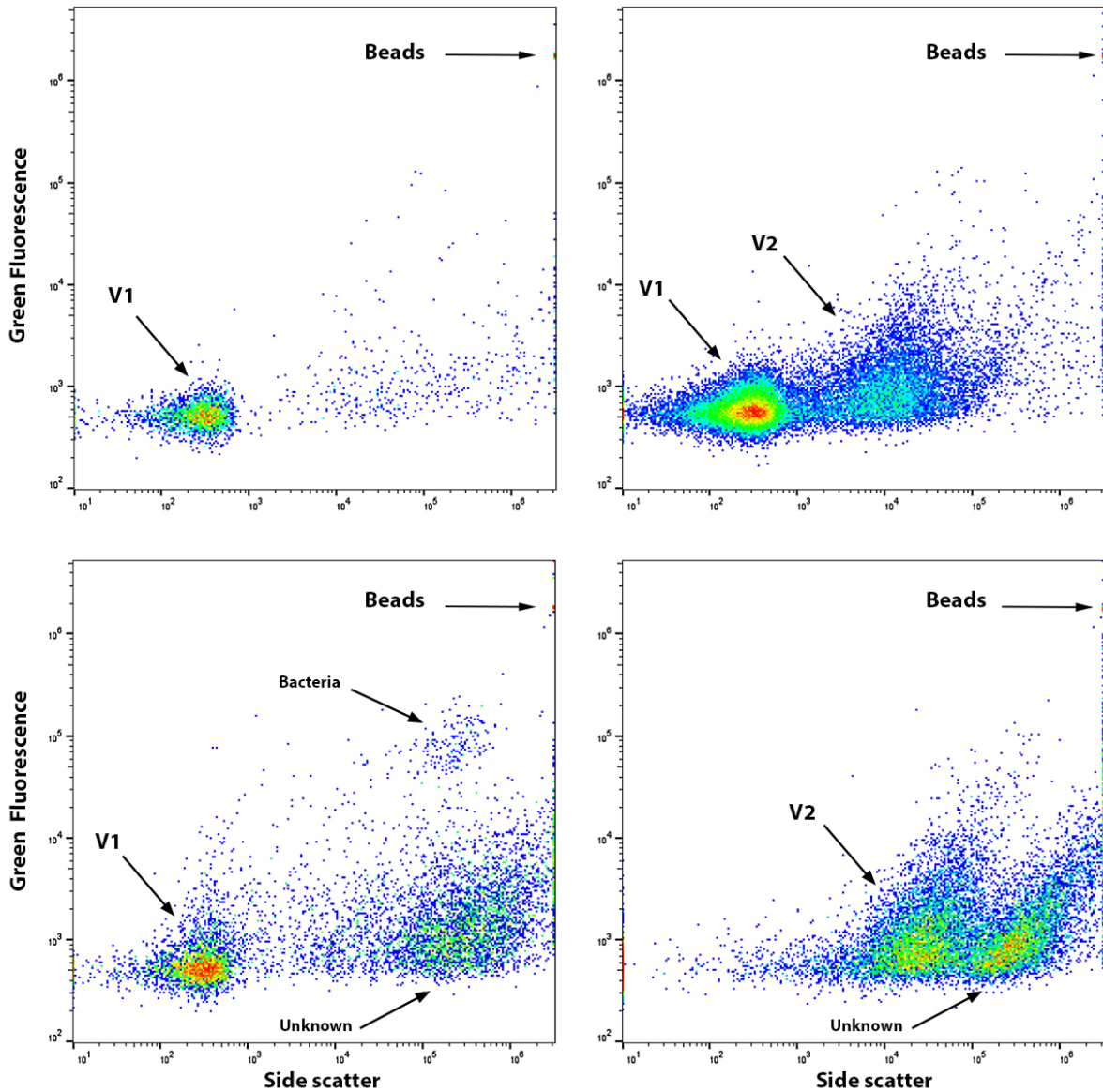


Figure 3: The four microbiological regions found in this study from samples of the glottis of *Tiliqua rugosa* using flow cytometry. X-axis is a standard log axis of the violet side scatter whereas Y-axis is the forward scatter measuring SYBR green fluorescence. V1 =Virus 1, V2 = Virus 2, Bacteria =Bacteria, Unknown = Unidentified region.



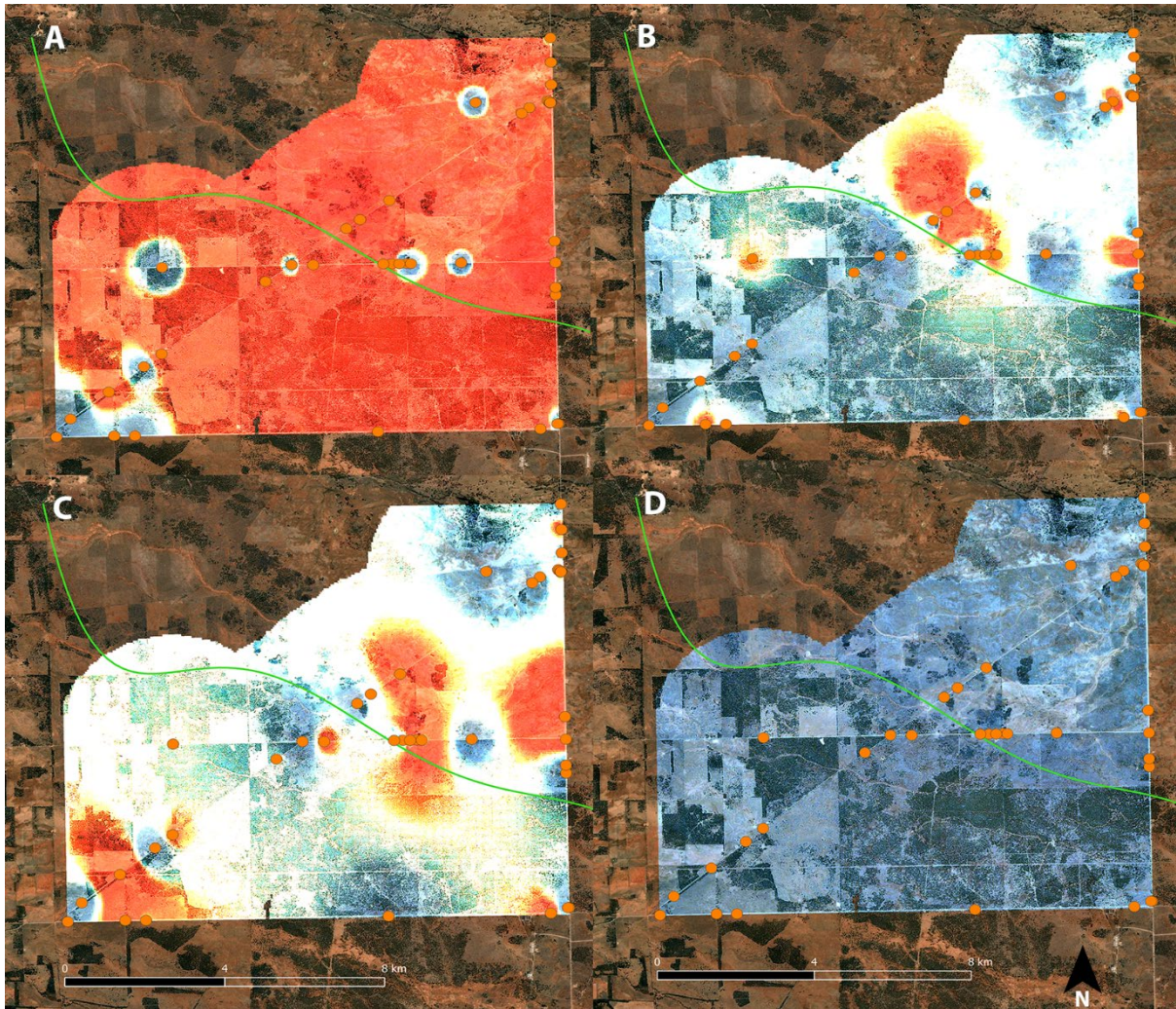
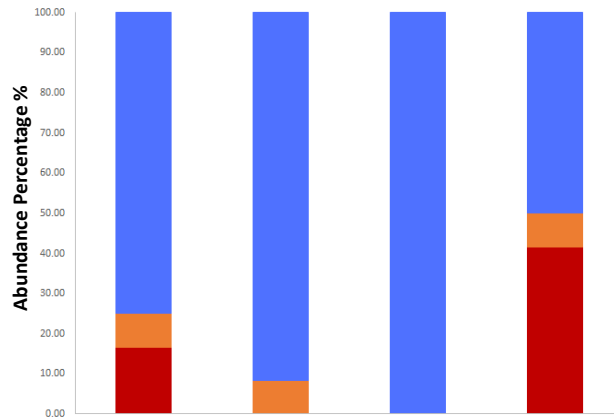
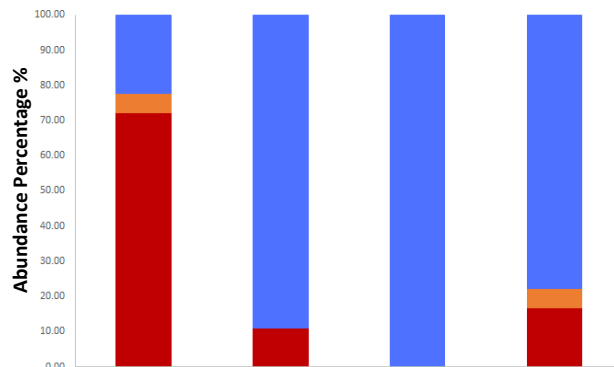


Figure 4: The abundance of Virus 1(A), Virus 2(B), Unknown (C), Bacteria (D) found in oral swabs mapped spatially using a weighted (2.00) interpolation analysis in QGIS (version 3.14) to identify hot spot zones. Abundance of microbiological regions is represented by blue = low range ($<3.11 \times 10^6$ particles per mL), white = medium range (between $3.11 \times 10^6 - 3.72 \times 10^6$ particles per mL), red= high range ($>3.72 \times 10^6$ particles per mL). Orange dots indicate sample locations of the *Tiliqua rugosa* individuals.

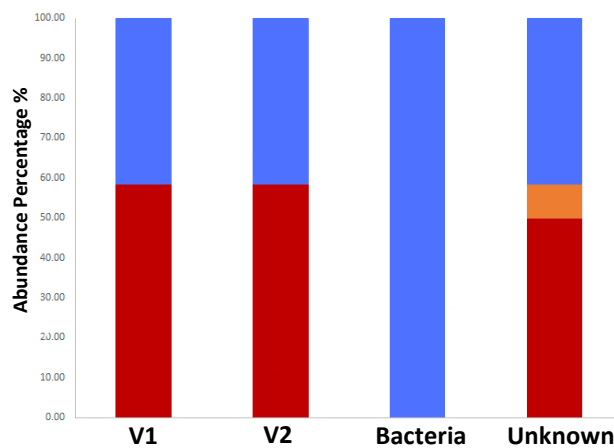
***Amblyomma limbatum* side**
(n=12)



Near Boundary
(n=18)



***Bothriocroton hydrosauri* side**
(n=12)



Microbiological Populations
■ High abundance ■ Medium abundance ■ Low abundance

Figure 5: Abundance percentages of each subpopulation (Virus1, Virus2, Bacteria, Unknown), grouped in relation to boundary position (northern side with *Amblyomma limbatum* side, southern side with *Bothriocroton hydrosauri* side, and near-boundary). Abundance was classified as high ($>3.72 \times 10^6$ particles per mL), medium (between $3.11 \times 10^6 - 3.72 \times 10^6$ particles per mL), and low ($< 3.11 \times 10^6$ particles per mL), when defining Inverse Weighted Distance interpolation gradients, and used consistently throughout the study.



Tables

Table 1 Kruskal-Wallis non-parametric testing for significance between three positions relative to the parapatric boundary (*Amblyomma limbatum* side, *Bothriocroton hydrosauri* side, and 'near-boundary'), for each sub-population (Virus1, Virus2, and Bacteria). Based on bootstrap of 10,000 permutations. Significant values are bolded

		Virus 1	Virus 2	Bacteria
Kruskal-Wallis H		8.23	3.25	.541
df		2	2	2
Asymp. Sig		.016	.197	.763
Monte Carlo Sig.	Sig.	.014	.204	.774
	95% C.I.			
	Lower Bound	.012	.196	.766
	Upper Bound	.016	.212	.782

Table 2: Mann-Whitney U non-parametric test for significance between two positions relative to the parapatric boundary (*Amblyomma limbatum* side and 'near-boundary'), for each subpopulation (Virus1, Virus2, and Bacteria).

		Virus 1	Virus 2	Bacteria
Mann-Whitney U		41.000	101.000	93.000
Wilcoxon W		119.000	179.000	264.000
Z		-2.836	-0.296	-0.635
Asymp. Sig (2-tailed)		0.005	0.767	0.525
Exact. Sig [2*(1-tailed Sig.)]		0.004	0.787	0.545
Monte Carlo Sig (2-tailed)	Sig.	0.003	0.786	0.545
	95% C.I.			
	Lower Bound	0.002	0.778	0.535
	Upper Bound	0.004	0.794	0.554



Data Availability

Data are stored on a GitHub repository and will be publicly available once published.



References

- Adan A, Alizada G, Kiraz Y, Baran Y, Nalbant A (2017). Flow cytometry: basic principles and applications. *Critical Reviews in Biotechnology* **37**: 163-176.
- Albery GF, Kirkpatrick L, Firth JA, Bansal S (2021). Unifying spatial and social network analysis in disease ecology. *Journal of Animal Ecology* **90**: 45-61.
- Ariel E (2011). Viruses in reptiles. *Veterinary Research* **42**: 100.
- Hisee A., Hisee M., McKerral J.C., Rosenbauer S.R., Paterson J.S., Mitchell J.G., Fallowfield H.J., (2020) Changes of viral and prokaryote abundances in a high rate algal pond using flow cytometry detection. *Water Sci Technol.* **82 (6)**: 1062–1069
- Becton DaC (2021). FlowJo™ Software (for Windows) [software application] V, Version 10.
- Blanco, I., Diego, I., Bueno, P., Fernández, E., Casas-Maldonado, F., Esquinas, C., Soriano, J. B., & Miravittles, M. (2017). Geographical distribution of COPD prevalence in Europe, estimated by an inverse distance weighting interpolation technique. *International Journal of Chronic Obstructive Pulmonary Disease* **13**: 57-67.
- Bouma MJ, Smallridge CJ, Bull CM, Komdeur J (2007). Susceptibility to infection by a haemogregarine parasite and the impact of infection in the Australian sleepy lizard *Tiliqua rugosa*. *Parasitology Research* **100**: 949-954.
- Brandell EE, Becker DJ, Sampson L, Forbes KM (2020). The rise of disease ecology. *bioRxiv*: 2020.2007.2016.207100.
- Brussaard CPD (2004). Optimization of procedures for counting viruses by flow cytometry. *Applied and environmental microbiology* **70**: 1506-1513.
- Bull C, Sharrad R, Petney T (1981). Parapatric boundaries between Australian reptile ticks. *The Proceedings of the Ecological Society of Australia* **11**: 95-107.
- Bull CM, Possingham H (1995). A model to explain ecological parapatry. *The American Naturalist* **145**: 935-947.
- Bull CM, Burzacott D (2001). Temporal and spatial dynamics of a parapatric boundary between two Australian reptile ticks. *Molecular Ecology* **10**: 639-648.
- Bull CM, Godfrey SS, Gordon DM (2012). Social networks and the spread of *Salmonella* in a sleepy lizard population. *Molecular Ecology* **21**: 4386-4392.
- Carlson-Jones JAP, Paterson JS, Newton K, Smith RJ, Dann LM, Speck P *et al.*, (2016). Enumerating Virus-Like Particles and Bacterial Populations in the Sinuses of Chronic Rhinosinusitis Patients Using Flow Cytometry. *PLOS ONE* **11**: e0155003.
- Carlson-Jones JAP, Kontos A, Kennedy D, Martin J, Lushington K, McKerral, Paterson JS, Smith RJ, Dann LM, Speck P, Mitchell, JG (2020). The microbial abundance dynamics of the paediatric oral cavity before and after sleep. *Journal of Oral Microbiology* **12**: 1741254.
- Comazzi S, Riondato F (2021). Flow Cytometry in the Diagnosis of Canine T-Cell Lymphoma. *Frontiers in veterinary science* **8**: 600963-600963.
- Dahlin CR, Hughes DF, Meshaka WE, Coleman C, Henning JD (2016). Wild snakes harbor West Nile virus. *One Health* **2**: 136-138.
- de Carvalho MPN, Queiroz-Hazarbassanov NGT, de Oliveira Massoco C, Sant'Anna SS, Lourenço MM, Levin G *et al.*, (2017). Functional characterization of neotropical snakes peripheral blood leukocytes subsets: Linking flow cytometry cell features, microscopy images and serum corticosterone levels. *Developmental & Comparative Immunology* **74**: 144-153.



- Garchitorena A, Sokolow SH, Roche B, Ngonghala CN, Jocque M, Lund A, Barry M, Mordecai E A, Daily GC, Jones JH, Andrews JR, Bendavid E, Luby SP, LaBeaud AD, Seetah K, Guégan JF, Bonds MH, De Leo GA, (2017). Disease ecology, health and the environment: a framework to account for ecological and socio-economic drivers in the control of neglected tropical diseases. *Philosophical Transactions of the Royal Society London B Biological Science* **372**: 37220160128
- Giles JR, Eby P, Parry H, Peel AJ, Plowright RK, Westcott DA *et al.*, (2018). Environmental drivers of spatiotemporal foraging intensity in fruit bats and implications for Hendra virus ecology. *Scientific Reports* **8**: 9555.
- Godfrey SS, Gardner MG (2017). Lizards, ticks and contributions to Australian parasitology: C. Michael Bull (1947–2016). *International Journal for Parasitology: Parasites and Wildlife* **6**: 295-298.
- Graham JL, Jaeger RF (1968). Inactivation of yellow fever virus by glutaraldehyde. *Appl Microbiol* **16**: 177-177.
- Harvell CD, Mitchell CE, Ward JR, Altizer S, Dobson AP, Ostfeld RS *et al.*, (2002). Climate warming and disease risks for terrestrial and marine biota. *Science* **296**: 2158-2162.
- Hoek G, Fischer P, Van Den Brandt P, Goldbohm S, Brunekreef B (2001). Estimation of long-term average exposure to outdoor air pollution for a cohort study on mortality. *Journal of Exposure Science & Environmental Epidemiology* **11**: 459-469.
- Hyndman T, Shilton C (2018). An update on Australian reptile infectious disease (Conference Proceedings).
- Klenk K, Snow J, Morgan K, Bowen R, Stephens M, Foster F, Gordy P, Beckett S, Komar N, Gubler D, Bunning M, (2004). Alligators as West Nile virus amplifiers. *Emerging infectious diseases* **10**: 2150-2155.
- Knapp LA (2005). The ABCs of MHC. *Evolutionary Anthropology: Issues, News, and Reviews* **14**: 28-37.
- Longo AV, Zamudio KR (2017). Environmental fluctuations and host skin bacteria shift survival advantage between frogs and their fungal pathogen. *The ISME journal* **11**: 349-361.
- Marschang RE (2011). Viruses Infecting Reptiles. *Viruses* **3**(11): 2087–2126
- Messina JP, Taylor SM, Meshnick SR, Linke AM, Tshetu AK, Atua B, Mwandagalirwa K, Emch M, (2011). Population, behavioural and environmental drivers of malaria prevalence in the Democratic Republic of Congo. *Malaria Journal* **10**: 161.
- O’Dea MA, Jackson B, Jackson C, Xavier P, Warren K (2016). Discovery and Partial Genomic Characterisation of a Novel Nidovirus Associated with Respiratory Disease in Wild Shingleback Lizards (*Tiliqua rugosa*). *PLOS ONE* **11**: e0165209.
- Parrish K, Kirkland PD, Skerratt LF, Ariel E (2021). Nidoviruses in Reptiles: A Review. *Frontiers in Veterinary Science* **8**.
- Paterson JS, Nayar S, Mitchell JG, Seuront L (2012). A local upwelling controls viral and microbial community structure in South Australian continental shelf waters. *Estuarine Coastal and Shelf Science* **96**: 197.
- Petney T, Bull C (1984). Microhabitat selection by two reptile ticks at their parapatric boundary. *Australian Ecology* **9**: 233-239.
- QGIS Development Team (2022). QGIS Geographic Information System. , 3.3 edn. QGIS Association.
- Rakus K, Ronsmans M, Vanderplasschen A (2017). Behavioral fever in ectothermic vertebrates. *Developmental & Comparative Immunology* **66**: 84-91.



- Reinhold JM, Lazzari CR, Lahondère C (2018). Effects of the Environmental Temperature on *Aedes aegypti* and *Aedes albopictus* Mosquitoes: A Review. *Insects* **9**: 158.
- Riondato F, Comazzi S (2021). Flow Cytometry in the Diagnosis of Canine B-Cell Lymphoma. *Frontiers in Veterinary Science* **8**.
- Rittenbury MS, Hench ME (1965). Preliminary evaluation of an activated glutaraldehyde solution for cold sterilization. *Ann Surg* **161**: 127-130.
- Rohr JR, Cohen JM (2020). Understanding how temperature shifts could impact infectious disease. *PLOS Biology* **18**: e3000938.
- Schumacher J (2011). Respiratory Medicine of Reptiles. *Veterinary Clinics: Exotic Animal Practice* **14**: 207-224.
- Shepard D: A two-dimensional interpolation function for irregularly-spaced data. *Proceedings of the 1968 23rd ACM national conference*. Association for Computing Machinery: 1968.
- Smallridge CJ, Bull CM (1999). Transmission of the blood parasite *Hemolivia mariae* between its lizard and tick hosts. *Parasitology Research* **85**: 858-863.
- Smallridge CJ, Bull CM (2000). Prevalence and intensity of the blood parasite *Hemolivia mariae* in a field population of the skink *Tiliqua rugosa*. *Parasitology Research* **86**: 655-660.
- Staines M, Bradford T, Graves SR, Bull S, Gardner MG (2020). Proposing a new hypothesis: *Rickettsia* spp. as a mechanism maintaining parapatry between two Australian reptile tick species. *Austral Ecology* **45**: 488-492.
- Vaughn LK, Bernheim HA, Kluger MJ (1974). Fever in the lizard *Dipsosaurus dorsalis*. *Nature* **252**: 473-474.
- Wieczorek M, Abualrous ET, Sticht J, Álvaro-Benito M, Stolzenberg S, Noé F, Freund C (2017). Major Histocompatibility Complex (MHC) Class I and MHC Class II Proteins: Conformational Plasticity in Antigen Presentation. *Frontiers in Immunology* **8**.
- Wilcox BA, Gubler DJ (2005). Disease ecology and the global emergence of zoonotic pathogens. *Environmental Health and Preventative Medicine* **10**: 263-272.
- Zimmerman L (2016). The Immune System in Reptiles. *Encyclopedia of Immunobiology*.
- Zimmerman Laura M, Vogel Laura A, Edwards Kevin A, Bowden Rachel M (2010). Phagocytic B cells in a reptile. *Biology Letters* **6**: 270-273.



Chapter 2: Supplementary Material

Table S1: The Abundance levels for the forty-two Individual *Tiliqua rugosa*. Percentage indicates the percent of individuals that were with that abundance level. Blue = low range ($<3.11 \times 10^6$ particles per mL), white = medium range (between 3.11×10^6 – 3.72×10^6 particles per mL), and red = high range ($>3.72 \times 10^6$ particles per mL). Unidentified population (Unknown) was detected in 97% of individuals but only 33% had high abundance. Virus 1 (V1) was detected in 95% of individuals with 52% in high abundance. Virus 2 (V2) was detected in all lizards but only 21% were in high abundance. While bacteria were in 92% of individuals, 100% was within the low abundance range.

Abundance Level	Unknown	V1	V2	Bacteria
# Individuals	41	40	42	39
% Detected	97.62	95.24	100.00	92.86
# Individuals	25	18	32	42
LOW %	59.52	42.86	76.19	100.00
# Individuals	3	2	1	0
MED %	7.14	4.76	2.38	0.00
# Individuals	14	22	9	0
HIGH %	33.33	52.38	21.43	0.00



Table S2: Mann-Whitney U non-parametric test for significance between two positions relative to the parapatric boundary (*Amblyomma limbatum* side and *Bothriocroton hydrosauri* side), for each subpopulation (Virus1, Virus2, Bacteria). Significant values are bolded.

		Virus 1	Virus 2	Bacteria	
Mann-Whitney U		41.500	40.000	63.000	
Wilcoxon W		119.500	118.000	141.000	
Z		-1.761	-1.848	-0.520	
Asymp. Sig (2-tailed)		0.078	0.065	0.603	
Exact. Sig [2*(1-tailed Sig.)]		0.078	0.068	0.630	
Monte Carlo Sig (2-tailed)	Sig.	0.076	0.068	0.623	
	95% C.I.	Lower Bound	0.071	0.063	0.614
		Upper Bound	0.081	0.073	0.633



Table S3: Mann-Whitney U non-parametric test for significance between 2 positions relative to the parapatric boundary (*Bothriocroton hydrosauri* side and ‘near boundary’), for each subpopulation (Virus1, Virus2, and Bacteria).

		Virus 1	Virus 2	Bacteria
Mann-Whitney U		86.000	77.000	98.500
Wilcoxon W		164.000	248.000	269.500
Z		-0.931	-1.312	-0.402
Asymp. Sig (2-tailed)		0.352	0.189	0.687
Exact. Sig [2*(1-tailed Sig.)]		0.368	0.200	0.692
Monte Carlo Sig (2-tailed)	Sig.	0.369	0.196	0.698
	95% C.I.			
	Lower Bound	0.359	0.188	0.689
	Upper Bound	0.378	0.204	0.707



Chapter 3: Foreword

Chapter 3 was initially designed with the assumption there would be a working antibody test to the *Shingleback nidovirus 1*. As such the overall aim was to combine the RT-qPCR with an indirect competitive enzyme-linked immunosorbent assay (icELISA) to determine whether a lizard was currently infected with the virus (RT-qPCR), or if it had ever been (icELISA). The icELISA could provide evidence of historical infection, while the RT-qPCR can only give current infection status at the time of sampling. Combining both methods was to provide some insight on whether the virus had historically crossed a state boarder as well as whether the lizards found in the surrounding Perth Hills were previously infected with the virus (icELISA), and where the *Shingleback nidovirus 1* was currently active (RT-qPCR). Unfortunately, the antibody test remains unvalidated. In order to preserve the rare samples from the Nullarbor and the south-east of Western Australia, the serum samples have been stored for long term storage to be used once the test is validated or another antibody test is created. Therefore, this chapter primarily focuses on the RT-qPCR samples that only provide a snapshot of where this virus was active at the time of sampling. However, the chapter does provide support that the *Shingleback nidovirus 1* is not present in the Mount Mary study site. Therefore, the identity of the two viruses (Virus 1 and 2) observed in Chapter 2, are likely new viruses for this host species. This Chapter is currently being prepared for peer-reviewed publication.



CHAPTER 3: Spatial distribution of the *Shingleback nidovirus 1* between Western Australia and South Australia using RT-qPCR

Robert L. O'Reilly¹ and Michael G. Gardner¹

¹ Flinders University, SA, Australia

Corresponding author: robert.liam.oreilly@gmail.com

Keywords: Virus distribution, Lizards, RT-qPCR, Reverse transcription PCR, Shingleback



Abstract

The importance of monitoring the distribution of viruses has become more apparent since the Covid-19 pandemic. By studying newly emerged viruses, not only would this benefit wildlife conservation but also prepare humans should a virus become zoonotic. Here, we aimed to determine the distribution of the *Shingleback nidovirus 1* between Perth and Adelaide, a virus associated with the bobtail flu in the Australian sleepy lizard, *Tiliqua rugosa*. This disease is an Upper Respiratory Tract Infection (URTI) inhibiting normal respiratory function, and has been isolated to the surround Perth Hills, Western Australia.

We aimed to determine whether the virus had spread from its restricted location in the Perth Hills, Western Australia, and crossed state border into South Australia. Anecdotal evidence from observations of symptomatic lizards suggests the bobtail flu had been observed in other states, including in at the long-term research site at Mount Mary, South Australia. Therefore, we sampled *Tiliqua rugosa* between Perth and Adelaide (total distance of 9949 km), in wide transects, taking oral swabs of the glottis. We used RT-qPCR to determine presence or absence of the virus in an individual. We found one positive sample (out of 91 samples) in a wild lizard east of the Perth Hills. We did not find any positive samples in South Australia (n = 60), or at the Mount Mary study site (n = 35). In the Mount Mary site, we travelled along transects that previously found two unknown viruses in >95% of individuals with the use of flow cytometry. So, while this study cannot rule it out, it is unlikely that either of the two viruses previously identified in South Australia are *Shingleback nidovirus 1*. We highlight the need for further research that uses serum samples to provide evidence on previous infection status to add to the history of this virus' distribution.



Introduction

The importance of discovering and monitoring emerging viruses has been brought into sharp focus since the global pandemic of SARS-CoV-2 began in 2019. Since the pandemic began, research into human and animal viruses has expanded in parallel with a greater appreciation of how emerging viruses can cause wide-spread economic and societal upheaval (Coccia 2021). Also, there are increasing concerns that climate change may increase the possibility of future spillover events as the distributions and abundances of wild animals and their vectors (e.g. ticks and mosquitos) shift (Carlson *et al.*, 2022; Reinhold *et al.*, 2018). Concerningly, Carlson *et al.* (2022) suggest that cross-species transmissions in wildlife will likely go undetected until there is a spillover event, which could threaten both human and wildlife populations. This highlights the importance of monitoring the epidemiology of viruses in wildlife hosts.

Technologies have almost evolved alongside Covid-19 as the need to screen, genome sequence samples, and determine the effects of Covid-19 on the public have put immense pressures on health care systems around the world (Iyengar *et al.*, 2020; Shrestha *et al.*, 2020). These technologies include flow cytometry (Moratto *et al.*, 2020), whole-genome sequencing (Nawaz *et al.*, 2021), and of course the two most publicly known, Rapid Antigen Tests (Albert *et al.*, 2021), and reverse transcription real-time polymerase chain reaction (RT-qPCR) (Morehouse *et al.*, 2021). Reverse transcription real-time polymerase chain reaction is a fast and reliable method that determines the presence of viral genome (Adams 2020); its utility has been demonstrated globally through its widespread use during the Covid-19 pandemic (Corman *et al.*, 2020; Sheridan 2020; Yelin *et al.*, 2020). The method involves creating complimentary DNA (cDNA) from the extracted viral RNA sample, then using specific primers for a viral gene and a fluorescent probe/quencher to bind to the single stranded cDNA. During the extension step in the polymerase reaction the quencher is separated from the fluorescent probe, allowing the emitting fluorescent signal to be detected — indicating the presence of that virus (Adams 2020). It is a versatile and highly sensitive method (Moreno-Contreras *et al.*, 2022; Yelin *et al.*, 2020). Here we use this method to test for the presence or absence of the *Shingleback nidovirus 1* in the widespread skink, *Tiliqua rugosa*.



Virus research in *Tiliqua rugosa* is relatively neglected as there is no large commercial value within this species. The majority of virus research comes from Perth, Western Australia, and is in relation to the *Shingleback nidovirus 1*— until recently, the only known virus of this species (Norval *et al.*, 2019; O’Dea *et al.*, 2016). Since the early 1990s the *T. rugosa* population in Perth has been severely affected over the years by an upper respiratory tract infection, a flu-like disease dubbed the ‘bobtail flu’. In one year, over 200 cases were brought into the Kanyana Wildlife Rehabilitation Centre by members of the public and wildlife rangers for treatment (Kanyana 2015; O’Dea *et al.*, 2016). These high case numbers, motivated research that aimed to discover the cause of bobtail flu (Moller 2014), ultimately leading to the discovery and partial genome characterisation of a virus species that was named Shingleback nidovirus 1 (O’Dea *et al.*, 2016). The virus species was initially classified as a coronavirus (*Coronaviridae*) but has since become a species of the genus *Pregotovirus* (subfamily: *Serpentovirinae*; family: *Tobaniviridae*; order: *Nidovirales*) (Parrish *et al.*, 2021; Walker *et al.*, 2019). Since then, more viruses have been discovered in *T. rugosa*. An adenovirus has been identified that is suspected to contribute to the bobtail flu in Perth (Hyndman and Shilton 2018) and Chapter 2 showed at least one new, yet to be identified, virus in *T. rugosa* using flow cytometry. As such, there is clearly more to be discovered in this species in terms of identifying the number of viruses this host is susceptible to.

As a species whose distribution ranges across the southern half of Australia and has a close interaction with humans (as a pet or as a delicacy), it is important to monitor known viruses and identify those that are still unknown. Here, we aimed to answer two hypotheses about the *Shingleback nidovirus 1* in southern Australian *T. rugosa*. First, we aimed to determine if the *Shingleback nidovirus 1* was currently active within South Australia or if still restricted to Western Australia. Second, we aimed to determine if one of the two viruses discovered in chapter 2, at the long-term study system at Mount Mary, SA, was the *Shingleback nidovirus 1*. The latter might explain some of the flu-like symptoms observed in those lizards (e.g., discharge from the eyes).

Methods

All required permits and permissions were obtained for this research: Animal Welfare Ethics Permit: E454/17; Department of Environment and Water (DEW): A23436-27; Department



of Biodiversity, Conservation and Attractions (WA permit): FO25000145; Institutional Biosafety Committee (IBC): 2019-07.

Sampling

Free-ranging animals between Adelaide and Perth (Cohort 1)

Sample collection took place from mid-September to early October 2019, during the Austral spring, when shingleback skinks are active (Brooker 2016; Godfrey and Gardner 2017).

Lizards were sampled opportunistically if they were encountered on major highways that connect Adelaide (in South Australia) to Esperance (in Western Australia, WA), and sampling continued along 400 km north-south transects (separated by 100 km west-east intervals) between Esperance and Perth (WA) (Figure 2). The intention was to sample across the natural range of shingleback skinks in SA and WA focussing on populations that would come into human contact along major highways. Shingleback skinks have been illegally imported into SA from WA (Heinrich *et al.*, 2022) and therefore animals from these sampling locations could facilitate the spread of Shingleback nidovirus 1 into SA.

Sample collection relied on the random encounter method, which entails driving along roads slowly and stopping to catch any shingleback skinks that are spotted; they are slow moving and do not require trapping or baiting (Bull and Burzacott 2001; Godfrey and Gardner 2017)..

Two oral swabs of the glottis were taken per individual, with each swab rotated on the glottis for 2x 360° turns before being stored in separate vials containing phosphate-buffered saline (PBS) (O’Dea *et al.*, 2016). Swab samples were stored at a consistent -18°C using a 40 L Engel freezer in the vehicle. Photos of the anterior aspect of the oral cavity as well as full length ventral and dorsal photos were taken using a Nikon D60..

In South Australia, each lizard was given a unique ID number represented by toe clips (Bull *et al.*, 1981; Godfrey and Gardner 2017) to prevent sampling the same lizard twice. The toes are available for future genetic analysis. However, in WA no toes were clipped due to permit restrictions. As the transects did not overlap and were travelled uni-directionally, it is unlikely that any lizards were resampled (Figure 2).

Free-ranging animals at Mount Mary, SA (Cohort 2)



Thirty-five samples were obtained from the field study site at Mount Mary, SA, in order to determine whether either of the two viruses discovered in Chapter 2 were the *Shingleback nidovirus 1* (Figure 3). Including one sample obtained from the ocular discharge of a lizard found with some flu-like symptoms. Due to the rare sighting of flu-like symptoms at this study site (RLO, pers.obs.), the individual was swabbed twice, and were stored in two different mediums. One swab stored in PBS like all other samples, however, the second swab was stored in RNAlater for the preservation of any viral RNA as an added precaution (Forster *et al.*, 2008; Wille *et al.*, 2018). Both samples were screened for the *Shingleback nidovirus 1* using the same RT-qPCR method. Samples were collected by travelling along transects using the same predetermined roads as in Chapter 1 and Chapter 2. Sampling method was consistent with the Adelaide-Perth trip. However, no photos or temperatures were taken, and swabs were snap frozen in liquid nitrogen.

Sick animals admitted for treatment, Perth, WA (Cohort 3)

Twenty suspected positive swab samples were obtained from Wattle Grove Veterinary Hospital, with the help of Kanyana Wildlife Rehabilitation Centre. These animals were wild before being admitted to the facilities after being discovered presenting flu-like symptoms by rangers and members of the public. Swabbing method was consistent with the other cohorts in this study.

RT-qPCR

Each oral swab had viral RNA extracted from the swabs using a MagMAX™-96 Viral RNA Isolation Kit (Applied Biosystems, USA) on a Thermo Scientific™ Kingfisher™ Duo automated sample extraction and purification system to reduce systematic error. The manufacturer's MadMax_Pathogen_High_Vol_DUO.bdz protocols were used. The reverse transcription real-time polymerase chain reaction (RT-qPCR) used a AgPath-ID™ One-Step RT-PCR kit (Applied Biosystems™) on the extracted viral RNA. This one step RT-qPCR method creates the cDNA with reverse transcription then performs the qPCR amplification in the one reaction (Adams 2020). This procedure reduces the chances of potential contamination, as well as reducing both random and experimental errors allowing for real time identification of infection in a presence or absence setting which is why it is used in clinical screening (Cerdeira *et al.*, 2021; Park *et al.*, 2022). The master mix contained: Nuclease free water (5.36 µl per sample); 2 x AgPath buffer (10 µl per sample); 25 x AmpliTaq Gold™ (0.8 µl per sample); Lizardnido-fwd:



CGGAGTGGACAAGTCGTGAA (10 µM; 0.8 µl per sample); Lizardnido-rev: GGACTCAGTGCGGTGAGAAA (10 µM; 0.8 µl per sample); Lizardnido-probe: 6FAM-CGTCGCCGGTCAGACAGCGAGCC –BHQ1 (10 µM; 0.24 µl per sample) created for this nidovirus, and 2 µl of extracted sample (O’Dea *et al.*, 2016).

A cycle threshold (Ct) value < 40 with a sigmoidal curve indicates a positive sample whereas a Ct value 40–45 with a sigmoidal curve is indeterminate (Figure 4) (O’Dea *et al.*, 2016). A Ct value that is undetectable is negative. To determine if the viral RNA extraction method and RT-qPCR methods was successful, a known positive sample was extracted using the kingfisher protocols and used for the RT-qPCR (Quntas 6 studio) along with two previously confirmed positive, viral RNA extractions obtained from virologist Tim Hyndman at Murdoch University. Negative control consisted of 2 ul of nuclease free water with the mastermix.

Results

Sampling

A total of 91 lizards were sampled in the twenty-two days of field work (Figure 2) between Perth and Adelaide (cohort 1). We were able to successfully collect oral swabs from all individuals. A further 35 lizards were sampled from Mount Mary study site (Figure 3) (cohort 2). One animal from the Mount Mary site, lizard ID 50008, showed potential flu symptoms with discharge from the ocular cavity. Twenty suspected positive swab samples were obtained from Wattle Grove Veterinary Hospital, with the help of Kanyana Wildlife Rehabilitation Centre (cohort 3). These samples were from lizards that had been brought in by members of the public, and wildlife rangers who had come across the animals displaying flu-like symptoms. A further two confirmed PCR positive samples were sent by virologist Tim Hyndman at Murdoch University, in the form of viral RNA extracted spin columns. These confirmed positives were used as controls.

RT-PCR

Of the 146 samples (cohort 1= 91; cohort 2 = 35; cohort 3 = 20), 17 were confirmed positive for *Shingleback nidovirus 1* (Table 1; Figure 4) based on the O’Dea *et al.*, (2016) protocols. Of the 20 shingleback skins from Kanyana/WGVH (cohort 3) that had signs consistent with bobtail flu, 16 were PCR-positive for *Shingleback nidovirus 1*. There was one positive sample found in a free-ranging shingleback skink from WA (cohort 1) (Table 1: Sample 22).. This



animal was active and showed no signs that were consistent with bobtail flu (Figure 5). There were no positive samples found in South Australia (cohort 1), including in the Mount Mary study site (cohort 2).



Discussion

Interpretation of results

The aim of this study was to test specific populations of WA and SA shingleback skinks for *Shingleback nidovirus 1*. These populations represented those that live near major road networks between Perth and Adelaide (cohort 1), those from rural locations at Mount Mary, SA (cohort 2), and those with signs of disease consistent with bobtail flu from peri-urban locations around Perth, WA (cohort 3). *Shingleback nidovirus 1* was detected by PCR only in one animal from cohort 1 and from 80% (16/20) of the animals from the symptomatic animals from cohort 3 (Table S3). Animal 22 (from cohort 1) showed no flu-like symptoms and was active. This asymptomatic infection is not particularly unusual, as O’Dea *et al.*, (2016) showed 12% of infected individuals had no overt signs of disease. It has been reported that the recovery rate of shingleback skinks with bobtail flu is 84% survival rate when treated with a combination of antibiotics and antiprotozoal medication, along with regular hydration (O’Dea *et al.*, 2016). However, these survival rates only relate to the period of time that these animals were being rehabilitated. Longer term survival rates and whether the infected individuals had cleared the nidovirus infection are unknown. It would be worthwhile for a future study to monitor for long term survival of those animals released after rehabilitation in conjunction with monitoring population sizes in the Perth Hills. We only found three lizards (Table S1; ID 18,19,20) in the Mundaring Park in the surrounding Perth Hills, when the species’ distribution in the area has been quite dense (Figure 1). Weather conditions at the time were optimal for lizard basking — warm days (28-37°C), no rain or wind (Table S1; ID 18,19,20 – ambient temperature).

No sample was PCR-positive for *Shingleback nidovirus 1* from the 35 skinks sampled at Mount Mary, South Australia (cohort 2). Of these animals, only one showed signs consistent with bobtail flu (this animal had ocular discharge) (Table S1). It is unknown what might have caused this animal’s bobtail flu-like signs of disease. If infectious, it may have been caused by *Shingleback nidovirus 1* in which case, the negative PCR result may have been due to intermittent shedding of virus or because the infection had since been cleared. Other infections (e.g. adenovirus or mycoplasma) should also be considered (Hyndman and Shilton 2018). The sample has been stored for long term storage and can be tested for these infections in the future. Another explanation is one of the two viruses found in Chapter 2



might be causing disease in only a few of these lizards while infecting the majority. Perhaps a reptile herpesvirus could be in this system as there are a number of reptile herpesviruses found in lizards (Ariel 2011; James *et al.*, 2004; Literak *et al.*, 2010; Marschang 2019; Wellehan *et al.*, 2005). Such viruses have previously been linked to conjunctivitis (Jacobson *et al.*, 1986), which may explain lizard ID 50008's symptom. The viruses in Chapter 2 could be any number of other viruses that infect lizards (Ariel 2011; Dervas *et al.*, 2020; Hyndman and Shilton 2018; Marschang 2011; Marschang *et al.*, 2021; Okoh *et al.*, 2021; Parrish *et al.*, 2021; Wirth *et al.*, 2018). However, it is also possible the symptoms of one lizard in the study site were not the result of a virus. Future research is needed to identify these viruses found in chapter 2, and then explore their aetiology and pathogenesis.

The results of this study may have been influenced by sampling bias (cohort 1 and cohort 2) as infected animals may have been less likely to have been sampled. Moderately-severely affected lizards are likely to be less-mobile and so would be encountered less-frequently than healthy individuals. It should also be noted that as reptiles have a limited capacity to induce a fever, some will behaviourally increase their temperatures by basking in areas with higher temperatures, and for longer periods of time to improve the immunological response to infection (Rakus *et al.*, 2017; Vaughn *et al.*, 1974). Therefore, it would still be expected to encounter infected individuals with our sampling method.

. The shingleback skinks from cohort 3 had signs of disease consistent with bobtail flu and so finding *shingleback nidovirus 1* in 80% of them was not unexpected. It was therefore interesting that the virus was not detected in free-ranging asymptomatic shingleback skinks from the Perth Hills region (as part of cohort 1)—an area near to the cohort 3 animals. These results are in agreement with the observed association between bobtail flu and the presence of *Shingleback nidovirus 1* (O'Dea *et al.* 2016) is consistent with there being an association between Shingleback that bobtail flu given the virus was detected in 80% of the animals from cohort 3. This association is clearly not perfect though as *Shingleback nidovirus 1* has also been found in asymptomatic individuals (O'Dea *et al.* 2016 and individual 22 from the present study). Additional sampling in the Perth Hills, could be conducted to provide additional data on the prevalence of *Shingleback nidovirus 1* in this area. However, in the Mount Mary site, the two viral sub-populations found in Chapter 2 were in > 95% of the lizards, and the same transects as this chapter were followed (Figure 7). This provides some



confidence that the sampling method would have captured the *Shingleback nidovirus 1* had it been one of the viruses observed in Chapter 2.

.

Conclusion

We made the first attempt at mapping the distribution of the *Shingleback nidovirus 1* between Perth and Adelaide (cohort 1). We discovered a positive sample south-east of Perth, where the virus has been previously detected (cohort 1). We did not find any positive samples in South Australia, including in our study site in Mount Mary (cohort 2). It is likely the viruses found in the Mount Mary study site (Chapter 2) are not the *Shingleback nidovirus 1* but either the adenovirus or new, yet to be identified, viruses in this species. Future research will need to use targeted sampling methods in WA and SA to confidently determine where the *Shingleback nidovirus 1* has spread to. Reverse transcription real-time PCR (RT-qPCR) is a fast and effective method for diagnosing many infections. However, RT-qPCR can only detect active viral infections and cannot be used to infer past infections. Future research should investigate historical infection using a validated antibody test on serum samples. There is also a need to identify the viruses found in the Mount Mary study system (Chapter 2); How these viruses might drive the selective pressures on *T. rugosa* that are discussed in Chapter 1; and determine whether these viruses infect other species of lizards or reptile in the study system.



Figures

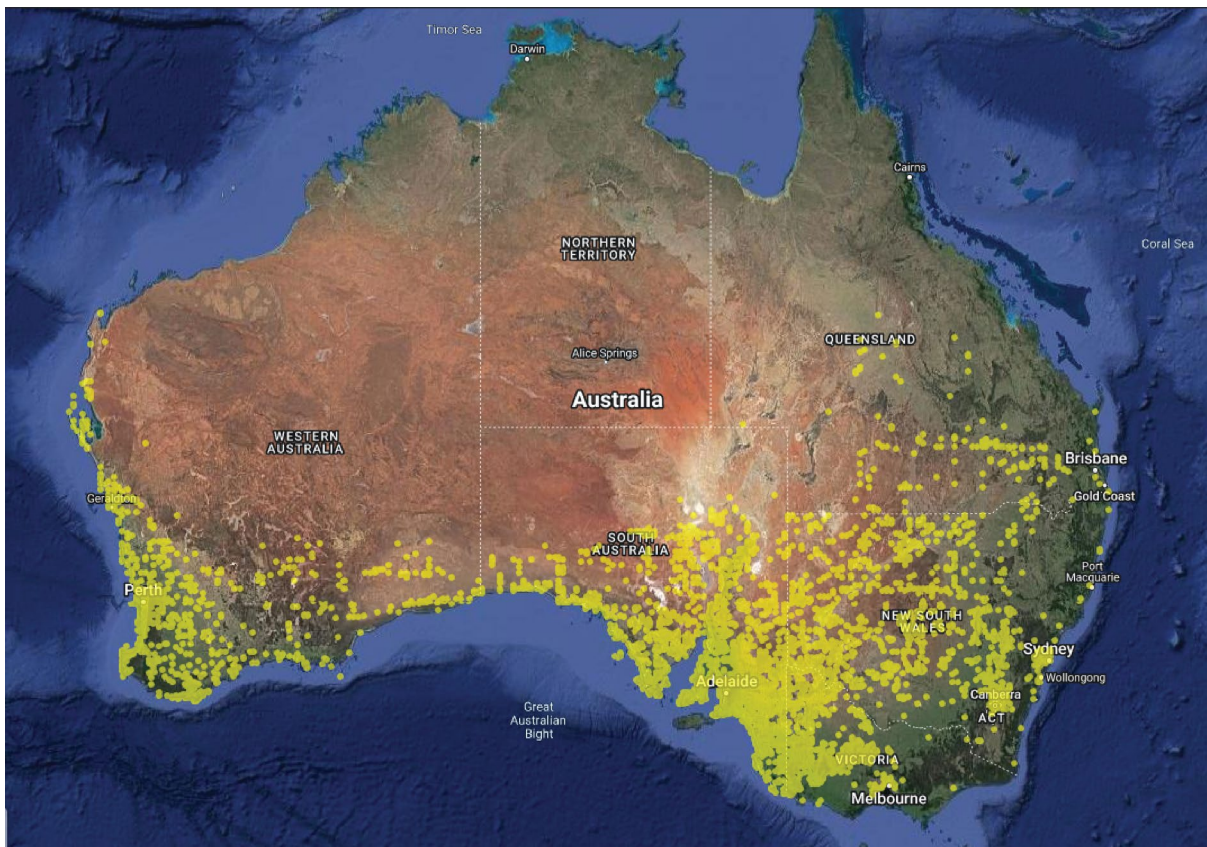


Figure 1: The reported distribution of *Tiliqua rugosa* across Australia by Atlas of Living Australia (Atlas of Living Australia website, Accessed 28 March 2022.). Yellow dot indicates occurrences where *Tiliqua rugosa* have been observed.



Figure 2: Green dots indicate the geographic locations of 91 *Tiliqua rugosa* sampled between Adelaide – Perth in Spring 2019. Red dots represent the 35 *Tiliqua rugosa* sampled at the study site in Mount Mary, South Australia.

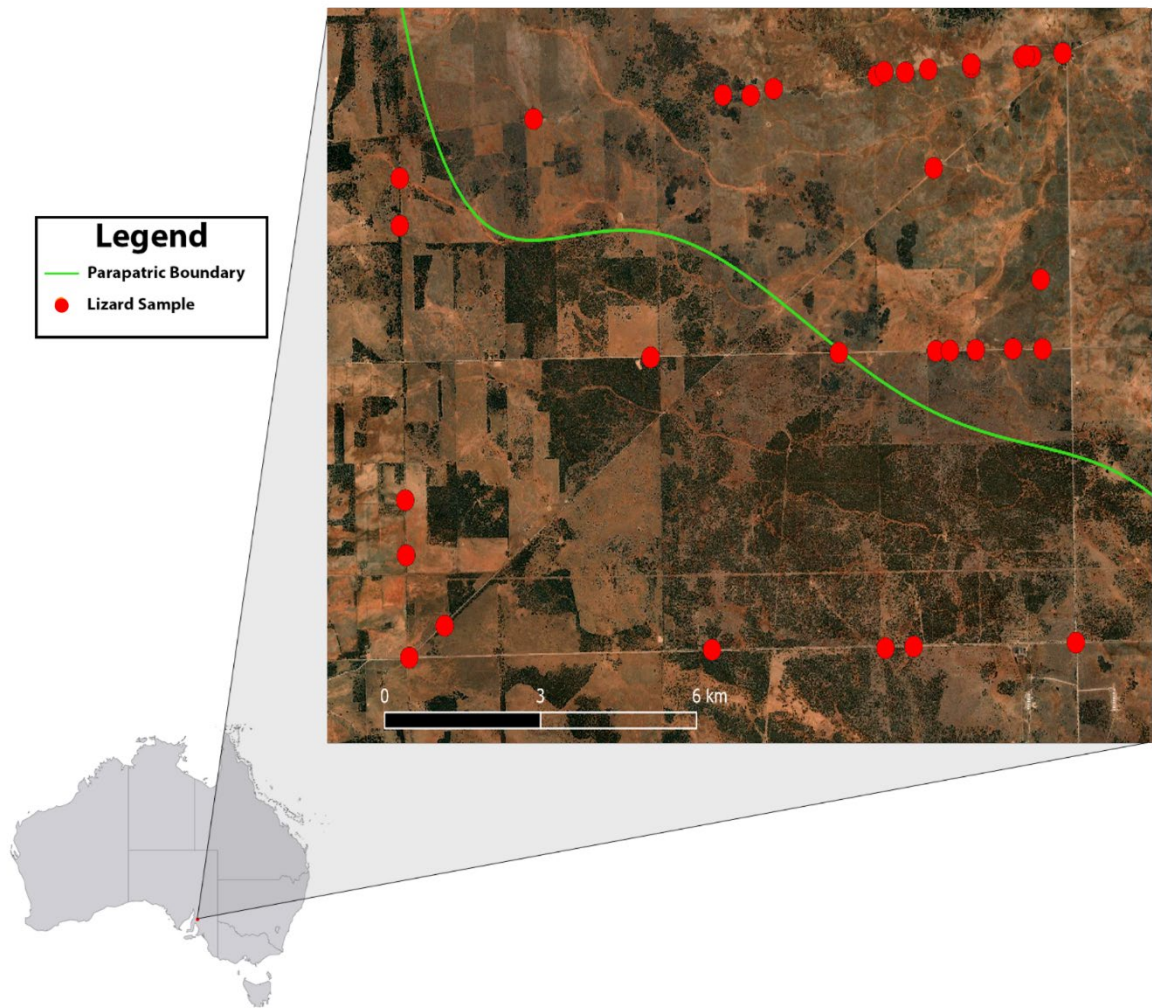


Figure 3: Red dots indicate the 35 *Tiliqua rugosa* that had oral swabs taken to test for the *Shingleback nidovirus 1* in the study site in Mount Mary, South Australia (-33.928306, 139.291000). Reverse Transcription real-time PCR (RT-qPCR) was used to determine whether the viruses found in Chapter 2 were the known virus associated with the bobtail flu. Green line indicates estimation of parapatric boundary

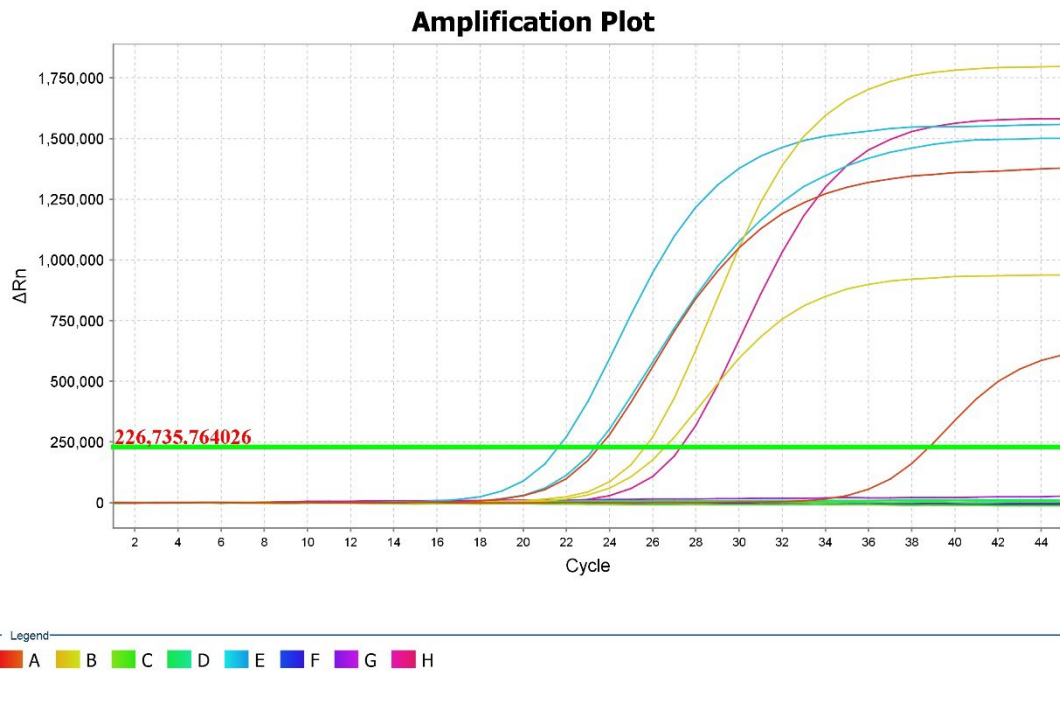


Figure 4: Graphical representation of the reverse transcription real-time PCR results indicating positive infection. Sigmoidal curves in relation to fluorescence and PCR cycle below 40 indicates the presence of the *Shingleback nidovirus 1*. PCR cycle number is represented on the x axis while report dye fluorescence (ΔR_n) is on the y axis. Green bar indicates threshold set at 1/3 of positive control curve, as per (O’Dea *et al.*, 2016). A-H indicate individual samples, each colour corresponds to the matching sigmoidal curve of the graph.



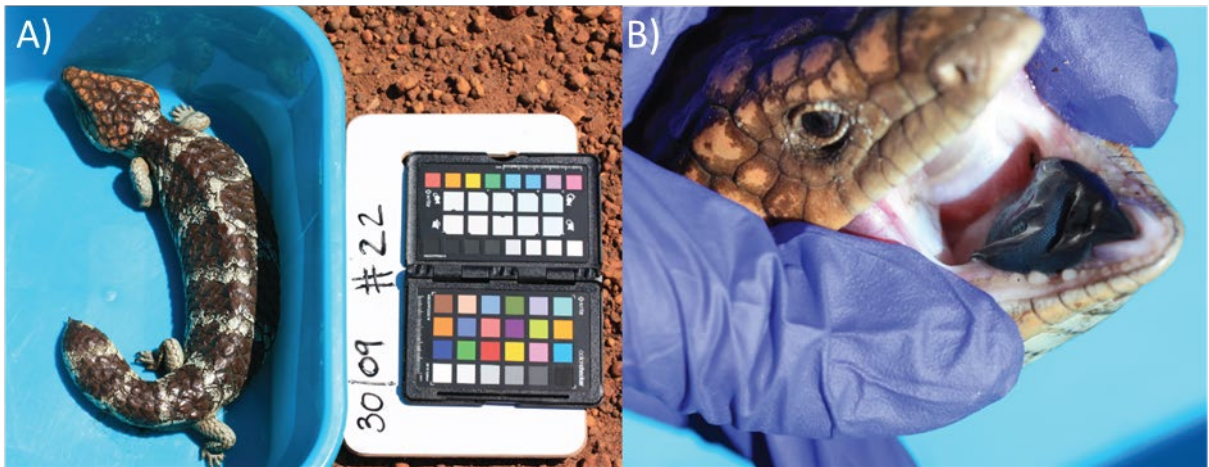


Figure 5: Animal 22, found to be infected with the *Shingleback nidovirus 1* in Western Australia between Quindanning and Williams (- 33.0181, 116.713), south-east of the Perth Hills where the virus is known to occur. The individual was very active, and no clinical flu-like symptoms.

A) Dorsal view of the infected individual. B) Right rostral causal, dorso-ventral oblique view of the infected individual, showing no clinical symptoms such as serous to mucopurulent mucus in the eyes or oral cavity

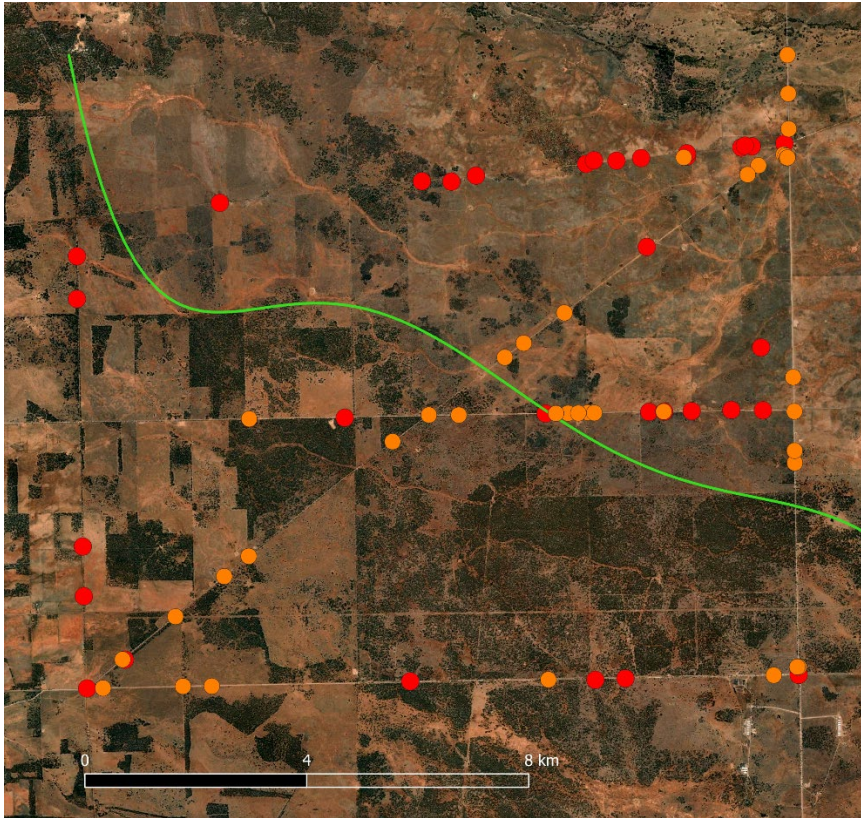


Figure 7: Comparative overlapping sample distributions of Chapter 2 and Chapter 3 at the Mount Mary study site in South Australia (-33.928306, 139.291000). Red dots indicates the samples used in Chapter 3's RT-qPCR, while the orange dots indicate the samples used in Chapter 2's flow cytometry.



Tables

Table 1: Summary of positive samples found in this study from the oral swabs of *Tiliqua rugosa*. All samples other than sample 22 (bold) were obtained from Kanyana Wildlife Rehabilitation Centre (Kanyana), Wattle Grove Veterinary Hospital (WGVH) or Tim Hyndman at Murdoch University. Reporter = fluorescence indicator, Quencher = Fluorescence inhibitor, CT = Cycle threshold, CT Threshold = Cycle threshold set at 1/3 of the sample's sigmoidal curve.

Sample Name	Reporter	Quencher	Ct Mean	Ct Threshold	Obtained
4 (Kanyana)	FAM	NFQ-MGB	31.460	391,300.259	Kanyana and WGVH
36789	FAM	NFQ-MGB	25.798	391,300.259	Kanyana and WGVH
36812	FAM	NFQ-MGB	24.936	391,300.259	Kanyana and WGVH
37084(a7)	FAM	NFQ-MGB	23.816	257,386.402	Kanyana and WGVH
39140(d1)'pos'	FAM	NFQ-MGB	20.522	257,386.402	Kanyana and WGVH
37050(a8)	FAM	NFQ-MGB	24.379	257,386.402	Kanyana and WGVH
37568(a9)	FAM	NFQ-MGB	28.051	257,386.402	Kanyana and WGVH
37259(a10)	FAM	NFQ-MGB	27.177	257,386.402	Kanyana and WGVH
37420(a11)	FAM	NFQ-MGB	23.161	257,386.402	Kanyana and WGVH
12 (Kanyana)	FAM	NFQ-MGB	22.556	335,672.866	Kanyana and WGVH
36309	FAM	NFQ-MGB	33.989	335,672.866	Kanyana and WGVH
36310	FAM	NFQ-MGB	21.733	226,735.764	Kanyana and WGVH
36483	FAM	NFQ-MGB	23.993	226,735.764	Kanyana and WGVH
10(kanya)	FAM	NFQ-MGB	24.593	226,735.764	Kanyana and WGVH
8(kanya)	FAM	NFQ-MGB	19.926	226,735.764	Kanyana and WGVH
9(kanya)	FAM	NFQ-MGB	25.612	226,735.764	Kanyana and WGVH
22*	FAM	NFQ-MGB	36.749	226,735.764	In the Wild, between Quindanning and Williams in Western Australia

* Sample **22** was found in the wild on the 2019 field trip across between Adelaide, South Australia, and Perth, Western Australia (-33.0181, 116.713)



Data Availability

Data are stored on a GitHub repository and will be publicly available once published.



References

- Adams G (2020). A beginner's guide to RT-PCR, qPCR and RT-qPCR. *The Biochemist* **42**: 48-53.
- Albert E, Torres I, Bueno F, Huntley D, Molla E, Fernández-Fuentes MÁ, Martínez M, Poujois S, Forqué L, Valdivia A, Solano de la Asunción C, Ferrer J, Colomina J, Navarro D (2021). Field evaluation of a rapid antigen test (Panbio™ COVID-19 Ag Rapid Test Device) for COVID-19 diagnosis in primary healthcare centres. *Clinical Microbiology and Infection* **27**: 472.e477-472.e410.
- Ariel E (2011). Viruses in reptiles. *Veterinary Research* **42**: 100.
- Arikan H, Çiçek K (2014). Haematology of amphibians and reptiles: a review. *North-Western Journal of Zoology* **10** 190-209.
- Atlas of Living Australia website. Species page:
<https://bie.ala.org.au/species/urn:lsid:biodiversity.org.au:afd.taxon:1a6623ab-8d46-4da0-957c-f27b663f7ef0>, Accessed 28 March 2022.
- Brooker M (2016). Bobtail skink (*Tiliqua rugosa*) observations on the Darling Scarp, Perth, Western Australia, 1985-2015 **30**: 131-147.
- Brown C (2007). Blood sample collection in lizards. *Lab Animal* **36**: 23-24.
- Bull C, Sharrad R, Petney T (1981). Parapatric boundaries between Australian reptile ticks. *The Proceedings of the Ecological Society of Australia* **11**: 95-107.
- Bull CM, Burzacott D (2001). Temporal and spatial dynamics of a parapatric boundary between two Australian reptile ticks. *Molecular Ecology* **10**: 639-648.
- Bull CM, Godfrey SS, Gordon DM (2012). Social networks and the spread of *Salmonella* in a sleepy lizard population. *Molecular Ecology* **21**: 4386-4392.
- Carlson CJ, Albery GF, Merow C, Trisos CH, Zipfel CM, Eskew EA *et al.*, (2022). Climate change increases cross-species viral transmission risk. *Nature*.
- Cerda, A., Rivera, M., Armijo, G., Ibarra-Henriquez, C., Reyes, J., Blázquez-Sánchez, P., Avilés, J., Arce, A., Seguel, A., Brown, A. J., Vásquez, Y., Cortez-San Martín, M., Cubillos, F., García, P., Ferres, M., Ramírez-Sarmiento, C. A., Federici, F., & Gutiérrez, R. A. (2021). A One-Step open RT-qPCR for SARS-CoV-2 detection. *medRxiv*: 2021.11.2029.21267000.
- Coccia M (2021). The impact of first and second wave of the COVID-19 pandemic in society: comparative analysis to support control measures to cope with negative effects of future infectious diseases. *Environmental Research* **197**: 111099.
- Corman VM, Landt O, Kaiser M, Molenkamp R, Meijer A, Chu DK, Bleicker T, Brünink S, Schneider J, Schmidt ML, Mulders DGJC, Haagmans BL, van der Veer B, van den Brink S, Wijsman L, Goderski G, Romette JL, Ellis J, Zambon M, Peiris M, Goossens H, Reusken C, Koopmans, MPG Drosten C (2020). Detection of 2019 novel coronavirus (2019-nCoV) by real-time RT-PCR. *Eurosurveillance* **25**: 2000045.
- Dervas, E., Hepojoki, J., Smura, T., Prähauser, B., Windbichler, K., Blümich, S., Ramis, A., Hetzel, U. and Kipar, A., 2020. Serpentoviruses: more than respiratory pathogens. *Journal of Virology*, **94**(18), pp.e00649-20.
- Doneley B, Monks D, Johnson R, Carmel B (2018). *Reptile medicine and surgery in clinical practice*. Wiley-Blackwell: Hoboken, New Jersey.
- Firth Bruce T, Belan I (1998). Daily and Seasonal Rhythms in Selected Body Temperatures in the Australian Lizard *Tiliqua rugosa* (Scincidae): Field and Laboratory Observations. *Physiological Zoology* **71**: 303-311.



- Forster JL, Harkin VB, Graham DA, McCullough SJ (2008). The effect of sample type, temperature and RNAlater™ on the stability of avian influenza virus RNA. *Journal of Virological Methods* **149**: 190-194.
- Fudge AM (2000). *Laboratory medicine : avian and exotic pets*. Saunders: Philadelphia.
- Godfrey SS, Gardner MG (2017). Lizards, ticks and contributions to Australian parasitology: C. Michael Bull (1947–2016). *International Journal for Parasitology: Parasites and Wildlife* **6**: 295-298.
- Heinrich S, Toomes A, Shepherd CR, Stringham OC, Swan M, Cassey P (2022). Strengthening protection of endemic wildlife threatened by the international pet trade: The case of the Australian shingleback lizard. *Animal Conservation* **25**: 91-100.
- Hyndman T, Shilton C (2018). An update on Australian reptile infectious disease (Conference Proceedings).
- International Committee on Taxonomy of Viruses. Virus taxonomy: 2020. v1 release - order nidovirales. In: *EC 52, Online Meeting, October 2020. Email ratification March 2021 (MSL #36)*. Elsevier
- Iyengar K, Mabrouk A, Jain VK, Venkatesan A, Vaishya R (2020). Learning opportunities from COVID-19 and future effects on health care system. *Diabetes & Metabolic Syndrome: Clinical Research & Reviews* **14**: 943-946.
- Jacobson ER, Gaskin JM, Roelke M, Greiner EC, Allen J (1986). Conjunctivitis, tracheitis, and pneumonia associated with herpesvirus infection in green sea turtles. *J Am Vet Med Assoc* **189**: 1020-1023.
- James FXW, Donald KN, Ling-ling L, Vivek K (2004). Three Novel Herpesviruses Associated With Stomatitis In Sudan Plated Lizards *Gerrhosaurus major* And A Black-Lined Plated Lizard *Gerrhosaurus nigrolineatus*. *Journal of Zoo and Wildlife Medicine* **35**: 50-54.
- Kanyana (2015). Kanyana Wildlife Centre 2014–2015 Annual Report: Perth, WA.
- Literak I, Robesova B, Majlathova V, Majlath I, Kulich P, Fabian P., Roubalova, E., 2010. Herpesvirus-associated papillomatosis in a green lizard. *Journal of Wildlife Diseases*, **46**(1), pp.257-262 (2010). Herpesvirus-Associated Papillomatosis in a Green Lizard. *Journal of Wildlife Diseases* **46**: 257-262.
- Marschang, R.E., 2011. Viruses infecting reptiles. *Viruses*, **3**(11), pp.2087-2126.
- Marschang RE (2019). *Emerging Reptile Viruses*, vol. Volume 9. Fowler's Zoo and Wild Animal Medicine Current Therapy.
- Marschang RE, Bogan J, Pollock C, Gandar F (2021). What's New in the Scientific Literature? Infectious Diseases of Reptiles: Peer-reviewed publications, January-June 2020. *Journal of Herpetological Medicine and Surgery* **30**: 185-193, 189.
- Moller CA (2014). The haematology of bobtail lizards (*Tiliqua rugosa*) in Western Australia: reference intervals, blood cell morphology, cytochemistry and ultrastructure. Masters thesis, Murdoch University, Perth.
- Moratto D, Chiarini M, Giustini V, Serana F, Magro P, Roccaro AM *et al.*, (2020). Flow Cytometry Identifies Risk Factors and Dynamic Changes in Patients with COVID-19. *Journal of Clinical Immunology* **40**: 970-973.
- Morehouse, Z.P., Samikwa, L., Proctor, C.M., Meleke, H., Kamdolozi, M., Ryan, G.L., Chaima, D., Ho, A., Nash, R.J. and Nyirenda, T.S., 2021. Validation of a direct-to-PCR COVID-19 detection protocol utilizing mechanical homogenization: A model for reducing resources needed for accurate testing. *Plos one*, **16**(8), p.e0256316..
- Moreno-Contreras, J., Espinoza, M.A., Sandoval-Jaime, C., Cantú-Cuevas, M.A., Madrid-González, D.A., Barón-Olivares, H., Ortiz-Orozco, O.D., Muñoz-Rangel, A.V., Guzmán-



- Rodríguez, C., Hernández-de la Cruz, M. and Eroza-Osorio, C.M., 2022. Pooling saliva samples as an excellent option to increase the surveillance for SARS-CoV-2 when re-opening community settings. *Plos one*, **17**(1), p.e0263114.
- Nawaz MS, Fournier-Viger P, Shojaee A, Fujita H (2021). Using artificial intelligence techniques for COVID-19 genome analysis. *Applied Intelligence* **51**: 3086-3103.
- Norval G, Ross KE, Sharrad RD, Gardner MG (2019). Taking stock: a review of the known parasites of the sleepy lizard, *Tiliqua rugosa* (Gray, 1825), a common lizard endemic to Australia. *Transactions of the Royal Society of South Australia*: 1-19.
- O’Dea MA, Jackson B, Jackson C, Xavier P, Warren K (2016). Discovery and Partial Genomic Characterisation of a Novel Nidovirus Associated with Respiratory Disease in Wild Shingleback Lizards (*Tiliqua rugosa*). *PLOS ONE* **11**: e0165209.
- Okoh GsR, Horwood PF, Whitmore D, Ariel E (2021). Herpesviruses in Reptiles. *Frontiers in Veterinary Science* **8**.
- Park H, Jung W, Jang H, Namkoong K, Choi K-Y (2022). One-Step RT-qPCR for Viral RNA Detection Using Digital Analysis. *Frontiers in Bioengineering and Biotechnology* **10**.
- Parrish K, Kirkland PD, Skerratt LF, Ariel E (2021). Nidoviruses in Reptiles: A Review. *Frontiers in Veterinary Science* **8**.
- Parsons SK, Bull CM, Gordon DM (2015). Spatial variation and survival of *Salmonella enterica* subspecies in a population of Australian sleepy lizards, *Tiliqua rugosa*. *Applied and Environmental Microbiology*.
- Rakus K, Ronsmans M, Vanderplasschen A (2017). Behavioral fever in ectothermic vertebrates. *Developmental & Comparative Immunology* **66**: 84-91.
- Raynaud A (1976). Lesions Cutanees A Structure Papillomateuse Associees A Des Virus Chez Le Lizard Vert (*Lacerta viridis Laur*).
- Reinhold JM, Lazzari CR, Lahondère C (2018). Effects of the Environmental Temperature on *Aedes aegypti* and *Aedes albopictus* Mosquitoes: A Review. *Insects* **9**: 158.
- Sheridan C (2020). Coronavirus and the race to distribute reliable diagnostics. *Nature Biotechnology* **38**: 382-384.
- Shrestha N, Shad MY, Ulvi O, Khan MH, Karamehic-Muratovic A, Nguyen U-SDT (2020). The impact of COVID-19 on globalization. *One Health* **11**: 100180.
- Vaughn LK, Bernheim HA, Kluger MJ (1974). Fever in the lizard *Dipsosaurus dorsalis*. *Nature* **252**: 473-474.
- Walker, P.J., Siddell, S.G., Lefkowitz, E.J., Mushegian, A.R., Dempsey, D.M., Dutilh, B.E., Harrach, B., Harrison, R.L., Hendrickson, R.C., Junglen, S. and Knowles, N.J., 2019. Changes to virus taxonomy and the International Code of Virus Classification and Nomenclature ratified by the International Committee on Taxonomy of Viruses (2019). *Archives of virology*, **164**(9), pp.2417-2429..
- Wellehan JFX, Nichols DK, Li L-I, Kapur V (2004). Three Novel Herpesviruses Associated with Stomatitis in Sudan Plated Lizards (*Gerrhosaurus major*) and a Black-Lined Plated Lizard (*Gerrhosaurus nigrolineatus*). *Journal of Zoo and Wildlife Medicine* **35**: 50-54.
- Wellehan, J.F., Johnson, A.J., Latimer, K.S., Whiteside, D.P., Crawshaw, G.J., Detrisac, C.J., Terrell, S.P., Heard, D.J., Childress, A. and Jacobson, E.R., 2005. Varanid herpesvirus 1: a novel herpesvirus associated with proliferative stomatitis in green tree monitors (*Varanus prasinus*). *Veterinary microbiology*, **105**(2), pp.83-92.
- Wille M, Yin H, Lundkvist Å, Xu J, Muradrasoli S, Järhult JD (2018). RNAlater® is a viable storage option for avian influenza sampling in logistically challenging conditions. *Journal of Virological Methods* **252**: 32-36.



- Wirth W, Schwarzkopf L, Skerratt LF, Ariel E (2018). Ranaviruses and reptiles. *PeerJ* **6**: e6083.
- Yelin, I., Aharony, N., Tamar, E.S., Argoetti, A., Messer, E., Berenbaum, D., Shafran, E., Kuzli, A., Gandali, N., Shkedi, O. and Hashimshony, T., 2020. Evaluation of COVID-19 RT-qPCR test in multi sample pools. *Clinical Infectious Diseases*, **71**(16), pp.2073-2078.
- Zhang, J., Finlaison, D.S., Frost, M.J., Gestier, S., Gu, X., Hall, J., Jenkins, C., Parrish, K., Read, A.J., Srivastava, M. and Rose, K., 2018. Identification of a novel nidovirus as a potential cause of large scale mortalities in the endangered Bellinger River snapping turtle (*Myuchelys georgesii*). *PloS one*, **13**(10), p.e0205209.



Chapter 3: Supplementary Material

Table S1: Supplementary sample data of *Tiliqua rugosa* on the 2019 Nullarbor field trip between South Australia and Western Australia. Data includes lizard body temperatures and average body temperature (Head, Body, Tail), as well as ambient temperature and observations. Positive sample bolded (Sample 22).

ID #	State	Lat	Long	Serum	Oral Swab	Ground (°C)	Head (°C)	Body (°C)	Tail (°C)	Average temp (°C)	Ambient temp (°C)	Observations
1	SA	-33.1018	137.1968	No	2	33.20	28.70	28.80	28.60	28.70	33	Very active and aggressive. No flu symptoms
2	SA	-33.1983	136.7611	No	2	38.30	33.00	31.10	33.00	32.37	33	No flu symptoms and aggressive
3	SA	-33.1184	136.7664	Yes	2	37.60	34.30	34.00	31.60	33.30	33	Placid. No clinical signs
4	SA	-33.1873	136.5558	Yes	2	28.80	30.60	30.80	30.50	30.63	31	No flu symptoms. Not aggressive,
5	SA	-31.5579	130.4839	Yes	2	13.50	16.10	17.80	16.20	16.70	15	Seemed to be healthy and active. No Flu symptoms
6	WA	-33.0330	121.5292	Yes	2	35.50	32.00	35.50	32.50	33.33	25	No flu symptoms. Tip of tail crushed. Urine was a brown red colour -
7	WA	-33.0931	121.6115	Yes	2	34.40	30.10	31.80	36.20	32.70	22	Very active-running. No flu symptoms



8	WA	-33.0931	121.6358	Yes	2	28.50	32.00	33.10	33.60	32.90	28	Active. No flu symptoms
9	WA	-33.1028	121.7321	Yes	2	29.90	36.70	38.30	33.10	36.03	25	Active. No flu symptoms
10	WA	-33.1250	121.8021	Yes	2	37.60	37.10	37.80	32.80	35.90	28	Active. No flu symptoms. Tail very thin, and scarred
11	WA	-33.1332	121.8039	Yes	2	34.80	33.40	34.80	31.60	33.27	29	Active. Basking in sun with head raised. No flu symptoms. Brown urine though
12	WA	-33.6520	121.3666	Yes	2	29.20	34.30	34.00	33.10	33.80	26	Very active. No flu symptoms
13	WA	-33.6529	121.3666	Yes	2	29.10	33.80	34.70	25.90	31.47	29	Very active. No flu symptoms. Clear urine
14	WA	-33.6932	121.3665	Yes	2	32.60	31.90	30.50	32.30	31.57	30.5	Very active. No symptoms. Left eye doesn't open fully.
15	WA	-33.7619	121.0424	Yes	2	30.80	34.30	36.30	32.20	34.27	29	Very active. No flu symptoms
16	WA	-33.5175	120.2802	Yes	2	33.20	33.10	34.20	33.00	33.43	33	Very active. No flu symptoms. Brown-red urine colour
17	WA	-33.5736	120.2792	Yes	2	37.10	33.60	32.50	32.60	32.90	32	Active. No flu symptoms.
18	WA	-32.0156	116.1896	Yes	2	36.90	35.60	36.70	34.10	35.47	37	Very active. No flu symptoms. Very red coloured head. And oral cavity



													also more red colouring than usual. Not infection red
19	WA	-32.1062	116.2144	Yes	2	23.80	29.00	29.60	24.30	27.63	31		Very active. No clinical signs of illness
20	WA	-32.5755	116.0498	Yes	2	23.80	30.50	30.30	29.40	30.07	28		Active. No Flu symptoms
21	WA	-33.0283	116.5813	Yes	2	38.60	37.20	37.00	35.50	36.57	27		Active. No Flu symptoms
22	WA	-33.0181	116.7126	Yes	2	41.50	35.90	34.90	30.20	33.67	30		Active. No flu symptoms. Prolapse
23	WA	-33.0129	116.7231	Yes	2	40.70	32.30	33.60	33.60	33.17	29		Very active and aggressive. No flu symptoms. Mouth vents very red
24	WA	-32.7118	116.8974	Yes	2	29.60	29.80	30.00	27.50	29.10	27		Not active. very thin. No flu symptoms. Toes missing on all feet.
25	WA	-32.2890	117.1682	Yes	2	38.60	30.40	31.50	32.60	31.50	22		Discoloured patch in throat. Active but slow. No flu symptoms
26	WA	-32.2870	117.1764	Yes	2	40.00	35.60	37.60	37.20	36.80	26		Active. No flu symptoms. Female paired with #27 who was following her.



27	WA	-32.2870	117.1764	Yes	2	40.00	34.90	25.60	34.60	31.70	26	Active. No flu symptoms. Male paired with #26
28	WA	-32.0679	117.0409	Yes	2	34.50	33.60	33.50	32.00	33.03	25	Very active. No flu symptoms. Oral cavity quite red
29	WA	-31.4861	117.0041	Yes	2	43.20	34.70	36.30	32.30	34.43	28	Active. No flu symptoms
30	WA	-31.4055	117.0082	Yes	2	40.70	37.00	36.50	37.20	36.90	30	Active. No flu symptoms
31	WA	-31.3430	117.9348	Yes	2	34.80	35.00	35.80	34.00	34.93	32	Active. No flu symptoms. Prolapse
32	WA	-31.4067	117.9456	Yes	2	35.50	34.60	33.80	30.90	33.10	29	Very, very active. No flu symptoms
33	WA	-31.4119	117.9349	Yes	2	37.40	35.80	35.20	34.10	35.03	30	Very active. No flu symptoms
34	WA	-31.5518	117.9304	Yes	2	41.50	35.30	34.60	33.40	34.43	31	Very active. No flu symptoms. Discoloration, sore, in throat. Scaring on top left jaw
35	WA	-31.5886	117.9897	Yes	2	36.70	30.50	30.10	29.70	30.10	31	Very active. No flu symptoms
36	WA	-31.6866	118.1057	Yes	2	41.60	34.40	33.00	32.30	33.23	28	Not active. Very thin. No flu symptoms
37	WA	-31.9222	118.1739	Yes	2	34.50	32.60	32.50	29.10	31.40	28	Very active. No flu symptoms
38	WA	-32.1124	118.2068	Yes	2	32.50	32.80	32.30	31.80	32.30	28	Very active. No flu symptoms. Struggles to



													put tongue away. White marks on tongue
39	WA	-32.2870	118.1854	Yes	2	30.10	28.30	30.80	29.50	29.53	28		Very active. No flu symptoms
40	WA	-32.6762	118.0031	Yes	2	40.80	34.30	36.00	35.70	35.33	32		Very active. No flu symptoms
41	WA	-32.6795	118.0047	Yes	2	40.50	35.40	33.30	34.50	34.40	31.5		Very active. No flu symptoms
42	WA	-32.6823	117.9764	Yes	2	33.70	32.20	32.00	31.90	32.03	28		Very active. No flu symptoms. White mark (scar?) across tongue
43	WA	-32.7327	117.8747	Yes	2	33.40	32.40	33.30	32.50	32.73	27.5		Very active. No flu symptoms
44	WA	-32.8640	117.8419	Yes	2	38.20	34.50	34.30	32.30	33.70	28.5		Very active. No flu symptoms
45	WA	-32.9467	117.8611	Yes	2	30.10	32.10	33.10	31.60	32.27	29.5		Very active. No flu symptoms
46	WA	-33.1504	117.6929	Yes	2	33.50	31.20	31.10	29.30	30.53	28		Very active. No flu symptoms
47	WA	-33.1966	117.6550	Yes	2	34.50	33.90	34.50	34.00	34.13	28.5		Very active. No flu symptoms
48	WA	-33.2114	117.6367	Yes	2	33.80	32.80	33.50	30.60	32.30	29		Very active. No flu symptoms
49	WA	-33.4344	117.5300	Yes	2	26.30	29.50	29.60	27.70	28.93	26		Very active. No flu symptoms.
50	WA	-33.9329	117.5489	Yes	2	24.70	26.20	26.10	25.00	25.77	23		Not active. Cold and early. No flu symptoms
51	WA	-33.9437	117.5687	Yes	2	29.30	27.90	28.60	27.20	27.90	22.5		Very active. No flu symptoms



52	WA	-33.8362	119.0315	Yes	2	30.80	31.70	32.10	30.80	31.53	27.5	Very active. No Flu symptoms
53	WA	-33.8439	119.0729	Yes	2	37.10	35.20	35.00	32.00	34.07	31	Very active. No flu symptoms. Interesting patterns
54	WA	-33.7808	119.1372	Yes	2	40.90	33.80	33.40	33.20	33.47	28	No Flu symptoms. Throat did have some excess clear saliva. Very active
55	WA	-33.7487	119.3487	Yes	2	36.40	36.60	37.20	34.00	35.93	29.8	No flu symptoms. Very active.
56	WA	-33.6458	119.3711	Yes	2	31.20	30.10	30.60	29.60	30.10	29	No flu symptoms. Very active.
57	WA	-33.3552	119.6483	Yes	2	28.10	26.10	27.60	26.50	26.73	25	Active. No flu symptoms.
58	WA	-33.3321	119.6745	Yes	2	29.20	27.60	27.40	27.30	27.43	27	No flu symptoms. Very active.
59	WA	-32.6575	119.0963	Yes	2	22.80	21.30	21.90	20.50	21.23	19	Inactive. Cold. No flu symptoms.
60	WA	-32.5683	119.0114	Yes	2	21.80	23.10	23.30	21.50	22.63	20	slow, not very active. Cold. No flu like symptoms, however, did notice small amount of white mucus directly on the



												glottis. Swabbed it.
61	WA	-32.6568	118.9093	Yes	2	27.80	28.30	28.30	26.60	27.73	22	No flu symptoms. Not very active, but it was still cold
62	WA	-32.2387	119.1093	Yes	2	34.40	29.40	30.60	27.90	29.30	24	Active. No flu symptoms
63	WA	-32.0817	119.1346	Yes	2	38.50	28.90	29.50	24.70	27.70	27	Very active. No flu symptoms
64	WA	-32.0355	119.1359	Yes	2	39.90	31.00	31.20	27.50	29.90	28	Active. No flu symptoms.
65	WA	-31.9314	119.1750	Yes	2	34.00	31.10	31.50	30.90	31.17	26	No flu symptoms. Not very active.
66	WA	-31.9303	119.1756	Yes	2	28.90	26.80	28.00	26.20	27.00	26	No flu symptoms. Active walking across road. Back scales are bit damaged
67	WA	-31.7726	119.2496	Yes	2	33.30	31.20	30.00	27.40	29.53	29	Active. No Flu symptoms
68	WA	-31.3941	119.3903	Yes	2	33.60	31.00	31.10	29.50	30.53	20	Very active. No flu symptoms.
69	WA	-31.3702	119.3135	Yes	2	34.00	22.90	25.40	24.90	24.40	22	Very active. Saliva a little thick but still clear in colour.
70	WA	-32.3182	125.0978	Yes	2	30.00	29.50	30.40	28.50	29.47	23	No flu symptoms. Very active
71	WA	-32.2999	125.2456	Yes	2	29.50	25.90	27.30	25.00	26.07	28	No flu symptoms. Active.



72	SA	-31.5769	129.8886	Yes	2	32.80	32.80	32.50	25.10	30.13	27	Very active. No flu symptoms. Phlegmy throat
73	SA	-31.5659	130.2415	Yes	2	-	-	-	-	-	27	No flu symptoms.
74	SA	-31.5001	130.7830	Yes	2	28.80	30.90	31.50	26.50	29.63	22	Very active. No flu symptoms
75	SA	-31.4499	130.9013	Yes	2	29.00	28.10	28.90	22.50	26.50	23	Phlegm in throat. Very active
76	SA	-32.0075	133.4675	Yes	2	33.10	33.30	33.00	28.40	31.57	28	Female, paired with #77. No flu symptoms. Active.
77	SA	-32.0075	133.4675	Yes	2	32.30	31.60	33.60	35.50	33.57	28	Male, paired with #76 (following). No flu symptoms. Active.
78	SA	-32.1268	133.7329	Yes	2	37.00	35.60	36.00	37.20	36.27	26	No flu symptoms. Active
79	SA	-32.1474	133.7565	Yes	2	38.60	34.80	34.00	31.20	33.33	32	Very active. No flu symptoms
80	SA	-32.1823	133.8467	Yes	2	47.50	34.10	34.30	35.40	34.60	28	Very active. No flu symptoms
81	SA	-32.1654	133.8852	Yes	2	49.10	34.50	35.30	37.60	35.80	29	Very active. No flu symptoms
82	SA	-32.6105	134.4997	Yes	2	39.90	36.50	35.70	36.30	36.17	30	Possible flu symptoms. Slight yellow mucus in nasal cavity. White phlegm in throat. Watery eyes. Body



												condition was normal. Still active.
83	SA	-32.6810	134.4347	Yes	2	37.00	37.10	37.20	37.00	37.10	30	Active. White phlegm in throat. Just down the same road as the suspected flu lizard #82
84	SA	-32.8493	134.7562	Yes	2	32.10	34.60	35.10	31.3	34.85	29	No flu symptoms. Active
85	SA	-34.1134	135.5839	Yes	2	28.10	33.60	34.30	30.00	32.63	22	Female, paired with #86. Very active. No flu symptoms
86	SA	-34.1134	135.5839	Yes	2	26.10	34.90	35.60	36.00	35.50	22	Male, paired with #85. No flu symptoms. Very active.
87	SA	-33.8826	135.7061	Yes	2	36.70	37.10	38.10	38.50	37.90	29	Very active. No flu symptoms
88	SA	-33.2330	135.6420	Yes	2	39.10	38.60	39.00	37.20	38.27	31	Very active. No flu symptoms
89	SA	-33.2247	136.0013	Yes	2	43.30	34.30	34.00	35.20	34.50	33	Male, paired with #90. Active. Thick white saliva (possibly phlegm)
90	SA	-33.2247	136.0013	Yes	2	43.30	34.20	34.50	34.40	34.37	33	Female, paired with #89. Active. Thick white saliva in oral cavity



91	SA	-33.2776	136.7007	Yes	2	35.50	30.60	31.70	30.70	31.00	31	Very active. No flu symptoms but thick white saliva
50008	SA	-33.8855	139.3551	No	2	42.50	38.80	37.70	37.70	38.10	NA	2 swabs of discharge from the eyes - 1 PBS & 1 RNAlater



Table S2: Lizards ID and samples collected obtained from the Mount Mary study site in South Australia, in 2019.

ID	State	Lat	Long	Oral swabs	SVL (cm)	Weight (g)
1	SA	-33.88687	139.33617	1	34	850
37050	SA	-33.88555	139.34679	1	26	750
37054	SA	-33.88539	139.34885	1	33.9	650
724	SA	-33.91811	139.35	1	36	756
773	SA	-33.88501	139.35519	1	34.4	800
10893	SA	-33.88637	139.33617	1	31	700
30600	SA	-33.88527	139.347475	1	28	625
30500	SA	-33.97167	139.21753	1	28	550
1141	SA	- 33.901414	139.217003	1	31	760
10835	SA	- 33.908364	139.216858	1	32	710
50910	SA	-33.9284	139.268647	1	32.7	950
1120	SA	- 33.971683	139.316658	1	30	700
36000	SA	-33.9671	139.225	1	24.1	210
32002	SA	- 33.901474	139.328054	1	34	800
50905	SA	-33.88637	139.33617	1	35.6	790
34400	SA	-33.97152	139.322517	1	29.5	550
11199	SA	-33.89314	139.24501	1	30.3	625
607	SA	-33.89019	139.28445	1	29	650
33000	SA	- 33.890332	139.290199	1	30	600
11819	SA	-33.88942	139.29501	1	31.2	610
1842	SA	-33.88781	139.3165	1	24.5	510
821	SA	-33.88725	139.31805	1	32	730



ID	State	Lat	Long	Oral swabs	SVL (cm)	Weight (g)
11715	SA	-33.88738	139.32243	1	31.7	800
12414	SA	-33.88702	139.32724	1	28	750
39000	SA	- 33.971395	139.35631	1	27.6	560
14811	SA	- 33.956685	139.21719	1	29.9	610
17304	SA	-33.9486	139.21716	1	29.2	690
14972	SA	-33.97141	139.280548	1	30.2	750
10750	SA	-33.92826	139.3078	1	30.2	550
4291?	SA	-33.92828	139.328	1	33	910
14162	SA	-33.92827	139.33092	1	30	820
35000	SA	-33.92825	139.33628	1	28.6	700
34040	SA	-33.92818	139.34402	1	30.7	760
34020	SA	-33.92831	139.35017	1	29.5	590

STable 3: Descriptive statistics of the number of positive samples for each cohort of *Tiliqua rugosa* sampled

Cohort	N	Mean of Positive samples	Mean std Error
1	91	1	0.0110
2	35	0	0.0000
3	20	16	0.0918



Chapter 4: Foreword

This Chapter looks at how the bobtail flu affects gene regulation in *Tiliqua rugosa* using transcriptomics. The Chapter used two sequencing technologies to overcome the absence of an annotated genome of this non-model organism. There were two groups of *T. rugosa* individuals selected for comparison: 1) a treatment group of four lizards that were euthanised after being diagnosed with the bobtail flu by qualified veterinarians, and were not responding to treatment. 2) a control group with four lizards that were euthanised after suffering major trauma (motor vehicle accident and dog attack).

Unfortunately, not every lizard was swabbed before euthanasia which would enable screening for the *Shingleback nidovirus 1*, one of the viruses associated with the bobtail flu. As survival with treatment is 86%, obtaining tissue took almost three years and therefore it was not feasible to wait for more samples. As such, groupings were based on diagnosis of the bobtail flu by veterinarians, rather than by a specific virus.

Scripts have been hyperlinked to a repository due to their size.



CHAPTER 4: Differential gene expression analysis of a non-model organism (*Tiliqua rugosa*) suggests upregulation of adaptive immune genes with the bobtail flu

Robert L. O'Reilly¹, Carmel Maher¹, Terry Bertozzi² and Michael G. Gardner¹

¹ Flinders University, Bedford Park, Adelaide, SA, Australia

² South Australian Museum, SA 5000, Australia

Corresponding author: robert.liam.oreilly@gmail.com

Keywords: Bobtail flu, Gene expression, *Shingleback nidovirus 1*, Reptile, Lizards, Non-model organism



Abstract

Understanding how a disease affects the host on a genetic level is an important part of systematic virology. The bobtail flu is an upper respiratory tract flu-like disease that affects *Tiliqua rugosa*, a widespread Australian skink that has close interactions with humans. This non-model organism currently does not have a reference genome therefore we used a combination of long read (Iso-seq) and short read (NovaSeq) sequences together to generate transcript expression levels of potentially hyper variable regions. We used tissue from eight *T. rugosa* individuals, four diagnosed with the bobtail flu by veterinarians, and four suffering from major trauma such as motor vehicle accident or dog attack. There were 109 differentially expressed transcripts, 18 upregulated and 91 down regulated. Of the 18 upregulated, 12 were for the adaptive immune system with immunoglobins IgL and IgY. The 91 downregulated consisted of 38 transcripts associated with immune system — the innate, adaptive, and the complementary.



Introduction

Systems virology focuses on the host-virus interaction. Specifically, the understanding of how a virus has entered the host's cells; if the virus suppressed the host's immune system; how it replicates using host resources; what mechanisms of the host are being used; and how the host system responds on a molecular, cellular, tissue, or organism level (Baig *et al.*, 2020; Sato 2021). These questions when explored can lead to better medical treatments that give back some sense of normalcy to those suffering (Gish *et al.*, 2015; Richman and Nathanson 2016). Such research is becoming more readily available as technology evolves. Availability of high throughput next generation technologies has increased over the years, making 'omics research, such as proteomics, transcriptomics, and genomics more accessible, even when applied to non-model organisms (Heck and Neely 2020; Misra *et al.*, 2019; Todd *et al.*, 2016). In recent years, 'omics research has increased rapidly not only due to accessibility and cost reduction, but also the recognition of applicability of developing innovations at this level of biological organisation (Allendorf *et al.*, 2010; Ouborg *et al.*, 2010).

One major issue with 'omics is assembling sequences. *De-novo* assembly is one way to assemble smaller fragments, without a reference genome, however, it is prone to errors due to miss-alignments of the smaller sequence fragments that can affect the results, leading to false conclusions. This issue is alleviated for model organisms that have an annotated reference genome, and are able to use '*ab-initio*' assembly (Martin and Wang 2011). An annotated reference genome allows researchers to deep sequence their organism with the confidence of mapping back to a complete genome with high capture rates and alignments while being able to identify genes that were differentially expressed. Non-model organism transcriptomics, however, must assemble transcripts essentially in the dark, with higher errors from miss alignments, lower capture rates, and unannotated differentially expressed genes (Martin and Wang 2011; Ungaro *et al.*, 2017). One way around these problems is to sequence long read transcripts that extend exon-intron gaps, in order to generate a pseudo reference with the help of open reading frame prediction programs (Amarasinghe *et al.*, 2020; Ungaro *et al.*, 2017). This then allows short read sequencing with greater depth to map back to the reference for expression levels reducing errors and pseudoalignments. This solution is particularly helpful with hypervariable gene regions, such as the Major



Histocompatibility Complex (MHC) immune genes. However, in some cases differentially expressed genes are so distant or unique that they will not align to anything on available databases.

The non-model organism, *Tiliqua rugosa*, is a long-lived, semi-social monogamous lizard that is distributed across the entire southern half of Australia. This species currently has no closely related reference genome available. In Perth, south-west of Australia, the *T. rugosa* population are known to suffer from the bobtail flu, an upper respiratory tract disease which presents flu-like symptoms. This disease has been mostly restricted to Perth and some regions of Western Australia since the early 1990's when it was first discovered, however, there are anecdotal reports of the bobtail flu in other states of Australia (Kanyana 2015; O'Dea *et al.*, 2016). In 2016, the bobtail flu was associated with the *Shingleback nidovirus 1*, a newly discovered virus and the first documented in this species (O'Dea *et al.*, 2016). Initially this partially characterised virus was classed as a *Coronaviridae*, subfamily *Torovirus*, in newly coined genus *Barnivirus* along with six other reptile nidoviruses (Dervas *et al.*, 2020, O'Dea *et al.*, 2016; Zhang *et al.*, 2018). However, these reptile nidoviruses were later reclassified into the family *Tobaniviridae*, subfamily *Serpentovirinae* by the International Committee on Taxonomy of Viruses (Dervas *et al.*, 2020; Parrish *et al.*, 2021; Walker *et al.*, 2019). There is also the suggestion that a recently discovered adenovirus, that has been found to infect lizards in the *Tiliqua* genus, may also contribute to the bobtail flu as a coinfection (Hyndman and Shilton 2018).

The bobtail flu is suspected to have had a severe impact on wild populations surrounding Perth Hills due to the number of sick *T. rugosa* brought into clinics. In one year, as many as 200 symptomatic lizards were brought into Kanyana Wildlife Rehabilitation Centre during 2014 (Kanyana 2015; O'Dea *et al.*, 2016). Based on this information, we aimed to determine how this disease, rather than a particular virus, affects the lizard's genes that play a role in immune response, either upregulation or down regulation of gene expression levels. This was achieved by combining two next generation sequencing technologies: Pacific Bioscience's long read Iso-Seq to create a pseudo reference to use with Illumina's NovaSeq 6000 for deep short read sequencing for expression levels. This project aimed to perform a differential analysis between *T. rugosa* with the flu-like symptoms, and those suffering from major trauma to determine how this disease influences the host's immune system.



Methods

Tissue collection

Spleen tissue was used for this analysis as we were interested in the immune response of *T. rugosa* to the bobtail flu (up-regulation or down-regulation). Playing a key role in immune response, the spleen is the appropriate tissue to target when performing immunological transcriptomics (Dettleff *et al.*, 2017, Priyam *et al.*, 2016, Talavera-López *et al.*, 2019, Tian *et al.*, 2021). Spleens were obtained from Wattle Grove Veterinary Clinic and Kanayana Wildlife Rehabilitation Centre, Perth, Western Australia, by qualified veterinarians from eight *T. rugosa* individuals over a three-year period. Four of these individuals were euthanised due to not responding to treatment and showing flu like symptoms — with two of these individuals having confirmed PCR positive tests for the *Shingleback nidovirus 1*. As the control, four individuals were euthanised after suffering major trauma (motor vehicle collisions or fatal dog attacks) and assessed for flu-like symptoms—open mouth breathing, discharge from the mouth or eyes, lethargy, loss of body condition (O’Dea *et al.*, 2016).

Spleens were removed within 30 minutes of drug induced euthanasia. These tissues were then cut into 5 mm thick pieces and immediately placed in vials containing RNAlater (Forster *et al.*, 2008; Kruse *et al.*, 201; Wille *et al.*, 2018). The vials were placed in the 4°C fridge for 24 hr before moving into the freezer (-20°C) until shipment. After arriving in Adelaide, tissue was stored at South Australian Reginal Facility for Molecular Evolution and Ecology (SARFMEE) in -80°C freezer until used.

As these animals were brought into the centres by members of the public, there is no detailed location data other than the Perth Hills. Only cause of death and tissue type were recorded, and only some animals were swabbed. Sexing of the lizards was done with genetic markers on the tissue (Stuart 2019), but due to the sampling restrictions, sex bias could not be fully accounted for.

Iso-Seq to generate a pseudo-reference genome

Iso-Seq by Pacific Biosciences (California, USA) creates long reads that span entire transcripts and do not require assembly, and is less prone to errors in comparison to short read sequencing alone when there is no reference genome (Beiki *et al.*, 2019). Longer reads with less assembly reduces errors in bioinformatic pipeline that could lead to false conclusions being made. Therefore, we used Iso-Seq to produce consensus transcripts that



were used as a scaffold for short read NovaSeq, that gives higher coverage, to map back to for the expression levels (Rhoads and Au 2015). Only one tissue sample was used for the transcripts and that was tissue “ORE9519A5” or “sample 6”. This sample was from the control group to provide a base reference, with the assumption that the length of the transcripts would cover the same number of functional genes as in the infected sample. Also, as Iso-Seq sequencing is deep, even genes expected to be lower expression will still be detected.

RNA extraction, PCR amplification, and cDNA synthesis

The selected tissue sample had total RNA extracted using RNeasy plus Mini Kit (Qiagen) following manufacturer’s protocols. The total RNA was then sent to SA Pathology to be quality assessed using an Agilent bioanalyser (nanochip) (Figure S1). Once the extracted RNA passed quality check (RIN score 7.3, concentration 77 ng/μl), cDNA was created using Clontech Smarter PCR DNA synthesis kit. Manufactures protocols ‘Procedure & Checklist-Iso-Seq™ template’ were used in preparation for the Sequel® Systems. Optimal PCR cycles for cDNA synthesis was determined using electrophoresis gel (Figure S2). Once optimal conditions were determined, cDNA was created for the sample and sent off to SA Pathology for a bioanalyser high sensitivity DNA assay to determine quality (Figure S3). As the cDNA was determined to meet sample submission quality, the cDNA was then sent to Ramaciotti Centre for Genomics, in Sydney, for sequencing on a SMART cell 8. We opted for no size selection transcripts with a length of up to 4kb.

Transcript assembly

Isoseq3

The bioinformatic pipeline consisted of multiple packages installed on Flinders University’s high performance computer (HPC) ‘DeepThought’ to process the computationally heavy datasets (Flinders 2021). Sequence data were retrieved from Ramaciotti in movie.subreads.bam format, and then processed initially using css (Circular Consensus Sequence) in the Isoseq3 (version 3.0.0) package’s pipeline to generate one representative sequence for each Zero Mode Waveguides (ZMW) (Pacific Biosciences 2018). Zero Mode Waveguides are part of the SMRT cell sequencing technologies that work together with Magbeads to ensure only the product complex is sequenced rather than any short insert SMRTbells, or adapter dimers also in solution (Pacific Biosciences 2018). Using the package



'lima' (version 3.48.3), primer removal and demultiplexing were performed on the circular consensus sequence SLE8055A4.ccs.bam output file. Primers were 'Clontech_5p: AAGCAGTGGTATCAACGCAGAGTACATGGGG', and 'NEB_Clontech_3p: GTACTCTGCGTTGATACTGCTT'. The function '--peek-guess' was also selected to remove any false positive signals ([Script 1: Sequence Data](#)). We removed poly(A) tails from the now full-length reads by using the isoseq3's function 'refine' before using the 'cluster' function ([Script 1: Sequence Data](#)). The Isoseq3 package has an optional step 'polish' which generates per base QVs for transcript consensus sequences using the refined output with the original subread file. While pacific biosciences state the results of this function are only improved marginally, particularly for the time consumed performing this. We erred on the side of conserved caution and performed 'polish' on the data, as there is currently no reference genome for this species, and we were creating a reference for data to map back to ([Script 1: Sequence Data](#)).

Cogent

Cogent (version 8.0.0) uses the high-quality transcripts generated in the Isoseq3 (version 3.0.0) program, and clusters them in gene families (based on transcript similarity) (Hun 2019). It creates K-mer profiles and then calculates a pairwise distance matrix before separating the transcript clusters into unique folders. Transcripts that do not fit a cluster are categorised as unassigned in the partition log ([Script 1: COGENT](#)). We then used a tailored script to reconstruct the contigs for each cluster as Cogent's 'reconstructing contigs' with K=30 did not work. The script loops through each of the clustered transcript folders cycling through K values until the reconstruction succeeds—up to K=99 before failing ([TBreconstructContig-edit.sh](#)). Minimap2 (version 2.23) was then used to map the high-quality transcripts generated in IsoSeq3 to the fake genome reference created in cogent, which were then sorted by kmer value ([Script 1: Minimap2](#)). In order to generate a single sequence per transcript, redundant isoforms needed to be collapsed. Redundant isoforms are variations in sequences for a particular transcript that is of various lengths (Wang et al., 2008). For example, the two sequences PB.1.1 and PB.1.2 means this locus PB.1 has two isoforms. We used the package cDNA_cupcake (version 28.0.0) to collapse these isoforms into one full length transcript for each canonical transcript, before extracting gene name, count, and abundance information ([Script 1: COGENT](#)).



ANGEL: Robust Open Reading Frame Prediction

We used the program ANGEL (version 3.0), and the CD-HIT (v4.7) dependency, that creates robust open reading frames from predictions based on a training-set data to obtain translated protein sequences, coding sequences, and untranslated regions. The coding sequences were then used for a NCBI BLASTx search (Fu *et al.*, 2012; Huang *et al.*, 2010; Tseng 2019). CD-HIT (v4.7) was then used separately on the Angel.cds translated protein files to cluster again to generate names to add to the reference list (Huang *et al.*, 2010; Li *et al.*, 2001).

BLASTX and BLAST2GO

A BLASTx (version 2.12.0+) analysis was performed on the translated protein sequences from the predicted coding sequences generated in ANGEL (ANGEL.cds) using Flinders University's 'DeepThought' HPC in order to autonomously identify the gene names of the transcripts in the reference list (Altschul *et al.*, 1990, Flinders 2021, NCBI Resource Coordinators 2016). The database created for the BLASTx used were downloaded from [Uniprot](#) (The UniProt Consortium 2021). Parameters were set as -max_target_seqs 1 -max_hsps 1 -evalue 0.00001 in format 6 for the data to be used in R. However, we also re-ran the results with the parameters -max_target_seqs 1 -max_hsps 5 -evalue 0.00001 in format 5 as the program Blast2GO can handle 5 hits per sequence and required format 5 to input the data ([Script 1: BLASTx](#)) (BioBam Bioinformatics 2019; Götz *et al.*, 2008). Gene IDs were inferred from the protein IDs identified in this BLASTx search using the [UniProt Retrieve/ID mapping tool](#) online portal.

Blast2GO uses the BLASTx results to map and annotate gene ontology, as well as identifies the distribution blast results of various levels and functions across three categories: Biological processes, Molecular functions, and Cellular Component.

NovaSeq

RNA extraction and assessment

Two separate RNA extractions (RNA mini kit, Qiagen) were performed for each of the eight spleen samples, following manufactures protocols, before being sent to SA Pathology to be run on a nanochip bioanalyser for quality control. The best extracted Total RNA replication



for each sample were selected to be sent to Ramaciotti Centre for Genomics (Sydney, Australia), for NovaSeq 6000 SP sequencing with 150bp paired end reads.

Mapping to transcripts

Quality analysis of the NovaSeq sequencing data were performed on each read end file (R1 and R2) for each sample on Flinders University's HPC 'DeepThought' using FastQC (Andrews 2010; Flinders 2021). There were no poor-quality samples, and adapters were removed by Ramaciotti, the R1 and R2 files were then imported directly into the program Kallisto (0.46.2) as it accepts paired-end reads in separate files (Bray *et al.*, 2016).

Kallisto pseudo-aligned reads to a reference list created from the Iso-seq data, with the two paired end NovaSeq files and generated a h5 output file format ([Kallisto.sh](#)) (Bray *et al.*, 2016). Quantification of estimated read counts was performed for each of the eight samples separately. Using R program (version 4.1.0), Rstudio (version 1.4.1717) with the edgeR package (version 3.34.1) (McCarthy *et al.*, 2012, Robinson *et al.*, 2009), the function 'catchKallisto' was used to obtain estimated transcript counts, and bootstrap samples to determine an over-dispersion coefficient for each transcript (Bray *et al.*, 2016). Sex and Cause of death were added to the h5 names in order to be able to determine sample groups once input into R.

Differential expression analysis in R

Each sample was assigned two group factors ([Script 1: Differential expression](#)). Factor 1 was sex, and factor 2 was Cause of Death (COD) and as we wanted to determine whether the cause of death influenced gene expression and accounted for sex as it is well known sex bias can influence differential expression analyses (Cox *et al.*, 2017; Lv *et al.*, 2021; Mayne *et al.*, 2016). Using EdgeR's DGE list each sample's counts, group, library size, transcript lengths, effective length, and overdispersion were created into an object. We explored the counts per million for each sample, regardless of group factor, and plotted the log distribution. Library size for each sample was then visualised with box plot to ensure the differential analysis was not skewed by variation in sequencing depth between samples. Sample variation was then visualised with a MDS plot of the log fold chains.



Group Factor differential analysis

Transcripts that had less than 5 reads per 2 samples were then filtered out before differential calculations for each group factor were performed: Calculate Normalisation Factors; estimateCommonDisp, in order to estimate a common dispersion value across all genes; and estimateTagwiseDisp, that uses an empirical Bayes method based on maximum likelihood to estimate tagwise dispersion (Robinson *et al.*, 2009). The top 25 differentially expressed genes, based on p-value, were then viewed ([Script 1: Group Factors](#)). Using the 'lma' (version 3.48.3) package in Rstudio, a summary of each group factor's differential analysis was generated to show how many transcripts were significantly up-regulated or down-regulated.

The differentially expressed transcripts were then subset from the non-significant transcripts to attach gene names and gene descriptions from the Blast2GO output file using Excel (version 2205). Due to the low number of these expressed transcripts identified using the automated method, these differentially expressed transcript sequences were then also manually used in nucleotide BLASTx on GenBank. By using NCBI Genbank for a manual BLASTx search, we were able to use other databases like ensembl rather than only using Uniprot.

Results

IsoSeq

RNA extraction and cDNA synthesis

The spleen tissue from sample 6, group factor major trauma, had RNA successfully extracted. Bioanalyser report determined the RNA extraction was suitable for cDNA synthesis with a RIN score of 7.30, and 77ng/ μ l concentration (Figure S1). PCR optimal cycling conditions were shown to be 14 cycles (Figure S2). The high sensitivity DNA assay on the SA pathology's bioanalyser showed 15 peaks, the highest peak at 1098bp while the highest concentration was at 2697bp (1210 pg/ μ l). The average length was 2145bp. The cDNA had minimal contamination and passed quality check to be sent off for IsoSeq sequencing (Figure S3).



Transcript Assembly

Isoseq3

Once sequence data was obtained the data was processed initially using isoseq3 css pipeline to generate one representative circular consensus sequence for each ZMW. There were 624247 ZMWs processed in css, and only 254 ZMWs (0.04%) with tandem repeats. Of the total ZMW input, 75% passed the program's filters. While 85% of the failed ZMW were due to lacking full passes ([Script 1: ZMW](#)). Afterwards, primers and poly A tails were successfully removed which was followed by clustering and polishing.

Cogent

Cogent created a k-mer profile and calculated pairwise distance on the isoseq3 output, that was then partitioned into 23100 separate folders by "gene family". It should be noted that gene family is a term used by the program, that in this scenario, represents transcript sequence similarity and not actual gene family. There were 3545 unassigned transcripts ([Script 1:Cogent](#)). Contigs were then reconstructed using reconstruct_contig.py in an adapted script ([TBreconstructContig-edit.sh](#)). As a result, there were 4199 contigs created as a pseudo reference ([Script 1:Cogent](#)). Minimap2 mapped 23528 sequences back to the reconstructed reference genome. We then collapsed transcript isoforms using cDNA_cupcake to return 15226 of the longest unique full-length transcripts.

ANGEL: Robust Open Reading Frame Prediction

Using the fasta file with the longest transcripts for each gene, a training dataset was created in ANGEL to predict 'dumb ORF' before creating a non-redundant training data set (angel classifier training). Finally, using 'angel_predict.py' the program returned: 11071 ANGEL.cds (coding sequences); 11071 in ANGEL.pep (proteins); and 16228 in ANGEL.utr (untranslated regions).

CD-HIT

The ANGEL.cds output was put into CD-HIT online, in order to cluster again based on protein translations of predicted open read frames and group the unique non-redundant canonical transcripts into putative genes/gene families. Without a reference or further annotation, the level of this clustering cannot be confirmed. The output, analysed in R, determined 45 transcripts in cluster 0, 40 in cluster 1, 11 in cluster 10, 5 in cluster 100, 3 in cluster 1000, and 3 in cluster 1001 ([Script 1: CD-HIT](#)).



Blastx and Blast2GO

The Uniprot's BLASTx search returned 10298 transcripts with hits. After exporting the list into Uniprot's online [Retrieve/ID mapping tool](#) to obtain gene names from UniprotID names, there were 6119 matches. 126 protein IDs did not match to anything. Two Uniprot IDs corresponded to multiple gene IDs. Uniprot ID P32969 corresponds to genes RPL9, RPL9P7, RPL9P8, and RPL9P9. Uniprot ID Q5ZJE4 corresponds to gene IDs RCJMB04_18o22 and SPRING. Duplicate Uniprot IDs were removed (n = 6115). Of the 6115 remaining Uniprot IDs, 5524 corresponded to unique gene IDs. This dataset was joined to the original Blastx search results of 10298 transcripts before filtering gene name with NAs. This left 9298 (of the 10298) that mapped to one of the 6115 gene IDs ([Script 1: Uniprot](#)). Blast2GO showed a total of 95,058 annotations, with the mean level at 7.2 (Figure S4). Annotated transcripts were primarily for biological processes (Figure S4).

NovaSeq

RNA extraction and assessment

Sixteen RNA extractions were performed on the eight tissue samples (2 per sample). However, neither of the extraction replicates for sample 1 passed the quality control for sequencing. Sample 1.1 had DNA contamination, while sample 1.2 was fragmented (Table S1). As such, another two extractions were performed on sample 1 (1.1.1, 1.1.2). Both were acceptable for sequencing (Table S1). The extraction replicate with the highest RIN score and RNA concentration were selected for sequencing (n=8) (Table 1)

FastQC

FastQC was run on the returned NovaSeq data for quality checks. Each sample had two files, R1 and R2 files. No sample read files were flagged as poor quality. Each file contained between 50 -75 million reads. Adapters had been removed by Ramaciotti, no duplicate sequences were flagged (Table S2).

Differential expression analysis

Library Exploration

Multidimensional scaling (MDS) plot for sample variation showed log fold chain dimension 1 was 36%, while dimension 2 was 20% of the variation with sample39140_2FLU_S3_Male as the greatest outlier (Figure S5). A box plot of the Log2 counts per million for each sample



showed similar counts per million, slightly over 5 million, with sample 39140_2FLU_S3_Male, again, as a slight outlier with below the mean log2 counts for each sample (Figure 1). A heatmap of the top 500 most variable genes showed some uniqueness in individuals 39140_2FLU_S3_Male, the most variable genes showing low level expression (Figure 2). Whereas sample 1_1_1MT_S8_Male had high expression levels (Figure 2)

Differential group factor: Cause of Death (COD)

. Of the total 8571 transcripts, 8560 were not significantly differentially expressed. However, there were eleven significantly expressed, six down-regulated and five up-regulated. Two of the eleven matched to a gene ontology on the Uniprot database, the human Immunoglobulin lambda-like polypeptide (Table S3). A manual BLASTx search of the differentially expressed transcript sequences returned a hit for all differentially expressed transcripts (Table S4). Four out of the five differentially expressed upregulated transcripts were associated with the immune system (Table S4). Whereas only one of the six downregulated were associated with the immune system (Table S4).

Differential group factor: SEX (no Cause of Death)

When defining group factor by sex only, of the total 8571 transcripts, there were eighteen significantly differentially expressed between groups, seven down regulated and eleven up regulated. Nine of the eleven up regulated transcripts returned a hit on the Uniprot database. Of the nine, only one was associated with the immune system 'IGSF2_HUMANImmunoglobulin superfamily member 2'. None of the seven down regulated transcripts returned a match on the Uniprot database (Table S5). After manually running a BLASTx search on the differentially expressed transcript sequences, all transcripts returned a match (Table S6). Of the eleven up regulated transcripts, four were associated with the immune system, whereas two of the seven down regulated were of the immune system (Table S6).

Differential group factor: Cause of Death sex differentiated (CODsex)

When sex was factored in with cause of death there were 109 differentially expressed transcripts, and 8462 not significant. Of the 109, eighteen were up regulated and 91 downregulated. The automated BLASTx search using the Uniprot database returned 57/109 matches (Table S7). Two of the eighteen up regulated were of the immune system in mice and chicken 'LAC2_MOUSEIg lambda-2 chain C region' and 'PDIA3_CHICKProtein disulfide-



isomerase' with twenty-two of the 91 downregulated transcripts were linked to the immune system (Table S7). A manual BLASTx of transcripts sequences, rather than transcript ID names, returned a match for 107/109 transcripts (Table S7). Twelve of the eighteen up regulated differentially expressed transcripts were associated with the immune system, with multiple isoforms of the adaptive immune system (Table 2). Of the 91 down regulated transcripts, the manual BLASTx returned 38 transcripts (41.7%) linked predominantly to the innate immune system (Table 2)

Discussion

Interpretation of results

We used two next generation sequencing technologies (Iso-seq and NovaSeq) for a differential gene expression analysis on *Tiliqua rugosa* suffering from the bobtail flu, compared to those that had suffered major trauma. By using Pacific Bioscience's Iso-seq to generate long read transcripts we were able to build a reference to map Illumina's short read NovaSeq to. This allowed us to reduce misalignments and pseudo-alignments prone to de novo assembly when conducting transcriptomics on a non-model organism without a reference genome (Ungaro *et al.*, 2017).

The differential analysis in the cause of death group when factoring in sex (CODsex), found 109 differentially expressed transcripts (Figure 3; Table S7). Twelve of the eighteen upregulated transcripts were associated with isoforms of immunoglobulin lambda-1 light chain-like (IGL1) and the immunoglobulin Y heavy chain constant region (IGY) in a variety of reptiles: the eastern fence lizard (*Sceloporus undulatus*), the Green Sea turtle (*Chelonia mydas*), the Leatherback sea turtle (*Dermochelys coriacea*), and the Green anole (*Anolis carolinensis*) (Table 2). These genes are associated with the adaptive immune system, as immunoglobulins, or antibodies, are glycoproteins responsible for binding to specific antibodies (Schroeder and Cavacini 2010). Immunoglobulin Y (IgY) molecules are in fact functionally the same as the human Immunoglobulin G (IgG) molecule that is responsible for antigen specific binding (Schroeder and Cavacini 2010; Zimmerman *et al.*, 2010). These differentially expressed upregulated transcripts between the control group and the bobtail flu group suggests infection was long enough to produce a secondary immune response (IgY) from the adaptive immune system, or the animals had been previously infected with the disease-causing agent. We cannot know which from these results, however, the



production of IgY requires maturation of naive antibodies to a specific antigen—this can take 6-8 weeks in reptiles (Zimmerman 2016).

Of the 91 differentially expressed transcripts (CODsex) that were downregulated, 38 of them were associated with the immune system. These sequences matched to a variety of reptiles: Common wall lizard (*Podarcis muralis*); Sand lizard (*Lacerta agilis*); Eastern fence lizard (*Sceloporus undulatus*); Central bearded dragon (*Pogona vitticeps*); and the Tiger rattle snake (*Crotalus tigris*) (Table2). The variable query cover and percentage of identify of the BLASTx results in Table2 can be explained by the fact those reptiles are distantly related to the *T. rugosa* and likely matched to the conserved regions of each gene. Ideally, an annotated genome would provide greater coverage however that is not currently possible.

A large portion (41.7%) of the 91 downregulated transcripts (CODsex) play a role in the innate immune response such as: Interleukin-1 receptor antagonist protein-like; interleukin-6; NF-kappa-B inhibitor alpha; interferon regulatory factor 1; interferon gamma receptor 1; toll-like receptor 5; neutrophil cytosol factor 1; and monocyte differentiation antigen CD14 (Table2). The differentially expressed transcripts such as Interferon (IFN) and Toll-like receptors (TLR) are antigen recognition molecules in the innate immune response (Lester and Li 2014; Taylor and Mossman 2013; Zou *et al.*, 2016). They then signal molecules like Interleukin (IL) and NF-Kappa-B inhibitors (NFkB) that are involved in a cascade of immune responses, for example, signalling pro inflammatory cytokines and cytotoxic immune cells (Akdis *et al.*, 2011; Doyle and O'Neill 2006).

Downregulation of these differentially expressed transcripts suggests that the host's innate immune signalling response is dysregulated when suffering from the bobtail flu, compared to those in the control group. This is interesting as the bobtail flu has been associated with at least one respiratory virus, the *Shingleback nidovirus 1* (O'Dea *et al.*, 2016). In fact, two of the four samples in the Flu group (Sample 4.2 and 39140.1) were PCR positive for the *Shingleback nidovirus 1* – The others were not tested.

The *Shingleback nidovirus 1* is a positive single strand RNA virus classified as a serpentovirus (Dervas *et al.*, 2020; O'Dea *et al.*, 2016; Parrish *et al.*, 2021; Walker *et al.*, 2019). All +RNA viruses delay or interrupt antiviral signalling as a mechanism for a more efficient viral replication and increase the chance of survival in the host (Scutigliani and Kikkert, 2017; Kikkert 2020). Although only 50% of the flu group were confirmed positive for the



Shingleback nidovirus 1, the observed downregulation of signal receptors (Interleukin-1 receptor antagonist protein-like; NF-kappa-B inhibitor alpha; interferon regulatory factor 1; interferon gamma receptor 1) does align with a RNA virus infection. Because the innate immune system is linked closely to the adaptive immune responses, this also indirectly affects the adaptive immune system, such as activating naïve T-cells to antigen-specific killers (CD8⁺ T-cells) (Bevan 2004; Kikkert 2020; Mahajan et al., 2021).

We expected there to be MHC class I differentially expressed transcripts as MHC class I is a key antigen recognition molecule of the adaptive immune system that identifies viruses, before presenting them to T-cells for destruction (Knapp, 2005). However, there were no MHC differentially expressed. It could be the animals were not infected long enough for the reptile's slow immune system to build a significant adaptive response, and the observed upregulation of IgY were the beginnings of an adaptive response (Zimmerman 2016)..

One major limitation with this study is the inconsistent swabbing of euthanised lizards for both groups. Although veterinarian diagnosis of symptomatic lizards with the bobtail flu is reliable, there is a low chance that individuals in the major trauma group could have been asymptomatic. All lizards for both groups should have been screened specifically for the *Shingleback nidovirus 1* and the adenovirus. We could have then associated the regulation of the adaptive and innate immune system observed in this study to one or more viruses rather than a disease. This would enable a clearer explanation of the regulation of signal pathways observed here with less speculation. Another potential limitation is the control group. Due to the trauma sustained by the group before euthanasia, a systemic immune response, such as inflammation, is likely (Maier *et al.*, 2008). However, euthanasia of healthy animals from the same local area was not feasible at the time.

This study brings about interesting questions: Is the downregulation of the innate immune system in response to disease a result of the *Shingleback nidovirus 1* infection? — 50% of the flu group were confirmed PCR positive. Were these animals also infected with the adenovirus that is thought to contribute to the bobtail flu? Can either virus cause the bobtail flu, independent of each other? Is the disease more severe or less with the presence of both? Is there viral interference or superinfection exclusion? Perhaps being taxonomically/genetically different viruses (ssRNA and dsDNA), they do not inhibit each other. Adenoviruses typically trigger multi-level host defences for detection and destruction



such as the TLR, IL1, 1L6, IFN, that our study showed were downregulated (Atasheva and Shayakhmetov 2016). If these are suppressed enough then its logical to expect the adenovirus, or any other opportunistic pathogen, has a better opportunity to survive the host's defences. Future research will need to explore these questions by screening for both viruses when repeating the experiment.

Conclusion

Our study found significantly differentially expressed transcripts associated with immune defence between groups diagnosed with the bobtail flu, and those suffering from major trauma. However, this research does create a lot of interesting questions on these lizards' immune response and possible viral coinfections as a result of a suppressed immune system. Future research should be conducted to answer these questions particularly further exploring coinfections in these reptiles. There is a platinum standard annotated genome for *Tiliqua rugosa* currently in development that will make future gene expression analyses more powerful and could further validate previous transcriptomic work on this species



Figures

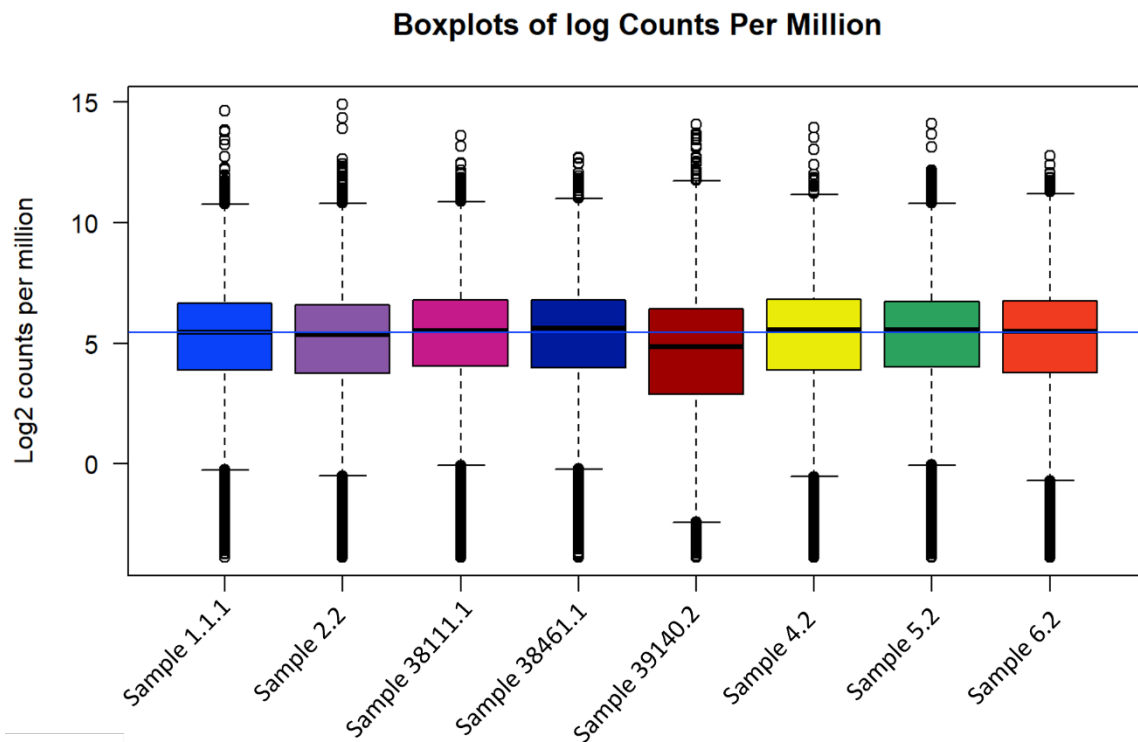
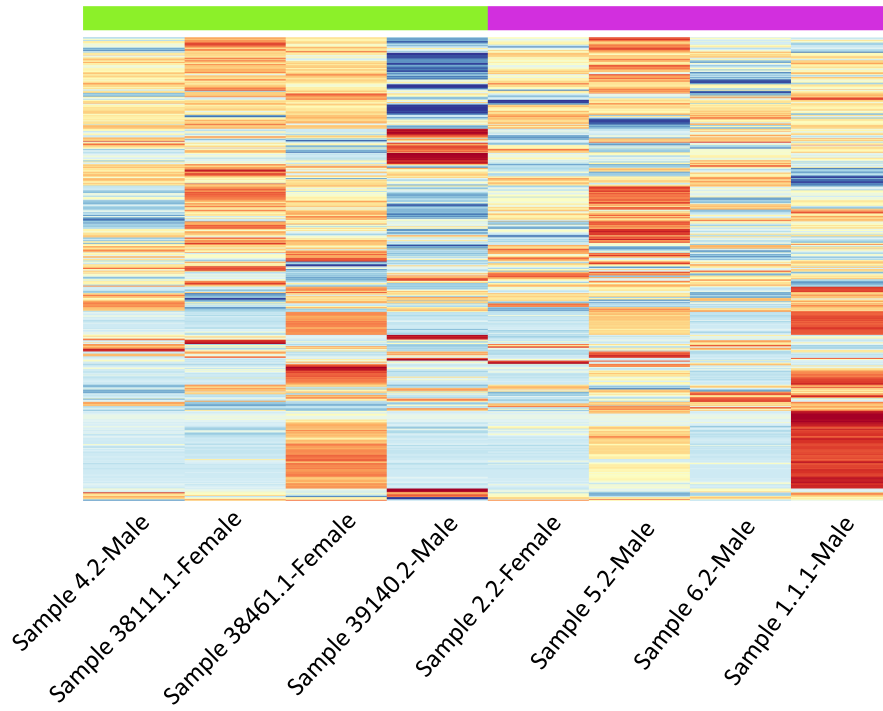


Figure1: Box plot of log counts per million for each sample. Figure shows normalised expression distributions. Blue dividing line represents median data, while individual boxes indicate upper and lower quartiles (top to bottom respectively).



Top 500 most variable genes across samples



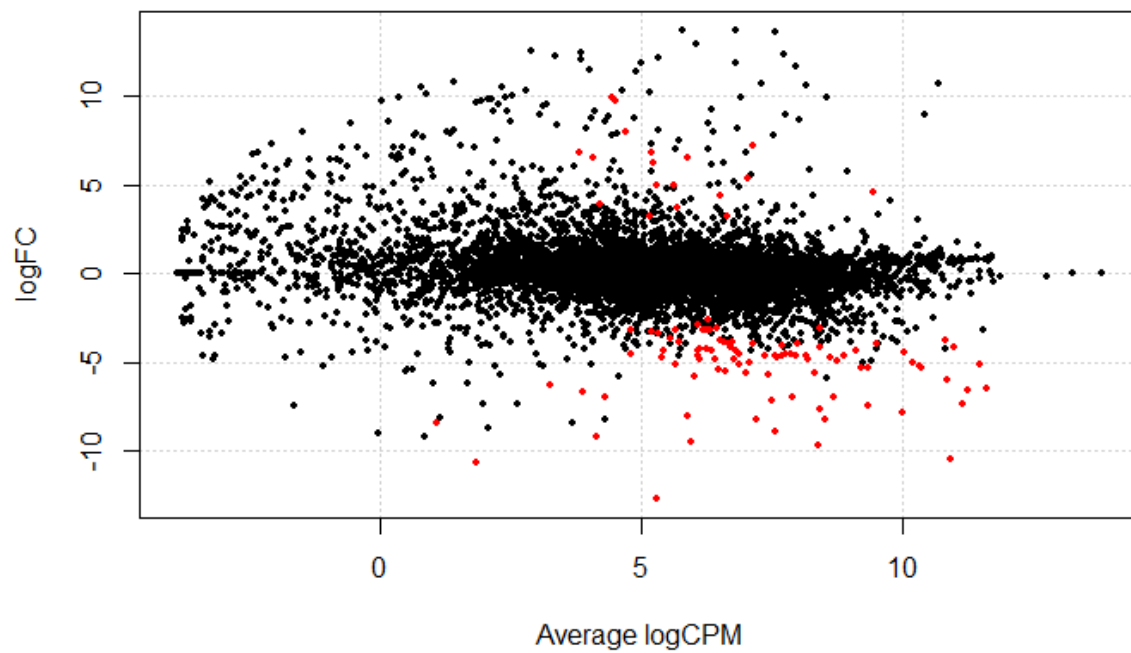


Figure 3: Visualise the logged Fold Change against Average logged counts per million, in expression of transcripts between Flu and Major Trauma groupings, using a plotsmear. Red indicates PValue < 0.05



Tables

Table 1: NovaSeq sample submission of Total RNA sent to Ramaciotti Centre for Genomics for sequencing. Samples obtained from the spleens of eight *Tiliqua rugosa* by qualified veterinarians (Wattle Grove Veterinary Hospital) in Western Australia.

Sample Submission names	Sample	Sex	Cause of Death	RIN Score	RNA_conc (ng/ul)	RNA area
RO-4.2FLU	4.2	Male	FLU	8.5	509	747.7
RO-38111.1FLU	38111.1	Female	FLU	8.8	344	583
RO-38461.1FLU	38461.1	Female	FLU	8.6	700	1186.2
RO-39140.2FLU	39140.2	Male	FLU	7.6	289	323.1
RO-2.2MT	2.2	Female	Major trauma	7.2	684	1047.1
RO-5.2MT	5.2	Male	Major trauma	9.5	431	633.1
RO-6.2MT	6.2	Male	Major trauma	8.5	356	523.4
RO-1.1.1MT	1.1.1	Male	Major trauma	7.7	613	685



Table 2: Group factor: ‘Cause of Death (sex)’: Differentially expressed transcripts and their descriptions that corresponded to some component of the immune system in reptiles. Descriptions are based on a manual BLASTx search of the transcript sequences. Expressed: 1 = upregulated, - 1 = downregulated.

TranscriptID	Sequence length	Expressed	Maunal Blastx Description - NCBI	Max Score	Total Score	Query Cover	E value	Per. Ident	Acc. Len	Accession
PB.435.2 b'13a0c1' path 118:76-1126(+) transcript/13736	1045	1	immunoglobulin lambda-1 light chain-like isoform X8 [<i>Sceloporus undulatus</i>]	260	260	67%	2.00E-82	59.15%	235	XP_042297772.1
PB.482.1 b'13a0c1' path 197:14-981(+) transcript/15717	968	1	immunoglobulin lambda-1 light chain-like isoform X10 [<i>Sceloporus undulatus</i>]	181	250	73%	7.00E-52	51.52%	235	XP_042297774.1
PB.487.1 b'13a0c1' path 205:0-1145(+) transcript/13689	1148	1	immunoglobulin lambda-1 light chain-like isoform X7 [<i>Sceloporus undulatus</i>]	164	268	60%	2.00E-55	56.29%	235	XP_042297771.1
PB.519.1 b'13a0c1' path 256:0-993(+) transcript/15646	992	1	immunoglobulin lambda variable 5-39 isoform X8 [<i>Chelonia mydas</i>]	204	204	68%	1.00E-60	50.00%	241	XP_043385604.1



TranscriptID	Sequence length	Expressed	Maunal Blastx Description - NCBI	Max Score	Total Score	Query Cover	E value	Per. Ident	Acc. Len	Accession
PB.581.1 b'13a0c1' path 337:189-1070(+) transcript/16392	880	1	immunoglobulin lambda-1 light chain-like isoform X10 [<i>Sceloporus undulatus</i>]	134	134	52%	6.00E-34	51.30%	235	XP_042297774.1
PB.584.1 b'13a0c1' path 340:0-1082(+) transcript/14311	1080	1	immunoglobulin lambda-1 light chain-like isoform X3 [<i>Dermochelys coriacea</i>]	270	270	68%	3.00E-85	54.00%	276	XP_043353662.1
PB.586.2 b'13a0c1' path 344:1-972(+) transcript/15761	972	1	immunoglobulin lambda-1 light chain-like isoform X8 [<i>Sceloporus undulatus</i>]	267	267	72%	2.00E-85	57.20%	235	XP_042297772.1
PB.604.1 b'13a0c1' path 368:0-1012(+) transcript/15392	1012	1	immunoglobulin lambda-1 light chain-like isoform X8 [<i>Sceloporus undulatus</i>]	252	252	68%	2.00E-79	53.88%	235	XP_042297772.1
PB.618.2 b'13a0c1' path 44:3-1072(+) transcript/14751	1071	1	immunoglobulin lambda-1 light chain-like isoform X8 [<i>Sceloporus undulatus</i>]	286	286	65%	2.00E-92	61.44%	235	XP_042297772.1



TranscriptID	Sequence length	Expressed	Maunal Blastx Description - NCBI	Max Score	Total Score	Query Cover	E value	Per. Ident	Acc. Len	Accession
PB.3525.1 b'9d81d9' path0:h75:0-2817(+) transcript/7028	1901	1	immunoglobulin Y heavy chain constant region [<i>Anolis carolinensis</i>]	436	436	68%	4.00E-144	51.13%	443	ABV66132.1
PB.4069.1 b'b1d8d5' path0:h293:0-2678(+) transcript/7688	1919	1	immunoglobulin Y heavy chain constant region [<i>Anolis carolinensis</i>]	475	475	70%	3.00E-159	51.10%	443	ABV66132.1
PB.6546.1 transcript/1383:0-3327(+) transcript/1383	3327	1	PREDICTED: leucine-rich repeat neuronal protein 3 [<i>Anolis carolinensis</i>]	521	1232	63%	0	88.93%	708	XP_003221250.1
PB.65.1 b'0305f0' path0:0-1536(+) transcript/10418	1536	-1	natural cytotoxicity triggering receptor 1-like [<i>Podarcis muralis</i>]	123	192	50%	3.00E-27	42.86%	317	XP_028607677.1
PB.72.2 b'035475' path0:2-1628(+) transcript/13640	1160	-1	interleukin-8-like [<i>Lacerta agilis</i>]	145	145	22%	1.00E-38	79.31%	104	XP_033026963.1



TranscriptID	Sequence length	Expressed	Maunal Blastx Description - NCBI	Max Score	Total Score	Query Cover	E value	Per. Ident	Acc. Len	Accession
PB.490.2 b'13a0c1' path 210:95-1035(+) transcript/15172	949	-1	immunoglobulin lambda-1 light chain-like isoform X12 [<i>Sceloporus undulatus</i>]	239	239	73%	1.00E-74	53.65%	234	XP_042297776.1
PB.593.1 b'13a0c1' path 352:280-974(+) transcript/18599	692	-1	immunoglobulin lambda-1 light chain-like isoform X14 [<i>Sceloporus undulatus</i>]	123	189	68%	3.00E-38	56.03%	234	XP_042297779.1
PB.613.1 b'13a0c1' path 38:50-906(+) transcript/16749	857	-1	immunoglobulin lambda-1 light chain-like isoform X10 [<i>Sceloporus undulatus</i>]	143	143	59%	2.00E-37	46.55%	235	XP_042297774.1
PB.871.2 b'1da525' path 1:1543-3709(+) transcript/5514	2168	-1	PREDICTED: putative helicase MOV-10 isoform X2 [<i>Anolis carolinensis</i>]	791	791	70%	0	76.61%	956	XP_008108050.1
PB.1265.1 b'30964e' path h0:0-3659(+) transcript/1072	3539	-1	intercellular adhesion molecule 5-like [<i>Zootoca vivipara</i>]	511	511	40%	5.00E-165	50.38%	545	XP_034957462.1



TranscriptID	Sequence length	Expressed	Maunal Blastx Description - NCBI	Max Score	Total Score	Query Cover	E value	Per. Ident	Acc. Len	Accession
PB.1265.2 b'30964e' pat h0:1-4332(+) transcript/330	4334	-1	intercellular adhesion molecule 5-like [<i>Zootoca vivipara</i>]	579	579	36%	0	54.92%	545	XP_034957462.1
PB.1276.1 b'315ed9' pat h0:0-1559(+) transcript/10267	1557	-1	LOW QUALITY PROTEIN: fos-related antigen 1 [<i>Podarcis muralis</i>]	336	336	53%	2.00E-108	83.09%	311	XP_028565992.1
PB.1299.1 b'32371b' pat h1:0-1999(+) transcript/6528	1998	-1	TNFAIP3-interacting protein 3-like isoform X1 [<i>Dermochelys coriacea</i>]	338	338	58%	6.00E-106	53.38%	408	XP_038271750.1
PB.1300.1 b'32371b' pat h2:0-1921(+) transcript/7402	1921	-1	PREDICTED: TNFAIP3-interacting protein 3 isoform X2 [<i>Alligator mississippiensis</i>]	327	327	54%	1.00E-102	55.49%	366	XP_006278146.1
PB.1378.3 b'3700c4' pat h1:14-2774(+) transcript/3391	2533	-1	TNFAIP3-interacting protein 1 isoform X3 [<i>Zootoca vivipara</i>]	886	886	71%	0	81.89%	628	XP_034961580.1



TranscriptID	Sequence length	Expressed	Maunal Blastx Description - NCBI	Max Score	Total Score	Query Cover	E value	Per. Ident	Acc. Len	Accession
PB.1463.1 b'3b03d2' pat h2:0-1787(+) transcript/8363	1783	-1	interleukin-1 receptor antagonist protein-like isoform X1 [<i>Podarcis muralis</i>]	242	242	27%	7.00E-73	72.05%	178	XP_028597091.1
PB.1464.1 b'3b03d2' pat h5:118-1846(+) transcript/9115	1732	-1	interleukin-1 receptor antagonist protein-like isoform X1 [<i>Podarcis muralis</i>]	251	251	30%	1.00E-76	69.71%	178	XP_028597091.1
PB.1489.1 b'3c6578' pat h0:0-1382(+) transcript/11978	1382	-1	interleukin-6 [<i>Pogona vitticeps</i>]	209	209	45%	3.00E-61	55.19%	219	XP_020637801.1
PB.1863.1 b'4ee890' pat h0:0-3659(+) transcript/883	3660	-1	neutrophil cytosol factor 1 [<i>Lacerta agilis</i>]	689	689	31%	0	83.29%	389	XP_033028282.1
PB.2071.4 b'58c046' pat h0:59-2811(+) transcript/2765	2748	-1	leukocyte immunoglobulin-like receptor subfamily A member 6 [<i>Varanus komodoensis</i>]	101	166	16%	1.00E-17	43.08%	719	XP_044303646.1



TranscriptID	Sequence length	Expressed	Maunal Blastx Description - NCBI	Max Score	Total Score	Query Cover	E value	Per. Ident	Acc. Len	Accession
PB.2602.1 b'74e2ed' pat h0:0-706(+) transcript/17892	706	-1	interferon regulatory factor 1 [<i>Sceloporus undulatus</i>]	229	229	49%	4.00E-71	89.66%	303	XP_042311195.1
PB.2603.1 b'74e2ed' pat h1:0-2391(+) transcript/4253	2392	-1	interferon regulatory factor 1 [<i>Sceloporus undulatus</i>]	375	375	34%	2.00E-120	72.50%	303	XP_042311195.1
PB.2603.2 b'74e2ed' pat h1:0-2387(+) transcript/6312	1950	-1	interferon regulatory factor 1 [<i>Varanus komodoensis</i>]	415	415	47%	8.00E-138	69.33%	302	XP_044310382.1
PB.3082.1 b'8a6ab3' pat h0:0-1943(+) transcript/6626	1943	-1	leukocyte elastase inhibitor-like isoform X1 [<i>Pogona vitticeps</i>]	654	654	64%	0	73.75%	453	XP_020669995.1
PB.3351.1 b'980835' pat h2:0-1705(+) transcript/9312	1706	-1	NF-kappa-B inhibitor alpha [<i>Podarcis muralis</i>]	138	138	12%	4.00E-32	92.86%	330	XP_028576521.1
PB.3377.1 b'993720' pat h0:0-2416(+) transcript/4249	2403	-1	interferon gamma receptor 1 [<i>Lacerta agilis</i>]	273	273	54%	2.00E-79	41.96%	433	XP_032999761.1



TranscriptID	Sequence length	Expressed	Maunal Blastx Description - NCBI	Max Score	Total Score	Query Cover	E value	Per. Ident	Acc. Len	Accession
PB.3650.3 b'a36ec8' pat h9:0-1953(+) transcript/6307	1954	-1	transcription factor jun-B isoform X1 [<i>Varanus komodoensis</i>]	239	508	43%	1.00E-126	89.92%	317	XP_044309937.1
PB.4156.1 b'b23a8a' pat h0:0-4868(+) transcript/178	4868	-1	tumor necrosis factor alpha-induced protein 3 [<i>Podarcis muralis</i>]	1049	1301	49%	0	75.56%	810	XP_028579370.1
PB.5257.2 b'e2b1f3' path 0:119-2644(+) transcript/9125	1752	-1	PREDICTED: complement factor B [<i>Gekko japonicus</i>]	629	685	88%	0	60.64%	770	XP_015260944.1
PB.5257.3 b'e2b1f3' path 0:1036-2644(+) transcript/9752	1606	-1	complement factor B [<i>Podarcis muralis</i>]	711	1014	91%	0	68.17%	1233	XP_028573449.1
PB.5622.1 b'f3d115' path 3:0-1784(+) transcript/11734	1412	-1	suppressor of cytokine signalling 3 [<i>Python bivittatus</i>]	397	397	46%	2.00E-134	94.09%	241	XP_007428564.2
PB.5622.2 b'f3d115' path 3:0-2439(+) transcript/4075	2440	-1	suppressor of cytokine signalling 3 [<i>Python bivittatus</i>]	396	396	27%	3.00E-129	94.09%	241	XP_007428564.2



TranscriptID	Sequence length	Expressed	Maunal Blastx Description - NCBI	Max Score	Total Score	Query Cover	E value	Per. Ident	Acc. Len	Accession
PB.5622.4 b'f3d115' path 3:0-2435(+) transcript/6684	2023	-1	suppressor of cytokine signaling 3 [<i>Python bivittatus</i>]	224	370	30%	1.00E-91	92.31%	241	XP_007428564.2
PB.6100.1 transcript/11390:0-1457(+) transcript/11390	1457	-1	TNFAIP3-interacting protein 3 [<i>Podarcis muralis</i>]	452	452	69%	4.00E-154	71.22%	343	XP_028600850.1
PB.6132.1 transcript/11542:0-1442(+) transcript/11542	1442	-1	cytospin-B isoform X1 [<i>Maylandia zebra</i>]	76.6	76.6	26%	2.00E-10	31.06%	1360	XP_024659847.1
PB.6180.1 transcript/11718:0-1345(+) transcript/11718	1345	-1	interleukin-8-like [<i>Pelodiscus sinensis</i>]	67.4	67.4	8%	1.00E-09	83.78%	104	XP_006125460.1
PB.6297.1 transcript/12432:0-1323(+) transcript/12432	1323	-1	monocyte differentiation antigen CD14 [<i>Crotalus tigris</i>]	396	396	76%	2.00E-131	64.53%	445	XP_039182068.1
PB.7798.1 transcript/2282:0-2882(+) transcript/2282	2882	-1	TNF receptor-associated factor 2-like [<i>Zootoca vivipara</i>]	317	545	37%	5.00E-144	74.55%	364	XP_034963066.1



TranscriptID	Sequence length	Expressed	Maunal Blastx Description - NCBI	Max Score	Total Score	Query Cover	E value	Per. Ident	Acc. Len	Accession
PB.7969.1 transcript/2499:0-2827(+) transcript/2499	2827	-1	interferon-inducible GTPase 5-like [<i>Chrysemys picta bellii</i>]	419	419	42%	3.00E-134	54.95%	397	XP_005314339.1
PB.8363.1 transcript/4274:0-2345(+) transcript/4274	2345	-1	toll-like receptor 5 [<i>Lacerta agilis</i>]	727	727	83%	0	65.70%	657	XP_033030737.1
PB.8970.1 transcript/7812:0-1907(+) transcript/7812	1907	-1	interferon-stimulated gene 20 kDa protein isoform X3 [<i>Chrysemys picta bellii</i>]	242	242	27%	1.00E-72	65.70%	174	XP_005294944.1



Data Availability

Data and scripts are stored on a GitHub repository and will be publicly available once published.



References

- Akdis M, Burgler S, Crameri R, Eiwegger T, Fujita H, Gomez E *et al.*, (2011). Interleukins, from 1 to 37, and interferon- γ : Receptors, functions, and roles in diseases. *Journal of Allergy and Clinical Immunology* **127**: 701-721.e770.
- Allendorf FW, Hohenlohe PA, Luikart G (2010). Genomics and the future of conservation genetics. *Nature Reviews Genetics* **11**: 697-709.
- Altschul SF, Gish W, Miller W, Myers EW, Lipman DJ (1990). Basic local alignment search tool. *Journal of Molecular Biology* **215**: 403-410.
- Amarasinghe SL, Su S, Dong X, Zappia L, Ritchie ME, Gouil Q (2020). Opportunities and challenges in long-read sequencing data analysis. *Genome Biology* **21**: 30.
- Andrews S (2010). FastQC: A Quality Control Tool for High Throughput Sequence Data.
- Atasheva S, Shayakhmetov DM (2016). Adenovirus sensing by the immune system. *Current opinion in virology* **21**: 109-113.
- Baig AM, Khaleeq A, Ali U, Syeda H (2020). Evidence of the COVID-19 Virus Targeting the CNS: Tissue Distribution, Host–Virus Interaction, and Proposed Neurotropic Mechanisms. *ACS Chemical Neuroscience* **11**: 995-998.
- Beiki, H., Liu, H., Huang, J., Manchanda, N., Nonneman, D., Smith, T.P.L., Reecy, J.M. and Tuggle, C.K., 2019. Improved annotation of the domestic pig genome through integration of Iso-Seq and RNA-seq data. *BMC genomics*, **20**(1), pp.1-19.
- Bevan, M (2004). Helping the CD8⁺ T-cell response. *Nat Rev Immunol* **4**: 595–602.
- BioBam Bioinformatics (2019). OmicsBox – Bioinformatics Made Easy, BioBam Bioinformatics. .
- Bray NL, Pimentel H, Melsted P, Pachter L (2016). Near-optimal probabilistic RNA-seq quantification. *Nature Biotechnology* **34**: 525-527.
- Cox RM, Cox CL, McGlothlin JW, Card DC, Andrew AL, Castoe TA (2017). Hormonally Mediated Increases in Sex-Biased Gene Expression Accompany the Breakdown of Between-Sex Genetic Correlations in a Sexually Dimorphic Lizard. *The American Naturalist* **189**: 315-332.
- Dervas E, Hepojoki J, Smura T, Prähauser B, Windbichler K, Blümich SS, Ramis A, Hetzel U, Kipar, A. (2020). Serpentoviruses: More than Respiratory Pathogens. *Journal of Virology* **94**: e00649-00620.
- Dettleff P, Moen T, Santi N, Martinez V (2017). Transcriptomic analysis of spleen infected with infectious salmon anemia virus reveals distinct pattern of viral replication on resistant and susceptible Atlantic salmon (*Salmo salar*). *Fish & Shellfish Immunology* **61**: 187-193.
- Doyle SL, O'Neill LA (2006). Toll-like receptors: from the discovery of NFkappaB to new insights into transcriptional regulations in innate immunity. *Biochemical Pharmacology* **72**: 1102-1113.
- Flinders U (2021). Deep Thought (HPC). Flinders University.
- Forster JL, Harkin VB, Graham DA, McCullough SJ (2008). The effect of sample type, temperature and RNeasy™ on the stability of avian influenza virus RNA. *Journal of Virological Methods* **149**: 190-194.
- Fu L, Niu B, Zhu Z, Wu S, Li W (2012). CD-HIT: accelerated for clustering the next-generation sequencing data. *Bioinformatics* **28**: 3150-3152.



- Gish RG, Given BD, Lai C-L, Locarnini SA, Lau JYN, Lewis DL, Schlupe, T (2015). Chronic hepatitis B: Virology, natural history, current management and a glimpse at future opportunities. *Antiviral Research* **121**: 47-58.
- Götz S, García-Gómez JM, Terol J, Williams TD, Nagaraj SH, Nueda MJ *et al.*, (2008). High-throughput functional annotation and data mining with the Blast2GO suite. *Nucleic Acids Res* **36**: 3420-3435.
- Heck M, Neely BA (2020). Proteomics in Non-model Organisms: A New Analytical Frontier. *J Proteome Res* **19**: 3595-3606.
- Huang Y, Niu B, Gao Y, Fu L, Li W (2010). CD-HIT Suite: a web server for clustering and comparing biological sequences. *Bioinformatics* **26**: 680-682.
- Hun HT, Elizabeth (2019). Cogent: Coding GENome reconstruction Tool.
- Hyndman T, Shilton C (2018). An update on Australian reptile infectious disease (Conference Proceedings).
- IsoSeq3 3.0.0 – SMRTtools 6.0.0.47835. Pacific Biosciences (2018). SMRT® Tools Reference Guide, Pacific Biosciences of California, Inc. Version 04
<https://www.pacb.com/support/software-downloads/>
- Kanyana (2015). Kanyana Wildlife Centre 2014–2015 Annual Report: Perth, WA.
- Kikkert M (2020). Innate Immune Evasion by Human Respiratory RNA Viruses. *Journal of innate immunity* **12**: 4-20.
- Kruse CPS, Basu P, Luesse DR, Wyatt SE (2017). Transcriptome and proteome responses in RNAlater preserved tissue of *Arabidopsis thaliana*. *PloS one* **12**: e0175943-e0175943.
- Kumar N, Sharma S, Barua S, Tripathi BN, Rouse BT (2018). Virological and Immunological Outcomes of Coinfections. *Clinical Microbiology Reviews* **31**: e00111-00117.
- Lester SN, Li K (2014). Toll-Like Receptors in Antiviral Innate Immunity. *Journal of Molecular Biology* **426**: 1246-1264.
- Li W, Jaroszewski L, Godzik A (2001). Clustering of highly homologous sequences to reduce the size of large protein databases. *Bioinformatics* **17**: 282-283.
- Lv M, Chen X, Huang X, Liu N, Wang W, Liu H (2021). Transcriptome Analysis Reveals Sexual Disparities between Olfactory and Immune Gene Expression in the Olfactory Epithelium of *Megalobrama amblycephala*. *International Journal of Molecular Sciences* **22**: 13017.
- Mahajan S, Choudhary S, Kumar P, Tomar S. (2021). Antiviral strategies targeting host factors and mechanisms obliging +ssRNA viral pathogens. *Bioorg Med Chem.* **46**:116356.
- Maier M, Wutzler S, Bauer M, Trendafilov P, Henrich D, Marzi I (2008). Altered gene expression patterns in dendritic cells after severe trauma: Implications for systemic inflammation and organ injury. *Shock.* **30(4)**: 344-351.
- Martin JA, Wang Z (2011). Next-generation transcriptome assembly. *Nature Reviews Genetics* **12**: 671-682.
- Mayne BT, Bianco-Miotto T, Buckberry S, Breen J, Clifton V, Shoubridge C, Roberts CT (2016). Large scale gene expression meta-analysis reveals tissue-specific, sex-biased gene expression in humans. *Frontiers in genetics*, **7** p.183.
- McCarthy DJ, Chen Y, Smyth GK (2012). Differential expression analysis of multifactor RNA-Seq experiments with respect to biological variation. *Nucleic Acids Research* **40**: 4288-4297.
- Misra BB, Langefeld C, Olivier M, Cox LA (2019). Integrated omics: tools, advances and future approaches. *Journal of Molecular Endocrinology* **62**: R21-R45.
- NCBI Resource Coordinators (2016). Database resources of the National Center for Biotechnology Information. *Nucleic Acids Res* **44**: D7-19.



- O’Dea MA, Jackson B, Jackson C, Xavier P, Warren K (2016). Discovery and Partial Genomic Characterisation of a Novel Nidovirus Associated with Respiratory Disease in Wild Shingleback Lizards (*Tiliqua rugosa*). *PLOS ONE* **11**: e0165209.
- Ouborg NJ, Pertoldi C, Loeschcke V, Bijlsma RK, Hedrick PW (2010). Conservation genetics in transition to conservation genomics. *Trends in genetics***26**: 177-187.
- Parrish K, Kirkland PD, Skerratt LF, Ariel E (2021). Nidoviruses in Reptiles: A Review. *Frontiers in Veterinary Science* **8**.
- Priyam M, Tripathy M, Rai U, Ghorai SM (2016). Tracing the evolutionary lineage of pattern recognition receptor homologues in vertebrates: An insight into reptilian immunity via de novo sequencing of the wall lizard splenic transcriptome. *Veterinary Immunology and Immunopathology* **172**: 26-37.
- Rhoads A, Au KF (2015). PacBio Sequencing and Its Applications. *Genomics Proteomics Bioinformatics* **13**: 278-289.
- Richman DD, Nathanson N (2016). Antiviral Therapy. *Viral Pathogenesis*: 271-287.
- Robinson MD, McCarthy DJ, Smyth GK (2009). edgeR: a Bioconductor package for differential expression analysis of digital gene expression data. *Bioinformatics* **26**: 139-140.
- Sato K (2021). The True Nature of Viruses Elucidated by Systems Virology. *Frontiers in Virology* **1**. p.808865
- Schroeder HW, Jr., Cavacini L (2010). Structure and function of immunoglobulins. *The Journal of allergy and clinical immunology* **125**: S41-S52.
- Scutigliani EM, Kikkert M. (2017) Interaction of the innate immune system with positive-strand RNA virus replication organelles. *Cytokine & Growth Factor Reviews*. **37**: 17-27.,
- Stuart, M 2019. Development of sex distinguishing markers in two species of social skinks from the sub family Egerniinae, Honours thesis, Flinders University, Adelaide.
- Talavera-López C, Bediako Y, Lin J-w, Joseph Valletta J, Recker M, Langhorne J (2019). Comparison of whole blood and spleen transcriptional signatures over the course of an experimental malaria infection. *Scientific Reports* **9**: 15853.
- Taylor KE, Mossman KL (2013). Recent advances in understanding viral evasion of type I interferon. *Immunology* **138**: 190-197.
- The UniProt Consortium (2021). UniProt: the universal protein knowledgebase in 2021. *Nucleic Acids Research* **49**: D480-D489.
- Tian Y, De Jesús Andino F, Khwatenge CN, Li J, Robert J, Sang Y (2021). Virus-Targeted Transcriptomic Analyses Implicate Ranaviral Interaction with Host Interferon Response in Frog Virus 3-Infected Frog Tissues. *Viruses* **13**: 1325.
- Todd EV, Black MA, Gemmell NJ (2016). The power and promise of RNA-seq in ecology and evolution. *Molecular ecology* **25**: 1224-1241.
- Tseng E, Ripp, F., Botsford, D., Dunn, C. (2019). ANGEL: Robust Open Reading Frame prediction, Pacific Biosciences.
- Ungaro A, Pech N, Martin J-F, McCairns RJS, Mévy J-P, Chappaz R, Gilles, A (2017). Challenges and advances for transcriptome assembly in non-model species. *PLOS ONE* **12(9)**: p.e0185020.
- Walker PJ, Siddell SG, Lefkowitz EJ, Mushegian AR, Dempsey DM, Dutilh BE, Harrach B, Harrison RL, Hendrickson, RC, Junglen S, Knowles NJ (2019). Changes to virus taxonomy and the International Code of Virus Classification and Nomenclature ratified by the International Committee on Taxonomy of Viruses (2019). *Archives of Virology* **164**: 2417-2429.



- Wang ET, Sandberg R, Luo S, Khrebtkova I, Zhang L, Mayr C, Kingsmore SF, Schroth GP, Burge CB (2008). Alternative isoform regulation in human tissue transcriptomes. *Nature*. **456(7221)**: 470-476.
- Wille M, Yin H, Lundkvist Å, Xu J, Muradrasoli S, Järhult JD (2018). RNAlater® is a viable storage option for avian influenza sampling in logistically challenging conditions. *Journal of Virological Methods* **252**: 32-36.
- Zhang J, Finlaison DS, Frost MJ, Gestier S, Gu X, Hall J, Jenkins C, Parrish K, Read AJ, Srivastava M, Rose K (2018). Identification of a novel nidovirus as a potential cause of large scale mortalities in the endangered Bellinger River snapping turtle (*Myuchelys georgesii*). *PLOS ONE* **13**: e0205209.
- Zimmerman L (2016). The Immune System in Reptiles. *Encyclopedia of Immunobiology*.
- Zimmerman LM, Vogel LA, Bowden RM (2010). Understanding the vertebrate immune system: insights from the reptilian perspective. *The Journal of Experimental Biology* **213**: 661.
- Zou J, Castro R, Tafalla C (2016). Chapter 7 - Antiviral Immunity: Origin and Evolution in Vertebrates. In: Malagoli D (ed). *The Evolution of the Immune System*. Academic Press. pp 173-204.

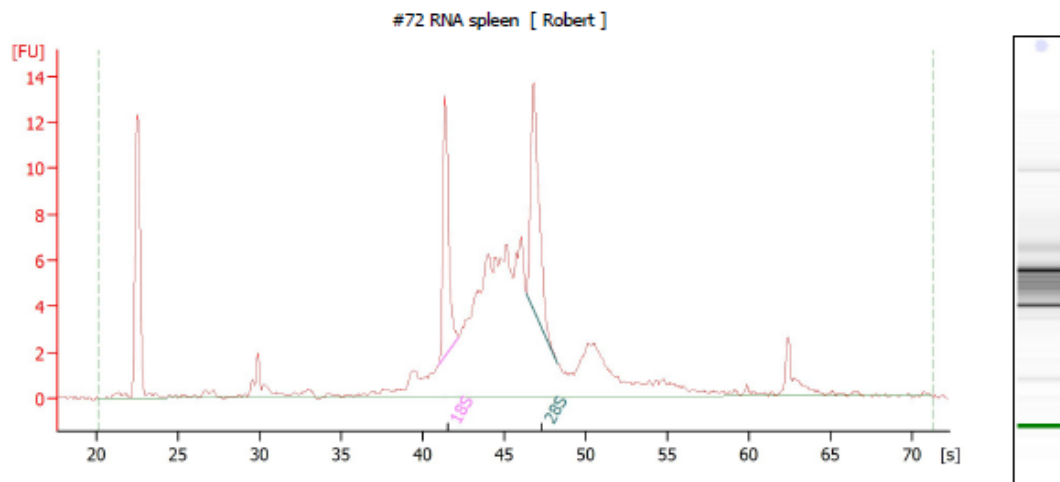


Chapter 4: Supplementary Material

ISOSEQ

Assay Class: Eukaryote Total RNA Nano
Data Path: E:\...Eukaryote Total RNA Nano_DE54704589_2019-02-06_17-40-42.xad
Created: 06/02/2019 17:40:41
Modified: 06/02/2019 18:04:00

Electropherogram Summary



Overall Results for sample 10 : #72 RNA spleen

RNA Area: 122.9
RNA Concentration: 77 ng/ μ l
rRNA Ratio [28s / 18s]: 1.2
RNA Integrity Number (RIN): 7.3 (B.02.08)
Result Flagging Color:
Result Flagging Label: RIN: 7.30

Fragment table for sample 10 : #72 RNA spleen

Name	Start Time [s]	End Time [s]	Area	% of total Area
18S	40.97	42.16	10.1	8.2
28S	46.34	48.25	12.6	10.2

Figure S1: Evaluation of total RNA extracted from spleen tissue of *Tiliqua rugosa* (sample ID ORE9519A4) using a bioanalyser nanochip. Determining quality to use in cDNA synthesis to be sent off for IsoSeq sequencing. RIN score 7.30 was acceptable.



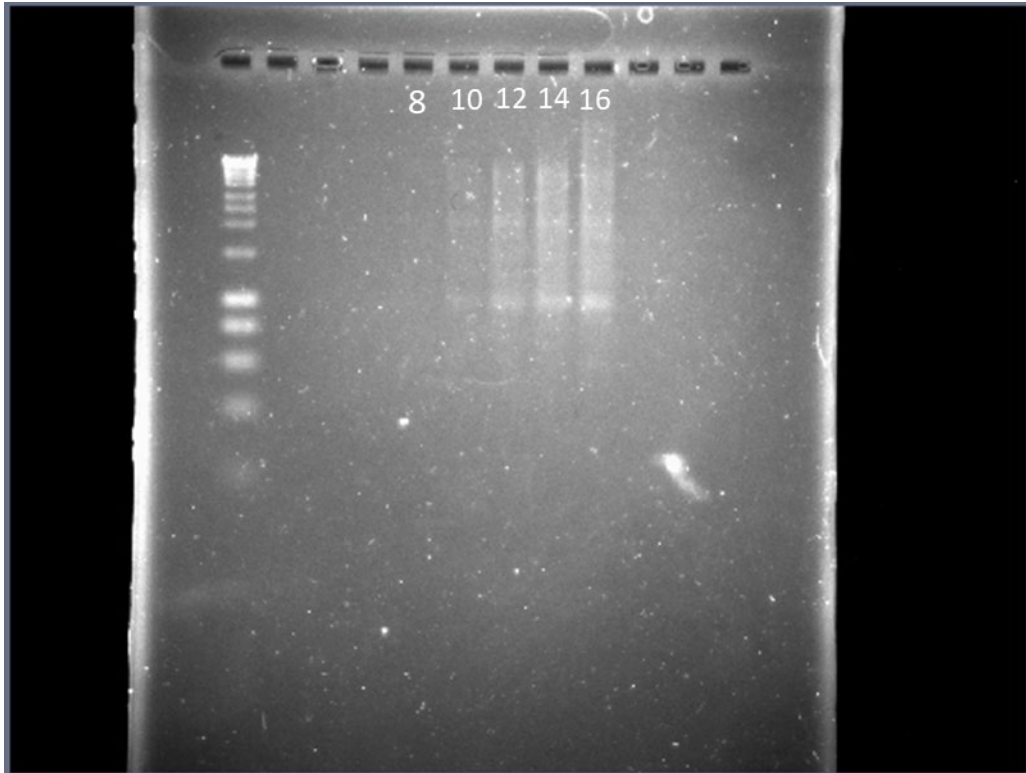


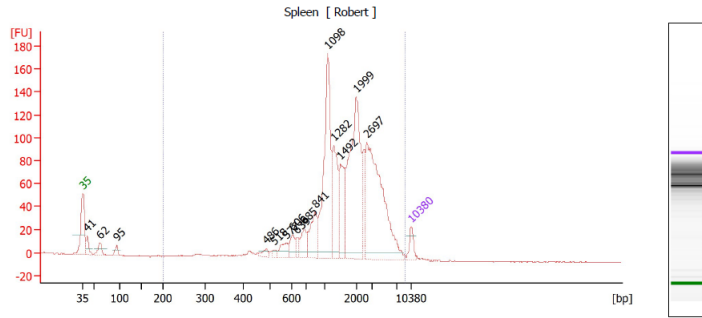
Figure S2: Determining optimal PCR cycles for Clontech's Smarter PCR cDNA synthesis kit, using electrophoresis gel at 90V for 60 minutes. Gel image shows PCR cycles 8,10,12,14,16. Cycle 14 was deemed optimal.



Assay Class: High Sensitivity DNA Assay
 Data Path: E:\...gh Sensitivity DNA Assay_DE54704589_2020-01-17_16-55-13.xad

Created: 17/01/2020 16:55:12
 Modified: 17/01/2020 17:37:05

Electropherogram Summary Continued ...



Overall Results for sample 6 : Spleen

Number of peaks found: 15 Corr. Area 1: 1,520.4
 Noise: 0.3

Peak table for sample 6 : Spleen

Peak	Size [bp]	Conc. [pg/μl]	Molarity [pmol/l]	Observations
1	35	125.00	5,411.3	Lower Marker
2	41	133.55	4,927.8	
3	62	120.50	2,946.3	
4	95	71.49	1,139.2	
5	486	45.39	141.6	
6	518	25.52	74.6	
7	577	98.18	257.6	
8	606	95.71	239.1	
9	639	51.22	121.4	
10	685	136.00	300.9	
11	841	274.46	494.6	
12	1,098	996.89	1,375.9	
13	1,282	433.10	512.1	
14	1,492	355.18	360.8	
15	1,999	1,088.94	825.4	
16	2,697	1,210.81	680.2	
17	10,380	75.00	10.9	Upper Marker

Region table for sample 6 : Spleen

From [bp]	To [bp]	Corr. Area	% of Total	Average Size [bp]	Size distribution in CV [%]	Conc. [pg/μl]	Molarity [pmol/l]	Color
200	9,005	1,520.4	97	2,145	66.5	4,996.35	5,404.8	■

Figure S3: Results of cDNA created from a Western Australian *Tiliqua rugosa* spleen sample in a high sensitivity DNA assay. Figure indicates sample with number of base pairs under 4000, with a small peak above 10,000bp and minimal contamination.



NOVASEQ Sup Material

Table S1: The summary results of quality control for all RNA extractions of spleen tissue samples from eight *Tiliqua rugosa* using SA Pathology's nanochip bioanalyser.

Sample	RIN Score	RNA_conc (ng/ul)	RNA area	Use (Y or N)	Notes
1.1	7.4	271	415.4	N	No good - DNA contamination
1.2	4.4	4770	7299.6	N	No good - Looks fragmented
2.1	3	1339	1967.1	N	No good - DNA contamination
2.2	7.2	684	1047.1	Y	OK
4.1	7.5	543	798.5	Y	OK
4.2	8.5	509	747.7	Y	OK - better than 4.1
5.1	6.2	991	1455.5	Y	No good - Looks fragmented
5.2	9.5	431	633.1	Y	OK
6.1	8.3	168	247	Y	OK
6.2	8.5	356	523.4	Y	OK
38461.1	8.6	700	1186.2	Y	OK
38461.2	8.5	558	945.1	Y	OK
38111.1	8.8	344	583	Y	OK
38111.2	4.7	321	543.4	N	No good. problem with baseline
39140.1	7.6	294	328.7	Y	OK
39140.2	7.6	289	323.1	Y	OK
1.1.1	7.7	613	685	Y	OK
1.1.2	7.6	245	273.6	Y	OK



Table S2: Next Generation Sequencing reports of the FASTQC analysis on the NovaSeq data for each sample. Number of reads per file were between 50–70 million, none were flagged as poor quality.

File Name	Total no. reads	Flagged As Poor Quality	Sequence Length (bp)	%GC
RO-4_2FLU_S7_R1	67,901,263	0	35-150	48
RO-4_2FLU_S7_R2	67,901,263	0	35-150	48
RO-38111_1FLU_S2_R1	74,186,282	0	35-150	48
RO-38111_1FLU_S2_R2	74,186,282	0	35-150	49
RO-38461_1_FLU_S5_R1	50,912,807	0	35-150	48
RO-38461_1_FLU_S5_R2	50,912,807	0	35-150	48
RO-39140_2FLU_S3_R1	60,871,336	0	35-150	47
RO-39140_2FLU_S3_R2	60,871,336	0	35-150	48
RO-2_2MT_S1_R1	70,405,254	0	35-150	49
RO-2_2MT_S1_R2	70,405,254	0	35-150	49
RO-5_2MT_S6_R1	69,405,994	0	35-150	48
RO-5_2MT_S6_R2	69,405,994	0	35-150	49
RO-6_2MT_S4_R1	63,612,346	0	35-150	47
RO-6_2MT_S4_R2	63,612,346	0	35-150	48
RO-1_1_1MT_S8_R1	60,988,133	0	35-150	49
RO-1_1_1MT_S8_R2	60,988,133	0	35-150	49



DIFFERENTIAL ANALYSIS SUP MATERIAL

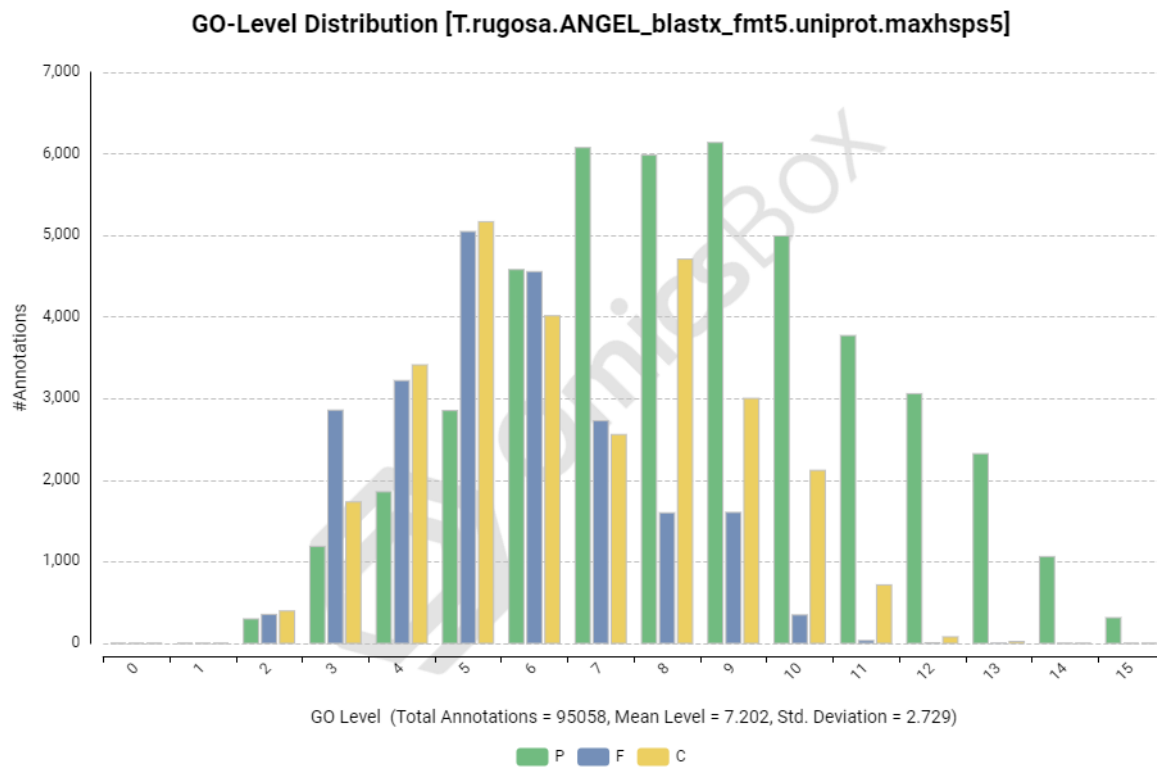


Figure S4: Blast2GO level distribution on the number of annotated transcripts. Input data was from the automated BLASTx output with max hits per sequence = 5, and evaluate= 0.0001 parameters. Green = transcripts responsible for Biological Processes (P), Blue = transcripts responsible for Molecular Function (F), and yellow = transcripts responsible for Cellular Components (C).



Library Exploration

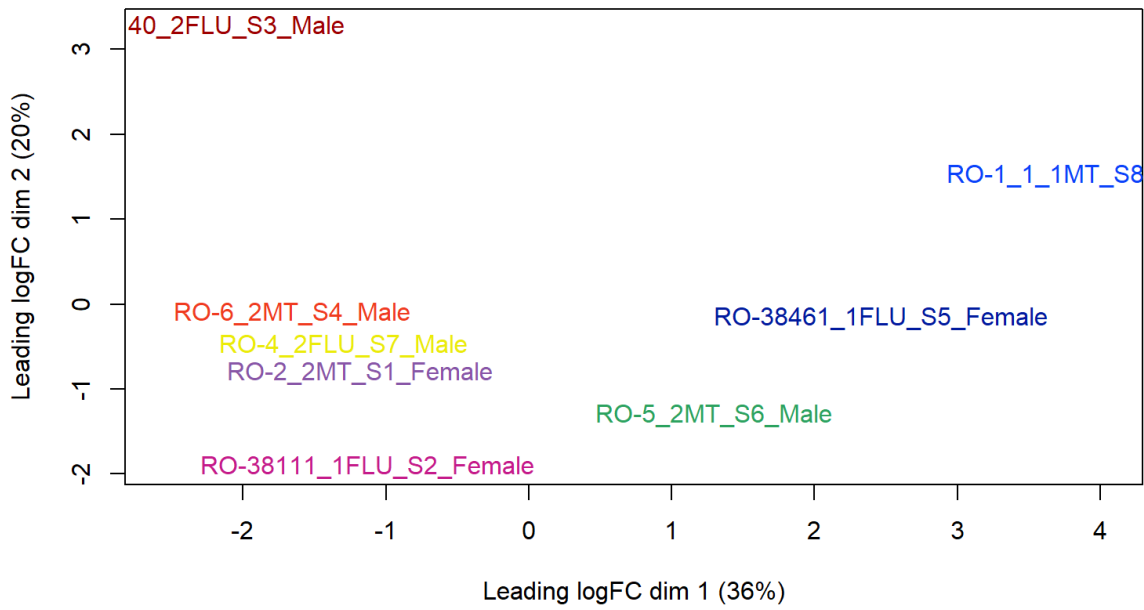
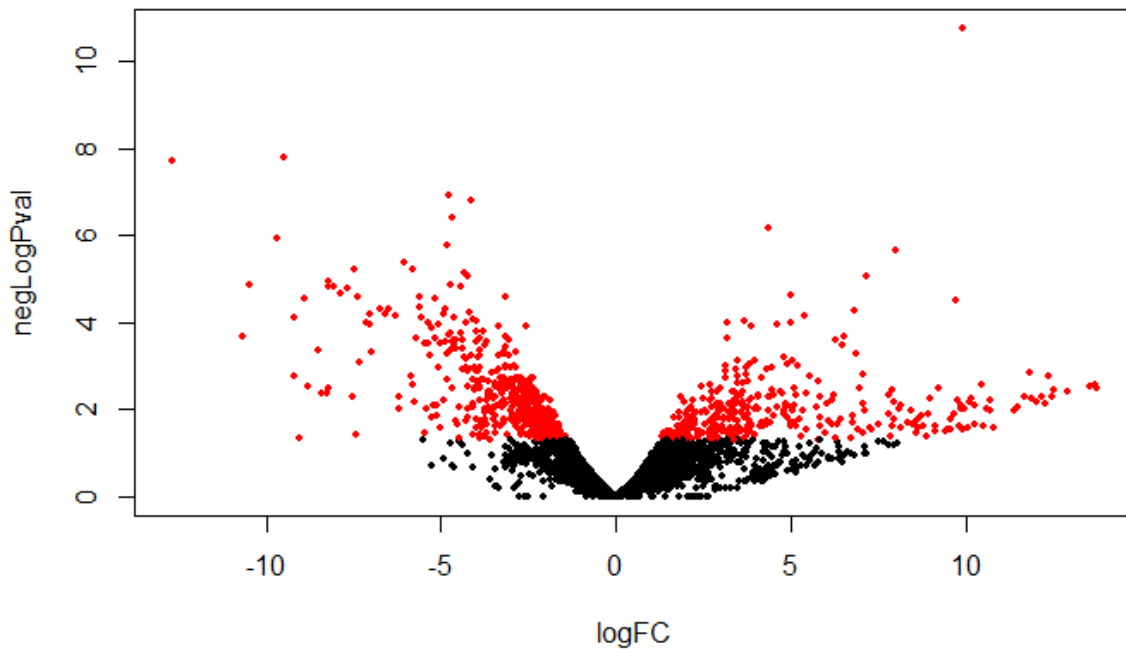


Figure S5: Multidimensional scaling (MDS) plot of samples, showing principal component analysis of log fold chain (logFC) to visualise the samples with the greatest variation.





FigureS6: Differential expression of transcripts between group factor 'Cause of Death' (Flu and Major Trauma) factoring in sex, using the negative Logged PValue against Logged Fold Change in expression: Red indicates a transcript with PValue < 0.05, and Log Fold change > 2



Table S3: Group factor 'Cause of Death': Differentially expressed transcripts for group factor using an automated blastx search with the Uniprot database. Expressed: 1= upregulated, -1= downregulated

TranscriptID	Expressed	Sequence Length	Automated blast2GP Description	Blast2GOLength	GO.Names	UniprotID	Gene	evalue	length
PB.3536.1 b'9d81d9' path90:0- 2798(+) transcript/80 17	1	1874	NA	NA	NA	NA	NA	NA	NA
PB.557.1 b'13a0c1' pa th309:2- 1064(+) transcript/14 202	1	1062	NA	NA	NA	NA	NA	NA	NA
PB.570.1 b'13a0c1' pa th324:0- 810(+) transcript/162 96	1	810	IgLL5_HUMANImmunoglobulin lambda-like polypeptide 5 OS= <i>Homo sapiens</i> OX=9606 GN=IGLL5 PE=2 SV=2	489	P:activation of immune response; P:lymphocyte mediated immunity; P:adaptive immune response based on somatic recombination of immune receptors built from immunoglobulin superfamily domains; P:defense response to other organism; F:antigen binding; ; C:cell surface; C:T cell receptor complex; C:IgG immunoglobulin complex	B9A064	igll5	3.48E-28	113
PB.5911.1 transcript/ 10352:0- 1549(+) transcript/10 352	1	1549	NA	NA	NA	NA	NA	NA	NA
PB.613.1 b'13a0c1' pa th38:50- 906(+) transcript/167 49	1	857	IgLL5_HUMANImmunoglobulin lambda-like polypeptide 5 OS= <i>Homo sapiens</i> OX=9606 GN=IGLL5 PE=2 SV=2	411	P:activation of immune response; P:response to tumor cell; P:lymphocyte mediated immunity; P:adaptive immune response based on somatic recombination of immune receptors built from immunoglobulin superfamily domains; P:endocytosis; P:phagocytosis; P:regulation of cellular process; P:defense response to other organism;	B9A064	igll5	1.29E-28	113



F:antigen binding; F:protein binding; C:extracellular space; C:cell surface; C:T cell receptor complex; C:IgG immunoglobulin complex

PB.1386.2 b'3771b8' path0:0- 896(+) transcript/164 12	-1	897	NA						
PB.2959.1 b'848714' path0:0- 1292(+) transcript/12 660	-1	1203	NA						
PB.4133.2 b'b1d8d5' path67:0- 2701(+) transcript/70 58	-1	1942	NA						
PB.4207.1 b'b549cd' path0:0- 4404(+) transcript/34 0	-1	4403	NA						
PB.4207.3 b'b549cd' path0:1956- 4417(+) transcript/40 07	-1	2460	NA						
PB.5120.2 b'dc60a2' path2:128- 1885(+) transcript/14 057	-1	1132	NA						



Table S4: Group factor 'Cause of Death': Annotation of differentially expressed transcripts using a manual blastx search of transcript sequences on NCBI GenBank

TranscriptID	Expressed	Sequence Length	Manual blastx description	Accession	Max Score	Total Score	Query Cover	E value	Per. Ident	Acc. Len
PB.3536.1 b'9d81d9' path90:0-2798(+) transcript/8017	1	1874	immunoglobulin Y heavy chain constant region [<i>Anolis carolinensis</i>]	ABV66132.1	437	437	69%	1.00E-144	51.13%	443
PB.557.1 b'13a0c1' path309:2-1064(+) transcript/14202	1	1062	<i>Anolis carolinensis</i> clone 10-48 lambda immunoglobulin light chain gene, partial cds	GU338719.1	163	163	19%	4.00E-35	80.95%	344
PB.570.1 b'13a0c1' path324:0-810(+) transcript/16296	1	810	immunoglobulin lambda-1 light chain-like isoform X10 [<i>Sceloporus undulatus</i>]	XP_042297774.1	144	144	59%	6.00E-38	45.96%	235
PB.5911.1 transcript/10352:0-1549(+) transcript/10352	1	1549	ADML protein [<i>Chunga burmeisteri</i>]	NWS58844.1	215	215	30%	1.00E-63	68.79%	164
PB.613.1 b'13a0c1' path38:50-906(+) transcript/16749	1	857	immunoglobulin lambda-1 light chain-like isoform X10 [<i>Sceloporus undulatus</i>]	XP_042297774.1	143	143	59%	2.00E-37	46.55%	235
PB.1386.2 b'3771b8' path0:0-896(+) transcript/16412	-1	897	heat shock protein 90 alpha [<i>Coturnix japonica</i>]	AAL83217.1	372	456	75%	5.00E-127	98.37%	230
PB.2959.1 b'848714' path0:0-1292(+) transcript/12660	-1	1203	GTP-binding nuclear protein Ran [<i>Python bivittatus</i>]	XP_007426723.1	440	440	52%	1.00E-152	100.00%	217
PB.4133.2 b'b1d8d5' path67:0-2701(+) transcript/7058	-1	1942	PREDICTED: LOW QUALITY PROTEIN: Ig epsilon chain C region [<i>Anolis carolinensis</i>]	XP_016852938.1	576	576	90%	0	47.99%	598
PB.4207.1 b'b549cd' path0:0-4404(+) transcript/340	-1	4403	collagen alpha-1(III) chain-like [<i>Podarcis muralis</i>]	XP_028572538.1	482	482	17%	1.00E-154	88.54%	315
PB.4207.3 b'b549cd' path0:1956-4417(+) transcript/4007	-1	2460	collagen alpha-1(III) chain-like [<i>Podarcis muralis</i>]	XP_028572538.1	482	482	30%	2.00E-161	88.54%	315
PB.5120.2 b'dc60a2' path2:128-1885(+) transcript/14057	-1	1132	PREDICTED: pancreatic alpha-amylase [<i>Anolis carolinensis</i>]	XP_003220126.1	694	694	97%	0	88.56%	512



Table S5: Group factor SEX: Differentially expressed transcripts for group factor using an automated blastx search with the Uniprot database. Expressed: 1= upregulated, -1= downregulated

TranscriptID	Expressed	Sequence Length	Automated blast2GP Description	Blast2GOLength	GO.Names	UniprotID	Gene	evaluate	length
PB.190.3 b'08c526' path1:1-2233(+) transcript/9192	1	1658	RGS1_MOUSERegulator of G-protein signaling 1 OS= <i>Mus musculus</i> OX=10090 GN=Rgs1 PE=2 SV=2	648	P:response to amphetamine; P:regulation of translation; P:immune response; P:G protein-coupled acetylcholine receptor signaling pathway; P:spermatogenesis; P:brain development; P:response to bacterium; P:negative regulation of phospholipase activity; P:negative regulation of cardiac muscle hypertrophy; P:negative regulation of MAP kinase activity; P:positive regulation of GTPase activity; P:brown fat cell differentiation; P:regulation of cellular component organization; P:relaxation of cardiac muscle;	Q9JL25	rgs1	2.73E-72	159
PB.231.1 b'0a4273' path0:0-1843(+) transcript/8362	1	1841	RAB3I_HUMANRab-3A-interacting protein OS= <i>Homo sapiens</i> OX=9606 GN=RAB3IP PE=1 SV=1	858	P:protein targeting to membrane; P:exocytosis; P:Golgi to plasma membrane transport; P:protein localization to organelle; P:regulation of catalytic activity; P:negative regulation of filopodium assembly; P:ciliary basal body-plasma membrane docking; F:guanyl-nucleotide exchange factor activity; F:kinase binding; F:identical protein binding; F:GTPase binding; C:nucleus; C:Golgi apparatus; C:centrosome; C:cytosol; C:lamellipodium; C:ciliary basal body; C:perinuclear region of cytoplasm; C:Golgi to plasma membrane transport vesicle; C:proximal dendrite	Q96QF0	rab3ip	6.62E-167	285
PB.2461.2 b'6e1acc' path237:0-1256(+) transcript/13237	1	1215	APOEB_DANREApolipoprotein Eb OS= <i>Danio rerio</i> OX=7955 GN=apoeb PE=2 SV=1	801	P:response to dietary excess; P:cholesterol catabolic process; P:cellular calcium ion homeostasis; P:response to oxidative stress; P:aging; P:protein localization; P:response to zinc ion; P:negative regulation of gene expression; P:positive regulation of cholesterol esterification; P:positive regulation of cholesterol efflux; P:lipid transport involved in lipid storage; P:positive regulation of neuron projection development; P:peripheral nervous system axon regeneration;	O42364	apoeb	2.18E-44	191



PB.2461.4 b'6e1acc' path2 37:0- 1258(+) transcript/14561	1	1084	APOE_ALLMIApolipoprotein E OS= <i>Alligator mississippiensis</i> OX=8496 GN=APOE PE=3 SV=2	738	P:response to dietary excess; P:cholesterol catabolic process; P:cellular calcium ion homeostasis; P:response to oxidative stress; P:aging; P:protein localization; P:response to zinc ion; P:negative regulation of gene expression; P:positive regulation of cholesterol esterification; P:positive regulation of cholesterol efflux; P:lipid transport involved in lipid storage; P:positive regulation of neuron projection development; P	POD MT6	apoe	1.53E- 51	204
PB.2727.2 b'7a1caf' path0: 1-1609(+) transcript/10710	1	1533	RBM3_MOUSERNA-binding protein 3 OS= <i>Mus musculus</i> OX=10090 GN=Rbm3 PE=1 SV=1	513	P:regulation of alternative mRNA splicing, via spliceosome; P:mRNA splice site selection; P:membrane protein ectodomain proteolysis; P:response to osmotic stress; P:gastrulation; P:response to UV; P:cold acclimation; P:embryo development ending in birth or egg hatching; P:cell migration; P:neurogenesis; P:negative regulation of cell growth; P:stress granule assembly; P:production of miRNAs involved in gene silencing by miRNA; P:hibernation	O890 86	rbm3	1.61E- 49	82
PB.3427.1 b'9b13cd' path0: 0-982(+) transcript/14773	1	981	IGSF2_HUMANImmunoglobulin superfamily member 2 OS= <i>Homo sapiens</i> OX=9606 GN=CD101 PE=1 SV=2	627	P:regulation of cellular process; C:membrane	Q930 33	cd101	3.60E- 21	182
PB.490.2 b'13a0c1' path21 0:95- 1035(+) transcript/15172	1	949	NA	NA	NA	NA	NA	NA	NA
PB.5141.2 b'dcb56b' path1 :7-1923(+) transcript/7534	1	1916	TCPB_MACFAT-complex protein 1 subunit beta OS= <i>Macaca fascicularis</i> OX=9541 GN=CCT2 PE=2 SV=3	1083	P:binding of sperm to zona pellucida; P:positive regulation of telomere maintenance via telomerase; P:translocation of peptides or proteins into host cell cytoplasm; P:protein stabilization; P:chaperone mediated protein folding independent of cofactor; P:chaperone-mediated protein complex assembly; P:positive regulation of telomerase activity; P:scaRNA localization to Cajal body; P:toxin transport;	Q4R6 F8	cct2	0	332



PB.5295.2 b'e412d4' path0:22-745(+) transcript/18688	1	657	PSB9_HUMANProteasome subunit beta type-9 OS= <i>Homo sapiens</i> OX=9606 GN=PSMB9 PE=1 SV=2	606	P:liver development; P:response to xenobiotic stimulus; P:response to bacterium; P:muscle atrophy; P:antigen processing and presentation; P:proteasome-mediated ubiquitin-dependent protein catabolic process; P:response to alkaloid; P:spleen development; P:thymus development; P:cellular response to electrical stimulus; P:cellular response to interleukin-1; P:cellular response to virus; P:response to benzene;	P28065	psmb9	1.05E-95	185
PB.593.1 b'13a0c1' path352:280-974(+) transcript/18599	1	692	NA	NA	NA	NA	NA	NA	NA
PB.871.2 b'1da525' path1:1543-3709(+) transcript/5514	1	2168	MOV10_CHICKPutative helicase MOV-10 OS= <i>Gallus gallus</i> OX=9031 GN=MOV10 PE=2 SV=1	1542	P:nuclear-transcribed mRNA catabolic process, nonsense-mediated decay; P:embryonic axis specification; P:male meiosis I; P:spermatogenesis; P:RNAi-mediated antiviral immune response; P:negative regulation of transposition, RNA-mediated; P:cellular component assembly; P:macromolecule localization; P:piRNA metabolic process; P:miRNA-mediated gene silencing by mRNA destabilization; P:DNA methylation involved in gamete generation; P:negative regulation of cell cycle	Q5ZKD7	mov10	0	499
PB.1003.1 b'249aa1' path0:0-5150(+) transcript/104	-1	5150	NA	NA	NA	NA	NA	NA	NA
PB.2927.2 b'82e0eb' path0:17-1813(+) transcript/8644	-1	1796	NA	NA	NA	NA	NA	NA	NA
PB.34.4 b'016a96' path0:0-2746(+) transcript/3015	-1	2683	NA	NA	NA	NA	NA	NA	NA
PB.487.1 b'13a0c1' path205:0-1145(+) transcript/13689	-1	1148	NA	NA	NA	NA	NA	NA	NA
PB.519.1 b'13a0c1' path256:0-993(+) transcript/15646	-1	992	NA	NA	NA	NA	NA	NA	NA
PB.5984.1 transcript/10757:0-1538(+) transcript/10757	-1	1538	NA	NA	NA	NA	NA	NA	NA
PB.6243.1 transcript/12113:0-1298(+) transcript/12113	-1	1298	NA	NA	NA	NA	NA	NA	NA



Table S6: Group factor 'SEX': Annotation of differentially expressed transcripts using a manual blastx search of transcript sequences on NCBI GenBank

TranscriptID_3	Expressed	Sequence Length	Manual blastx	Accession	Max Score	Total Score	Query Cover	E value	Per. Ident	Acc. Len
PB.190.3 b'08c526' path1:1-2233(+) transcript/9192	1	1658	regulator of G-protein signaling 1 [<i>Varanus komodoensis</i>]	XP_044295223.1	300	300	36%	8.00E-96	76.47%	205
PB.231.1 b'0a4273' path0:0-1843(+) transcript/8362	1	1841	<i>rab-3A-interacting protein</i> [<i>Podarcis muralis</i>]	XP_028602488.1	503	862	75%	4.00E-170	91.96%	461
PB.2461.2 b'6e1acc' path237:0-1256(+) transcript/13237	1	1215	apolipoprotein E [<i>Pogona vitticeps</i>]	XP_020668207.1	298	376	65%	5.00E-95	66.83%	336
PB.2461.4 b'6e1acc' path237:0-1258(+) transcript/14561	1	1084	apolipoprotein E [<i>Pogona vitticeps</i>]	XP_020668207.1	342	342	66%	1.00E-112	66.39%	336
PB.2727.2 b'7a1caf' path0:1-1609(+) transcript/10710	1	1533	RNA-binding protein 3 [<i>Varanus komodoensis</i>]	KAF7243844.1	174	174	16%	4.00E-48	100.00%	162
PB.3427.1 b'9b13cd' path0:0-982(+) transcript/14773	1	981	immunoglobulin superfamily member 2 [<i>Pogona vitticeps</i>]	XP_020666406.1	202	202	63%	4.00E-54	59.15%	1038
PB.490.2 b'13a0c1' path210:95-1035(+) transcript/15172	1	949	immunoglobulin lambda-1 light chain-like isoform X12 [<i>Sceloporus undulatus</i>]	XP_042297776.1	239	239	73%	1.00E-74	53.65%	234
PB.5141.2 b'dcb56b' path1:7-1923(+) transcript/7534	1	1916	T-complex protein 1 subunit beta isoform X1 [<i>Numida meleagris</i>]	XP_021240819.1	591	983	86%	0	86.03%	621
PB.5295.2 b'e412d4' path0:22-745(+) transcript/18688	1	657	PREDICTED: proteasome subunit beta type-9 [<i>Anolis carolinensis</i>]	XP_003230744.2	316	316	84%	9.00E-107	89.19%	211
PB.593.1 b'13a0c1' path352:280-974(+) transcript/18599	1	692	immunoglobulin lambda-1 light chain-like isoform X14 [<i>Sceloporus undulatus</i>]	XP_042297779.1	123	189	68%	3.00E-38	56.03%	234
PB.871.2 b'1da525' path1:1543-3709(+) transcript/5514	1	2168	PREDICTED: putative helicase MOV-10 isoform X2 [<i>Anolis carolinensis</i>]	XP_008108050.1	791	791	70%	0	76.61%	956
PB.1003.1 b'249aa1' path0:0-5150(+) transcript/104	-1	5150	venom factor-like [<i>Podarcis muralis</i>]	XP_028568231.1	2591	2591	96%	0	75.33%	1653
PB.2927.2 b'82e0eb' path0:17-1813(+) transcript/8644	-1	1796	protein disulfide-isomerase A3 [<i>Sceloporus undulatus</i>]	XP_042332148.1	848	913	75%	0	91.85%	503
PB.34.4 b'016a96' path0:0-2746(+) transcript/3015	-1	2683	elongation factor 2 [<i>Alligator sinensis</i>]	XP_006017577.1	1589	1589	94%	0	93.99%	915
PB.487.1 b'13a0c1' path205:0-1145(+) transcript/13689	-1	1148	immunoglobulin lambda-1 light chain-like isoform X7 [<i>Sceloporus undulatus</i>]	XP_042297771.1	164	268	60%	2.00E-55	56.29%	235



PB.519.1 b'13a0c1' path256:0-993(+) transcript/15646	-1	992	immunoglobulin lambda variable 5-39 isoform X8 [<i>Chelonia mydas</i>]	XP_043385604.1	204	204	68%	1.00E-60	50.00%	241
PB.5984.1 transcript/10757:0-1538(+) transcript/10757	-1	1538	ras-related and estrogen-regulated growth inhibitor-like protein isoform X1 [<i>Sceloporus undulatus</i>]	XP_042326445.1	305	411	39%	4.00E-98	90.91%	204
PB.6243.1 transcript/12113:0-1298(+) transcript/12113	-1	1298	GSTA2 transferase [<i>Alaudala cheleensis</i>]	NXQ31533.1	382	382	51%	3.00E-129	82.43%	222



Table S7: Group factor Cause of Death, with sex factored: 109 transcripts significantly differentially expressed: Expressed: 1= up regulation, -1= down regulation. Descriptions in bold indicate the transcript is associated with the immune system.

TranscriptID_3	Sequenc e length	Expr esse d	Descriptions from Automated blastx search- Uniprot database	Maunal Blastx Description - NCBI	Max Score	Total Score	Query Cover	E value	Per. Ident	Acc. Len	Accession
PB.34.4 b'016a96' path0:0-2746(+) transcript/3015	2683	1	EF2_CALJAElongation factor 2 OS= <i>Callithrix jacchus</i> OX=9483 GN=EEF2 PE=2 SV=1	elongation factor 2 [<i>Alligator sinensis</i>]	1589	1589	94%	0	93.99%	915	XP_006017577.1
PB.435.2 b'13a0c1' path118:76-1126(+) transcript/13736	1045	1	NA	immunoglobulin lambda-1 light chain-like isoform X8 [<i>Sceloporus undulatus</i>]	260	260	67%	2.00E-82	59.15%	235	XP_042297772.1
PB.482.1 b'13a0c1' path197:14-981(+) transcript/15717	968	1	NA	immunoglobulin lambda-1 light chain-like isoform X10 [<i>Sceloporus undulatus</i>]	181	250	73%	7.00E-52	51.52%	235	XP_042297774.1
PB.487.1 b'13a0c1' path205:0-1145(+) transcript/13689	1148	1	NA	immunoglobulin lambda-1 light chain-like isoform X7 [<i>Sceloporus undulatus</i>]	164	268	60%	2.00E-55	56.29%	235	XP_042297771.1
PB.519.1 b'13a0c1' path256:0-993(+) transcript/15646	992	1	NA	immunoglobulin lambda variable 5-39 isoform X8 [<i>Chelonia mydas</i>]	204	204	68%	1.00E-60	50.00%	241	XP_043385604.1
PB.581.1 b'13a0c1' path337:189-1070(+) transcript/16392	880	1	LAC2_MOUSEI g lambda-2 chain C region OS= <i>Mus musculus</i> OX=10090 GN=Iglc2 PE=1 SV=1	immunoglobulin lambda-1 light chain-like isoform X10 [<i>Sceloporus undulatus</i>]	134	134	52%	6.00E-34	51.30%	235	XP_042297774.1
PB.584.1 b'13a0c1' path340:0-1082(+) transcript/14311	1080	1	NA	immunoglobulin lambda-1 light chain-like isoform X3 [<i>Dermochelys coriacea</i>]	270	270	68%	3.00E-85	54.00%	276	XP_043353662.1
PB.586.2 b'13a0c1' path344:1-972(+) transcript/15761	972	1	NA	immunoglobulin lambda-1 light chain-like isoform X8 [<i>Sceloporus undulatus</i>]	267	267	72%	2.00E-85	57.20%	235	XP_042297772.1
PB.604.1 b'13a0c1' path368:0-1012(+) transcript/15392	1012	1	NA	immunoglobulin lambda-1 light chain-like isoform X8 [<i>Sceloporus undulatus</i>]	252	252	68%	2.00E-79	53.88%	235	XP_042297772.1
PB.618.2 b'13a0c1' path44:3-1072(+) transcript/14751	1071	1	NA	immunoglobulin lambda-1 light chain-like isoform X8 [<i>Sceloporus undulatus</i>]	286	286	65%	2.00E-92	61.44%	235	XP_042297772.1
PB.1003.1 b'249aa1' path0:0-5150(+) transcript/104	5150	1	NA	venom factor-like [<i>Podarcis muralis</i>]	2591	2591	96%	0	75.33%	1653	XP_028568231.1
PB.2927.2 b'82e0eb' path0:17-1813(+) transcript/8644	1796	1	PDIA3_CHICK Protein disulfide-isomerase A3 OS= <i>Gallus gallus</i> OX=9031 GN=PDIA3 PE=2 SV=1	protein disulfide-isomerase A3 [<i>Sceloporus undulatus</i>]	848	913	75%	0	91.85%	503	XP_042332148.1



PB.3171.2 b'8e55ed' pat h0:1002-3110(+) transcript/5891	2123	1	AP1M1_MOUSEAP-1 complex subunit mu-1 OS= <i>Mus musculus</i> OX=10090 GN=Ap1m1 PE=1 SV=3	adaptor related protein complex 1 subunit mu 1 [<i>Pipistrellus kuhlii</i>]	226	226	15%	5.00E-66	98.18 %	159	KAF6283224.1
PB.3525.1 b'9d81d9' pat h75:0-2817(+) transcript/7028	1901	1	NA	immunoglobulin Y heavy chain constant region [<i>Anolis carolinensis</i>]	436	436	68%	4.00E-144	51.13 %	443	ABV66132.1
PB.4069.1 b'b1d8d5' pat h293:0-2678(+) transcript/7688	1919	1	NA	immunoglobulin Y heavy chain constant region [<i>Anolis carolinensis</i>]	475	475	70%	3.00E-159	51.10 %	443	ABV66132.1
PB.6243.1 transcript/12113:0-1298(+) transcript/12113	1298	1	NA	GSTA2 transferase [<i>Alaudala cheleensis</i>]	382	382	51%	3.00E-129	82.43 %	222	NXQ31533.1
PB.6546.1 transcript/1383:0-3327(+) transcript/1383	3327	1	NA	PREDICTED: leucine-rich repeat neuronal protein 3 [<i>Anolis carolinensis</i>]	521	1232	63%	0	88.93 %	708	XP_003221250.1
PB.8009.1 transcript/2685:0-2727(+) transcript/2685	2727	1	NA	two pore calcium channel protein 1-like isoform X2 [<i>Lacerta agilis</i>]	120	1205	84%	0	87.47 %	795	XP_033000882.1
PB.65.1 b'0305f0' path0:0-1536(+) transcript/10418	1536	-1	KI3X1_HUMANPutative killer cell immunoglobulin-like receptor-like protein KIR3DX1 OS= <i>Homo sapiens</i> OX=9606 GN=KIR3DX1 PE=5 SV=2	natural cytotoxicity triggering receptor 1-like [<i>Podarcis muralis</i>]	123	192	50%	3.00E-27	42.86 %	317	XP_028607677.1
PB.72.2 b'035475' path0:2-1628(+) transcript/13640	1160	-1	IL8_CHICKInterleukin-8 OS= <i>Gallus gallus</i> OX=9031 GN=CXCL8 PE=2 SV=1	interleukin-8-like [<i>Lacerta agilis</i>]	145	145	22%	1.00E-38	79.31 %	104	XP_033026963.1
PB.190.3 b'08c526' path 1:1-2233(+) transcript/9192	1658	-1	RGS1_MOUSERegulator of G-protein signaling 1 OS= <i>Mus musculus</i> OX=10090 GN=Rgs1 PE=2 SV=2	regulator of G-protein signaling 1 [<i>Varanus komodoensis</i>]	300	300	36%	8.00E-96	76.47 %	205	XP_044295223.1
PB.231.1 b'0a4273' path 0:0-1843(+) transcript/8362	1841	-1	RAB3I_HUMANRab-3A-interacting protein OS= <i>Homo sapiens</i> OX=9606 GN=RAB3IP PE=1 SV=1	rab-3A-interacting protein [<i>Podarcis muralis</i>]	452	715	71%	0	88.43 %	430	XP_026304235.1
PB.307.2 b'0dc0c0' path 0:1146-1815(+) transcript/19051	669	-1	NA	NA	NA	NA	NA	NA	NA	NA	NA
PB.490.2 b'13a0c1' path 210:95-1035(+) transcript/15172	949	-1	NA	immunoglobulin lambda-1 light chain-like isoform X12 [<i>Sceloporus undulatus</i>]	239	239	73%	1.00E-74	53.65 %	234	XP_042297776.1
PB.593.1 b'13a0c1' path 352:280-974(+) transcript/18599	692	-1	NA	immunoglobulin lambda-1 light chain-like isoform X14 [<i>Sceloporus undulatus</i>]	123	189	68%	3.00E-38	56.03 %	234	XP_042297779.1
PB.613.1 b'13a0c1' path 38:50-906(+) transcript/16749	857	-1	IGLL5_HUMANImmunoglobulin lambda-like polypeptide 5 OS= <i>Homo sapiens</i> OX=9606 GN=IGLL5 PE=2 SV=2	immunoglobulin lambda-1 light chain-like isoform X10 [<i>Sceloporus undulatus</i>]	143	143	59%	2.00E-37	46.55 %	235	XP_042297774.1



PB.871.2 b'1da525' path 1:1543-3709(+) transcript/5514	2168	-1	MOV10_CHICKPutative helicase MOV-10 OS= <i>Gallus gallus</i> OX=9031 GN=MOV10 PE=2 SV=1	PREDICTED: putative helicase MOV-10 isoform X2 [<i>Anolis carolinensis</i>]	791	791	70%	0	76.61 %	956	XP_008108050.1
PB.940.1 b'21a70f' path 0:0-753(+) transcript/17868	753	-1	NA	PREDICTED: cathelicidin-1-like [<i>Gekko japonicus</i>]	148	148	48%	1.00E-40	59.02 %	174	XP_015277842.1
PB.1176.1 b'2d348d' pat h0:0-2500(+) transcript/3667	2498	-1	CCN2_PIGCCN family member 2 OS= <i>Sus scrofa</i> OX=9823 GN=CCN2 PE=2 SV=1	PREDICTED: connective tissue growth factor [<i>Gekko japonicus</i>]	629	629	39%	0	97.27 %	349	XP_015276741.1
PB.1265.1 b'30964e' pat h0:0-3659(+) transcript/1072	3539	-1	ICAM1_PANTRIintercellular adhesion molecule 1 OS= <i>Pan troglodytes</i> OX=9598 GN=ICAM1 PE=2 SV=2	intercellular adhesion molecule 5-like [<i>Zootoca vivipara</i>]	511	511	40%	5.00E-165	50.38 %	545	XP_034957462.1
PB.1265.2 b'30964e' pat h0:1-4332(+) transcript/330	4334	-1	ICAM1_MACMUIintercellular adhesion molecule 1 OS= <i>Macaca mulatta</i> OX=9544 GN=ICAM1 PE=2 SV=1	intercellular adhesion molecule 5-like [<i>Zootoca vivipara</i>]	579	579	36%	0	54.92 %	545	XP_034957462.1
PB.1276.1 b'315ed9' pat h0:0-1559(+) transcript/10267	1557	-1	FOSL1_RATFos-related antigen 1 OS= <i>Rattus norvegicus</i> OX=10116 GN=Fosl1 PE=2 SV=1	LOW QUALITY PROTEIN: fos-related antigen 1 [<i>Podarcis muralis</i>]	336	336	53%	2.00E-108	83.09 %	311	XP_028565992.1
PB.1299.1 b'32371b' pat h1:0-1999(+) transcript/6528	1998	-1	NA	TNFAIP3-interacting protein 3-like isoform X1 [<i>Dermochelys coriacea</i>]	338	338	58%	6.00E-106	53.38 %	408	XP_038271750.1
PB.1300.1 b'32371b' pat h2:0-1921(+) transcript/7402	1921	-1	NA	PREDICTED: TNFAIP3-interacting protein 3 isoform X2 [<i>Alligator mississippiensis</i>]	327	327	54%	1.00E-102	55.49 %	366	XP_006278146.1
PB.1378.3 b'3700c4' pat h1:14-2774(+) transcript/3391	2533	-1	TNIP1_HUMANTNFAIP3-interacting protein 1 OS= <i>Homo sapiens</i> OX=9606 GN=TNIP1 PE=1 SV=2	TNFAIP3-interacting protein 1 isoform X3 [<i>Zootoca vivipara</i>]	886	886	71%	0	81.89 %	628	XP_034961580.1
PB.1436.1 b'3a0103' pat h0:0-2015(+) transcript/6690	2014	-1	STX11_MOUSESyntaxin-11 OS= <i>Mus musculus</i> OX=10090 GN=Stx11 PE=1 SV=1	syntaxin-11 [<i>Zootoca vivipara</i>]	270	504	41%	4.00E-132	82.28 %	288	XP_034964722.1
PB.1463.1 b'3b03d2' pat h2:0-1787(+) transcript/8363	1783	-1	IL1RA_TURTRIinterleukin-1 receptor antagonist protein OS= <i>Tursiops truncatus</i> OX=9739 GN=IL1RN PE=2 SV=1	interleukin-1 receptor antagonist protein-like isoform X1 [<i>Podarcis muralis</i>]	242	242	27%	7.00E-73	72.05 %	178	XP_028597091.1
PB.1464.1 b'3b03d2' pat h5:118-1846(+) transcript/9115	1732	-1	IL1RA_PIGInterleukin-1 receptor antagonist protein OS= <i>Sus scrofa</i> OX=9823 GN=IL1RN PE=2 SV=1	interleukin-1 receptor antagonist protein-like isoform X1 [<i>Podarcis muralis</i>]	251	251	30%	1.00E-76	69.71 %	178	XP_028597091.1
PB.1489.1 b'3c6578' pat h0:0-1382(+) transcript/11978	1382	-1	IL6_CHICKInterleukin-6 OS= <i>Gallus gallus</i> OX=9031 GN=IL6 PE=2 SV=1	interleukin-6 [<i>Pogona vitticeps</i>]	209	209	45%	3.00E-61	55.19 %	219	XP_020637801.1
PB.1559.1 b'3fd528' pat h0:0-2368(+) transcript/4374	2370	-1	TRIM7_MOUSEE3 ubiquitin-protein ligase TRIM7 OS= <i>Mus musculus</i> OX=10090 GN=Trim7 PE=2 SV=2	zinc finger protein RFP isoform X1 [<i>Chelonia mydas</i>]	403	403	66%	6.00E-128	47.15 %	541	XP_037768270.1
PB.1560.1 b'3fd528' pat h1:0-2294(+) transcript/4768	2294	-1	TRI27_HUMANZinc finger protein RFP OS= <i>Homo sapiens</i> OX=9606 GN=TRIM27 PE=1 SV=1	zinc finger protein RFP-like [<i>Chelonoidis abingdonii</i>]	399	399	69%	2.00E-127	45.02 %	480	XP_032630233.1



PB.1590.1 b'414790' pat h0:0-3897(+) transcript/664	3897	-1	STEA4_HUMANMetalloredutase STEAP4 OS= <i>Homo sapiens</i> OX=9606 GN=STEAP4 PE=1 SV=1	metalloredutase STEAP4 [<i>Podarcis muralis</i>]	712	712	35%	0	80.25 %	471	XP_028607051.1
PB.1669.2 b'45e6de' pat h0:0-1740(+) transcript/9128	1733	-1	EBP_HUMAN3-beta-hydroxysteroid-Delta(8),Delta(7)-isomerase OS= <i>Homo sapiens</i> OX=9606 GN=EBP PE=1 SV=3	3-beta-hydroxysteroid-Delta(8),Delta(7)-isomerase [<i>Pogona vitticeps</i>]	400	400	39%	4.00E-134	81.39 %	231	XP_020653388.1
PB.1863.1 b'4ee890' pat h0:0-3659(+) transcript/883	3660	-1	NCF1_BOVINNeutrophil cytosol factor 1 OS= <i>Bos taurus</i> OX=9913 GN=NCF1 PE=2 SV=1	neutrophil cytosol factor 1 [<i>Lacerta agilis</i>]	689	689	31%	0	83.29 %	389	XP_033028282.1
PB.2071.4 b'58c046' pat h0:59-2811(+) transcript/2765	2748	-1	NA	leukocyte immunoglobulin-like receptor subfamily A member 6 [<i>Varanus komodoensis</i>]	101	166	16%	1.00E-17	43.08 %	719	XP_044303646.1
PB.2133.1 b'5d067b' pat h0:0-1902(+) transcript/7292	1902	-1	NADK_MOUSENAD kinase OS= <i>Mus musculus</i> OX=10090 GN=Nadk PE=1 SV=2	NAD kinase isoform X1 [<i>Lacerta agilis</i>]	573	820	70%	0	95.56 %	446	XP_033012254.1
PB.2231.1 b'632ea6' pat h0:0-2516(+) transcript/3750	2506	-1	SNX10_HUMANSorting nexin-10 OS= <i>Homo sapiens</i> OX=9606 GN=SNX10 PE=1 SV=2	sorting nexin-10 [<i>Chrysemys picta bellii</i>]	329	329	24%	7.00E-104	89.55 %	202	XP_005297032.1
PB.2440.2 b'6d4960' pat h0:1084-2106(+) transcript/15284	1025	-1	RINI_RATRibonuclease inhibitor OS= <i>Rattus norvegicus</i> OX=10116 GN=Rnh1 PE=1 SV=2	RINI inhibitor [<i>Anseranas semipalmata</i>]	145	354	34%	2.00E-35	67.52 %	456	NXI65525.1
PB.2461.2 b'6e1acc' pat h237:0-1256(+) transcript/13237	1215	-1	APOEB_DANREApolipoprotein Eb OS= <i>Danio rerio</i> OX=7955 GN=apoeb PE=2 SV=1	apolipoprotein E [<i>Pogona vitticeps</i>]	298	376	65%	5.00E-95	66.83 %	336	XP_020668207.1
PB.2461.4 b'6e1acc' pat h237:0-1258(+) transcript/14561	1084	-1	APOE_ALLMIApolipoprotein E OS= <i>Alligator mississippiensis</i> OX=8496 GN=APOE PE=3 SV=2	apolipoprotein E [<i>Pogona vitticeps</i>]	342	342	66%	1.00E-112	66.39 %	336	XP_020668207.1
PB.2477.2 b'6e5906' pat h0:1771-3988(+) transcript/6022	2202	-1	TGM1_RABITProtein-glutamine gamma-glutamyltransferase K OS= <i>Oryctolagus cuniculus</i> OX=9986 GN=TGM1 PE=2 SV=2	protein-glutamine gamma-glutamyltransferase K [<i>Varanus komodoensis</i>]	355	355	41%	1.00E-106	77.92 %	844	XP_044276906.1
PB.2550.1 b'72524d' pat h0:0-1536(+) transcript/10726	1537	-1	RND1_HUMANRho-related GTP-binding protein Rho6 OS= <i>Homo sapiens</i> OX=9606 GN=RND1 PE=1 SV=1	rho-related GTP-binding protein Rho6 [<i>Lacerta agilis</i>]	468	468	45%	1.00E-161	97.41 %	232	XP_032993946.1
PB.2602.1 b'74e2ed' pat h0:0-706(+) transcript/17892	706	-1	IRF1_CHICKInterferon regulatory factor 1 OS= <i>Gallus gallus</i> OX=9031 GN=IRF1 PE=2 SV=1	interferon regulatory factor 1 [<i>Sceloporus undulatus</i>]	229	229	49%	4.00E-71	89.66 %	303	XP_042311195.1
PB.2603.1 b'74e2ed' pat h1:0-2391(+) transcript/4253	2392	-1	IRF1_CHICKInterferon regulatory factor 1 OS= <i>Gallus gallus</i> OX=9031 GN=IRF1 PE=2 SV=1	interferon regulatory factor 1 [<i>Sceloporus undulatus</i>]	375	375	34%	2.00E-120	72.50 %	303	XP_042311195.1
PB.2603.2 b'74e2ed' pat h1:0-2387(+) transcript/6312	1950	-1	IRF1_CHICKInterferon regulatory factor 1 OS= <i>Gallus gallus</i> OX=9031 GN=IRF1 PE=2 SV=1	interferon regulatory factor 1 [<i>Varanus komodoensis</i>]	415	415	47%	8.00E-138	69.33 %	302	XP_044310382.1
PB.3082.1 b'8a6ab3' pat h0:0-1943(+) transcript/6626	1943	-1	PAI2_HUMANPlasminogen activator inhibitor 2 OS= <i>Homo sapiens</i> OX=9606 GN=SERPINB2 PE=1 SV=2	leukocyte elastase inhibitor-like isoform X1 [<i>Pogona vitticeps</i>]	654	654	64%	0	73.75 %	453	XP_020669995.1



PB.3244.1 b'92b6e7' pat h0:0-3460(+) transcript/1178	3460	-1	SIGL5_HUMANSialic acid-binding Ig-like lectin 5 OS= <i>Homo sapiens</i> OX=9606 GN=SIGLECS PE=1 SV=1	sialic acid-binding Ig-like lectin 13 isoform X1 [<i>Zootoca vivipara</i>]	404	404	49%	7.00E-124	43.45 %	572	XP_034976873.1
PB.3297.2 b'9598b3' pat h0:2-2686(+) transcript/3062	2677	-1	RDH10_HUMANRetinol dehydrogenase 10 OS= <i>Homo sapiens</i> OX=9606 GN=RDH10 PE=1 SV=1	retinol dehydrogenase 10 [<i>Podarcis muralis</i>]	621	621	38%	0	95.04 %	341	XP_028592529.1
PB.3324.1 b'96fa12' pat h0:0-1064(+) transcript/15494	1010	-1	B2LA1_MOUSEBcl-2-related protein A1 OS= <i>Mus musculus</i> OX=10090 GN=Bcl2a1 PE=1 SV=1	bcl-2-related protein A1 isoform X1 [<i>Sceloporus undulatus</i>]	215	215	51%	1.00E-65	62.07 %	175	XP_042332292.1
PB.3351.1 b'980835' pat h2:0-1705(+) transcript/9312	1706	-1	IKBA_HUMANNF-kappa-B inhibitor alpha OS= <i>Homo sapiens</i> OX=9606 GN=NFKBIA PE=1 SV=1	NF-kappa-B inhibitor alpha [<i>Podarcis muralis</i>]	138	138	12%	4.00E-32	92.86 %	330	XP_028576521.1
PB.3358.1 b'984964' pat h0:0-630(+) transcript/19237	630	-1	NA	NA	NA	NA	NA	NA	NA	NA	NA
PB.3377.1 b'993720' pat h0:0-2416(+) transcript/4249	2403	-1	INGR1_HUMANInterferon gamma receptor 1 OS= <i>Homo sapiens</i> OX=9606 GN=IFNGR1 PE=1 SV=1	interferon gamma receptor 1 [<i>Lacerta agilis</i>]	273	273	54%	2.00E-79	41.96 %	433	XP_032999761.1
PB.3650.3 b'a36ec8' pat h9:0-1953(+) transcript/6307	1954	-1	JUNB_RATTranscription factor jun-B OS= <i>Rattus norvegicus</i> OX=10116 GN=Junb PE=1 SV=2	transcription factor jun-B isoform X1 [<i>Varanus komodoensis</i>]	239	508	43%	1.00E-126	89.92 %	317	XP_044309937.1
PB.3778.2 b'a92240' pat h0:1-1156(+) transcript/13684	1156	-1	P2Y13_HUMANP2Y purinoceptor 13 OS= <i>Homo sapiens</i> OX=9606 GN=P2RY13 PE=1 SV=3	P2Y purinoceptor 13-like [<i>Lacerta agilis</i>]	532	532	86%	0	84.23 %	336	XP_033006336.1
PB.3835.1 b'abb05b' pat h0:0-1905(+) transcript/7829	1905	-1	PML_HUMANProtein PML OS= <i>Homo sapiens</i> OX=9606 GN=PML PE=1 SV=3	Protein PML [<i>Varanus komodoensis</i>]	267	267	42%	2.00E-80	50.74 %	293	KAF7237817.1
PB.3836.1 b'abb05b' pat h1:0-2560(+) transcript/3523	2566	-1	PML_HUMANProtein PML OS= <i>Homo sapiens</i> OX=9606 GN=PML PE=1 SV=3	protein PML-like [<i>Lacerta agilis</i>]	441	441	72%	3.00E-138	41.59 %	812	XP_033016605.1
PB.3969.1 b'b1b56f' pat h0:0-4460(+) transcript/321	4460	-1	PNPH_HUMANPurine nucleoside phosphorylase OS= <i>Homo sapiens</i> OX=9606 GN=PNP PE=1 SV=2	Purine nucleoside phosphorylase [<i>Ophiophagus hannah</i>]	548	548	20%	7.00E-180	84.44 %	325	ETE69996.1
PB.4156.1 b'b23a8a' pat h0:0-4868(+) transcript/178	4868	-1	TNAP3_HUMANTumor necrosis factor alpha-induced protein 3 OS= <i>Homo sapiens</i> OX=9606 GN=TNFAIP3 PE=1 SV=1	tumor necrosis factor alpha-induced protein 3 [<i>Podarcis muralis</i>]	104 9	1301	49%	0	75.56 %	810	XP_028579370.1
PB.4424.1 b'c02052' pat h0:0-3453(+) transcript/1197	3454	-1	PDE4B_HUMANcAMP-specific 3',5'-cyclic phosphodiesterase 4B OS= <i>Homo sapiens</i> OX=9606 GN=PDE4B PE=1 SV=1	cAMP-specific 3',5'-cyclic phosphodiesterase 4B isoform X1 [<i>Pseudonaja textilis</i>]	108 2	1082	48%	0	94.15 %	564	XP_026555922.1
PB.4528.1 b'c5be3e' pat h0:0-1182(+) transcript/13730	1177	-1	NA	peripheral myelin protein 22-like [<i>Podarcis muralis</i>]	115	115	40%	1.00E-26	50.31 %	159	XP_028598369.1
PB.4646.1 b'cc721f' pat h0:0-2086(+) transcript/6226	2086	-1	FFAR2_RATFree fatty acid receptor 2 OS= <i>Rattus norvegicus</i> OX=10116 GN=Ffar2 PE=1 SV=1	free fatty acid receptor 2-like [<i>Zootoca vivipara</i>]	421	421	44%	9.00E-139	66.03 %	356	XP_034974610.1



PB.5141.2 b'dcb56b' pat h1:7-1923(+) transcript/7534	1916	-1	TCPB_MACFAT-complex protein 1 subunit beta OS= <i>Macaca fascicularis</i> OX=9541 GN=CCT2 PE=2 SV=3	T-complex protein 1 subunit beta isoform X1 [<i>Numida meleagris</i>]	591	983	86%	0	86.03 %	621	XP_021240819.1
PB.5257.2 b'e2b1f3' pat h0:119-2644(+) transcript/9125	1752	-1	CFAB_BOVINComplement factor B OS= <i>Bos taurus</i> OX=9913 GN=CFB PE=1 SV=2	PREDICTED: complement factor B [<i>Gekko japonicus</i>]	629	685	88%	0	60.64 %	770	XP_015260944.1
PB.5257.3 b'e2b1f3' pat h0:1036-2644(+) transcript/9752	1606	-1	CFAB_PONPYComplement factor B OS= <i>Pongo pygmaeus</i> OX=9600 GN=CFB PE=3 SV=1	complement factor B [<i>Podarcis muralis</i>]	711	1014	91%	0	68.17 %	1233	XP_028573449.1
PB.5286.1 b'e39877' pat h0:0-4685(+) transcript/1006	3550	-1	TNAP2_HUMAN tumor necrosis factor alpha-induced protein 2 OS= <i>Homo sapiens</i> OX=9606 GN=TNFAIP2 PE=1 SV=2	PREDICTED: tumor necrosis factor alpha-induced protein 2 [<i>Gekko japonicus</i>]	689	689	58%	0	59.34 %	702	XP_015261979.1
PB.5295.2 b'e412d4' pat h0:22-745(+) transcript/18688	657	-1	PSB9_HUMANProteasome subunit beta type-9 OS= <i>Homo sapiens</i> OX=9606 GN=PSMB9 PE=1 SV=2	PREDICTED: proteasome subunit beta type-9 [<i>Anolis carolinensis</i>]	316	316	84%	9.00E-107	89.19 %	211	XP_003230744.2
PB.5622.1 b'f3d115' pat h3:0-1784(+) transcript/11734	1412	-1	SOCS3_CHICKSuppressor of cytokine signaling 3 OS= <i>Gallus gallus</i> OX=9031 GN=SOCS3 PE=2 SV=1	suppressor of cytokine signaling 3 [<i>Python bivittatus</i>]	397	397	46%	2.00E-134	94.09 %	241	XP_007428564.2
PB.5622.2 b'f3d115' pat h3:0-2439(+) transcript/4075	2440	-1	SOCS3_CHICKSuppressor of cytokine signaling 3 OS= <i>Gallus gallus</i> OX=9031 GN=SOCS3 PE=2 SV=1	suppressor of cytokine signaling 3 [<i>Python bivittatus</i>]	396	396	27%	3.00E-129	94.09 %	241	XP_007428564.2
PB.5622.4 b'f3d115' pat h3:0-2435(+) transcript/6684	2023	-1	SOCS3_BOVINSuppressor of cytokine signaling 3 OS= <i>Bos taurus</i> OX=9913 GN=SOCS3 PE=2 SV=1	suppressor of cytokine signaling 3 [<i>Python bivittatus</i>]	224	370	30%	1.00E-91	92.31 %	241	XP_007428564.2
PB.5779.1 b'fbfe89' pat h0:0-1488(+) transcript/11142	1488	-1	GA45B_HUMANGrowth arrest and DNA damage-inducible protein GADD45 beta OS= <i>Homo sapiens</i> OX=9606 GN=GADD45B PE=1 SV=1	growth arrest and DNA damage-inducible protein GADD45 beta [<i>Podarcis muralis</i>]	265	265	31%	2.00E-83	89.81 %	158	XP_028569769.1
PB.5908.1 transcript/10343:0-1585(+) transcript/10343	1585	-1	NA	radiation-inducible immediate-early gene IEX-1 [<i>Varanus komodoensis</i>]	218	218	33%	4.00E-64	62.16 %	181	XP_044275535.1
PB.6100.1 transcript/11390:0-1457(+) transcript/11390	1457	-1	NA	TNFAIP3-interacting protein 3 [<i>Podarcis muralis</i>]	452	452	69%	4.00E-154	71.22 %	343	XP_028600850.1
PB.6132.1 transcript/11542:0-1442(+) transcript/11542	1442	-1	NA	cytospin-B isoform X1 [<i>Maylandia zebra</i>]	76.6	76.6	26%	2.00E-10	31.06 %	1360	XP_024659847.1
PB.6180.1 transcript/11718:0-1345(+) transcript/11718	1345	-1	NA	interleukin-8-like [<i>Pelodiscus sinensis</i>]	67.4	67.4	8%	1.00E-09	83.78 %	104	XP_006125460.1
PB.6297.1 transcript/12432:0-1323(+) transcript/12432	1323	-1	NA	monocyte differentiation antigen CD14 [<i>Crotalus tigris</i>]	396	396	76%	2.00E-131	64.53 %	445	XP_039182068.1



PB.6375.1 transcript/12875:0-1283(+) transcript/12875	1283	-1	NA	TRAF-interacting protein with FHA domain-containing protein A [<i>Varanus komodoensis</i>]	201	201	39%	5.00E-58	56.29%	237	XP_044284233.1
PB.6492.1 transcript/13537:0-1167(+) transcript/13537	1167	-1	NA	tumor necrosis factor receptor superfamily member 12A [<i>Podarcis muralis</i>]	164	164	26%	5.00E-46	85.71%	122	XP_028559053.1
PB.6596.1 transcript/14092:0-1144(+) transcript/14092	1144	-1	NA	PREDICTED: ubiquitin-like protein ISG15 [<i>Gekko japonicus</i>]	208	208	38%	1.00E-60	66.22%	290	XP_015280625.1
PB.6754.1 transcript/15130:0-1038(+) transcript/15130	1038	-1	NA	butyrophilin subfamily 1 member A1-like [<i>Pogona vitticeps</i>]	314	314	71%	4.00E-103	59.36%	268	XP_020671464.1
PB.6806.1 transcript/1552:0-3255(+) transcript/1552	3255	-1	NA	LIM domain kinase 1 isoform X1 [<i>Pogona vitticeps</i>]	106	1065	55%	0	91.24%	605	XP_020657296.1
PB.7156.1 transcript/17937:0-745(+) transcript/17937	745	-1	NA	AN1-type zinc finger protein 2A isoform X1 [<i>Zootoca vivipara</i>]	294	294	69%	6.00E-98	78.03%	173	XP_034987218.1
PB.7351.1 transcript/19273:0-613(+) transcript/19273	613	-1	NA	cathelicidin-3-like [<i>Lacerta agilis</i>]	147	147	56%	4.00E-41	59.48%	150	XP_033022221.1
PB.7798.1 transcript/2282:0-2882(+) transcript/2282	2882	-1	NA	TNF receptor-associated factor 2-like [<i>Zootoca vivipara</i>]	317	545	37%	5.00E-144	74.55%	364	XP_034963066.1
PB.7969.1 transcript/2499:0-2827(+) transcript/2499	2827	-1	NA	interferon-inducible GTPase 5-like [<i>Chrysemys picta bellii</i>]	419	419	42%	3.00E-134	54.95%	397	XP_005314339.1
PB.8001.1 transcript/2643:0-2756(+) transcript/2643	2756	-1	NA	protein PML [<i>Varanus komodoensis</i>]	503	649	79%	2.00E-175	44.44%	778	XP_044306531.1
PB.8252.1 transcript/3744:0-2470(+) transcript/3744	2470	-1	NA	thioredoxin reductase 1, cytoplasmic [<i>Podarcis muralis</i>]	976	976	66%	0	85.84%	639	XP_028602813.1
PB.8358.1 transcript/4240:0-2402(+) transcript/4240	2402	-1	NA	E3 ubiquitin-protein ligase TRIM7-like isoform X1 [<i>Lacerta agilis</i>]	434	567	59%	1.00E-150	60.10%	484	XP_032998252.1
PB.8363.1 transcript/4274:0-2345(+) transcript/4274	2345	-1	NA	toll-like receptor 5 [<i>Lacerta agilis</i>]	727	727	83%	0	65.70%	657	XP_033030737.1
PB.8399.1 transcript/4457:0-2360(+) transcript/4457	2360	-1	NA	aldehyde dehydrogenase family 1 member A3 [<i>Podarcis muralis</i>]	995	995	65%	0	95.91%	513	XP_028562186.1
PB.8443.1 transcript/4681:0-2287(+) transcript/4681	2287	-1	NA	urokinase plasminogen activator surface receptor [<i>Pogona vitticeps</i>]	465	465	43%	4.00E-155	65.58%	339	XP_020668472.1



PB.8536.1 transcript/513 :0- 4086(+) transcript/513	4086	-1	NA	sodium- and chloride-dependent neutral and basic amino acid transporter B(0+) [<i>Sceloporus undulatus</i>]	944	944	46%	0	80.78 %	640	XP_042333656.1
PB.8599.1 transcript/546 8:0- 2179(+) transcript/5468	2179	-1	NA	NA	NA	NA	NA	NA	NA	NA	NA
PB.8640.1 transcript/567 1:0- 2151(+) transcript/5671	2151	-1	NA	fibronectin isoform X1 [<i>Zootoca vivipara</i>]	766	1850	70%	0	70.51 %	2379	XP_034994873.1
PB.8676.1 transcript/585 1:0- 2083(+) transcript/5851	2083	-1	NA	uncharacterized protein LOC117667923 [<i>Pantherophis guttatus</i>]	119	119	34%	2.00E-25	34.88 %	289	XP_034277428.1
PB.8743.1 transcript/635 9:0- 2048(+) transcript/6359	2048	-1	NA	deoxyribonuclease-1-like 2 [<i>Protobothrops mucrosquamatus</i>]	380	380	38%	4.00E-124	71.21 %	276	XP_015667481.1
PB.8858.1 transcript/708 0:0- 1993(+) transcript/7080	1993	-1	NA	tumor necrosis factor [<i>Varanus komodoensis</i>]	275	275	34%	3.00E-84	57.63 %	231	XP_044275697.1
PB.8970.1 transcript/781 2:0- 1907(+) transcript/7812	1907	-1	NA	interferon-stimulated gene 20 kDa protein isoform X3 [<i>Chrysemys picta bellii</i>]	242	242	27%	1.00E-72	65.70 %	174	XP_005294944.1
PB.9006.1 transcript/807 2:0- 1875(+) transcript/8072	1875	-1	NA	2'-5'-oligoadenylate synthase 1A-like [<i>Podarcis muralis</i>]	462	462	54%	1.00E-155	66.67 %	356	XP_028566472.1
PB.9108.1 transcript/856 2:0- 1798(+) transcript/8562	1798	-1	NA	forkhead box protein S1-like [<i>Sceloporus undulatus</i>]	513	513	80%	4.00E-173	64.24 %	561	XP_042319057.1



Summary and Discussion

This PhD project aimed to address five main questions that explore the pathogen-host interactions between the sleepy lizard (*Tiliqua rugosa*) and viruses.

- 1) Could ectoparasites (potentially virus vectors) cause a genetic change at genome wide and MHC markers in a population of sleepy lizards?
- 2) Are there viruses infecting *T. rugosa* at the Mount Mary study system in South Australia, and do their abundances vary over a known ecological gradient and tick parapatric boundary?
- 3) How widespread is the *Shingleback nidovirus 1* throughout its known distribution in Western Australia urban areas where most of the infected lizards have been reported?
- 4) Has the Shingleback virus spread into South Australia, as informed by observations of sick lizards in this region, including in the Mount Mary study site?
- 5) How does the bobtail flu, associated with viruses, affect the lizard host's immune responsive genes?

Chapter 1 associated the Major Histocompatibility Complex class I genotypes of *Tiliqua rugosa*, with a tick parapatric boundary and ecological gradient at a fine-scale. Here I showed that allele frequency at a single MHC class I locus varied with tick type, that there was heterozygosity deficiency, and positive selection at this locus. It is possible that these two tick species act as the vectors for pathogens across this region. As MHC class I is responsible for the antigen recognition molecule that detects viruses, before binding and presenting them to T-cells (Knapp 2005; Schwensow *et al.* 2017; Trowsdale 2011). My findings suggest pathogen mediated selection is occurring in *T. rugosa*. However, this study cannot determine the cause of these selection pressure but research has begun to explore this further.

Also in Chapter 1, I then used genome-wide SNPs to determine whether there is evidence of selective differentiation across the entire genome. Whether the result is simply reflective of wider population structure or if the differentiation is restricted to a small, possibly functional, region of the lizard's genome supporting what has been observed with the MHC



gene. I found no evidence that these patterns were due to host genetic clusters, as no population structure was identified in *T. rugosa* at this site however, there did seem to be some pattern (Chapter 1; Figure 4). Further work is required to determine if the ticks are vectors of viruses. Whilst these are only preliminary results, they do lead on to further research that can take place within this system that might help to elucidate the observed pressures on *T. rugosa*, and possibly what maintains the tick parapatric boundary (Godfrey and Gardner 2017). The limitation of this study is that group delineation in this chapter were based on tick species attached at the time of sampling, which does not necessarily reflect the full life history of *T. rugosa* that can live up to 40 years in the wild (Jones *et al.*, 2016). The lizards could have had more than one species of tick attached to it in its long life. Future work could use the long-term dataset to determine the lifetime tick infestation type of each lizard and relate this to genotypes at further immune gene loci. Using DArTSeq sequencing on lizards that have been repeatedly captured over the 40-year period that have consistently only had one type of tick species attached, could give more support to the group delineations, and explore further the possibility that ectoparasites might be causing differentiation in these lizards due to the role of MHC loci in mate selection.

Since Chapter 1 suggests pathogen mediated selection is occurring at the Mount Mary study site, Chapter 2 explored whether there were viruses in the system that might not be using the ticks as vectors. Viral abundance variations over the ecological gradient could also explain the MHC results of Chapter 1. Therefore, Chapter 2 used oral swabs of *T. rugosa* and flow cytometry to identify viral subpopulations in the oral cavity, as the only known viruses in this host species are respiratory viruses. The data were then used to calculate viral abundances and then visually identify 'hot spots' across the Mount Mary study site.

The use of flow cytometry to calculate viral abundances is a novel technique for use on reptiles, but has been applied to children (Carlson-Jones *et al.*, 2020). I identified two distinct viral sub-populations in the system, with significant viral abundance differences between those on the arid *Amblyomma limbatum* side of the site and those grouped along the parapatric boundary. The lizards grouped as 'near boundary' and *Bothriocroton hydrosauri* side had similar viral abundances of Virus 1 (Chapter 2: Figure 5). Perhaps Virus 1 has limited survival capacity in the more arid conditions in the north-east of the study site. It could be these viral abundance differences observed, are the cause of the



selective pressures on *T. rugosa* in the south-west of the site. Unfortunately, flow cytometry does not identify the virus. Therefore, the next step is to sample more across the site and use flow cytometry along with genome wide sequencing to identify/classify them taxonomically. However, this research identified two unknown viral sub-populations in this system that vary over the ecological gradient in the site. An interesting idea for future research when collecting oral swabs for flow cytometry would be to also take biological samples (blood or toes) to MHC genotype the lizards. This may then elucidate the MHC selection found in Chapter 1 if an association is found between these viruses and MHC genotype.

Chapter 3 aimed to determine whether the *Shingleback nidovirus 1* was currently active in the Mount Mary site, and, if so, if it was elsewhere in South Australia (SA), potentially having spread from the assumed source location in Perth, Western Australia (WA). Using reverse transcription PCR (RT-qPCR), currently the only method for detecting the virus, the study found no positive samples in the Mount Mary site, or in South Australia across main entry point from WA – the Nullarbor. As discussed in Chapter 3, one positive viral sample was identified in the collections of wild individuals (cohort 1) from a region of WA where the virus has been previously observed. This individual showed no flu-like symptoms at the time of sampling. It has been noted that 12% individuals infected with the *Shingleback nidovirus 1* do not show signs of disease (O’Dea *et al.*, 2016).

The sampling method applied in this study highlights that even remote areas, animals can still be screened for viruses, with normal and safe storage, combined with the RT-qPCR methods. This attempt at determining whether the *Shingleback nidovirus 1* had crossed a state border in wild populations is also the first of its kind (Parrish *et al.*, 2021). If this method was combined with a validated antibody test it would be a powerful method to determine the spread of the virus, and where it has been historically. Unfortunately attempts to develop a validated antibody test (icELISA) were not successful, perhaps once virus isolation is achieved then a neutralising antibody test could be developed. Future research into the virus’ distribution should apply a more targeted sampling regime and spend more time in selected areas where sick lizards have been observed. However, this would have to be with coordinated groups sampling synchronously in various locations



between Western Australia and South Australia, as the *T. rugosa* are only active for three months of the year making in depth sampling across such large distances difficult.

Although the flow cytometry samples of Chapter 2 were not screened for the *Shingleback nidovirus 1* using this RT-qPCR method of Chapter 3, the sample distribution of the Mount Mary, South Australia site in Chapters 2 and 3 do overlap (Chapter 3; Figure 6). As Chapter 2 showed Virus 1 to be in 95% of individuals sampled, and Virus 2 to be in 100% of individuals sampled, we can be reasonably confident that the viruses found in Chapter 2 were not the *Shingleback nidovirus 1*. This therefore means that *T. rugosa* has at least one newly observed virus, possibly two if the known *T. rugosa* adenovirus is also eliminated in future studies.

To build on the explorations of host-pathogen interactions, viral discovery and distributions, as well their ability to act as selective genetic drivers in this host. Chapter 4 aimed to determine how a disease associated with a virus influences the regulation of the *T. rugosa*'s immune system. The *Shingleback nidovirus 1*, and the adenovirus, are currently the only viruses known to infect *T. rugosa* and have been associated with the bobtail flu. It is not yet known whether the bobtail flu requires one or both viruses to be life threatening. Of course, environmental conditions, other opportunistic pathogens, as well as host specific factors could also contribute to the severity of the disease. Nevertheless, chapter 4 assessed the differential expression levels between *T. rugosa* displaying bobtail flu, and those suffering from major trauma to determine how the disease impacts the host's immune system using transcriptomics. The chapter had to attempt this without the use of a reference genome, that makes assembly of highly variable and short length genes difficult without false alignment errors. I found downregulation of innate immune system genes responsible for antigen detection and various isoforms of only two different immunoglobulins upregulated (IGY and IGL1).

If the *Shingleback nidovirus 1* is the key contributor of the bobtail flu, then it could be that this suppression of the innate system allows the adenovirus a better opportunity to infect the host. Of course, the adenovirus' contribution to the disease needs to be explored first. Future research should use healthy control animals to reduce the confounding noise that could be obscuring the results in Chapter 4. The animals from both groups should be screened for all known, or suspected, contributors to the bobtail flu disease (currently,



Shingleback nidovirus 1 and adenovirus). Screening would provide more confidence in the control group as currently there is a low possibility of asymptomatic animals, which would influence the results found here. Future research should also explore the severity of the disease and response to treatment when diagnosed with coinfections of the adenovirus (Hyndman and Shilton 2018) and *Shingleback nidovirus 1* (O’Dea *et al.*, 2016) and compare with a single infection of either virus. The adenovirus has been detected in other lizards in the *Tiliqua* genus (Hyndman and Shilton 2018). However, the *Shingleback nidovirus 1* has yet to be reported in other species. Therefore, understanding where this virus is and how it affects the known host is important should other species be susceptible. Particularly for species like the endangered *Tiliqua adelaidensis*, as no virus research has been conducted on this species yet (Cogger 2014; Smith *et al.*, 2009).

Research into reptile pathogens is becoming more common as human interactions are more frequent. This increased frequency has shown the spread of pathogens from squamates to humans (Whiley *et al.*, 2017). So there is a real concern about the possibility of spreading the *Shingleback nidovirus 1*, and other yet unknown pathogens, globally by a species with close interactions with humans (from pets to delicacies), and has been found illegally exported to other parts of the world (Asia, Europe, and North America) (Heinrich *et al.*, 2022). This greatly increases the potential to infect other domestic/wild lizards—or even other animals— and emphasises the importance of viral research in this species.

Conclusion

My thesis contributes significantly to the 40-year long term research at Mount Mary that is continuously conducted on these lizards (Godfrey and Gardner 2017). This thesis shows there are selective pressures present, and one, possibly two, new viruses previously unknown in this system and species. I also explored how the bobtail flu, the only disease currently known to be threatening this species (Norval *et al.*, 2019), affects the host on a genetic level. The results of which suggests a mechanism that could explain the, not yet supported, idea that the adenovirus is contributing to the bobtail flu with the suppression of the innate immune system enabling opportunistic pathogens a greater chance to survive in the host. This significantly adds to what is known about the bobtail flu, and how the host’s immune system responds to it. This thesis adds significantly to what is known about host-pathogen interactions in a non-model organism.



References

- Atasheva S, Shayakhmetov DM (2016). Adenovirus sensing by the immune system. *Current opinion in virology* **21**: 109-113.
- Carlson-Jones JAP, Kontos A, Kennedy D, Martin J, Lushington K, McKerral J Paterson JS, Smith RJ, Dann LM, Speck P, Mitchell JG (2020). The microbial abundance dynamics of the paediatric oral cavity before and after sleep. *Journal of Oral Microbiology* **12**: 1741254.
- Cogger H (2014). *Reptiles and amphibians of Australia*. CSIRO publishing.
- Dervas E, Hepojoki J, Smura T, Prähauser B, Windbichler K, Blümich S, Ramis A, Hetzel U, Kipar A (2020). Serpentoviruses: More than Respiratory Pathogens. *Journal of Virology* **94**: e00649-00620.
- Godfrey SS, Gardner MG (2017). Lizards, ticks and contributions to Australian parasitology: C. Michael Bull (1947–2016). *International Journal for Parasitology: Parasites and Wildlife* **6**: 295-298.
- Heinrich S, Toomes A, Shepherd CR, Stringham OC, Swan M, Cassey P (2022). Strengthening protection of endemic wildlife threatened by the international pet trade: The case of the Australian shingleback lizard. *Animal Conservation* **25**: 91-100.
- Hyndman T, Shilton C (2018). An update on Australian reptile infectious disease (Conference Proceedings).
- Jones AR, Bull CM, Brook BW, Wells K, Pollock KH, Fordham DA (2016). Tick exposure and extreme climate events impact survival and threaten the persistence of a long-lived lizard. *Journal of Animal Ecology* **85**: 598-610.
- Kikkert M (2020). Innate Immune Evasion by Human Respiratory RNA Viruses. *Journal of innate immunity* **12**: 4-20.
- Knapp LA (2005). The ABCs of MHC. *Evolutionary Anthropology: Issues, News, and Reviews* **14**: 28-37.
- Norval G, Ross KE, Sharrad RD, Gardner MG (2019). Taking stock: a review of the known parasites of the sleepy lizard, *Tiliqua rugosa* (Gray, 1825), a common lizard endemic to Australia. *Transactions of the Royal Society of South Australia*: 1-19.
- O’Dea MA, Jackson B, Jackson C, Xavier P, Warren K (2016). Discovery and Partial Genomic Characterisation of a Novel Nidovirus Associated with Respiratory Disease in Wild Shingleback Lizards (*Tiliqua rugosa*). *PLOS ONE* **11**: e0165209.
- Parrish K, Kirkland PD, Skerratt LF, Ariel E (2021). Nidoviruses in Reptiles: A Review. *Frontiers in Veterinary Science* **8**.
- Schwensow N, Mazzoni CJ, Marmesat E, Fickel J, Peacock D, Kovaliski J, Sinclair R, Cassey P, Cooke B, Sommer S (2017). High adaptive variability and virus-driven selection on major histocompatibility complex (MHC) genes in invasive wild rabbits in Australia. *Biological Invasions* **19**: 1255-1271.
- Smith AL, Gardner MG, Fenner AL, Bull CM (2009). Restricted gene flow in the endangered pygmy bluetongue lizard (*Tiliqua adelaidensis*) in a fragmented agricultural landscape. *Wildlife Research* **36**: 466-478.
- Trowsdale J (2011). The MHC, disease and selection. *Immunology Letters* **137**: 1-8.
- Walker PJ, Siddell SG, Lefkowitz EJ, Mushegian AR, Dempsey DM, Dutilh BE, Harrach B, Harrison RL, Hendrickson RC, Junglen S, Knowles NJ (2019). Changes to virus taxonomy and the International Code of Virus Classification and Nomenclature ratified by the



International Committee on Taxonomy of Viruses (2019). *Archives of Virology* **164**: 2417-2429.

Whiley H, Gardner, MG, Ross K (2017). A review of *Salmonella* and squamates (lizards, snakes and amphisbians): implications for public health. *Pathogens* **6**(3): 38

